Understanding the role of gamma delta (γδ) T cells in pancreatic cancer metastasis

Mark Lawrence, BSc(Hons)

Thesis submitted in fulfilment of the requirements for the Degree of Doctor of Philosophy

College of Medical, Veterinary and Life Sciences (MVLS)

Institute of Cancer Sciences

Cancer Research UK Beatson Institute

Garscube Estate, Switchback Road

Glasgow, G61 1BD

United Kingdom

January 2022

Abstract

Pancreatic ductal adenocarcinoma (PDAC) is a lethal malignancy with a 1-year survival rate of 5.6% and a 10-year survival rate of <1%. In Scotland, 3 in 5 people with pancreatic cancer are diagnosed at late-stage metastatic disease, and surgical resection remains the only effective cure for patients with non-metastatic disease. Given late-stage diagnosis and low rates of surgical resection, understanding the mechanisms of metastatic disease is of the utmost importance. In breast cancer, IL-17A$^+$ gamma delta (γδ) T cells are potently pro-metastatic and drive myeloid cell expansion which impairs anti-metastatic CD8$^+$ T cells. In PDAC, IL-17A has been implicated in early-stage PDAC progression, and γδ T cells have been shown to be abundant in human PDAC. Therefore, I sought to understand the role of γδ T cells in PDAC metastasis, and if they can promote metastasis in a similar manner as seen in breast cancer.

Using spontaneous $Kras^{G12D};Trp53^{R172H};Pdx1-Cre$ (KPC) mice, I have phenotyped γδ T cells in mouse PDAC and assessed their role in PDAC tumourigenesis and metastasis. In short, IL-17A$^+$ γδ T cells are significantly infiltrated into PDAC tumours, and Vγ6$^+$ γδ T cells (considered IL-17A-producers) are expanded in KPC spleen. Crucially, the absence of γδ T cells in KPC mice leads to a two-fold reduction in the incidence of spontaneous liver metastasis. Contrasting with breast cancer, γδ T cells do not mediate crosstalk with neutrophils by systemic cytokine production, but instead communicate locally with tumour-associated macrophages within the PDAC TME. Furthermore, γδ T cells promote the expansion of the embryonic-derived (tissue-resident) macrophage compartment, which have greater pro-tumour function than monocyte-derived macrophages.

These results reveal that tumour-infiltrated γδ T cells in PDAC display a pro-tumour phenotype, and that γδ T cells are indispensable for metastatic dissemination. They also reveal a novel phenotype where γδ T cells mediate crosstalk with macrophages specifically within the primary PDAC tumour. Further work is required to understand the mechanism of this crosstalk, but these findings may have important implications for the identification of future targets of anti-metastatic therapies.

Author's Declaration

I declare that I am the sole author of this thesis and that all work presented is my own, unless stated otherwise. No part of this thesis has been submitted for any other degree or award.

Mark Lawrence

Acknowledgments

Firstly, I would like to thank my supervisor Seth Coffelt for the opportunity to work on this project, and for all the help and support he has given me over the last four years. Your passion for science is infectious, and your guidance and constant encouragement throughout the PhD were invaluable. I am truly thankful to have had such a supportive supervisor.

To all the members of M32, past (Rhona and Sarah) and present (Anna, Rob, Wilma, Toshi, Liam and Amy). I could not have wished to work with better people, you guys honestly made M32 such a fun lab to work in. Thanks for all the morning coffee and breakfast rolls, listening to my rants about mice and the Fortessa, and for all your help throughout this project. Special thanks to Anna for always being there for support and advice, and for patiently answering my (many) questions. Wilma, for being my desk-mate and for putting up with me the last few months, you really helped keep me sane. Finally, Rob and Sarah, I'm so lucky to have had friends like you to turn to throughout the PhD, thanks for all the good times, Paesano trips and liquid therapy.

Thank you to all the members of R10 for your help with mouse training and checks, particularly Jen and Saadia, and a shout out to the other PCUK Future Leaders — Declan, Laura, Sigi and Rachael, and the honorary Future Leader, Dale for going through the PhD together. Thank you to my panel review members Prof Rob Nibbs and Prof Laura Machesky for their input throughout the PhD. Thank you to Colin Nixon and the histology team for all their work, and to Billy Clark and Robin Shaw for their help with the bulk RNA-seq experiments. Additionally, I would like to thank Pancreatic Cancer UK (PCUK), who funded this PhD.

Away from the lab, I would like to thank my family, particularly my parents and sister Deborah, who have supported me unconditionally in everything I have done. Without their support I would not be where I am today, and I can't thank them enough. Finally, I would like to thank my partner, Josie. You have been a constant source of encouragement throughout the PhD, and you always believed in me even when I didn't believe in myself. I can't put into words how grateful I am for everything you have sacrificed to help me succeed, I could not have done this without you.

List of Tables

List of Figures

List of abbreviations

ADCC	Antibody-mediated cell-dependent cytotoxicity
ADEX	Aberrantly Differentiated Endocrine Exocrine
ADM	Acinar-ductal metaplasia
BMDM	Bone marrow-derived macrophage
BTK	Bruton's tyrosine kinase
C57BL/6	Commonly used genetically identical inbred mouse strain
CA	Chronically active
CAF	Cancer-associated fibroblast
CCL/CXCL	Chemokine ligand
CCR/CXCR	Chemokine receptor
CD	Cluster of differentiation
CK-19	Cytokeratin 19
CM	Conditioned media
CRC	Colorectal cancer
CTGF	Connective tissue growth factor
CTLA-4	Cytotoxic T-lymphocyte-associated antigen 4
DC	Dendritic cell
DCLK	Doublecortin-like kinase
DEGA	Differentially expressed gene analysis
DNAM-1	DNAX accessory molecule-1
E20	Embryonic day (n)
EAE	Experimental autoimmune encephalomyelitis
ECM	Extracellular matrix
EMT	Epithelial-mesenchymal transition
ESC	Embryonic stem cell
FAP	Fibroblast activation protein
FAS	Cell surface death receptor
FLT3	FMS-like tyrosine kinase 3
FOV	Field of view
FSC	Forward scatter
GATA3	GATA binding protein 3
GEMM	Genetically engineered mouse model
GFP	Green fluorescent protein
GM-CSF	Granulocyte-macrophage colony stimulating factor
HCC	Hepatocellular carcinoma
HNF6	Hepatocyte nuclear factor 6
HSC	Hematopoietic stem cell
HSTC	Hepatic stellate cell
ID8	passaged C57BL/6 murine ovarian surface epithelial cells
IFN	interferon
IHC	Immunohistochemistry
IL1R1	interleukin 1 receptor 1
IPMN	Intraductal papillary mucinous neoplasm

ISH	*In situ* hybridisation
IV	Intravenous
JAK	Janus kinase
KC	Kupffer cell
KC (mouse)	LSL-Kras^{G12D};Pdx1-Cre
KEP	K14^{Cre};Cdh1$^{F/F}$;Trp53$^{F/F}$
KFE	Ela1-CreERT2; KrasG12D; Fbw7$^{+/+}$
KPC	LSL-Kras^{G12D};LSL-Trp53$^{R172H/+}$;Pdx1-Cre
KPL	Kras^{G12D};Trp53$^{fl/fl}$;R26^{tm1}
KPP	Kras$^{G12D/+}$;Ptf1a$^{ER-Cre/+}$;Pten$^{f/f}$
LIF	Leukaemia inhibitory factor
LPS	Lipopolysaccharide
MAM	Metastasis-associated macrophage
MCN	Mucinous cystic neoplasm
M-CSFR	Macrophage colony stimulating factor receptor
MDSC	Myeloid-derived suppressor cell
MHC	Major histocompatibility complex
MICA/B	MHC class I polypeptide-related sequence A
MMP	Matrix metalloproteinase 9
MMTV	Mouse mammary tumour virus
NMF	Non-negative matrix factorisation
MSC	Mesenchymal stem cell
NK	Natural killer
NKG2A/D	NK group 2 member A/D
NOS	Nitric oxide synthase
NSCLC	Non-small cell lung cancer
OT	Ova-specific T cell
PBMC	Peripheral blood mononuclear cell
PD-L1	Programmed death ligand 1
PDAC	Pancreatic ductal adenocarcinoma
PDGF	Platelet-derived growth factor
PDPN	Podoplanin
PDX1	Pancreatic and duodenal homeobox 1
PERT	Pancreatic enzyme replacement therapy
PI3K	Phosphoinositide 3-kinase
PKF	Ptf1a$^{cre/+}$; LSL-Kras^{G12D}; Tgfbr2$^{flox/flox}$
PMN	Premetastatic niche
PSC	Pancreatic stellate cell
RORyt	RAR-related orphan receptor gamma
SHP1/2	Src homology 2 domain-containing protein tyrosinephosphatase 1/2
SMA	Smooth muscle actin
SMAD4	Smad family member 4
SSC	Side scatter

STAT1/3	Signal transducer and activator of transcription 1/3
TAM	Tumour-associated macrophage
TAN	Tumour-associated neutrophil
TCR	T cell receptor
Tcrd	T cell receptor delta
T_{FH}	T follicular helper cell
TGF-ß	Transforming growth factor beta
TIGIT	T cell and IgG ITIM domain
TIL	Tumour-infiltrating lymphocyte
TME	Tumour microenvironment
TNF-alpha	Tumour-necrosis factor alpha
TRAIL	Tumour necrosis factor apoptosis inducing ligand
TRAV15N	T cell receptor alpha variable 15N-1
TRM	Tissue-resident macrophage
ULBP1	UL16 binding protein 1
VCAM	Vascular cell adhesion molecule
WT	Wild type
YFP	Yellow fluorescent protein
αß T cell	Alpha beta T cell
γδ T cell	Gamma delta T cell

Table of Contents

Chapter 1   Introduction.

1.1 Development of PDAC.

1.1.1 Overview of PDAC.

Pancreatic cancer is an umbrella term that describes endocrine and exocrine malignancies. Endocrine malignancies, defined as *pancreatic neuroendocrine tumours (PNETs),* develop following transformation and aberrant growth of hormone-producing islet cells, and account for less than 5% of overall pancreatic cancer cases. The commonest pathology is *pancreatic ductal adenocarcinoma* (PDAC), an exocrine malignancy that accounts for nearly 90% of all pancreatic cancer cases. (Rawla et al., 2019) Currently in Scotland, patients diagnosed with PDAC have a survival rate of just 5.6%, and a 10-year survival rate <1%. PDAC commonly develops asymptomatically, with clinical symptoms presenting often only when a patient has progressed to metastatic disease — in Scotland, 3 in 5 people are diagnosed with late-stage disease. These dismal survival rates have barely changed since the 1970s and are even more concerning when one considers PDAC incidence rates — increased by 17% between 1993-2017 in the UK, and projected to increase by 6% between 2014-2035. (Smittenaar et al., 2016) This trend is not UK-restricted, as data from the US predicts that PDAC will become the second leading cause of cancer related mortality within the next decade. (Rahib et al., 2014) The deadly combination of low and static survival rates, the projected increases in incidence and mortality, and the prevalence of metastatic disease reinforces that PDAC is a cancer of severe unmet clinical need. Considering that surgical resection remains the only effective cure for PDAC, a greater understanding of PDAC biology is fundamental to improve early disease detection and develop anti-tumour therapies, with the aim of improving patient survival.

1.1.2 Disease Classification.

Precision medicine aims to improve patient survival by subtyping tumours based on distinct molecular signatures, which enables patient therapy stratification. Different cancer types are driven through a heterogenous mix of driver mutations, numerous subverted cellular programs, and the acquisition of additional mutations with disease progression, all of which contribute to disease

classification. Numerous in-depth studies have confirmed that the initiating mutation of oncogenic KRAS (>90%) along with TP53 (64%), SMAD4 (21%) and CDKN2A (17%) are the four major genetic changes observed in human PDAC, and drive progression from precursor lesions to invasive carcinoma. (Orth et al., 2019, Biankin et al., 2012, Waters and Der, 2018) Despite the consensus surrounding PDAC driver mutations, a commonality in the classification of PDAC subtypes is lacking. The principle of PDAC molecular subtyping is to establish distinct classifications through the identification of molecular signatures and biological processes unique to each subset. Given that PDAC is driven by numerous oncogenes, somatic mutations and epigenetic changes, the mutational signatures of individual PDAC tumours are diverse. In lieu of such diversity, several studies have classified PDAC subtypes through various approaches, including global gene expression analysis, non-negative matrix factorisation (NMF) and whole genome/deep exome sequencing.(Collisson et al., 2011, Moffitt et al., 2015, Bailey et al., 2016)

Firstly, Collinsson et al. utilised global gene expression analysis to define three subtypes: *Classical*, *Quasimesenchymal* and *Exocrine-like*.(Collisson et al., 2011) "Classical" subtypes had high expression of adhesion and epithelial-associated genes, higher GATA6 and KRAS expression and longer post-resection survival.(Collisson et al., 2011) Comparatively, "Quasimesenchymal" subtypes had higher expression of mesenchyme-associated genes, poorer post-resection survival and reduced GATA6 and KRAS expression.(Collisson et al., 2011) "Classical" and "Quasimesenchymal" cell lines also had greater sensitivity to erlotinib and gemcitabine treatment, respectively. The "Exocrine-like" subtype was less well-defined, simply identified as having elevated expression of tumour-associated digestive enzyme genes.(Collisson et al., 2011) One caveat of this classification is the failure to separate tumour-derived signatures from stromal signatures in Exocrine-like subtypes.(Moffitt et al., 2015) Given that PDAC is dominated by a dense desmoplastic stroma, more recent subtyping focussed on distinguishing between the expression profiles of normal, PDAC and stromal tissues.(Moffitt et al., 2015) Using virtual micro-dissection with NMF, four distinct tumour- (*Basal* and *Classical*) and stroma-specific (*Normal* and *Activated*) subtypes were defined; tumour subsets are distinct from stromal subsets as the overexpression of stromal specific signatures was restricted to

CAFs and not tumour cells.(Moffitt et al., 2015) "Normal stroma" was associated with post-resection survival of 24 months, and increased expression of *pancreatic stellate cell* (PSC) markers; and "Activated stroma" had upregulated macrophage genes (ITCAM and CCL13/18), increased expression of MMP9 and FAP (fibroblast activation protein) and lower survival (15 months) compared to "Normal stroma".(Moffitt et al., 2015) "Classical tumour" subtypes exhibited increased survival (19 months) when compared to "Basal tumour" subtypes (11 months), and the majority of metastatic samples were classified as "Basal tumour" subtypes.(Moffitt et al., 2015) However, more recently the application of whole-genome and deep-exome sequencing has further characterised PDAC into four distinct groups – *Squamous, Pancreatic Progenitor, Aberrantly Differentiated Endocrine Exocrine (ADEX)* and *Immunogenic.*(Bailey et al., 2016) "Squamous" tumours have poor prognosis and are characterised by increased p53 mutations, which confers more aggressive metastatic disease; expression of TP63ΔN which regulates epithelial cell plasticity and EMT; and increased protumour TGF-β and Wnt signalling.(Bailey et al., 2016, Morton et al., 2010) The "Pancreatic Progenitor" subtype is defined by transcription factors that determine pancreatic lineage. This includes PDX1, as all ductal, endocrine and exocrine cells derive from PDX1$^+$ progenitors, and *hepatocyte nuclear factor* (HNF) transcription factors that define terminally differentiated pancreatic β cells.(Bailey et al., 2016) "ADEX" subtypes are a subclass of "Pancreatic Progenitors" as the expression profile identifies terminally differentiated pancreatic cells.(Bailey et al., 2016) "ADEX" tumours also exhibit both endocrine and exocrine lineages, whereas non-transformed pancreas expresses endocrine or exocrine.(Bailey et al., 2016) Finally, "Immunogenic" tumours are characterised by immune infiltrates — particularly pathways associated with B cell signalling, antigen presentation, CD4$^+$/CD8$^+$ T cells and TLR signalling.(Bailey et al., 2016)

To summarise, classification of PDAC subtypes based on global RNA expression profiles reveals distinct subtypes, but the inclusion of stromal expression signatures provides greater clarity on the molecular composition of PDAC subtypes. The above classifications all identify subsets with poorer prognosis and show that inter-patient molecular heterogeneity is associated with differential therapy responses. Therefore, using subtype classification as part of a precision

medicine approach can help stratify patients to more tailored therapeutic regimens, but may also identify suitable candidates for clinical trial enrolment. However, there is a lack of consensus surrounding PDAC subtyping, owing to the degree of overlap between classifications — particularly between Bailey and Collisson subtypes.(Bailey et al., 2016) Thus, whilst the application of molecular subtyping has the potential for clear patient benefit, the clinical application is lacking due to the absence of consensus.

1.1.3 Kras mutations.

The three RAS genes (HRAS, NRAS and KRAS) share homologous sequences and function, and are one of the most frequently mutated genes in cancer — occurring in roughly 27% of cancers.(Waters and Der, 2018) Of these, Kras is the predominant form and is particularly dominant in PDAC with roughly 92% of PDAC cases exhibiting Kras mutations.(Witkiewicz et al., 2015) In PDAC, the most frequent mutations occur at residue G12 (89%), which is a substitution point mutation from glycine (G), then to aspartate (D, 41%), valine (V, 34%) and arginine (R, 16%).(Witkiewicz et al., 2015) Homeostatic Ras protein is normally inactive and bound to GDP, but the activation of receptor tyrosine kinase leads to short-lived interactions between Ras-GTP which then subsequently drives a variety of intracellular signalling cascades.(Waters and Der, 2018) The point mutations described above results in permanent interactions between Kras-GTP, which causes constitutive overexpression of cellular pathways that drive proliferation. Given its near-universal expression within PDAC, including within early precursor lesions, Kras mutations are considered to be the initiating event of PDAC tumourigenesis.(Morris et al., 2010) However, despite the strong association of Kras with developed PDAC, evidence suggests ductal epithelial cells are refractory to oncogenic Kras alone, and that additional mutations including inflammatory stimuli are required to drive neoplastic lesion formation and subsequent PDAC development.(Ferreira et al., 2017, Brembeck et al., 2003, Kopp et al., 2012)

1.1.4 P53 mutations.

Mutations to tumour suppressor p53 are fundamental in enabling cancer cell proliferation, survival and metastatic spread; and with mutations occurring in

>50% of all human cancers, it is considered to be the most commonly mutated gene.(Perri et al., 2016) To summarise its broad function, p53 prevents the proliferation of damaged, stressed and transformed cells by directing repair mechanisms or apoptotic cell clearance.(Olovnikov et al., 2009) In PDAC, p53 mutations are found in roughly 50-75% of cases, where missense gain-of-function mutations dominate and drive PDAC progression through the subversion of senescence.(Morton et al., 2010) Using *in vivo* modelling, it was found that KC mice (*Pdx1-Cre-GFP; LSL-Kras$^{G12D/+}$*) readily develop premalignant PanIN lesions by 2 months, but do not progress to advanced PDAC. However, KPC mice (*Pdx1-Cre-GFP; LSL-Kras^{G12D};LSL-Trp53$^{R172H/+}$*) expressing a mutant copy of p53 rapidly progressed to PDAC — showing that mutant p53^{R172H} drives tumourigenesis. (Morton et al., 2010) Whilst both KC and KPC mice express comparable levels of senescence-associated β-galactosidase and p21 in PanIN precursors, PDAC tumours from KPC mice had no observable β-galactosidase, low expression of p21 but high levels of p53 expression. This indicates that accumulated p53^{R172H} mutations fail to activate p21, which subverts senescence mechanisms that would normally restrain PDAC progression.(Morton et al., 2010) Finally, it was found that KPC mice had increased metastatic incidence when compared to p53 null *LSL-Trp53$^{loxP/+}$* (KP^{fl}C) mice — 65% and 0%, respectively.(Morton et al., 2010) Therefore, gain-of-function mutant p53 facilitates PDAC progression through subversion of senescence, and increases the metastatic potential of PDAC.

Further studies have tried to elucidate the mechanisms of mutant p53-driven metastasis, with one notable example utilising RNA sequencing to transcriptionally profile KPC cells lines and identify downstream mediators of mutant P53.(Weissmueller et al., 2014) Following small hairpin RNA (shRNA) depletion of mutant p53 from KPC cells lines, differential gene expression analysis (DEGA) highlighted *platelet-derived growth factor receptor b* (PDGFRb), which regulates proliferation, survival and migration. WT p53 normally interacts with p63/73, which would repress PDGFRb. p73 overexpression in KP^{fl}C cell lines impairs PDGFRb activity through the formation of a complex with NF-Y, and mutant p53^{R172H} interrupts the p73/NF-Y complex and abrogates repression of PDGFRb.(Weissmueller et al., 2014) Modulation of PDGFRb expression in KPC cell lines through shRNA significantly reduces metastatic colonisation, indicating that mutant p53 can modulate metastasis by impairing p73/NF-Y localisation, which

increases PDGFRb expression and PDAC cell invasiveness.(Weissmueller et al., 2014) Thus, the acquisition of mutant p53, in addition to oncogenic Kras, is a fundamental driver of PDAC tumour progression and also underpins metastatic disease.

1.1.5 Precursor Lesions.

There has previously been conjecture within the literature as to the exact cellular origins of PDAC, but the name *pancreatic ductal adenocarcinoma* suggests it arises from ductal epithelial cells. This was postulated due to tumour architecture exhibiting morphological similarities to ducts, and the observation that pancreatic ductal hyperplasia, now referred to as neoplastic lesions, was found with increased incidence in patients with pancreatic cancer.(Hruban et al., 2000) These lesions can be separated into 3 categories: pancreatic intraepithelial neoplasia (PanIN), intraductal papillary mucinous neoplasm (IPMN) and mucinous cystic neoplasm (MCN), however, the focus here is on PanINs.(Hruban, 2008)

PanIN lesions are the most well-known PDAC precursor lesion, and the development of PDAC through PanINs is a stepwise process characterised by the accumulation of genetic mutations through each developmental stage (Figure 1-1). PanINs develop asymptomatically within the ductal epithelium and can be classed as low-grade (PanIN-1A/1B), intermediate grade (PanIN-2) and high-grade (PanIN-3).(Hruban, 2008, Distler et al., 2014) Despite the abnormal morphological changes, PanIN lesions do not breach the basement membrane and are considered non-invasive precursors.(Hruban, 2008, Distler et al., 2014) PanIN1A lesions maintain a columnar morphology, but exhibit cellular elongation, cytoplasmic expansion, and a papillary growth pattern (finger-like projections). PanIN-1B lesions can be identified by the presence of invaginations. Genetic mutations associated with PanIN-1 lesions include the activation of oncogenic Kras, followed by inactivation of p16/CDKN2A — these initiate lesion formation and facilitates progression to PanIN-2, respectively.(Hruban, 2008, Distler et al., 2014) PanIN-2 lesions are characterised by invaginations and nuclear changes such as a loss of basal polarity and nuclear crowding due to p16 inactivation. Finally, PanIN-3 lesions are characterised by severe nuclear atypia, identifiable mitosis, luminal budding and the loss of p53 and Smad4 tumour

suppressor genes.(Hruban, 2008, Distler et al., 2014) PanIN-3 lesions are the penultimate step prior to invasive carcinoma (PDAC), and have previously been described as *carcinoma in situ.*

Figure removed as it contains 3rd party copyright material, and permission for inclusion has not been granted.

Figure 1-1 PDAC develops sequentially through precursor PanIN lesions.
Invasive PDAC develops through precursor PanIN lesions following transformation of pancreatic acinar cells through ADM. PanIN lesions are characterised by distinct morphological changes that are driven by the accumulation of genetic mutations in a stepwise manner – initially oncogenic Kras, followed by CDKN2A, p53 and SMAD4. Taken from Orth et al., 2019.

1.1.6 Cellular Origin of PDAC

Pancreatic tissue consists of 3 main components – acinar, ductal and islet cells. Acinar and ductal cells combine to form the exocrine compartment (85%) and islet cells form the endocrine compartment (15%) and produce insulin and glucagon.(Pandol, 2010) As the histological features of PDAC closely resemble ductal architecture, a ductal origin was initially proposed. Early genetically engineered mouse models (GEMMs) of pancreatic cancer, such as the *Pdx1-Cre; LSL-Kras^{G12D}* (KC) mouse, were developed following the identification of transcription factors that direct pancreatic progenitor cell fate – expression of both *Pdx1* (E8/8.5) and *p48/Ptf1* (E9/9.5) induces development of mature pancreatic cells.(Jørgensen et al., 2007) The pancreas-specific expression of Kras^{G12D} through Pdx1-Cre recombination led to precursor lesions that recapitulated PanINs seen in human disease, however, only 2/29 mice subsequently developed invasive and metastatic PDAC.(Hingorani et al., 2003) Despite the early (E8-9.5) expression of *Pdx1-Cre* in all pancreatic progenitor cells, the KC mouse alone is not sufficient to determine the cellular origin of PDAC, and subsequent models have been developed to address this shortcoming.

1.1.7 Ductal Origin of PDAC

Whilst oncogenic Kras mutation is fundamental for PDAC initiation, there is evidence that ductal cells are refractory to $Kras^{G12D}$ *alone*, and that additional mutations are required for ductal cell progression to PDAC. Conditional expression of Kras through the cytokeratin-19 (*Ck-19*) promoter resulted in $Kras^{G12D}$ expression specifically within ductal epithelial cells.(Brembeck et al., 2003) However, following duct-specific $Kras^{G12D}$ recombination there was increased NK cell-mediated lysis of transformed cells and upregulation of N-cadherin in response to stress-associated morphogenesis — N-cadherin maintains cellular interactions and prevents ductal transformation to PanIN lesions.(Brembeck et al., 2003) Additionally, although KC mice exhibited PanINs similar to human disease, invasive carcinoma rarely develops and often there is no detectable carcinoma at 30 weeks, indicating ductal cells are refractory to $Kras^{G12D}$ mutations alone.(Hingorani et al., 2003, Aguirre et al., 2003) However, PanIN progression is characterised by the sequential acquisition of somatic mutations following $Kras^{G12D}$ mutation. The combination of $Kras^{G12D}$ with *p16* mutations (*Pdx1-Cre*; $Kras^{G12D}$; $Ink4a/Arf^{flo/lox}$) resulted in highly invasive tumours between 7-11 weeks; and combining $Kras^{G12D}$ with *Smad4* mutation (*Pdx1-Cre*; $Kras^{G12D}$; $Smad4^{lox/lox}$) significantly increased the grade and size of PanIN lesions, increased tumour development and significantly reduced survival.(Aguirre et al., 2003, Bardeesy et al., 2006) In KPC mice *(Pdx1-Cre; LSL-$Kras^{G12D}$;LSL-$Trp53^{R172H}$)* the addition of mutant $p53^{R172H}$ enables cells with oncogenic $Kras^{G12D}$ to overcome senescence mechanisms, and confers increased metastatic potential.(Morton et al., 2010) This cumulative evidence shows whilst ductal cells are indeed refractory to oncogenic $Kras^{G12D}$ alone, the accumulation of *p16*, *Smad4* and $p53^{R172H}$ mutations enhances the formation of PanIN lesions, and promotes the development of invasive carcinoma from ductal cells.

1.1.8 Acinar Origin of PDAC

Despite the evidence that ductal cells can develop into PanIN lesions following $Kras^{G12D}$ initiation and additional mutations, there is strong evidence that acinar cells are more responsive to $Kras^{G12D}$ mutation. To address this, GEMMs with $Kras^{G12D}$ combined with deletion of tumour suppressor Fbw7 ($Fbw7^{+/+}$) were conditionally expressed in either ductal or acinar cells using the cytokeratin-19

(*CK-19-Cre^{ER}*) or elastase promoters (*Ela1-Cre^{ERT2}*), respectively.(Ferreira et al., 2017) In *Ela1-CreERT2*; *KrasG12D*; *Fbw7$^{+/+}$* (KFE) mice, it was found that they had a significantly higher number of PanIN lesions when compared to *Ck19-Cre^{ER}*; *Kras^{G12D}*; *Fbw7$^{+/+}$* (KFCk) mice. Furthermore, whilst KFCk mice were able to develop PDAC, they had no detectable PanIN lesions. PDAC was instead preceded by ductal cell expansion, loss of cellular polarity and cellular tufting. In comparison, KFE mice exhibited overt PanIN lesion development — suggesting that whilst acinar and ductal compartments are both capable of developing into PDAC, only acinar-specific Kras^{G12D} mutation leads to PanIN precursor lesions.(Ferreira et al., 2017) A summary of acinar- and duct-derived PDAC development is shown in Figure 1-2.

Additional evidence from Kopp et al. supports an acinar PDAC origin.(Kopp et al., 2012) Using *Sox9-Cre^{ER}*; *Kras^{G12D}*; *R26R^{YFP}* mice, Kras^{G12D} was recombined in ductal cells and tagged with a YFP promoter for lineage-tracing — *Pft1a-Cre^{ER}*; *Kras^{G12D};R26R^{YFP}* mice were also used for acinar compartment tracing.(Kopp et al., 2012) It was found that *Sox9-Cre^{ER}* mice had largely normal histology and rarely developed into PanINs. Conversely, *Ptf1a-Cre^{ER}* mice displayed considerable PanIN lesion development, 112-fold higher frequency than that of *Sox9-Cre^{ER}* mice.(Kopp et al., 2012) The acinar origin was further investigated in two models of acinar-restricted tamoxifen-inducible GEMMs using the Elastase (*Kras^{G12D}*; *Ela-CreERT2$^{Tg/+}$*) and Mist1 (*Kras^{G12D}*; *Mist1$^{CreERT2/+}$*) promoters, and 60% of mice exhibited overt PanIN lesion formation 2 months post-induction followed by PDAC development.(Habbe et al., 2008) This shows that PDAC can arise from the acinar compartment, and that acinar cells have a greater propensity to develop into PanIN lesions than ductal cells. Additionally, this demonstrates that acinar cells exhibit a certain plasticity, and that Kras^{G12D} mutation can induce acinar cells to acquire a ductal morphology — achieved through a process known as *acinar-ductal metaplasia* (ADM).

Figure removed as it contains 3rd party copyright material, and permission for inclusion has not been granted.

Figure 1-2 PanIN lesions arise from transformed acinar cells.
Acinar cells receive oncogenic signals through Kras[G12D] mutations, undergo ADM and progress to PDAC through precursor PanIN lesions. Ductal-derived PDAC forms following oncogenic Kras[G12D] mutations which causes ductal cell proliferation, loss of cellular polarity and the eventual formation of ductal structures in a PanIN-independent manner. Taken from Ferreira et al., 2017.

1.1.9 Acinar-Ductal Metaplasia.

ADM is defined a physiological response of the pancreas to injury, whereby acinar cells revert to a progenitor state, adopt a ductal phenotype and undergo proliferation to aid in organ repair.(Storz, 2017) ADM is a crucial homeostatic process that serves to regenerate cell populations, and is characterised by the repression of acinar genes and the expression of ductal genes within the acinar compartment.(Shi et al., 2013) During homeostasis, ADM is reversible and self-limiting; however, oncogenic Kras signalling through PI3K isoforms maintains acinar plasticity, prevents the re-differentiation of transformed acinar cells and leads to persistent and unresolving ADM.(Baer et al., 2014)

1.1.10   Repression of acinar identity.

Several transcription factors help to maintain acinar identity, but no individual transcription factor is a master regulator of lineage commitment. However, *pancreas transcription factor 1 complex* (Ptf1a) is considered crucial in maintaining acinar identity.(Campos et al., 2013) Normally, Ptf1a forms a complex with RBPJl, which interacts with GATA6 to maintain acinar identity, and loss of Ptf1a/GATA6 leads to persistent ADM characterised by extensive inflammatory macrophage infiltrate.(Martinelli et al., 2016) In PDAC, the induction of ADM in Ptf1a knockout (Ptf1a$^{-/-}$) GEMMs sensitises cells to oncogenic Kras and leads to carcinoma development.(Krah et al., 2015) Another transcription factor that contributes to a loss of acinar identity is KLF4, which is

known to have roles in cellular differentiation, cell cycle, apoptosis and inflammation.(Ghaleb and Yang, 2017) Increased KLF4 expression is found in human and mouse PanIN cells, but not in normal pancreatic tissue, suggesting it plays a role in PanIN formation.(Wei et al., 2016) Using a ductal ligation assay to induce ADM, KLF4 was found to be significantly increased along with ductal marker cytokeratin-19 (CK-19), and the ablation of KLF4 is also sufficient to abrogate ADM, even in the presence of oncogenic Kras.(Wei et al., 2016) Further investigation revealed that oncogenic Kras drives KLF4 overexpression, leading to a downregulation of acinar gene Ptf1a and an upregulation of CK-19 ductal marker, resulting in the repression acinar identity.(Wei et al., 2016)

1.1.11   Gain of ductal/progenitor identity.

The repression of acinar genes is one aspect of ADM, the other being the induction of ductal genes such as Sox9 and *hepatocyte nuclear factor 6* (HNF6). During embryogenesis, Sox9 maintains progenitor cell turnover, and lineage-tracing experiments have shown Sox9+ pancreatic progenitors give rise to acinar and ductal cells.(Aguilar-Medina et al., 2019) However, Sox9 expression is restricted to ductal and centroacinar cells in adult pancreas, so the abundant Sox9 in PanIN lesions supported the ductal origin.(Aguilar-Medina et al., 2019) However, Sox9 expression in acinar-derived metaplastic ducts from *Ela1-CreERT2; Kras*^{G12D} mice indicates Sox9 drives ductal reprogramming during Kras-driven ADM.(Morris et al., 2010) During ADM, and in the context of Kras activation, upregulation of Sox9 and CK-19 ductal markers are observed in metaplastic acinar cells, and has been shown to be downstream of HNF6.(Prévot et al., 2012) Over-expression of HNF6 with adenoviral transduction in acinar cells upregulates ductal genes (Sox9 and CK-19), and simultaneously represses acinar gene signatures such as Mist1, Ptf1a and amylase.(Prévot et al., 2012) This demonstrates that ADM is a multifaceted process reliant on several distinct mechanisms, and it is unlikely that an individual signal will be responsible for initiating ADM alone.

1.1.12 Chronic inflammation is driven by IL-1β, which also drives Neoplastic Development.

Since ADM is a physiological response to intrinsic stress and damage, it is crucial that pancreatic inflammation is transient and self-limiting, as continued inflammatory insults will lead to permanent tissue dysregulation. In PDAC, chronic pancreatitis is a well-defined risk factor as it leads to unresolved and persistent ADM, which sensitise cells to oncogenic Kras mutations.(Marrache et al., 2008) One notable driver of chronic pancreatitis is the inflammatory cytokine IL-1β, with higher IL-1β associated with increased disease severity.(Marrache et al., 2008) When IL-1β overexpression is restricted to pancreatic acinar cells it leads to pancreas-specific cellular proliferation, apoptosis, fibrosis and persistent ADM.(Marrache et al., 2008) Chronic pancreatitis is not only crucial for maintaining persistent ADM, but also for the development of PanIN lesions and subsequent PDAC in adult mice.(Guerra et al., 2007) Using an inducible mouse model ($Kras^{+/LSLG12Vgeo};Elas\text{-}tTA/tetO\text{-}Cre$), acinar-specific $Kras^{G12V}$ expression was controlled by a tet-off system, where doxycycline repression of $Kras^{G12V}$ enabled the temporal control of oncogenic recombination.(Guerra et al., 2007) In the absence of doxycycline, $Kras^{G12V}$ recombination is followed by ADM in late embryonic development, leading to extensive PanIN lesions and PDAC.(Guerra et al., 2007) However, the removal of doxycycline at 60 days of age (P60) did not lead to ADM or PanIN lesions, suggesting that oncogenic Kras alone is not sufficient facilitate ADM and PanINs in adult acinar cells.(Guerra et al., 2007) Given that chronic pancreatitis is a major risk factor in human disease, GEMMs can model this through treatment of low dose caerulein, which induces the secretion of exocrine enzymes to mediate chronic pancreatitis.(Willemer et al., 1992) Chronic treatment of low dose caerulein combined with the removal of doxycycline in P60 mice led to diffuse ADM, extensive high grade PanIN lesions and the development of invasive PDAC.(Guerra et al., 2007) This indicates that recombination of oncogenic Kras in adult acinar cells requires additional stimuli, such as IL-1β-mediated chronic pancreatitis, to form PanINs and subsequent PDAC.

1.1.13   Role of macrophages in ADM.

Chronic pancreatitis is a key aspect of ADM, as it is characterised by an extensive immune infiltrate, notably macrophages. In caerulein-induced ADM, depletion of macrophages (by macrophage toxin gadolinium chloride hexahydrate) is sufficient to abrogate ADM formation, and culture of pancreatic acinar cells with macrophage-conditioned media (CM) increased ductal and reduced acinar gene expression — suggesting a central role for macrophages in ADM formation.(Liou et al., 2013) Further to this, cytokine profiling of macrophage CM found increased TNF and CCL5. Blocking of TNF and CCL5 in acinar cell and macrophage co-cultures represses ADM through the inhibition of NK-κB signalling and MMP-9 production in acinar cells. (Liou et al., 2013) Therefore, ADM can be initiated by macrophage activation, as macrophage-derived products drive a loss of acinar cell identity and upregulate ADM-inducing factors.

In addition to IL-1β and TNF-α, IL-6 has also been shown to be important in PDAC, as IL-6 correlates with poor prognosis and is increased in patients with metastatic disease compared to non-metastatic patients.(van Duijneveldt et al., 2020) IL-6 is produced by numerous cell types, including macrophages, and binding of IL-6 to IL-6R leads to Jak2 signalling and phosphorylation of Stat3 (pStat3), which drives anti-apoptotic mechanisms, increased proliferation and immune modulation.(van Duijneveldt et al., 2020) Normal pancreata do not exbibit pStat3, but it is present in high levels within human PDAC and PanIN lesions.(Lesina et al., 2011) Furthermore, in GEMMs that have pancreas-specific Stat3 inactivation *(Ptf1a-Cre^{ex1};Kras^{G12D};Stat3^{Δ}panc)*, the loss of pStat3 prevents the formation of PanIN lesions and results in higher levels of apoptosis.(Lesina et al., 2011) This indicates that pStat3 signalling contributes to early PDAC tumorigenesis by regulating proliferative and apoptotic mechanisms to drive PanIN progression. Conventionally, pStat3 activity is driven by Jak2 signalling following IL-6R binding its cognate ligand IL-6, with pStat3 activity controlled endogenously through the action of Socs3 inhibitor.(Wang and Sun, 2014) However, acinar cells do not express the IL-6R, with the activation of pStat3 occurring through IL-6 trans-signalling. This is a process whereby IL-6 forms a complex with a soluble form of the IL-6R, which then induces pStat3 signalling within cells that do not express the IL-6R, such as acinar cells.(Lesina et al.,

2011) The importance of IL-6 in PDAC is shown in *Ptf1a-Cre^ex1^;Kras^G12D^;Il6^−/−^* mice which have impaired IL-6 trans-signalling, resulting in fewer PanIN lesions and reduced lesion severity.(Lesina et al., 2011) Additionally, reconstitution of bone marrow from IL-6^−/−^ donors in irradiated *Ptf1a-Cre^ex1^;Kras^G12D^* mice did not facilitate high grade PanIN development, unlike IL-6-competent donors which developed high grade PanINs.(Lesina et al., 2011) Finally, loss of pStat3 regulator Socs3 in *Ptf1a-Cre^ex1^;Kras^G12D^;Socs^Δ/Δ^* mice leads to accelerated PanIN development, indicating that loss of Stat3 regulation can also drive PDAC tumourigenesis.(Lesina et al., 2011) Therefore, macrophage-derived IL-6 can mediate Stat3 signalling in acinar cells through IL-6 trans-signalling, which modulates acinar cell proliferation and apoptosis to drive PanIN development; additionally, the loss of Socs3-mediated Stat3 regulation can also drive PanIN development. This cumulative evidence shows that whilst macrophage-driven inflammation induces ADM, macrophage-derived products such as TNF-α and IL-6 can also directly influence early PDAC tumourigenesis.

1.1.14 Changes in macrophage polarisation facilitates PanIN development.

Given the evidence that macrophages can establish ADM, the preceding step to precursor PanIN lesions, macrophages clearly play a central role in PDAC initiation and progression. When unresolving ADM occurs in the presence of Kras^G12D^ mutations and chronic pancreatitis, macrophage behaviour can be subverted from inflammatory to a more pro-fibrotic state.(Xue et al., 2015) During chronic pancreatitis in mice, inflammatory cytokines such as IL-1β and IL-6 become reduced and pro-fibrotic cytokines like TGF-β are increased.(Xue et al., 2015) This fluid nature is characteristic of macrophages, which are highly heterogeneous immune cells that can change their functionality based on signals from the local cytokine milieu. ADM initiation is driven by inflammatory macrophages, which are characterised through the production of cytokines such as IL-1β, TNF-α, and IFN-γ; they are also identified through nitric oxide synthase (NOS) production and the promotion of inflammatory responses.(Lin et al., 2019) During tumour development, macrophages are re-polarised and acquire a *tumour-associated macrophage* (TAM) phenotype, which is highly immunosuppressive and enables metastatic growth through immune subversion and promotion of fibrosis.(Lin et al., 2019) TAMs are identifiable through the

production of anti-inflammatory cytokines such as IL-4, IL-10, IL-13 and TGF-β, and the expression of CD163, CD206 and Ym1.(Lin et al., 2019) Within human PanIN1/2 lesions, inflammatory macrophages (iNOS^{+}) and TAMs (CD163^{+} or Ym1^{+}) are found at a ratio of 1:2.(Liou et al., 2013) Furthermore, *p48*[Cre]; *Kras*[G12D] mice exhibited a 3-fold increase in Ym1^{+} TAMs in PanIN regions, with the dominant populations in regions of ADM was found to be iNOS[+] inflammatory macrophages.(Liou et al., 2013) This demonstrates that inflammatory macrophages drive ADM establishment, but become repolarised to TAM phenotype either prior to, or following, PanIN development.

1.1.15   PanINs subvert macrophage phenotype to facilitate outgrowth.

In vitro studies have confirmed that peritoneal iNOS[+] inflammatory macrophages can be re-polarised to a Ym1^{+} TAM phenotype by the presence of IL-4/IL-13 in culture.(Liou et al., 2017) Further to this, the presence of IL-13 within areas of murine ADM and PanINs indicates that the early preneoplastic microenvironment may be responsible for TAM polarisation.(Liou et al., 2017) Pancreatic stellate cells (PSCs) and CD4^{+} T$_h$2 cells are known sources of IL-13, however, *in situ hybridisation* (ISH) revealed co-expression of IL-13 with DCLK1^{+} and α-tubulin^{+} tuft cells, also confirmed by flow cytometry of DCLK1 [+] tuft cells.(Liou et al., 2017) Healthy murine pancreas is devoid of tuft cells; however, the presence of ADM and neoplasia mediates tuft cell formation where they play a role in tissue repair to maintain pancreatic homeostasis.(DelGiorno et al., 2020) The application of IL-13 neutralising antibody reduces macrophages in PanIN regions, specifically an 80% decrease in F4/80[+]Ym-1^{+} TAMs in PanIN1 regions, but no change to inflammatory F4/80[+]Stat1^{+} macrophages.(Liou et al., 2017) The reduction of TAMs also correlates with reduced fibrosis, along with reduced Ki67 expression and pErk1/2, which are markers of proliferating PanIN lesions.(Liou et al., 2017) Therefore, macrophages initiate ADM and drive PanIN lesion formation, which leads to the activation of tuft cells in response to neoplastic transformation. The subsequent release of IL-13 from tuft cells within PanIN lesions then polarises macrophages to a TAM phenotype, which enhances stromal deposition, cellular proliferation and drives PanIN progression.(Liou et al., 2017)

The unresolving inflammation associated with neoplastic transformation is a major contributing factor to TAM polarisation in early tumourigenesis. However, cancer-associated inflammation is not comprised solely of a single macrophage phenotype — microarray data from various tumour types indicates that inflammatory macrophage (IL-1β, TNF-α, CXCL2 and Socs3) and TAM (Arginase 1) gene signatures are both present within tumours.(Kratochvill et al., 2015) TAMs eventually become the dominant population through disrupting a balance between inflammatory macrophage and TAM phenotype. Macrophage populations have differential signalling mechanisms and mediators; inflammatory macrophages signal through NF-κB which activates various effector genes such as TNF-α, and TAMs are driven by IL-4/IL-13 which activates Stat6 to upregulate TAM effector genes.(Liu et al., 2017, Biswas and Mantovani, 2010) When bone marrow-derived macrophages (BMDMs) were cultured with M-CSF and IL-13 with or without TNF-α, the presence TNF-α was found to repress TAM gene signatures.(Kratochvill et al., 2015) More specifically, inflammatory macrophage-derived TNF-α impairs IL-13-driven upregulation of TAM genes, acting as a negative regulator of TAM activity in early tumourigenesis. However, continued PanIN lesion expansion leads to increased production of IL-13, which overpowers the TNF-α-mediated repression and enables the expansion of TAM phenotypes in the TME. Thus, TAMs are a fundamental immune cell in the early PDAC TME, particularly for PanIN progression and the establishment of an immune-suppressive TME.

1.2   PDAC Tumour Microenvironment (TME).

1.2.1 Cancer-associated fibroblasts (CAFs) play major roles within the PDAC TME.

Despite the clear importance of macrophages in PDAC tumourigenesis, the PDAC TME is immune-quiescent, resulting from the immune-suppressive mechanisms that facilitate tumourigenesis. The outgrowth of PDAC is heavily reliant upon this suppressive TME, which also consists of a significant stromal compartment that drives a desmoplastic reaction characterised by overt fibrosis. As with tumour initiation, there is no single factor that solely maintains the TME; it is instead characterised by a complex network of immune-suppressive inflammatory infiltrate and cancer-associated fibroblasts (CAFs) which influence tumour growth, invasion and metastasis through a variety of mechanisms.(Bolm et al., 2017)

CAFs can be generated from bone-marrow-derived mesenchymal stem cells (MSCs), pancreatic stellate cells (PSCs) and from the pancreas-resident fibroblast population. (Bolm et al., 2017) MSC-derived CAFs originate from bone marrow and differentiate into α-smooth muscle actin$^+$ (αSMA) CAFs (myofibroblasts) through TGF-β-driven mechanisms.(Quante et al., 2011) MSC-derived CAFs also express pro-tumour IL-6 and CXCL12, which helps further recruit MSCs through CXCR4-dependent mechanisms.(Quante et al., 2011) In the context of PDAC, isolated cancer-associated MSCs (CA-MSC) were found to enhance PDAC cell invasive potential and proliferation in co-culture, and through CA-MSC conditioned media, wich suggests a secretory mechanism that drives PDAC proliferation.(Waghray et al., 2016) Compared to other CAF populations, CA-MSCs isolated from human PDAC were found to exclusively produce *granulocyte-macrophage colony stimulating factor* (GM-CSF), with cognate receptor expression also observed on CK-19+ PDAC cells in human PDAC.(Waghray et al., 2016) GM-CSF knockout through shRNA in CA-MSCs abrogated the proliferation and invasion of PDAC cells, and the addition of exogenous GM-CSF restored PDAC proliferation.(Waghray et al., 2016) Thus, a component of the PDAC CAF population is capable of directly promoting PDAC cell proliferation and invasion through crosstalk mediated by CAF-derived GM-CSF.

Despite the evidence that CA-MSCs are capable of driving PDAC cell proliferation and invasive potential, the CAF subset that is regarded as providing the majority of the stromal reaction are PSC-derived.(Öhlund et al., 2014) During homeostasis, PSCs are considered to be quiescent cells, distinguishable through their stellate morphology, and are found throughout the exocrine pancreas in periductal and periacinar regions.(Awaji and Singh, 2019) Normal physiological function of PSCs is to maintain ECM homeostasis, and they become activated as part of the wound-healing response.(Ferdek and Jakubowska, 2017) PSCs can be activated by *platelet-derived growth factor* (PDGF) and TGF-β which leads to PSCs acquiring a myofibroblast phenotype, characterised through the expression of α-SMA.(Öhlund et al., 2014) α-SMA$^+$ CAFs produce matrix metalloproteinases (MMPs) which are ECM-degrading products, along with fibronectin and collagen (type I, III and IV) to remodel the ECM — this forms the basis of the desmoplastic reaction.(Öhlund et al., 2014) During acute inflammation, the activation of apoptotic mechanisms within fibroblasts normally ensures this ECM remodelling is transient.(Öhlund et al., 2014) However, during the chronic inflammation associated with neoplastic transformation, fibroblast activation is maintained and leads to extensive fibrotic deposition.(Awaji and Singh, 2019) Thus, CAF populations within PDAC are highly heterogenous and have diverse functions which range from direct crosstalk, and the promotion of proliferation and cell invasion, or promoting the desmoplastic reaction through matrix remodelling and fibrotic deposition.

The activation and reprogramming of PSCs to CAFs is driven by a multitude of soluble factors, notable examples include TGF-β, PDGF, IL-1 and IL-6 — all factors that are present within the early TME following neoplastic cell transformation.(Öhlund et al., 2014) The ability to respond to a diverse range of activating signals further indicates CAF plasticity, with the term "CAF" used as an umbrella term that belies the true population heterogeneity, which has been poorly studied and defined until recently. Within PDAC, there exists a variety of biomarkers that can identify CAFs; this includes α-SMA, fibroblast activation protein (FAP), podoplanin (PDPN) and PDGFRα/β — however, biomarker expression alone cannot identify PDAC CAF subpopulations.(Pereira et al., 2019) Instead, CAFs are defined through a variety of factors such as biomarker expression and spatial location within the PDAC TME (Figure 1-3). The

heterogeneity of PDAC CAFs was demonstrated through immunofluorescence staining of human PDAC CAFs, which revealed differential expression of α-SMA — α-SMA^{high} FAP$^+$ CAFs were found in close proximity to PDAC cells and were classed as *myofibroblastic CAFS* (myCAFs).(Öhlund et al., 2017) Co-culture of murine PSCs with KPC organoids confirmed that PSC-derived CAFs expressing high levels of α-SMA were found in close proximity to PDAC organoids.(Öhlund et al., 2017) Secretome analysis of the conditioned media from the co-culture revealed elevated expression of inflammatory cytokines, notably IL-6.(Öhlund et al., 2017) Trans-well cultures confirmed that PSCs were the source of IL-6, and produced other cytokines such as IL-11 and leukaemia inhibitory factor (LIF) in a paracrine signalling axis between KPC cells.(Öhlund et al., 2017) However, despite culturing of PSCs with organoid conditioned media establishing CAF phenotype (FAP$^+$ and PDGFR$^+$), the upregulation of IL-6, IL-11 and LIF RNA levels occurred with a reduction in α-SMA RNA and protein levels — indicating a loss of myofibroblastic CAF phenotype.(Öhlund et al., 2017) Based on this, two mutually exclusive CAF populations were defined; firstly, α-SMA^{high} IL-6^{low} myCAFs found proximally to PDAC cells; and secondly, more distally located α-SMA^{low} IL-6^{high} CAFs that do not require direct cell-cell contact to mediate cytokine production — these were termed inflammatory CAFs (iCAFs) due to their ability to produce inflammatory cytokines.(Öhlund et al., 2017) Additionally, CAFs that express high MHC II in response to local IFN-γ can activate CD4$^+$ T cell by TCR ligation and are termed antigen-presenting CAFs (apCAFs). These apCAFs can also convert to myCAFs under certain conditions, but for simplicity I will herein focus on myCAFs and iCAFs.(Elyada et al., 2019) Single cell RNA-sequencing confirms that myCAFs and iCAFs are two distinct populations, and are characterised by upregulated TGF-β and JAK/STAT signalling pathways, respectively.(Biffi et al., 2019) Regarding iCAFs, IL-1α has been shown to drive the production of inflammatory factors such as IL-6 from CAFs, and IL-1α receptor (IL1R1) expression on CAFs confirms an ability to respond to NF-κB activating ligands such as IL-1α.(Tjomsland et al., 2011, Biffi et al., 2019) In both human and murine PSC culture, IL-1α leads to the upregulation of various inflammatory cytokines such as IL-1α, IL-6, LIF, CXCL1 and G-CSF at the expense of α-SMA expression and TGF-β signalling.(Biffi et al., 2019) Despite IL-1α driving inflammatory cytokine production, the action of LIF was found to be

indispensable for the activation of JAK/STAT signalling, and maintains the iCAF lineage in an autocrine manner – an illustration summarising iCAF and myCAF differentiation can be found below (Figure 1-3).(Biffi et al., 2019) Conversely, myCAFs are established through TGF-β signalling, which was found to impair iCAFs through the inhibition of JAK/STAT signalling through IL-1R downregulation.(Biffi et al., 2019) Thus, since both IL-1α and TGF-β drive iCAF and myCAF differentiation through antagonising signalling mechanisms, respectively, CAF lineage commitment is believed to be determined through the physical location within the TME. In summary, myCAFs are located proximally to PDAC cells, as PDAC-derived TGF-β establishes myCAF identity through antagonising IL-1α signalling; conversely, the more distally located CAFs respond to IL-1α signalling in the absence of TGF-β-mediated inhibition, and become iCAFs that produce a variety of inflammatory cytokines.(Biffi et al., 2019)
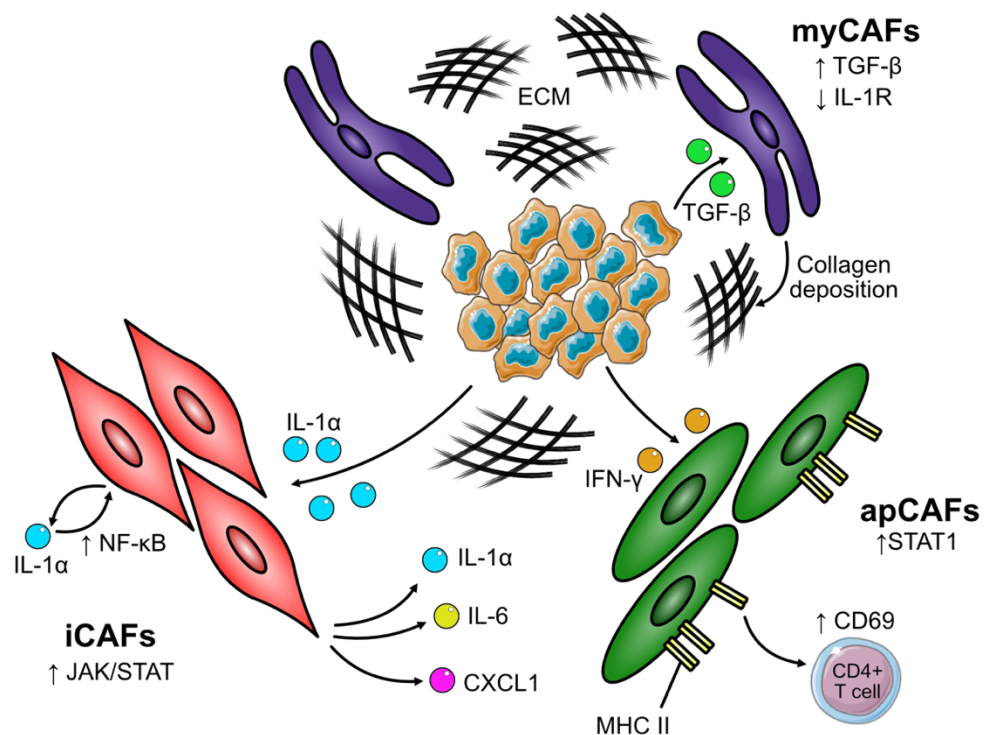
Figure 1-3 CAF populations within the PDAC TME are heterogeneous.
Tumour-secreted TGF-β acts on proximally located PSCs within the TME, leading to TGF-β signalling and repression of IL-1α signalling. TGF-β signalling directs myCAF differentiation, identifiable through expression of α-SMA and the production of collagen which contributes to the PDAC stromal reaction. Tumour-secreted IL-1α acts on more distal PSCs and mediates NF-κB signalling following IL-1R signalling. NF-κB signalling leads to production of LIF, which maintains iCAFs through an autocrine signalling loop that upregulates IL-1R expression. NF-κB also drives Jak/STAT signalling which establishes an inflammatory phenotype through the production of pro-tumour mediators including IL-1α, IL-6, G-CSF and CXCL1. Finally, IFN-γ upregulates MHC II expression on PSCs to promote apCAF development, which increases CD69 expression on CD4^{+} T cells. *Adapted from Biffi et al, 2018 & Elyada et al, 2019.*

By understanding CAF heterogeneity, signalling and effector mechanisms, it is hoped that this will translate into potential for therapeutic exploitation. Current standard of care regimens such as gemcitabine are largely ineffective in PDAC, as the dense stromal compartment presents a barrier to agent delivery.(Dalin et al., 2019) Logically, it has previously been believed that depletion of the stromal compartment, particularly the collagen-producing α-SMA$^+$ myofibroblasts (myCAFs), would enable improved delivery of chemotherapeutic agents and improve survival.(Özdemir et al., 2014) However, myofibroblast depletion in both early and late stage PDAC led to reduced survival, as undifferentiated tumours resulted in increased tumour invasion.(Özdemir et al., 2014) Further to this, loss of sonic hedgehog (Shh) in PDAC led to increased tumour aggressiveness and reduced survival, as Shh signalling promotes the desmoplastic reaction.(Rhim et al., 2014) However, it is hoped that a greater understanding of CAF heterogeneity and the underlying mechanisms will enable the development of more sophisticated therapeutic regimens. For example, in iCAF development IL-1α activates JAK/STAT signalling within PSCs which leads to LIF production which maintains iCAFs through autocrine signalling.(Biffi et al., 2019) However, LIF is a pleiotropic cytokine and binds to its cognate receptor on PDAC cells, leading to the activation of pro-tumour STAT3 signalling, which regulates proliferative and anti-apoptotic mechanisms.(Lesina et al., 2011) Genetic depletion of LIFR in KPC mice *(Lifr$^{flox/flox}$)* was found to significantly increase survival, delay PanIN progression and reduce pro-tumour GM-CSF and CCL11.(Shi et al., 2019) Further to this, iCAF-derived IL-6 is also known to be pro-tumourigenic through the direct induction of STAT3.(Lesina et al., 2011) Pharmacological inhibition of IL-6 through impaired mTOR signalling prevented CAF production of IL-6, compromising tumour growth and reduced PDAC chemoresistance.(Duluc et al., 2015) Finally, apCAFs are also found in the PDAC TME which respond to IFN-γ, this upregulates STAT1 and MHC molecules, leading to increased CD69 expression on CD4$^+$ T cells.(Elyada et al., 2019) Thus, a greater understanding of CAF heterogeneity will lead to tailored therapies that are more specific than complete CAF ablation, leading to improved therapies with fewer adverse effects.

1.2.2 Immune cells play a fundamental role in PDAC.

The interplay between the immune system and cancer is a fundamental aspect of malignant disease, with the subversion of anti-tumour immune mechanisms central in driving tumour outgrowth. This is known as cancer immunoediting, which is defined by three stages; elimination, equilibrium and escape.(Dunn et al., 2004, Mittal et al., 2014) "Elimination" occurs when malignant transformation and inflammation recruit innate and adaptive immune cells to drive early anti-tumour responses.(Dunn et al., 2004, Mittal et al., 2014) Immune-mediated elimination is initially effective at restraining tumour growth, however, strong immune selection pressure drives the evolution of tumour cells that resist immune clearance — this state is defined as "Equilibrium".(Dunn et al., 2004, Mittal et al., 2014) During equilibrium, development of an immune-suppressive TME actively subverts anti-tumour responses through various mechanisms, and leads to the final "Escape" phase, which is characterised by tumour outgrowth and immune-suppression.(Dunn et al., 2004, Mittal et al., 2014) In PDAC, TME development is characterised by a strong desmoplastic reaction, which restricts immune cell infiltration, drives chemoresistance and impairs anti-tumour immune responses.(Wachsmann et al., 2012) Thus, the impairment of anti-tumour immune responses is key in driving the growth, invasiveness and metastatic potential of PDAC cells.(Liu et al., 2019) One major characteristic of the PDAC TME is the immunosuppressive immune infiltrate, particularly myeloid cells, which play a central role in driving tumourigenesis.(Noy and Pollard, 2014) However, the general immune suppressive functions of myeloid cells are often attributed to myeloid-derived suppressor cells (MDSC), which have been shown to correlate with cancer stage and metastatic burden.(Diaz-Montero et al., 2009, Stromnes et al., 2014) Data from KPC mice further indicates that MDSCs are major component of the PDAC TME, drive immune suppression and are associated with metastasis.(Bayne et al., 2012) However, the term MDSC encompasses a heterogenous population of myeloid cells that includes monocytes and neutrophils, which both have distinct pro-tumour functions within the PDAC TME, and their identification and biochemical function remain controversial.(Steele et al., 2016, Candido et al., 2018, Zhu et al., 2017) Consequently, the functions of specific myeloid populations such as neutrophils and macrophages in PDAC will be discussed further.

1.2.3 Macrophages in PDAC.

Macrophages are a major component of the PDAC TME and function as phagocytic cells of the innate immune system, and are important cytokine producing cells.(Arango Duque and Descoteaux, 2014) Macrophages are also highly plastic cells and have diverse effector functions that are polarised by the local cytokine milieu, promoting either pro-inflammatory or immune-regulatory functions.(Arango Duque and Descoteaux, 2014) In PDAC tumourigenesis, macrophage polarisation is subverted within the TME and establishes a TAM phenotype that is potently immunosuppressive.(Habtezion et al., 2016) The polarisation of TAMs is crucial for PDAC progression, as they are not only immune-suppressive, but drive early tumourigenesis, PDAC invasiveness, chemotherapy resistance and metastasis.(Lin et al., 2019, Liou et al., 2013, Liou et al., 2017, Céspedes et al., 2016, Nielsen et al., 2016, Ireland et al., 2016)

1.2.4 TAM Polarisation in PDAC.

As mentioned above, the plastic function of macrophages is shaped by the local cytokine milieu, which promotes the development of inflammatory or regulatory macrophage phenotypes.(Cui et al., 2016) Briefly, inflammatory macrophages derive from circulating monocytes and respond to IFN-γ and inflammatory signals such as LPS.(Yang et al., 2020, Arango Duque and Descoteaux, 2014) Following activation, they produce IL-1β, IFN-γ, TNF-α, and other cytokines such as IL-6 and IL-23; they are also identifiable through surface expression of CD86, CD11b and CXCR3, and they clear infections through phagocytosis and the promotion of Th1 immune responses.(Yang et al., 2020, Arango Duque and Descoteaux, 2014) Conversely, pro-tumour TAMs respond to IL-4, IL-10, IL-13 and TGF-β, with macrophage colony stimulating factor (M-CSF) also implicated; TAMs are CD163^{+} and CD206^{+} and produce TGF-β, IL-10, matrix metalloproteinases (MMP) and chemoattractant molecules such as CCL2, CCL5 and VEGF (Figure 1-4).(Yang et al., 2020, Arango Duque and Descoteaux, 2014) This phenotypic switch is fundamental in PDAC tumourigenesis, and was primarily thought to be driven by the recruitment and polarisation of monocyte-derived macrophages.

During normal physiological responses to pancreatic injury, inflammatory macrophages accumulate and exert pro-inflammatory function through

production of IL-1β, TNF-α and IL-6, facilitated through NF-κB signalling.(Liou et al., 2013) However, inflammatory responses are normally transient and self-limiting, but the presence of chronic pancreatitis and oncogenic Kras signalling maintains continuous NF-κB expression in a positive feedback loop, contributing to unresolving inflammation.(Daniluk et al., 2012) As previously described, chronic pancreatitis is a major PDAC risk factor as it is dominated by immune-regulatory phenotypes, particularly CD206^{+} macrophages expressing IL-10 and TGF-β.(Xue et al., 2015) During chronic pancreatitis, which can be considered the early TME, this re-polarisation of macrophages is directed by pancreatic stellate cells (PSC), which are proximally located to macrophages.(Xue et al., 2015) PSC conditioned medium contains high levels of IL-4/13, and upregulates the expression of CD206 on bone marrow-derived macrophages (BMDM) along with the capacity to produce IL-10 and TGF-β.(Xue et al., 2015) TAM polarisation is further cemented through a positive feedback loop, as CD206^{+} TAMs upregulate IL-4Rα to become more responsive to IL-4/13, and the production of TGF-β along with platelet-derived growth factor (PDGF) increases the production of IL-4/13 from PSCs.(Xue et al., 2015) Additionally, IL-13 production from tuft cells in early PanIN lesions further contributes to the polarisation of TAMs, and cements the immunosuppressive nature of the early TME.

The maintenance of these TAM populations was hypothesised to be through CCL2-mediated recruitment of monocyte-derived macrophages from bone marrow to the PDAC TME, as patients with high CCL2 have increased macrophage infiltration and reduced survival.(Sanford et al., 2013) Under homeostatic conditions, stromal cells express CXCL12 within the bone marrow, which binds to CXCR4 on monocytes acting as a retention signal.(Wang et al., 2009) Under inflammatory conditions, CCL2 upregulation activates CCR2 on bone marrow monocytes, and desensitises the CXCR4 retention signal, enabling the mobilisation of inflammatory monocytes.(Wang et al., 2009, Jung et al., 2015) CCL2 expression is attributable to a number of cancer-associated cells, including fibroblasts, cancer cells and myeloid cells.(Gschwandtner et al., 2019) Indeed, blockade of CCR2 signalling, although combined with CXCR2 blockade, has been shown to improve therapeutic responses in PDAC, suggesting monocyte mobilisation may be an important attribute of PDAC tumourigenesis.(Nywening et al., 2018)

Upon entry to the PDAC TME, monocytes must undergo differentiation to macrophages, which is thought to be driven by tumour-derived M-CSF, an important macrophage survival signal.(Hunter et al., 2009) M-CSF has also been demonstrated to upregulate macrophage characteristics associated with TAMs, such as expression of CD206 and IL-10 production; and also increases expression of tumour-associated genes such as CCL2 and TGF-β.(Svensson et al., 2011) The importance of TAM-associated M-CSF signalling has been demonstrated in a number of preclinical GEMMs, that show M-CSF/M-CSFR signalling is crucial for pro-tumour TAM activity in PDAC.(Zhu et al., 2014, Candido et al., 2018) Blockade of M-CSFR signalling using tyrosine kinase inhibitor (PLX3397) not only reduces F4/80+ macrophage infiltration in orthotopic PDAC models, but also leads to increased inflammatory gene expression (*Ifng* and *Stat1*), and increased expression genes associated with T cell recruitment (*Cxcl10, Ccl3 and Ccl4*) and cytotoxic lymphocyte (*Infg, CD8a and Prf1*) gene signatures.(Zhu et al., 2014) Additionally, the interruption of M-CSFR signalling led to increased death of CD206+ TAMS, reduced expression of immune-suppressive genes (*Il10, Tgfb1, Arg1*) and increased anti-tumour gene signatures — indicating that the M-CSF functions as a crucial regulator of pro-tumour TAM activity in PDAC.(Zhu et al., 2014) Autochthonous KPC models more accurately recapitulate PDAC, and M-CSFR blockade (AZD7507) in KPC mice further confirms reduced macrophage infiltration (*Csf1r, Arg1 and Mrc1*), enriched CTL gene signatures (*Cd69, Cd8 and Gzma*) and impaired collagen deposition and fibroblast activation.(Candido et al., 2018) Additionally, M-CSFR blockade reduced pro-tumour IL-6 and IL-10 production, impaired PD-L1+ TAMs in the PDAC TME and led to reductions in tumour mass — confirming the central role of M-CSF in driving TAM activity.(Candido et al., 2018) Finally, M-CSF also influences PDAC subtype development, as M-CSFR blockade switches from poor prognosis squamous subtype to more favourable immunogenic and ADEX subtypes.(Candido et al., 2018) Therefore, M-CSF not only plays a fundamental role in driving pro-tumour TAM activity in the PDAC TME, and but also contributes to the squamous subtype of human PDAC.(Candido et al., 2018, Bailey et al., 2016) Thus, the literature details that PDAC TAMs can be derived from bone marrow progenitors, and driven through inflammatory CCL2-mediated recruitment and that tumour-derived M-CSF induces differentiation to protumour TAM phenotype.

1.2.5 Tissue-resident macrophages can promote PDAC tumourigenesis.

There is evidence that suggesting that not only are monocyte-derived macrophages important for PDAC tumourigenesis, but that embryonic-derived macrophages are also important pro-tumour cells. Macrophages are heterogenous and can derive either from Flt3+ hematopoietic stem cell (HSC) progenitors during adult haematopoiesis, or from embryonic-derived macrophages where they persist as a self-renewing population.(Wynn et al., 2013) Orthotopic transplantation of KPC cells into CCR2-deficient (CCR2$^{-/-}$) mice reduces PDAC TAM populations by 50% but did not impact tumour growth — indicating that whilst monocyte-derived macrophages contribute to the TAM population, they might be dispensable in PDAC development.(Zhu et al., 2017) Using the *FLt3-Cre*$^+$; *LSL-YFP* (Flt3-Cre^{YFP}) reporter mouse, lineage tracing revealed that YFP$^+$ TAMs are defined as monocyte-derived and develop from HSC progenitors through FLt3 upregulation and express high levels of MHC II; conversely, embryonic-derived TAMS (YFP$^-$) develop independently of Flt3$^+$ HSC progenitors, and are distinct through lower expression of MHC II.(Zhu et al., 2017) Treatment with anti-M-CSFR on E13 depleted embryonic-derived macrophages, significantly reduced TAM populations and delayed PDAC progression, illustrating MHC II^{lo} embryonic-derived TAMs drive PDAC progression when monocyte-derived TAMs are reduced.(Zhu et al., 2017) The delineation between the two macrophage populations has been previously demonstrated in the literature; with yolk-sac (embryonic) macrophages identified as F4/80^{bright}, *Flt3*$^-$, *Cx3cr1*$^+$ and controlled by the transcription factor *Maf*; and HSC-derived macrophages identifiable through expression of *Gata2* and *Ccr2* which control monocyte differentiation and recruitment, respectively.(Schulz et al., 2012) However, CCR2$^{-/-}$ mice still retain some Ly6C$^+$ monocytes in the circulation, and as CCR2 is required for 80-90% of macrophage infiltration from the periphery, some monocyte-derived macrophage populations remain.(Hsieh et al., 2014) Furthermore, the depletion of inflammatory monocytes by CCR2 inhibition (PF-04136309) in orthotopic PDAC models demonstrates enhanced anti-tumour immunity and reduced metastatic dissemination; and high levels of CCR2/CCL2 have poor prognosis in human patients following resection. (Sanford et al., 2013) Additionally, the role of bone marrow-derived macrophages is multi-faceted, as recent evidence has detailed they can promote PDAC cancer progression by

converting to cancer-associated fibroblast-like cells in response to conditioned media, which then leads to increased invasive potential of pancreatic cancer cells.(Iwamoto et al., 2021) Thus, PDAC TAM populations exhibit diverse ontogeny, and there is a greater appreciation of the pro-tumour function of TAMs derived from embryonic macrophage populations which can promote tumourigenesis through pro-fibrotic effector functions. However, the pro-tumour role of monocyte-derived macrophages also indicates a fundamental role in PDAC tumour progression, suggesting both TAM populations have non-redundant function in PDAC progression.

1.2.6 TAMs have potent immune-suppressive function.

TAMs develop in response to the immune-suppressive cytokine milieu and exert diverse effector functions that promote PDAC growth; this includes the production of immune-regulating cytokines such as IL-10 and TGF-β; driving angiogenesis and chemoresistance; and enhancing PDAC cell invasion and metastatic potential.(Smith et al., 2018, Mittal et al., 2015, McBride et al., 2002, Linton et al., 2018, Xian et al., 2017, Nielsen et al., 2016)

IL-10 is a pleiotropic cytokine produced by TAMs, and drives immune suppression through inhibition of costimulation, Treg recruitment and the impairment of APCs and CTLS and significantly correlates with poor survival in human PDAC.(Saraiva and O'Garra, 2010, Smith et al., 2018, Mittal et al., 2015, McBride et al., 2002, Candido et al., 2018, Poh and Ernst, 2021, Feng et al., 2018) In the absence of IL-10 signalling, CD80/86 costimulatory molecules bind to CD28 on T cells to augment TCR signalling.(Akdis et al., 2000) IL-10R signalling activates the tyrosine phosphatase SHP-1, which dephosphorylates CD28 and impairs costimulation to induce anergy, where T cells become functionally inert.(Taylor et al., 2007, Joss et al., 2000) Additionally, IL-10 can also directly impede CTL responses by impairing TCR/CD8 molecule co-localisation.(Smith et al., 2018) IL-10R signalling activates STAT3, an immunoregulatory transcription factor, which activates Mgat5.(Smith et al., 2018) Mgat5 then restricts TCR clustering by binding Galectin (Gal3), impeding TCR/CD8 co-localisation and reducing the antigen sensitivity of CTLs.(Smith et al., 2018) IL-10R signalling has also been shown to impair IL-12 production in DCs, which negatively impacts on CTL responses in preclinical breast cancer models and also impairs the ability of APCs

to present antigen.(Ruffell et al., 2014, Mittal et al., 2015) DCs normally respond to type 1 IFN and upregulate MHC II and CD80/86 molecules to become fully licensed, which reduces the activation threshold of T cells.(Mittal et al., 2015) IL-10R signalling in macrophages upregulates March-1, an E3 ubiquitin ligase, which increases lysosomal degradation of MHC II and CD80/86 and impairs macrophage antigen-presenting capacity.(Mittal et al., 2015) In DCs, IL-10 also impairs antigen presentation through March-1 independent pathways, as STAT3 phosphorylation activates Socs3, a transcription factor that prevents NF-kB translocation in DCs, impairing Th1 differentiation and promoting autocrine IL-10 secretion by DCs.(Schülke, 2018) Finally, IL-10 in the presence of TGF-β promotes FOXP3+ Treg differentiation through STAT3-dependent mechanisms.(Hsu et al., 2015) Thus, macrophage-derived IL-10 in PDAC TME is a potent immune-suppressive cytokine that inhibits APC presentation of cognate antigen, establishes T cell anergy through impaired costimulation, and directly impairs anti-tumour CTLs.

In addition to IL-10, TAM-derived TGF-β can induce epithelial-mesenchymal transition (EMT), promote ECM remodelling, cancer stemness and contributes to chemotherapy resistance in PDAC.(Yamazaki et al., 2014, Zhang et al., 2019, Xian et al., 2017) TAMs are major sources of TGF-β in the PDAC TME, and expression of TGF-β negatively correlates with survival in late stage PDAC.(Poh and Ernst, 2021, Principe et al., 2016) Firstly, TGF-β enhances the invasive potential of PDAC cells through EMT; a process characterised through loss of cell-cell interactions, epithelial junction proteins and basal polarity.(Wang et al., 2017) Continuous TGF-β signalling also leads to Smad accumulation, which stimulates the release of ECM products such as collagen, and activates fibrosis-associated genes within CAFs.(Ahmed et al., 2017) In addition, Smad-independent TGF-β signalling activates PI3-K and mTOR signalling which drives cytoskeleton reorganisation to induce EMT.(Zhang et al., 2013) TGF-β signalling is also associated with increased tumour size, metastasis incidence and poor survival.(Yamazaki et al., 2014, Katsuno et al., 2013, Yeh et al., 2018) TGF-β also induces cancer cell stemness, specifically through CD51^{+} TAMs, and activates stemness-related transcripts within PDAC cancer cells.(Zhang et al., 2019) Another function of TAM-derived TGF-β is the promotion of chemoresistance, as treatment of TAMs with simvastatin impairs TGF-β1

signalling and sensitises PDAC cells to gemcitabine.(Zhang et al., 2020a, Xian et al., 2017) Additionally, PDAC-derived exosomes can also drive the production of VEGF, IL-1β, IL-6, TNF-α and MMP9 from TAMs.(Linton et al., 2018) VEGF in particular is proangiogenic and contributes to chemoresistance through increasing TME interstitial fluid pressure.(Gremonprez et al., 2015) PDAC exosomes have also been implicated in the priming pre-metastatic niche (PMN) through metastasis-associated macrophages (MAM).(Costa-Silva et al., 2015, Nielsen et al., 2016) More specifically, PDAC exosome-educated Kupffer cells (KC) release TGF-β, which activates hepatic stellate cells (HSTC) and promotes fibronectin production, this enables metastasis-associated macrophage (MAM) accumulation and priming of the PMN.(Costa-Silva et al., 2015) MAMs in the PDAC PMN have greater expression of ECM proteases, particularly granulin, which leads to production of fibronectin and periostin by HSTCs, which drives pro-metastatic fibrosis.(Nielsen et al., 2016)
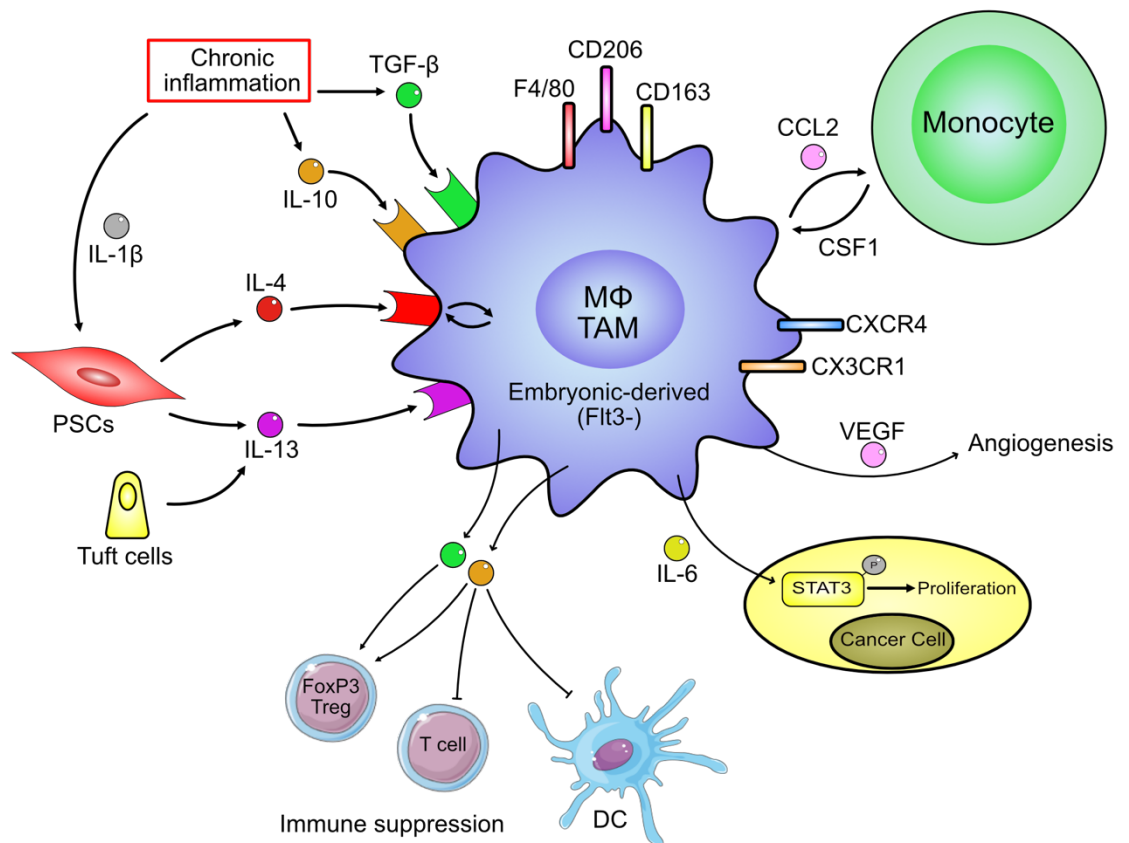
Figure 1-4 Pro-tumour TAMs have diverse function in PDAC.
TAM polarisation occurs during chronic pancreatitis, which causes an accumulation of polarising cytokines IL-4, IL-13, IL-10 and TGF-β. High IL-1β activates PSCs to produce IL-4 and IL-13, and IL-13 is also produced by tuft cells in precursor PanIN lesions in early tumourigenesis. IL-10 and TGF-β increase in response to chronic inflammation and drive TAM polarisation and immune suppression. Pro-tumour TAM populations arise from embryonic-derived (tissue-resident) macrophages that are Flt3-independent and are F4/80^{hi}, CD206^{+}, CD163^{+}, CXCR4^{+} and CX3CR1^{+}. TAM populations are partly replenished through CCL2-mediated recruitment and differentiation of monocytes through M-CSF (CSF1). TAM-derived IL-6 directly promotes PDAC cell proliferation through phosphorylation of STAT3, and they also produce VEGF to promote angiogenesis. IL-10 impairs DC antigen presentation and expression of CD28 costimulatory molecules to directly impair anti-tumour immunity, and synergises with TGF-β to promote development of FoxP3^{+} Tregs, which in turn produce TGF-β and IL-10 to suppress immune activity.

1.2.7 Neutrophils in PDAC

Despite macrophages being defined as the most dominant leukocyte population within the PDAC TME, neutrophils also play a crucial role. Under homeostatic conditions, excessive neutrophil mobilisation is controlled through retention signals such as CXCL12/CXCR4 signalling and integrin expression (VCAM-1) within bone marrow.(Eash et al., 2010, Coffelt et al., 2016) Whilst neutrophils are able to egress under homeostatic conditions, the chronic inflammation associated with tumourigenesis overrides neutrophil retention signals and results in neutrophilia; for example, granulocyte colony stimulating factor (G-CSF) actively

represses CXCL12 in bone marrow and CXCR4 expression on neutrophils, respectively.(Eash et al., 2010, Kim et al., 2006) Additionally, the CXCR4 retention signal is also abrogated through peripheral expression of chemokine ligands CXCL1-3 and CXCL5-8, which bind to cognate receptors CXCR1 and CXCR2 on neutrophils to promote egress.(Eash et al., 2010, Coffelt et al., 2016) These mechanisms are often subverted during oncogenesis and enable excessive neutrophil production, mobilisation and pro-tumourigenic polarisation. One of the most significant pro-tumour roles for neutrophils in tumourigenesis is in the metastatic cascade, with pro-metastatic function detailed in several cancer settings.(Coffelt et al., 2015, Steele et al., 2016, Cools-Lartigue et al., 2013) In the KEP ($K14^{Cre};Cdh1^{F/F};Trp53^{F/F}$) mouse model of spontaneous breast cancer, TAM-derived IL-1β stimulates the production of IL-17 from γδ T cells, which leads to downstream production of G-CSF and the mobilisation of immature iNOS$^+$ neutrophils, which results in suppression of CD8$^+$ T cells and enables metastatic colonisation. (Coffelt et al., 2015) Expansion of neutrophils within the TME is often associated with undifferentiated tumours and poor prognosis in PDAC.(Reid et al., 2011) In particular, the over-expression of neutrophil chemoattractant CXCL5 correlates with poor survival, indicating that CXCR2-mediated neutrophil recruitment is a tumour-promoting mechanism in PDAC.(Li et al., 2011a)

1.2.8 CXCR2 drives tumour-promoting neutrophils in PDAC.

Cumulative evidence within the literature implicates the CXCR2 axis as a driving force for tumourigenesis through several mechanisms, most notably the recruitment of pro-metastatic neutrophils that restrain effective infiltration of effector T cells into the TME. (Steele et al., 2016, Chao et al., 2016) In human PDAC, CXCR2 expression along with its ligands CXCL2/8 are upregulated compared to normal pancreas, with increased CXCL2/CXCR2 expression by MPO$^+$ cells (neutrophils) correlating with poorer prognosis. (Steele et al., 2016) Thus, high CXCR2 expression is associated with poor prognosis, and therapeutic blockade has demonstrated augmentation of anti-tumour immunity. Additionally, PDAC cells are also capable of producing CXCL1/2 to mediate the crosstalk between PDAC cells and neutrophils within the TME, a crucial facet of PDAC tumourigenesis.(Steele et al., 2016, Nywening et al., 2018, Stromnes et al., 2014) Thus, Steele et al. looked to determine the role of CXCR2 signalling in

spontaneous PDAC through CXCR2-deficient KPC mice (*KPC;Cxcr2$^{-/-}$*).(Steele et al., 2016) Interestingly, *KPC;Cxcr2$^{-/-}$* mice display no survival benefit; however, loss of infiltrating neutrophils confers an almost complete reduction in spontaneous metastases, reduced fibrotic reaction and increased CD3$^+$ T cell infiltration — indicating a central role for CXCR2 in promoting metastasis and contributing to the immunosuppressive desmoplastic stroma in PDAC.(Steele et al., 2016) Pharmacological inhibition through CXCR2 inhibitors(CXCR2i) pepducin and AZ13381758 were successful at abrogating spontaneous metastases, but also conferred significant survival benefit.(Steele et al., 2016) Treatment of late-stage palpable KPC tumours first with CXCR2i enabled greater T cell infiltration and was followed by anti-PD-1 therapy; this resulted in a sensitisation of late-stage KPC mice to immunotherapy and a significant extension of survival of mice treated with combined CXCR2i and PD-1 therapy.(Steele et al., 2016) Given the high rates of metastatic disease within PDAC patients, further uncovering CXCR2 function within the PDAC TME could potentially provide substantial clinical benefit.

The immunosuppressive and pro-tumour function of TANs is further shown through TCGA analysis of human PDAC samples, which demonstrate that high TAN infiltration correlates with the squamous subtype and poor prognosis.(Chao et al., 2016, Bailey et al., 2016) Significantly high levels of CXCL5 and CXCR2 transcripts specifically within PDAC cells were associated with TAN infiltration, and also correlated with oncogenic Kras expression.(Chao et al., 2016) Therefore, oncogenic Kras and CXCL5 expression within PDAC cells can promote crosstalk between PDAC cells and recruited TANs to drive tumourigenesis. (Chao et al., 2016) The subcutaneous implantation of KPC cells into *Cxcr2$^{-/-}$* mice demonstrated significant impairments to tumour growth, but had no observable differences in F4/80$^+$ TAM populations, CD31$^+$ endothelial cells or FoxP3 Tregs, but instead exhibited increased memory (CD44^{hi}CD62L$^+$) and effector (CD44^{hi}CD62L$^-$) effector T cells in the PDAC TME. This demonstrates that PDAC/neutrophil crosstalk is mediated through CXCR2 and is an important aspect of the immunosuppressive TME in PDAC.(Chao et al., 2016)

1.2.9 CXCR2 exerts additional pro-tumour functions in PDAC.

Whilst CXCR2 signalling drives primary tumour growth and metastatic dissemination in PDAC, CXCR2 signalling also directs tumour-stroma interactions which promotes angiogenesis, and enhances PDAC cell invasive and metastatic potential.(Saintigny et al., 2013, Ijichi et al., 2011, Matsuo et al., 2009a) Effective tumour-stromal crosstalk is crucial to PDAC tumourigenesis, and $Ptf1a^{Cre/+};Kras^{G12D};Tgfbr2^{flox/flox}$ mice detailed how the secretion of CXCR2 ligands maintain this synergistic relationship, as $Ptf1a^{Cre/+};Kras^{G12D}$ promotes the formation of precursor PanIN lesions and the addition of $Tgfbr2^{flox/flox}$ drives invasive PDAC.(Ijichi et al., 2011) PanIN lesions with intact TGF-β signalling have relatively low expression of CXCR2 ligands; however, PDAC cells with mutated TGF-β secrete high levels of CXCL1 and CXCL5 which bind CXCR2 expressed on stromal fibroblasts.(Ijichi et al., 2011) More specifically, PDAC-derived CXCR2 ligands upregulate the expression of connective tissue growth factor (CTGF) which strongly promotes fibrosis and is further augmented by TGF-β signalling.(Ijichi et al., 2011, Lipson et al., 2012) CXCR2 is also expressed on vascular endothelial cells, and production of CXCR2 ligands by PDAC cells promotes angiogenesis and confers increased invasive potential of vascular endothelial cells *in vitro*.(Matsuo et al., 2009b, Matsuo et al., 2009a) In $Ptf1a^{cre/+};\ LSL-Kras^{G12D};\ Tgfbr2^{flox/flox}$ (PKF) mice, it was found that PDAC cell—conditioned media (PKF CM) was capable of stimulating CXCL1, CXCL2 and CXCL3 production by CAFs, and the invasion and migration of PDAC cells was significantly enhanced through the addition of CAF-CM — suggesting feedback loops of CXCR2 ligands within the TME between PDAC and stromal cells.(Sano et al., 2019) $PKF;CXCR2^{+/-}$ mice displayed no survival benefit but had significant reductions in CD31$^+$ tumour microvessel density, further reinforcing the role the CXCR2 axis plays in promoting PDAC angiogenesis.(Sano et al., 2019) In summary, neutrophils play a fundamental role in PDAC by directly promoting tumourigenesis, contributing to the immunosuppressive TME and facilitating metastatic dissemination through the CXCR2 chemokine axis. However, CXCR2 signalling has additional protumour mechanisms independent of neutrophils and can mediate tumour-stroma crosstalk, angiogenesis and contribute to the characteristic desmoplastic reaction.

1.2.10   NK cells in PDAC.

Natural killer (NK) cells are another class of innate immune cells that have been implicated in cancer. More specifically, their potent cytotoxic mechanisms direct anti-tumour immune surveillance, and higher levels of NK cells are associated with reduced metastatic incidence in several human cancers.(López-Soto et al., 2017) NK cells make up between 5-10% of peripheral blood mononuclear cells (PBMC), and respond rapidly to virally infected and transformed cells; human NK cells are CD3$^-$CD16$^+$CD56$^+$ and sub-categorised into CD16^{bright}CD56^{dim} (cytotoxic) and CD16^{dim}CD56^{bright} (tissue-resident) subsets; murine NK cells are CD3$^-$NKp46$^+$/NK1.1$^+$ and are divided into CD49a$^-$DX5$^+$ (circulating) and CD49a$^+$DX5$^-$ (tissue-resident) subsets.(Wu et al., 2020, Jewett et al., 2020, Sojka et al., 2014) NK cell activity is tightly regulated by activating and inhibitory signals. To become activated, NK cells have natural cytotoxicity receptors (NCRs) such as NKp30/44/46, which direct NK cell-mediated lysis and the production of inflammatory cytokines.(Huntington et al., 2020, Kumar, 2018) Additionally, natural-killer group 2, member D (NKG2D) activates NK cells by binding to MICA, MICB and ULBP1-6 proteins that are upregulated during cell stress and transformation.(Huntington et al., 2020, Paul and Lal, 2017) Finally, NK cells also express DNAX accessory molecule-1 (DNAM-1), which binds to CD155 on infected and transformed cells, and is an important costimulatory molecule that directs NK-mediated lysis.(Huntington et al., 2020, Kumar, 2018, Paul and Lal, 2017) With regard to NK cell inhibition, one of the major routes to NK cell control is through classical inhibitory receptors known as killer immunoglobulin-like receptors (KIRs), which induce a strong inhibitory effect on NK cells by signalling through inhibitory ITIM motifs. An example includes the inhibitory KIRs KIR2DL1-3, which bind to MHC molecules (HLA-C) and prevent NK cell activation; however, the absence of MHC molecules enables NK cell activation through the concept of "missing self", where stressed and virally infected cells downregulate MHC I expression to avoid CD8$^+$ T cell-mediated cytotoxicity.(Miller, 2018) Another example of an MHC-associated inhibitory receptor expressed by NK cells is NKG2A/CD94, which binds to HLA-E to restrain NK cell activation. Finally, non-MHC-related inhibitory receptors include T-cell Ig and ITIM domain (TIGIT), which actively competes with DMAN-1 to bind CD155, and programmed cell death-1 (PD-1) which bind to PD-L1 to restrain NK cells. (Huntington et al., 2020, Cao et al., 2020) NK cell activation can also be mediated through cytokine

signalling — specifically IL-12R, IL-15R, IL18R and IL-21R binding to cognate ligands.(Huntington et al., 2020) Thus, NK cell independence from antigen-specific routes of activation is a crucial aspect of their anti-tumour function.

1.2.11   Anti-tumour NK cell effector mechanisms.

Once activated, the cytotoxic activity of NK cells is mediated by two distinct mechanisms — granule exocytosis of perforin and granzyme and the activation of death receptor pathways such as FasL and TRAIL.(Smyth et al., 2005) Granule exocytosis mediates apoptotic cell death, and is directed through cytotoxic granules which contain proteases and pore-forming proteins.(Prager and Watzl, 2019) These granules maintain an acidic pH which restrains the activity of granzyme and perforin, and they become activated in neutral pH when released into the immune synapse following NK cell activation — perforin forms transmembrane channels that facilitates entry of granzymes such as Granzyme B and A which drive apoptosis.(Prager and Watzl, 2019) Activation of NK cells also induces expression of FasL on the surface of NK cells, which binds to Fas receptor (CD95) on target cells and results in the cleavage of caspase 8/10 — this drives apoptosis through loss of mitochondrial outer membrane potential.(Prager and Watzl, 2019) TRAIL-mediated cell death acts in a similar manner, with TRAIL expression on activated NK cells directing similar apoptotic mechanisms.(Prager and Watzl, 2019)

1.2.12   NK cells are impaired in PDAC.

Despite the importance of NK cell cytotoxic function, there is evidence that NK cell activity is impaired in PDAC. In PDAC patients, tumour-infiltrating NK cells have reduced activating receptors NKG2D and NKp30, impaired IFN-γ production, and increased expression of anti-inflammatory IL-10 — suggesting a more regulatory NK phenotype in PDAC patients.(Marcon et al., 2020) Furthermore, NK cells make up a tiny proportion (0.3%) of the TIL population found in PDAC patients, when compared with other lymphocytes.(Lim et al., 2019) Expression of CXCR2 ligands is high in PDAC tissue but infiltrated NK cells were found to have reduced CXCR2 expression in PDAC patients, which indicates impaired NK cell recruitment.(Lim et al., 2019) Over-expression of CXCR2 in NK cells through CXCR2-expressing lentivirus rescues NK cell migrational capacity towards PDAC

cells; therefore, impaired NK cell trafficking in PDAC is attributable to reduced CXCR2 expression on NK cells.(Lim et al., 2019) In preclinical models of PDAC, NK cell cytotoxic capacity in KC mice mirrors NK cell impairment seen in obesity, a major PDAC risk factor.(Kaur et al., 2018) More specifically, pro-tumour IL-6 from pancreatic adipose tissue synergises with NK-derived IL-6 to impair IFN-γ production and cytotoxic function of NK cells. This functionally translates in to reduced tumour killing capacity, where NK cells are incapable of killing precursor PanIN lesions.(Kaur et al., 2018) Thus, despite anti-tumour function, NK cell activity is also subverted in PDAC with reduced cytotoxic capacity and cytokine production resulting in the growth of NK cell-resistant PDAC cells.

1.2.13   Dendritic cells in PDAC.

Although innate immune cell activity is a main feature of PDAC tumourigenesis, the subversion of adaptive immune responses by impairment of dendritic cells (DC) is also important. DCs can be split into three distinct categories: plasmacytoid DCs (pDC), monocyte-derived DCs (moDC) and conventional DCs (cDC).(Murphy, 2012) pDCs are located throughout the periphery and are major sources of type I interferon (IFN), and are crucial for the early detection of viral infections.(Gardner and Ruffell, 2016, Murphy, 2012) MoDCs form during inflammatory responses and are highly plastic cells that exert numerous effector functions in response to the diverse inflammatory milieu.(Gardner and Ruffell, 2016) Finally, cDCs are the major DC subset that activates T cells, as they present exogenous and endogenous antigen on MHC I and II, respectively, to drive both CD4 and CD8 T cell activation.(Gardner and Ruffell, 2016) Until recently, the role of cDCs in cancer was largely unknown, however, the "*Cancer Immunity Cycle*" outlines the role of DCs in activating anti-tumour immunity (Figure 1-5).(Chen and Mellman, 2013)

> Figure removed as it contains 3rd party copyright material, and permission for inclusion has not been granted.

Figure 1-5 The Cancer Immunity Cycle
Adaptive anti-tumour immunity is established in a stepwise manner and is characterised through the priming and activation of anti-tumour T cells. Firstly, apoptosis and necrosis of cancer cells leads to the release of cancer antigens within the tumour TME. Cancer antigens are then processed by DCs within the TME, leading to DC maturation and licensing. DC licensing is characterised through the expression of MHC molecules; the upregulation of costimulatory molecules such as CD80/86 that provide additional signals to activate T cells; the production of T cell-stimulating cytokines such as IL-2/12; and finally, the upregulation of chemokine receptors such as CCR7 that direct DC trafficking to draining lymph nodes. This cycle activates anti-tumour immune responses and drives the expansion of cytolytic T cell populations. *Taken from Chen and Mellman, 2013.*

To induce effector T cell responses, fully licensed DCs provide three distinct signals — activation, survival, and differentiation.(Murphy, 2012) Naïve CD4$^+$ T cells are initially activated through the recognition of peptide/MHC complexes via the TCR, and costimulatory molecules on the surface of DCs provide additional stimuli for full activation. More specifically, CD80/86 (B7.1/7.2) molecules on DCs bind CD28 receptors on CD4$^+$ T cells, which leads to the autocrine production of IL-2, a crucial survival signal that promotes proliferation.(Murphy, 2012) Following this, DC-derived cytokines direct the development of distinct helper T cell subsets, including T_H1, T_H2, T_H17, T follicular helper (T_{FH}) and also regulatory T cell (T_{reg}) subsets — this differentiation signal provides context to help establish appropriate immune responses.(Murphy, 2012) More specifically, DC-derived IFN-γ and IL-12 encourages T-bet$^+$ T_H1 cells; IL-4 drives GATA3$^+$ T_H2 development; TGF-β, IL-6 and IL-13 promote RORγt$^+$ T_H17 cells; and finally, TGF-β and IL-6 alone drive FOXP3$^+$ T_{reg} and Bcl6$^+$ T_{FH} subsets, respectively.(Murphy, 2012) CD8$^+$ CTLs require additional costimulation rather than a differentiation signal owing to their potent cytotoxicity — this often provided by CD4$^+$ T cells which produce IL-2 or by increased costimulatory molecule expression on DCs.(Murphy, 2012) Thus, following recognition of endogenous cross-resented antigen by MHC I/CD8 TCR

complex, the additional stimuli from CD4⁺ T cells promotes CD8 CTL activation and subsequent differentiation. In the context of cancer, this is known as the *"Cancer Immunity Cycle"*, which details how DCs direct adaptive anti-tumour immunity.(Chen and Mellman, 2013) In short, TME-resident DCs can internalise cancer antigen following cancer cell apoptosis or necrosis. During internalisation, the TME inflammatory milieu promotes the upregulation of costimulatory molecules, antigen presenting machinery and chemokine receptors, known as DC licensing.(Chen and Mellman, 2013) Mature DCs then migrate to draining lymph nodes and present cancer-associated antigens to naïve T cells, induce T cell activation and establish anti-tumour immunity.(Chen and Mellman, 2013) Several tumour escape mechanisms subvert this cycle; firstly, tumours with low immunogenicity provide insufficient antigen for DCs; secondly, dense tumour stroma acts as a physical barrier for DC migration; impaired DC maturation leads to immune tolerance; and finally, immunosuppressive cytokines within the TME directly subvert anti-tumour immune responses.(Chen and Mellman, 2013) There is growing evidence that subversion of DC function, specifically antigen-presenting cDCs, is an important aspect of PDAC tumourigenesis.

1.2.14   cDC paucity promotes immune dysfunction in PDAC.

cDCs are highly specialised cells, and promote anti-tumour immune responses by transporting tumour antigen to draining lymph nodes and cross-presenting exogenous tumour antigen to activate CD8⁺ CTLs.(Gardner and Ruffell, 2016) cDCs can be further subclassified into two groups; cDC1s cross-present exogenous antigen on MHC I to activate CD8⁺ CTLs, they require IRF8, Batf3 and ID2 transcription factors for differentiation and express XCR1, CD103 and CD24; cDC2s activate CD4⁺ helper T cells through tumour antigen expression on MHC II, they rely on IRF4 and ZEB2 transcription factors for development and express CD172a.(Schlitzer et al., 2015, Noubade et al., 2019) Previously, lymphoid-resident CD8α⁺cDC1s were defined as the cross-presenting DC population that activated anti-tumour CTLs, however, recent developments indicate that migratory CD103⁺ cDC1s are more important.(Salmon et al., 2016, Roberts et al., 2016) Roberts et al first showed that CD103⁺ DCs are essential antigen trafficking cells, and prime anti-tumour CD8⁺ T cell responses in tumour settings through CCR7-dependent trafficking mechanisms.(Roberts et al., 2016) More specifically,

CD103^{+} cDC1s were the dominant antigen trafficking population throughout tumour development in B78ChOVA models (OVA expression with MCherry reporter), and formed longer interactions with OT-I T cells when compared to lymph node-resident CD8α DCs.(Roberts et al., 2016) Additionally, following antigen internalisation, migratory CD103^{+} DCs express significant levels of surface CCR7, revealing a CCR7-dependent trafficking mechanism following antigen internalisation.(Roberts et al., 2016) Further studies have shown that CD103^{+} cDC1s have intrinsic anti-tumour effect, as anti-PD-L1 therapy in B16 transplantable models confers survival benefit, but the absence of Batf3 transcription factor ($Batf3^{-/-}$) abrogates the anti-tumour effect of anti-PD-L1.(Salmon et al., 2016) The anti-tumour role of cDC1s only extends to the activation of CD8 CTLs in the tumour draining lymph node (dLN), and does not enhance their infiltration into tumours.(Salmon et al., 2016) Only combined therapy of anti-PD-L1 with FLT3 ligation and poly I:C, which mobilise DC precursors and upregulate costimulatory molecules, respectively, improved CTL infiltration.(Salmon et al., 2016) Thus, whilst migratory cDC1s can facilitate tumour antigen trafficking to tumour dLN, DC paucity, high checkpoint molecule expression and insufficient T cell activation in the TME significantly restrains anti-tumour immune responses.

There is emerging evidence that dysfunctional DC activity contributes to the poor immune responses observed in PDAC.(Hegde et al., 2020, Meyer et al., 2018, Lin et al., 2020) Murine PDAC tissue not only has fewer cDCs compared to $Kras^{G12D};Trp53^{fl/fl};R26^{tm1}$ (KPL) model of lung adenocarcinoma, but they are also functionally impaired — CD103^{+}CD24^{+} cDC1s are 10-fold fewer in premalignant KPC mice than KPL mice, and are 79-fold fewer in late stage disease.(Hegde et al., 2020) In KPC-OG mice (OVA and GFP expression), Flt3 ligation combined with CD40 agonist treatment increased MHC and CD80/86 expression, and also enhanced CTL infiltration and resulted in reduced GFP expression, indicating immune selection pressures associated with tumour clearance.(Hegde et al., 2020) Therefore, KPC mice exhibit dysfunctional DCs that are insufficient to prime anti-tumour CD8^{+} responses. Evidence within the literature indicates that DC paucity could result from tumour-induced myelopoiesis, which promotes the expansion of immune-suppressive myeloid cells at the expense of cDC populations.(Meyer et al., 2018) In MMTV-PyMT and KPC GEMMs, pre-DC (FLT3^{+}

CD11c$^+$) and cDC1 (FLT3$^+$ CD11c$^+$ MHC II$^+$ CD24$^+$) populations in bone marrow and blood were significantly reduced compared to WT control groups, due to upregulated monocyte genes at the expense of cDC (*Irf8, Zbtb46 and Batf3*) gene programs.(Meyer et al., 2018) *Irf8* is a fundamental transcription factor that drives the commitment to cDC lineage and is also associated with patient outcome in PDAC patients — with reduced *Irf8* expression correlating with increased cDC1 impairment and poorer prognosis.(Meyer et al., 2018) G-CSF has been shown to impair *Irf8* expression through the upregulation of STAT3, which then leads to the expansion of granulocyte populations.(Netherby et al., 2017) Indeed, neutralisation of G-CSF in PyMT-B6 mice leads to restored *Irf8* expression, suggesting that G-CSF in tumour settings modulates *Irf8* to expand granulocytes at the expense of cDC populations.(Meyer et al., 2018) DC dysfunction in early PDAC tumourigenesis has also been explored, and it was found that cDCs in PDAC have partial upregulation of costimulation markers.(Lin et al., 2020) Specifically, cDCs in PDAC have upregulated CD40 and CD86 molecules but no changes were observed in CD80, MHC II and PD-L1 when compared to PanIN, indicating impaired CD8$^+$ T cell priming.(Lin et al., 2020) Interestingly, it was found that depletion of IL-6, which is elevated in pancreatic neoplasia restored cDC1 numbers and further shows that chronic inflammation in early PDAC neoplasia can promote cDC paucity and contribute to impaired CTL responses.(Lin et al., 2020)

1.3 γδ T cells in cancer.

1.3.1 Basic background of γδ T cells.

γδ T cells are innate-like lymphocytes that are found in greater numbers at mucosal and epithelial sites.(Komori et al., 2006) Although considered an unconventional T cell, γδ T cells develop from the same precursor as conventional αß T cells in the thymus.(Petrie et al., 1992) Gene rearrangement of ß, γ and δ chains in double negative (DN) thymocytes determines T cell lineage commitment, as different TCR configurations give differential signal strengths and modulates levels of lineage-committing transcription factors (Id3) and E-proteins.(Hayes et al., 2010, Fahl et al., 2018) Strong signals from γδ TCRs induces high levels of *Id3*, strongly repressing E-proteins to commit to γδ lineage; weaker signals from αß TCRs only mildly represses E-proteins due to lower *Id3* levels and facilitates αß lineage commitment.(Fahl et al., 2018, Lauritsen et al., 2009) Following commitment to the γδ lineage, γδ T cells can either acquire function in the periphery or exit the thymus with pre-defined effector function.(Parker and Ciofani, 2020)

1.3.2 Development of γδ T cells and characterisation.

In humans, γδ T cells can be classified into two distinct groups based on their δ chain usage — Vδ1 and Vδ2.(Wu et al., 2017, Vantourout and Hayday, 2013) Vδ1 T cells also are identifiable through the expression of Vγ2/3/4/5/8 chains and are found in the periphery; Vδ2 T cells predominately express the Vγ9 chain and are circulating cells that can respond to phosphoantigens — human Vγ9δ2 cells respond to tumour antigen, display antigen presenting capacity and cytotoxic function and have been studied extensively for therapeutic exploitation.(Wu et al., 2017, Lawand et al., 2017) In mice, γδ T cells develop in a series of waves during embryogenesis; firstly, Vγ5[+] DETCs appear at E13 and produce IFN-γ; Vγ6^{+} cells develop at E14 and are major sources of IL-17; finally Vγ1[+] and Vγ4^{+} cells emerge with pleiotropic cytokine function and produce IFN-γ, IL-17A, TNF and IL-4 (Figure 1-6).(Parker and Ciofani, 2020, Prinz et al., 2013, Silva-Santos et al., 2015) However, murine γδ T cells can be further categorised based on surface marker expression, transcription factor expression and effector function — which is either pro- or anti-tumourigenic in the context of cancer.(Silva-Santos et al.,

2015) Anti-tumour γδ T cells are identifiable through CD27^{+}, IL-2Rß^{+}, NK1.1^{+} and high CD45RB surface markers, the production of IFN-γ and through the expression of transcription factor T-bet; conversely, pro-tumour γδ T cells are CD27^{−}, but express CCR6, low CD45RB, produce IL-17A and express the transcription factor RORγt.(Silva-Santos et al., 2015, Parker and Ciofani, 2020) A key feature of γδ T cells is their ability to become activated either through MHC-independent routes such as cytokines within the local milieu, or in response to TCR stimulation and NKG2D ligation.(Silva-Santos et al., 2015) Elucidation of γδ T cell-activating ligands remains elusive, as the TCR antigen type remains unidentified, and TCR-antigen affinity is generally low which presents technical difficulties in ligand identification.(Deseke and Prinz, 2020) NKG2D, a stress-associated receptor that responds to the upregulation of stress molecules in infected or transformed cells, plays a key role in innate tumour surveillance and is a major recognised route of γδ T cell activation.(Huntington et al., 2020, Paul and Lal, 2017) However, more appropriate in the context of cancer is the ability of γδ T cells to respond to local cytokine milieu. It has been well documented that protumour γδ T cells respond to IL-1ß and IL-23 to upregulate IL-17A production; and anti-tumour γδ T cells upregulate IFN-γ and cytotoxic molecules following NKG2D ligation and also in response to local cytokines such as IL-2 and IL-15 independently of TCR stimulation.(Kong et al., 2009, Ribot et al., 2021)
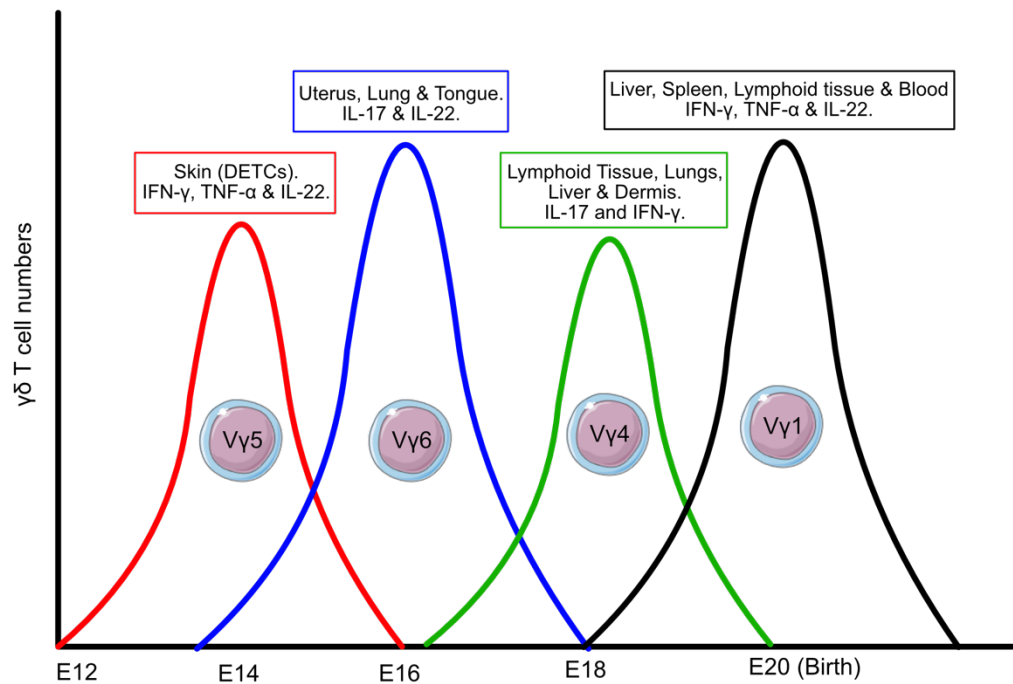
Figure 1-6 γδ T cells arise in distinct developmental waves throughout embryogenesis.
γδ T cells arise in developmental waves throughout embryogenesis, with each wave giving rise to distinct γδ T cell lineages that have different TCRs, effector function and tissue-homing properties. Firstly, Vγ5+ DETCs develop at E13 and specifically home to the skin, where they provide important barrier function through IFN-γ production. Next, Vγ6+ cells develop at roughly E16 where they colonise tissues in the uterus, lung, tongue adipose tissue and brain; they also produce IL-17A and are identifiable through CCR6 expression. Vγ4+ cells arise around E18 and exhibit polyfunctionality through production of IL-17A and IFN-γ, these cells home to lymphoid tissue, lungs, liver, and dermis. Finally, Vγ1+ cells develop peri-natally (from E20/birth) and are found in the liver, spleen, blood, and lymphoid tissue where they produce IL-17A and IFN-γ. Vγ7+ γδ T cells have not been included above, as they develop extra-thymically within the small intestine. *Adapted from Prinz et al, 2013 and Ribot et al, 2021.*

1.3.3 Anti-tumour γδ T cell function in cancer.

The anti-tumour function of γδ T cells was first described by Hayday et al., who demonstrated that loss of γδ T cells results in increased incidence of cutaneous malignancy.(Girardi et al., 2001) This was due to the cytotoxic effector function initiated by NKG2D ligation on γδ T cells by NKG2D ligand Rae-1, which is a stress related MHC-I molecule upregulated during tumourigenesis.(Girardi et al., 2001, Jung et al., 2012) This seminal study demonstrated that not only can γδ T cells exert protumour function, but that distinct tissue compartments may influence γδ T cell function due to the differential expression of NKG2D in different tissues.(Girardi et al., 2001) Further anti-tumour γδ function is observed in the transgenic adenocarcinoma of the mouse prostate (TRAMP) model, which mimics human prostate cancer through expression of SV40 Tag oncogene expression in the prostate epithelium.(Liu et al., 2008, Gelman, 2016)

TRAMP mice crossed with γδ T cell-deficient mice (TRAMP;TCRδ$^{-/-}$) were found to have greater tumour burdens than TRAMP controls, indicating γδ T cells contribute to tumour immune surveillance in murine prostate cancer.(Liu et al., 2008) Furthermore, subcutaneous injection of TRAMP cells was followed by adoptive transfer of expanded γδ T cells, which are cytolytic against TRAP cells *in vitro*. Adoptively transferred γδ T cells localise to tumour tissues, and mice treated with expanded γδ T cells exhibited lower tumour burdens than control mice.(Liu et al., 2008) This not only confirms anti-tumour γδ T cell function, but also highlights the therapeutic potential of adoptively transferred expanded anti-tumour γδ T cells.(Liu et al., 2008) γδ T cells in the periphery also have a predilection for IFN-γ production following TCR stimulation, further upregulated by the Th1-polarising cytokine IL-12.(Yin et al., 2002) Additionally, TCR signalling in the presence of IL-4, a Th2-polarising cytokine, also results in T-bet upregulation, indicating that γδ TCR stimulation promotes the development of anti-tumour IFN-γ$^+$ γδ T cells.(Yin et al., 2002)

As mentioned previously, the development of γδ T cell subsets in mice give rise to distinct subtypes with diverse cytokine production, for example Vγ1$^+$ and Vγ4$^+$ subsets are both capable of producing IFN-γ and IL-17.(Silva-Santos et al., 2015) However, activated Vγ4$^+$ cells have been shown to have greater capacity for IFN-γ production than Vγ1$^+$ cells, and display cytotoxic capacity toward tumour cells *in vitro*, directed through TCR ligation.(He et al., 2010) Finally, in the murine B16 melanoma model, tumour-infiltrating Vγ4$^+$ cells express greater levels of perforin than Vγ1$^+$ cells, indicating that Vγ4$^+$ cells have protective capacity in preclinical mouse cancer models.(He et al., 2010) Human γδ T cells, specifically the cytotoxic Vγ9$^+$Vδ2$^+$ subset, direct Fas/FasL-mediated apoptosis and induce the expression of TRAIL receptors that can sensitise cancer cells to γδ T cell cytotoxicity — indicating that γδ T cells can exert tumour killing function through multiple mechanisms.(Li et al., 2011b, Tawfik et al., 2019) Finally, there is evidence that γδ T cells direct tumour killing through *antibody-mediated cell-dependent cytotoxicity* (ADCC), as using bi-specific antibodies to Vγ9 and Her2/neu (expressed on PDAC cells) enhances γδ T cell cytotoxicity towards PDAC cells.(Oberg et al., 2014) Thus, anti-tumour functions of γδ T cells are highly diverse and have been well-documented in a variety of different cancer settings (Figure 1-7)
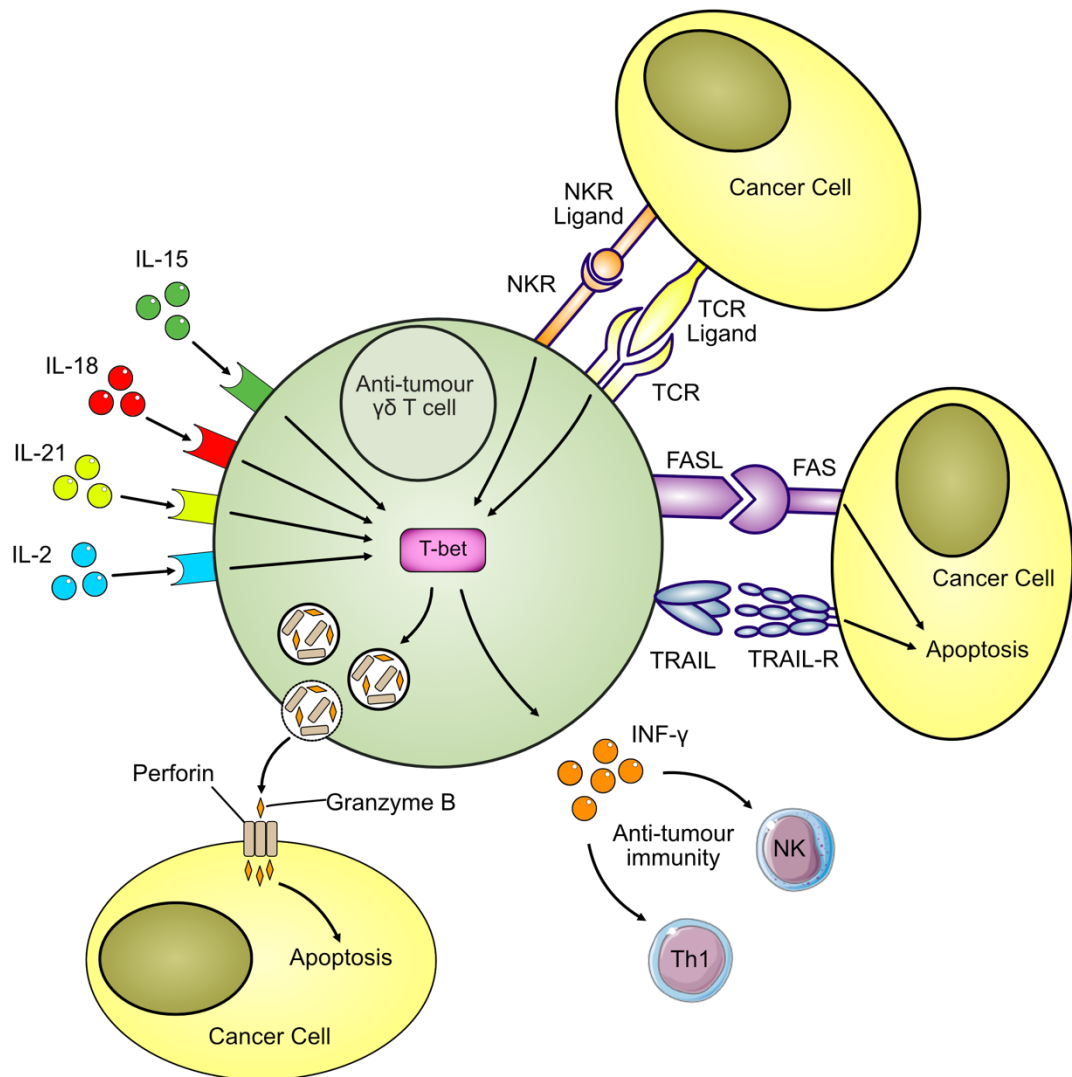
Figure 1-7 γδ T cells have diverse anti-tumour functions.
γδ T cells can exert anti-tumour functions through a variety of mechanisms. Activation through the TCR, by yet undefined ligands, mediates the upregulation of T-bet and drives INF-γ⁺ γδ T cell development. Expression of NKR ligands (MICA/B and Rae-1) to NKRs also activates anti-tumour γδ T cells and leads to IFN-γ production, which drives anti-tumour immunity through induction of Th1 immune responses and cytolytic NK cell development. Pro-tumour γδ T cell activation is augmented through the action of IL-15, IL-18 and IL-21, along with survival signal IL-2, which upregulate T-bet transcription factor. Pro-tumour γδ T cells also drive cancer cell apoptosis through FAS/FASL and TRAIL/TRAIL-R, and through the release of cytolytic granules that contain perforin and granzyme to induce apoptosis. *Adapted from Silva-Santos et al, 2019.*

1.3.4 Pro-tumour γδ T cell function in cancer.

The pro-tumour function of γδ T cells has been studied in numerous preclinical cancer models, and they have hugely diverse effector functions that can shape the TME through a variety of mechanisms including immune suppression, facilitating angiogenesis, directly influencing tumour proliferation, and driving metastatic dissemination. However, as previously stated above, pro-tumour γδ T

cells are generally identified through surface markers (notably the absence of CD27) and TCR usage, but particularly through the production of pro-tumour IL-17A (Figure 1-8).
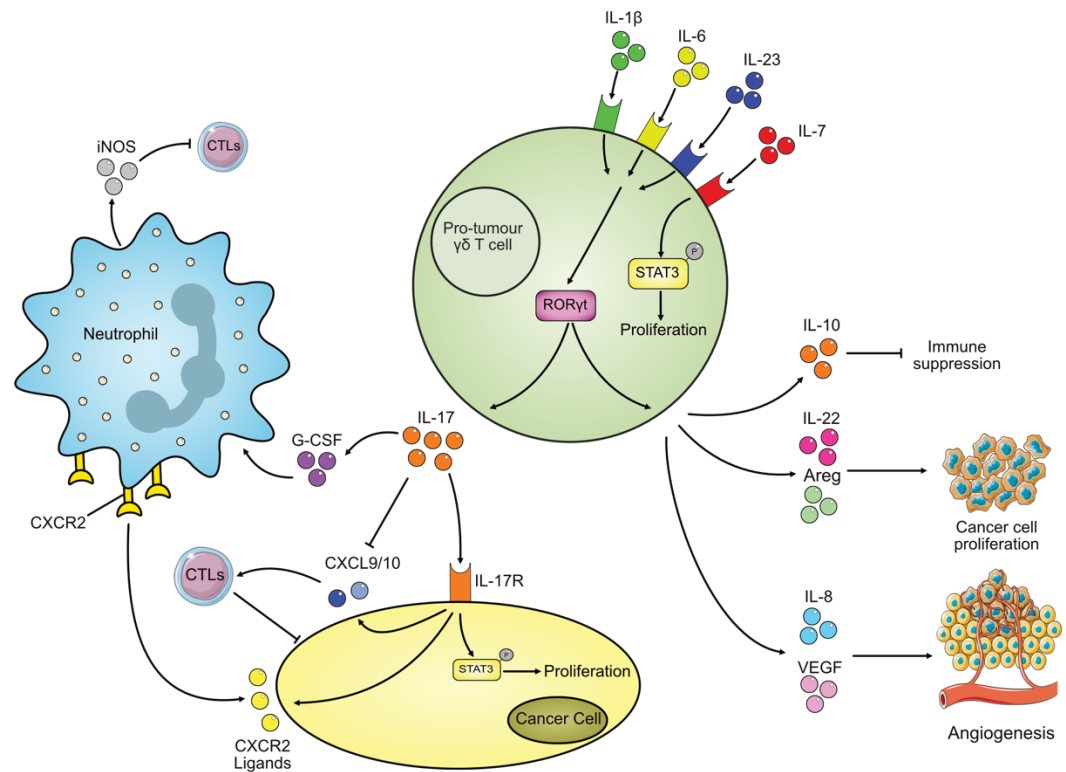
Figure 1-8 γδ T cells have potent pro-tumour mechanisms in a variety of cancer settings. Pro-tumour functions of γδ T cells are heterogenous, but centres on the production of IL-17A by RORγt⁺ γδ T cells. The presence of IL-1β, IL-6, IL-23 and IL-7 promote the expansion of IL-17A-producing γδ T cells, with IL-7 also acting as a survival signal to promote γδ T cell proliferation. IL-17A production directly induces cancer cell proliferation, impairs CXCL9/10-mediated recruitment of anti-tumour lymphocytes, but also upregulates tumour cell production of CXCR2 ligands to recruit pro-metastatic myeloid cells. γδ T cells also drive immune suppression through IL-10 production and stimulate cancer cell proliferation through the production of IL-22 and amphiregulin (Areg). Production of IL-8 and VEGF also helps promote tumour growth and metastatic dissemination through angiogenesis. *Adapted from Silva-Santos et al, 2019.*

In preclinical models of breast cancer, γδ T cells have been shown to have potent pro-tumour function by facilitating metastatic dissemination.(Coffelt et al., 2015) In *K14cre;Cdh1^{F/F};Trp53^{F/F}* (KEP) mice, a model of spontaneous breast cancer, tumour-derived IL-1β activates Vγ4⁺CD27⁻ γδ T cells to produce IL-17A.(Coffelt et al., 2015) The production of IL-17A was found to regulate the expansion of immature immune-suppressive neutrophils that produced iNOS to facilitate metastatic dissemination through the inhibition of cytotoxic CD8⁺ T cells.(Coffelt et al., 2015) In other experimental metastasis models have confirmed IL-17A-producing Vγ6⁺ T cells as potent pro-metastatic cells that are

regulated through Type I IFNs — revealing that pro-tumour γδ T cells are a heterogenous population.(Patin et al., 2018) This is further highlighted through single cell analysis of γδ T cells in the breast cancer pre-metastatic niche (PMN), which reveals that γδ T cell populations become more diverse in response to tumours.(Edwards et al., 2021) In steady state, CD27⁻ γδ T cells with enriched IL-17A signatures are found within a single cluster; whereas in response to tumour-derived IL-1ß and IL-23, pro-tumour Vγ4⁺/6⁺ γδ T cells expand into seven clusters expressing genes associated with pro-tumour IL-17A⁺ γδ T cells.(Edwards et al., 2021) In human breast cancer, patients with high γδ T cell infiltration have poor survival, as high γδ T cell infiltration also correlates with advanced stage and lymph node metastasis.(Ma et al., 2012) Finally, despite human Vγ9Vδ⁺ γδ T cells not producing IL-17A, they are capable of driving tumourigenesis and subvert anti-tumour immunity through the production of IL-8 and IL-10, respectively, further highlighting the central role of γδ T cells in breast cancer tumourigenesis.(Chabab et al., 2020)

γδ T cells are found in greater numbers in mucosal sites — particularly within gut tissue.(Komori et al., 2006) This population of γδ T cells are called *intraepithelial lymphocytes* (IELs) and are generally regarded as tissue-resident cells that play a central role in maintaining barrier integrity and gut homeostasis.(Suzuki et al., 2020) As with breast cancer, the pro-tumour role of γδ T cells in CRC largely centres upon their capacity to produce IL-17A and modulate immune responses.(Suzuki et al., 2020) In murine CRC, driven through loss of APC (*Cdx2-Cre;Apc^{F/Wt}*), impaired barrier integrity leads to IL-23 signalling driven by infiltrating myeloid cells, which upregulates IL-17A responses and results in reduced tumour growth.(Grivennikov et al., 2012) Additional studies using *APC^{Min/+}* mice crossed with IL-17A⁻/⁻ mice demonstrate reduced IL-6, IL-23 and IL-1ß and also reduced tumour development, implicating IL-17A⁺ γδ T cells drive tumourigenesis.(Chae et al., 2010) IL-17RA signalling is shown to be crucial for early CRC tumourigenesis, as ablation of IL-17RA signalling leads to reduced proliferation of transformed cells and loss of pro-tumour STAT3 signalling in early lesion development.(Wang and Sun, 2014) Further research has shown that a major pro-tumour function of IL-17A signalling is through the impairment of anti-tumour immunity, as IL-17A signalling was found to inhibit CXCL9/10 from CRC cells, which negatively impacts the recruitment of CTLs to tumours.(Chen et

al., 2019b) In human CRC, Vδ1+CD27− cells are the dominant cell population compared to CD27+IFN-γ+ γδ T cells found in normal colorectal tissue, suggesting a phenotypic switch to pro-tumour.(Wu et al., 2014) This pro-tumour function is activated through IL-23, which promotes IL-17A production along with IL-8 and GM-CSF, which promote angiogenesis and myeloid cell expansion, respectively.(Wu et al., 2014) The dominant Vδ1 subtype also shows a significant proportion of CD39+FOXP3+ cells that have high levels of checkpoint molecules (CTLA-4/PD-1), suggesting a strong regulatory phenotype.(Hu et al., 2017) The regulatory phenotype is further indicated through production of IL-10, GM-CSF and TGF-β1; but is mainly exerted through the adenosine pathway where co-expression of CD39 and CD73 enables the phosphoydrolysis of ATP to AMP, and then converts AMP to immune-suppressive adenosine.(Hu et al., 2017, Chabab et al., 2020) Tumour-infiltrating Vδ1+CD39+ γδ T cells also correlate with advanced CRC stage, tumour size and lymph node metastasis, so may be used as a prognostic indicator in CRC patients.(Hu et al., 2017)

The heterogenous pro-tumour function of γδ T cells is further observed in HCC and ovarian cancer, which are driven by IL-17A-producing Vγ4+ and Vγ6+ γδ T cells, respectively.(Ma et al., 2014, Rei et al., 2014) In HCC, IL-17A-producing Vγ4+ T cells were not found to directly alter tumour cell proliferation, but instead reduce CD8+ memory cells, IFN-γ effector function and drive the production of CXCL5 by tumour cells to recruit pro-tumour immune-suppressive myeloid cells.(Ma et al., 2014) In preclinical ovarian models, tumour-derived IL-7 promotes the expansion of Vγ6+IL-17-producing γδ T cells, which produce angiogenic factors (VEGFA and Ang-2) and recruit small peritoneal macrophages that drive angiogenesis and proliferation of cancer cells.(Rei et al., 2014, Chen et al., 2019a) This further reinforces that the crosstalk between γδ T cells and myeloid compartments are fundamental in driving a variety of tumour subtypes.

In lung cancer, there is strong evidence to show that IL-22/IL-22R are overexpressed in lung cancer, exhibit immunomodulatory properties and directly enhance proliferation, migration, and invasion of NSCLC cells.(Bi et al., 2016) γδ T cells are found to be major sources of IL-22 in Kras-driven lung cancer, and IL-22−/− mice demonstrate lower IL-17 and IL-6/STAT3 signalling, reduced Ki67 and EGR expression, and reduced lung lesions which further reinforces a central role for IL-22-producing γδ T cells in NSCLC.(Khosravi et al., 2018) Another route of

pro-tumour γδ T cell function is established through IL-1β and IL-23 signalling following loss of microbial homeostasis during neoplastic transformation, which leads to the expansion of tissue-resident RORγt⁺ Vγ6⁺CD27⁻ γδ T cells.(Jin et al., 2019) The expansion of a pro-tumour γδ T cell subset occurs with increased expression of neutrophil attractants (CXCL2 and G-CSF), increased IL-1R1 and IL-23 to increase γδ T cell responsiveness and production of amphiregulin (Areg), which can drive tumour cell proliferation in a dose-dependent manner.(Jin et al., 2019) Therefore, microbiota-activated γδ T cells in lung can directly stimulate tumour cell proliferation, and can influence lung inflammation through pro-tumour myeloid cell recruitment.(Jin et al., 2019)

Finally, despite being classified as an immunologically cold tumour, there is a growing appreciation of the role γδ T cells play in pancreatic cancer (PDAC), where they have been shown to play a pathogenic role in PDAC TME.(McAllister et al., 2014) In normal tissues, γδ T cells (RORγt⁺) are rarely found but increase roughly 50-fold in PanIN lesions — the expression of oncogenic Kras also drives IL-17A production from γδ T cells.(McAllister et al., 2014) Pancreatic GEMMs with genetic ablation of IL-17A demonstrate reduced collagen deposition, a less aggressive stromal reaction and more normal histology when compared to IL-17A$^{+/+}$ mice — pharmacological inhibition of IL-17A results in reduction of PanIN lesions.(McAllister et al., 2014) Additionally loss of IL-17A expressions leads to reduced *Il6* transcripts which indicates protumour function of IL-17A-producing γδ T cells in early pancreatic carcinoma.(McAllister et al., 2014) Further exploration has shown that IL-17A in early PanIN lesion development exerts the protumour function through the regulation of tuft cell development, and establishes stem cell marker upregulation in PanIN lesions to drive their development to invasive carcinoma.(Zhang et al., 2018) Mice overexpressing IL-17A have more extensive PanIN lesions expressing the tuft cell marker DCLK-1, one of the major dysregulated genes associated with Embryonic Stem Cell signature expressed during blockade of IL-17A.(Zhang et al., 2018) Neutralisation of IL-17A signalling also impairs neutrophil recruitment to PDAC tumours, which is mediated through the upregulation of CXCR2 ligands from KPC cells leading to CD8⁺ impairment.(Zhang et al., 2020b) Chronic IL-17 signalling in PDAC mediates pancreatitis through peptidyl arginine deaminase type IV (Padi4) neutrophil aggregates, which also drives NETosis — a process whereby Padi4 promotes the

release of chromatin-rich *neutrophil extracellular traps* (NETs).(Zhang et al., 2020b) Orthotopic KPC transplantation into Padi4$^{-/-}$ mice displayed greater sensitisation to anti-PD-1 therapy, demonstrating that IL-17-driven neutrophil recruitment in PDAC can contribute to chemotherapy resistance.(Zhang et al., 2020b) In human PDAC, γδ T cells were found to constitute a large proportion of the TIL population, and in murine PDAC γδ T cells were found to be predominately Vγ4$^+$ and produced pro-tumour cytokines such as IL-10 and IL-17A.(Daley et al., 2016) γδ T cells are recruited to PDAC TME through CCR2, CCR5 and CCR6, but were not found to directly influence tumour cell growth; instead, higher levels of Galectin-9 and PD-L1 indicated immune checkpoint control, which translated into reduced tumour levels of IFN, TNF and reduced effector function from CTLs.(Daley et al., 2016) Thus, infiltrating γδ T cells in PDAC modulate anti-tumour immunity through checkpoint ligation. There is further evidence that human γδ T cells in PDAC also exert protumour functions, as they have been observed proximal to pancreatic stellate cells (PSCs), are associated with increased expression of ECM-related genes, and induce expression of protumour IL-6 from PSCs.(Seifert et al., 2020) Therefore, the protumour function in preclinical murine models confirms that subsets of γδ T cells are potent protumour cells that can exert their functions through a variety of mechanisms. Furthermore, these protumour mechanisms are often context-dependent and have great potential for use in more tailored therapies.

1.3.5 Summary

Thus, the evidence discussed above reveals the potent pro-tumour capabilities of γδ T cells in a variety of cancer settings. Most notably in breast cancer, where IL-17A+ γδ T cells promote G-CSF production, the expansion of immature and immune-suppressive neutrophils and this leads to the impairment of anti-metastatic CD8+ T cells. Given the additional evidence that IL-17A delays precursor PanIN lesions; that γδ T cells promote PDAC tumourigenesis through impairment of anti-tumour immunity; and that neutrophil populations are potently pro-metastatic in PDAC; the role of γδ T cells in the PDAC metastatic cascade warrants further investigation, particularly the crosstalk with neutrophils. An illustrated summary of breast cancer metastatic cascade can be seen below, along with key papers that indicate a similar mechanism may be found in PDAC.
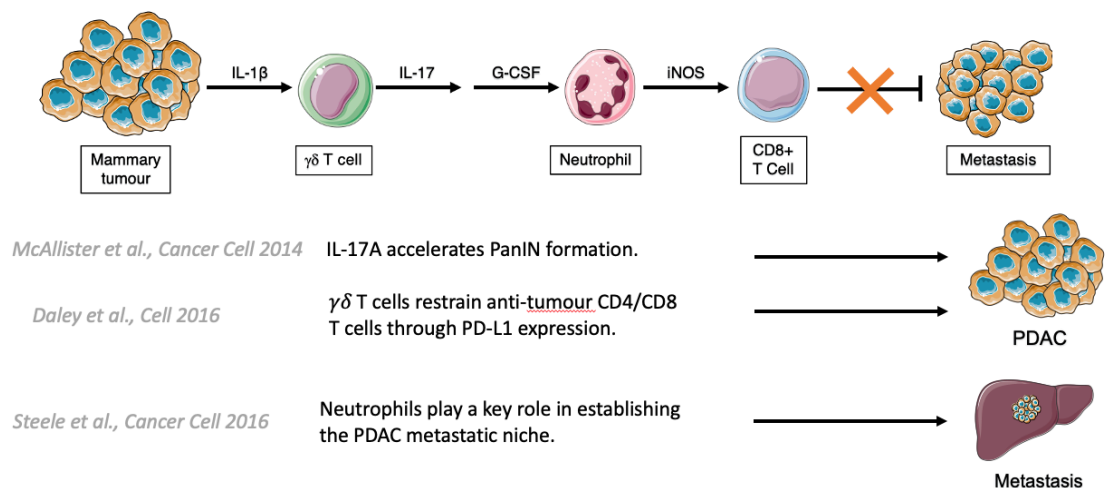
Figure 1-9 Illustrated summary of the potential γδ T cell-driven metastatic cascade in PDAC. In breast cancer, γδ T cells drive a metastatic cascade through IL-17A, which expands immune-suppressive and immature neutrophils to impair anti-metastatic CD8+ T cells. In PDAC, IL-17A has been shown to accelerate PanIN formation, and γδ T cells have been shown to impair anti-tumour CD4/CD8 T cells to restrain anti-tumour immunity; additionally, neutrophils have been demonstrated as potent pro-metastatic cells. This cumulative evidence suggests the crosstalk between γδ T cells and neutrophils may promote PDAC metastasis in a similar manner to breast cancer.

Aims and Hypothesis.

I hypothesise that IL-17A$^+$ γδ T cells play an important role in directing metastatic disease in murine PDAC. Evidence has shown that IL-17A$^+$ γδ T cells drive breast cancer metastasis through neutrophil expansion and impairment of anti-metastatic CD8$^+$ T cells. In PDAC, there is evidence that IL-17A signalling promotes PDAC progression, and γδ T cells constitute a major proportion of the tumour-infiltrating lymphocyte population. Additionally, given that neutrophils and macrophages are central for PDAC tumourigenesis and metastasis, I also hypothesise that γδ T cells direct metastasis by mediating crosstalk with pro-tumour myeloid cells. These hypotheses will be tested through the following experimental aims:

1. Determine if γδ T cells infiltrate the primary PDAC TME and metastatic niche, and then characterise their phenotype in both tissues.

2. Determine whether the genetic ablation of γδ T cells in KPC tumour-bearing mice affects PDAC progression and metastatic dissemination.

3. Determine the impact of γδ T cells on the primary PDAC TME and in the metastatic niche.

Chapter 2   Materials and Methods

2.1 Mice.

All animal experiments were performed under licenses issue by the UK Home Office under the Animals (Scientific Procedures) Act, 1986 and approved by the Animal Welfare and Ethical Review Board (AWERB). Mice were housed in *individually ventilated cages* (IVC) and has access to standard diet and water *ad libitum*. Mice were ear clipped to enable identification and provide tissue samples for genotyping through Transnetyx (Cordoba, TN, USA). Following genotyping, $Pdx1^{Cre};Kras^{G12D};Trp53^{R172H}$ (KPC) mice were identified, monitored three times weekly and culled once exhibiting symptoms that indicated humane clinical endpoint. Mice were maintained on C57BL/6 background, and both male and female tumour-bearing mice were used for experiments.

2.1.1 KPC mice.

Tumours in KPC mice are driven through the conditional expression of *Lox-STOP-Lox Kras^{G12D}* and *Lox-STOP-Lox Trp53^{R172H}*, which are controlled through a Cre-recombinase (*Pdx1-Cre*). Expression of *Pdx1-Cre* results in the excision of *Lox-STOP-Lox* sites and the expression of $Kras^{G12D/+}$ and $Trp53^{R172H/+}$ in a pancreas-specific manner.(Hingorani et al., 2005) KPC mice faithfully recapitulate the progression, clinical manifestations, and histopathological features of human PDAC. KPC mice have no observable neoplasia at birth, by 6 weeks they develop non-invasive PanIN precursor lesions, and by 10 weeks they display full spectrum of PanIN lesions as well as locally invasive PDAC and desmoplastic stroma. Clinical manifestations indictive of human clinical endpoint include cancer-associated cachexia, jaundice, ascites overt primary tumour growth and severe hunching. Finally, the KPC tumour microenvironment mirrors human PDAC with minimal vascularisation, extensive fibrosis, potent immune suppression, and metastatic dissemination to liver, lung and diaphragm. Metastatic incidence is observed in roughly 80% of KPC specimens on mixed background, but only around 40% of KPC specimens on C57BL/6 background

2.1.2 γδ T cell-deficient KPC mice (KPC;Tcrd$^{-/-}$).

KPC mice were crossed with *Tcrd*^{tm1Mom} mice. Mice homozygous for *Tcrd*^{tm1Mom} are deficient for γδ T cells due to targeted knockout of the T cell receptor delta (Tcrd) chain but exhibit normal αß (CD4$^+$/CD8$^+$) T cell populations.

2.2 Fluorescence-activated cell sorting (FACS)

2.2.1 Immune cell isolation from PDAC tissue.

PDAC tissue was harvested from KPC and KPC;Tcrd$^{-/-}$ mice that had reached human clinical endpoint, and were collected in 1X *phosphate-buffered saline* (PBS), and were held on ice. Tumours were then manually chopped in Corning® 100mm x 20mm petri dish using scalpel prior to enzymatic dissociation. Once homogenised, tumour tissue was transferred to gentleMACs C-tube (130-096-334, Miltenyi) containing 2.35mL RPMI 1640 or DMEM with 100μl Enzyme D, 50μl Enzyme R and 12.5μl Enzyme A. Manufacturer's instructions were followed, and samples were dissociated using gentleMACs Octodissociator (Miltenyi) program "37_m_TDK_2" for tough tumour dissociation at 37℃. Following enzymatic dissociation, the suspension was transferred to 50mL falcon tube through a 70μM filter, and 2mL fetal calf serum (FCS) was pour over to neutralise enzyme activity. The suspension was then centrifuged at 1500rpm for 5 minutes at 4℃, and supernatant was discarded. Pellets were resuspended in 1X RBC lysis buffer (Invitrogen), vortexed and incubated at room temperature (RT) for 3 mins, then centrifuged at 1500rpm for 5 minutes at 4℃. 1X RBC Lysis buffer was prepared through dilution of 10X RBC Lysis Buffer in distilled water. Pellets were then resuspended in 1mL FACs buffer (1X PBS + 0.5% BSA) (A7906-100A, Sigma Aldrich) prior to Percoll centrifugation.

2.2.2 Immune cell isolation from liver tissue.

Liver tissue was harvested from KPC and KPC;Tcrd$^{-/-}$ mice that had reached human clinical endpoint, and were collected in 1X PBS, and were held on ice. Livers were transferred to gentleMACs C-tube containing 4.7mL DMEM with 200μl Enzyme D, 100μl Enzyme R and 20μl Enzyme A and were finely chopped using scissors prior to enzymatic dissociation. Manufacturer's instructions were followed, and samples were dissociated at 37℃ by gentleMACs Octodissociator

along program "37_m_LIDK_1". Following enzymatic dissociation, the suspension was transferred to 50mL falcon tube through a 70µm filter, and 2mL *fetal calf serum* (FCS) was pour over to neutralise enzyme activity. The suspension was then centrifuged at 1500rpm for 5 minutes at 4°C, and supernatant was discarded. Pellets were resuspended in 1X RBC lysis buffer, vortexed and incubated at room temperature (RT) for 3 mins, then centrifuged at 1500rpm for 5 minutes at 4°C. An additional RBC lysis step was performed if required. Pellets were then resuspended in 1mL FACs buffer prior to Percoll centrifugation.

2.2.3 Immune cell isolation from spleen tissue.

Spleen tissue was harvested from KPC and KPC;Tcrd$^{-/-}$ mice that had reached human clinical endpoint, and were collected in 1X PBS, and were held on ice. Spleens were then mashed through 70µM filter into a 50mL Falcon tube, and 10mL of FACS buffer was flushed through the filter. Samples were then centrifuged at 1500rpm for 5 minutes at 4°C, and supernatant was discarded. Pellets were resuspended in 1X RBC lysis buffer, vortexed and incubated at room temperature (RT) for 3 minutes, then centrifuged at 1500rpm for 5 minutes at 4°C. An additional RBC lysis step was performed. Pellets were then resuspended in 1mL FACs buffer prior to counting via haemacytometer.

2.2.4 Lymphocyte enrichment by percoll gradient centrifugation.

15mL Falcon tubes were coated with 10% FCS in DMEM, this was to aid the formation of different density phases. Three different percoll concentrations were then made — 80%, 40% and 20%. PDAC and liver suspension were centrifuged at 1500rpm for 5 minutes at 4°C, supernatants were discarded, and pellets resuspended in 3mL 40% percoll. 10% FCS/DMEM was then replaced with 3mL 80% percoll in the 15mL falcon tubes, and 3mL cell suspensions (in 40% percoll) was gently poured into falcon tube via the wall using a P1000 pipette. 1mL of 20% percoll was then gently added on top of the 40% phase via the wall of the tube. Samples were then centrifuged at 1800rpm with no\lowest brake setting for 30 minutes at 21°C. Following centrifugation, all the 20% and half of the 40% phase was aspirated, and roughly 2mL of the 40/80% interphase was collected and transferred into a new 50mL falcon tube with an additional 8mL of FACS buffer. Samples were then centrifuged at 1800rpm for 5 minutes at room

temperature, and the supernatant was discarded. Cell pellets were then resuspended in 1mL FACS buffer prior to counting via hemacytometer.

2.2.5 Isolation of immune cells from adipose tissue.

Adipose tissue from subcutaneous (SubAT), epididymal (EpiAT) and brown (BrAT) adipose tissue were harvested from KPC and KPC;Tcrd$^{-/-}$ mice that had reached humane clinical endpoint. Fat tissue was dried on paper towel prior to recording weight, and were then transferred to 3mL of RPMI (Gibco) on ice. All adipose tissue was digested in 4mL of 1mg/mL Type II Collagenase (Worthington Biochem; Cat # LS00416) in RPMI (Gibco). Prior to dissociation, adipose tissue was finely chopped with scissors until homogenous, transferred to 4mL 1mg/mL collagenase II solution and then incubated at in a shaker at 37°C for 25 minutes at 100rpm. Following incubation, samples were removed and stored on ice to neutralise collagenase II activity and were then filtered through 70μM mesh filter. Samples were then centrifuged at 300g for 5 minutes at 4°C, supernatant was discarded and pellet was resuspended in 200μl RPMI prior to counting via hemacytometer.

2.2.6 Counting of immune cells for FACS staining.

Cells were counted manually using "Neubauer Improved Brightline" haemocytometer. Aliquots of cell suspensions were diluted 1:10 (PDAC and liver) or 1:100 (spleen) in 0.4% Trypan Blue Stain (Gibco) and 10μL of diluted cell suspensions was used to count haemocytometer chamber. For optimal antibody staining I aimed to plate 2×10^6 cells for PDAC, spleen and liver.

2.3 Fluorescence-activated cell sorting (FACS)

2.3.1 List of Antibodies

Table 1 List of antibodies used in flow cytometric analysis.

Marker	Fluorochrome	Clone	Dilution (Stock)	Manufacturer
CD103	BV421	2E7	1:200 (0.2mg/ml)	Biolegend
CD11b	Brilliant Violet 785	M1/70	1:800 (0.2mg/ml)	eBioscience
CD11b	APC-eFluor780	M1/70	1:800 (0.2mg/ml)	eBioscience
CD11c	PE	N418	1:400 (0.2mg/ml)	Biolegend
CD11c	APC-eFluor780	N418	1:200 (0.2mg/ml)	Invitrogen
CD19	APC-eFluor780	1D3	1:400 (0.2mg/ml)	eBioscience
CD19	FITC	eBio1D3	1:800 (0.5mg/ml)	eBioscience
CD226	BV605	TX42.1	1:200 (0.2mg/ml)	Biolegend
CD24	BUV737	M1/69	1:200 (0.2mg/ml)	BD Bioscience
CD27	PE/Dazzle 594	LG.3A10	1:400 (0.2mg/ml)	Biolegend
CD3	BV650	17A2	1:100 (0.1mg/ml)	Biolegend
CD317	Pe-Cy7	eBio927	1:400 (0.2mg/ml)	eBioscience
CD3	FITC	145-2C11	1:100 (0.5mg/ml)	eBioscience
CD4	BV605	GK1.5	1:100 (0.2mg/ml)	Biolegend
CD4	APC-eFluor780	GK1.5	1:200 (0.2mg/ml)	Invitrogen
CD44	PerCP-Cy5.5	IM7	1:50 (0.2mg/ml)	Biolegend
CD45	BV605	30-F11	1:100 (0.1mg/ml)	Biolegend
CD49a	BUV395	Ha31/8	1:100 (0.2mg/ml)	BD
CD64	Pe-Cy7	X54-5/7.1	1:50 (0.2mg/ml)	Biolegend
CD69	BV510	BV510	1:50 (0.1mg/ml)	Biolegend
CD8	BUV395	53-6.7	1:100 (0.2mg/ml)	BD Bioscience
CD8	APC-eFluor780	53-6.7	1:100 (0.2mg/ml)	Invitrogen
CD80	APC	16-10A1	1:50 (0.2mg/ml)	eBioscience
CD96	PE	3.3	1:50 (0.2mg/ml)	Biolegend
CX3CR1	Pe	SA011F11	1:200 (0.2mg/ml)	Biolegend
CXCR4	AlexaFluor647	L276F12	1:50 (0.5mg/ml)	Biolegend
DX5	FITC	DX5	1:200 (0.5mg/ml)	Biolegend
EpCAM/CD326	APC-eFluor780	G8.8	1:100 (0.2mg/ml)	eBioscience
F4/80	BV650	BM8	1:50 (0.2mg/ml)	Biolegend
γδTCR	FITC	GL3	1:200 (0.5mg/ml)	eBioscience
γδTCR	PE	GL3	1:100 (0.2mg/ml)	Biolegend
Granzyme B	AlexaFluor-647	GB11	1:50 (0.2mg/ml)	Biolegend
IFN-γ	PE-Cy7	XMG1.2	1:200 (0.2mg/ml)	eBioscience
IL-17A	PE	eBio17B7	1:100 (0.2mg/ml)	eBioscience
Ly6C	PeDazzle	HK1.4	1:200 (0.2mg/ml)	Biolegend
Ly6G	BUV395	1A8	1:50 (0.2mg/ml)	BD Bioscience
MHCII	PerCP-eFluor710	M5/114.15.2	1:100 (0.2mg/ml)	eBioscience
NK1.1	Brilliant Violet 421	PK136	1:50 (25μg/ml)	Biolegend
Ter-119	FITC	TER-119	1:100 (0.5mg/ml)	eBioscience
TIGIT	PerCP-eFluor710	GIGD7	1:200 (0.2mg/ml)	eBioscience
TruStain FcX (CD16/32)	—	93	1:50 (0.5mg/ml)	Biolegend
TNF-α	BV711	MP6-XT22	1:200 (0.2mg/ml)	BD
Viability Dye (Zombie Green)	—	—	1:400	Biolegend
Viability Dye (Zombie NIR)	—	—	1:400	Biolegend
Vδ6.3	APC	C504.17C	1:100 (0.2mg/ml)	Biolegend
Vγ1	PE	2.11	1:200 (0.2mg/ml)	Biolegend
Vγ2/4	PE-Cy7	UC3-10A6	1:100 (0.2mg/ml)	eBioscience
XCR1	BV421	ZET	1:200 (0.2mg/ml)	Biolegend

2.3.2 Cytokine Stimulation

Isolated immune cells from PDAC, liver and spleen were plated on 96 well V bottom plates (Thermo), centrifuged at 2000rpm for 2 minutes at 4℃ and then resuspended in 200μl of stimulation medium and incubated for 3 hours at 37℃. T cell stimulation medium consisted of 8% FCS (Gibco), 0.5% β-mercaptoethanol (Gibco), 1% penicillin/streptomycin (Sigma) in IMDM (Gibco). Cell Activation Cocktail (with Brefeldin A) was diluted 1:500 in T cell stimulation medium to 1X concentration. Cell Activation Cocktail (with Brefeldin A) (Biolegend) is a pre-mixed solution containing PMA (phorbol 12-myristate-13-acetate), ionomycin and Brefeldin A. Cells are stimulated and activated by PMA/ionomycin to induce cytokine production and Brefeldin A inhibits protein transport in the Golgi apparatus to prevent cytokine secretion. The retention of cytokines then enables their detection by flow cytometry through intracellular staining with fluorophore-conjugated antibodies.

2.3.3 Extracellular staining.

Following cytokine stimulation, cells were centrifuged at 2000rpm for 2 minutes at 4℃ and washed in 100μl FACS buffer to remove cytokine stimulation cocktail. Cells were then centrifuged at 2000rpm for 2min at 4℃, then resuspended in 50μL Fc Blocking Buffer, consisting of TruStain FcX™ (anti-mouse CD16/32) (Biolegend) diluted 1:50 in FACS Buffer. TruStain FcX (Fc Block) binds to murine CD16 and CD32, otherwise known as IgG Fc receptor III (FcR III) and FcR II, respectively, to prevent non-specific binding of fluorophore-conjugated antibodies to Fc regions. Cells were incubated with Fc blocking solution for 20 minutes at 4℃, then 50μL of extracellular antibody mix was added and incubated for 30 minutes at 4℃. Stock solution of extracellular antibodies was created at 2X concentration in BD Brilliant Stain Buffer (BD). Cells were then centrifuged at 2000rpm for 2 minutes at 4℃, washed in 100μl FACS buffer, centrifuged at 2000rpm for 2 minutes at 4℃, washed in 1X PBS and centrifuged at 2000rpm for 2 minutes at 4℃. Cells were then resuspended in 100μL of appropriate live\dead marker (Zombie Green or Zombie NIR viability dye) (423112, 423106, Biolegend) and incubated for 20 minutes at 4℃. Live\dead marker does not permeate viable cell membranes, but dead cells with compromised membrane integrity are labelled. Viability dyes were diluted

1:1400 in PBS. Following incubation, cells were centrifuged at 2000rpm for 2 minutes at 4℃, washed with FACS buffer, centrifuged at 2000rpm for 2 minutes at 4℃ and then resuspended in 100μL IC Fixation Buffer (Invitrogen) for 20 minutes at 4℃.

2.3.4 Intracellular Staining

Following fixation incubation, cells were centrifuged at 2000rpm for 2 minutes at 4℃ and were resuspended in 100μL 1X Permeabilization Buffer (Invitrogen). 1X permeabilization buffer was prepared through 10-fold dilution of 10X permeabilization buffer in distilled water. Cells were then centrifuged at 2000rpm for 2 minutes at 4℃ and resuspended in 100μL of intracellular antibody mix. Intracellular antibody mix was prepared at 1X concentration in permeabilization buffer, and FMO controls were prepared for all intracellular stains. Cells were then incubated for 30 minutes at 4℃. Cells were then washed twice in FACS buffer, centrifuged at 2000rpm for 2 minutes at 4℃, and then resuspended in 100μL FACs buffer. Cells were then filtered into 5mL FACS tubes for acquisition.

2.3.5 Acquisition and analysis

Prior to acquisition, UltraComp eBeads™ Compensation Beads (Invitrogen) were prepared. First, 50μL of FACS buffer was transferred to 1.4mL U-bottom FACSs tubes (Micronic), along with 1μL of antibody to create a single stain control. Compensation beads were vortexed for a 40 seconds, and 25μL of beads was added to each single stain antibody. Unstained beads were also prepared. Acquisition was then performed on LSRFortessa™ (BD Bioscience) using DIVA acquisition software, with data analysis performed with FlowJo software v9 (FlowJo, LLC).

2.4 Histology

2.4.1 Immunohistochemistry staining

Immunohistochemistry IHC) staining was performed in house by the CRUK Beatson Histology department. All haematoxylin & eosin (H&E), IHC, *in situ* hybridisation (ISH) and Pico-Sirius Red staining was performed on 4μm tissue

slices cut from formalin fixed paraffin embedded (FFPE) sections. Sections were mounted on blank slides and were placed in a 60℃ oven for 2 hours. Staining was then either performed on Agilent AutostainerLink48, Lecia Bond Rx Autostainer, or performed manually in the case of Pico-Sirius Red. All sections were finished by rinsing with tap water, dehydrated through 1x 1 minute bath in 70% ethanol, transferred to 100% ethanol for 2x 1 minutes, and finally to 3x 30 second Xylene baths. All stained sections had coverslips fixed in Xylene with DPX mountant (SEA-1300-00A, Cell Path). All IHC and Pico-Sirius Red staining were then scanned at x20 magnification and quantified on HALO Image Analysis software.

Table 2 List of antibodies used in IHC staining.

Antibody	Clone	Dilution	Manufacturer	Catalog #	Secondary Ab
αSMA	1A4	1:25,000	Sigma-Aldrich	A2547	Mouse EnVision
Caspase 3	ASP-175	1:500	Cell Signalling	9661	Rabbit EnVision
CD3	SP7	1:100	Abcam	ab16669	Rabbit Envision
CD31	—	1:75	Abcam	ab28364	Rabbit EnVision
M-CSFR	SP211	1:60	Abcam	ab183316	Rabbit EnVision
F4/80	CI:A3-1	1:100	Abcam	ab6640	Rat ImmPRESS
FOXP3	D608R	1:200	Cell Signalling	12653	Rabbit Envision
Ki67	D3B5	1:1000	Cell Signalling	12202	Rabbit EnVision
Ly6G	IA8	1:60,000	BioXcell	BE0075-1	Rat ImmPRESS
NKp46/NCR1	—	1:200	R&D Systems	af225	Goat ImmPRESS
Podoplanin	RTD4E10	1:4000	Abcam	ab11936	anti-hamster
pSMAD3	EP823Y	1:50	Abcam	ab52903	Rabbit EnVision

2.4.2 Agilent AutostainerLink48

The following antibodies were stained on Agilent AutostainerLink48; αSMA (A2547, Sigma-Aldrich), CD31 (ab28364, Abcam), FOXP3 (12653, Cell Signalling), NKp46 (af225, R&D Systems) and Podoplanin (ab11936, Abcam). Sections were dewaxed by Agilent pre-treatment module and underwent *heat-induced epitope retrieval* (HIER). αSMA, FOXP3 and Podoplpanin sections underwent antigen retrieval using low pH target retrieval solution (TRS) (K8005, Agilent) and heated to 97℃ for 20 minutes; CD31 and NKp46 sections underwent antigen retrieval using high pH TRS (K8004, Agilent) and heated to 97℃ for 20 minutes. Following HIER, all sections were rinsed in flex wash buffer (K8007, Agilent), followed by peroxidase blocking (S2024, Agilent) for 5 minutes followed by flex buffer washing. Sections then underwent additional blocking steps for 20 minutes; αSMA with mouse Ig blocking kit (MKB-2213, Vector Labs), NKp46 with blocking serum in the Goat ImmPRESS kit (MP-7405, Vector Labs), and Podoplanin with 1%

normal rabbit serum (X0902, Agilent). Primary antibodies targeting αSMA, CD31, FOXP3, NKp46 and Podoplanin (optimised dilutions and relevant information can be found in Table 2) were then incubated for 35 minutes. Prior to addition of secondary antibody, sections were washed with flex wash buffer and then incubated with secondary antibodies for 30 minutes; αSMA with Mouse Envision (K4001, Agilent), CD31 with Rabbit Envision (K4003, Agilent), FOXP3 with Rabbit Envision (K4003, Agilent), NKp46 with anti-Goat ImmPRESS (MP-7405, Vector Labs) and Podoplanin with rabbit anti-hamster (18893, Invitrogen), and sections were then rinsed with flex wash buffer. Podoplanin underwent an additional 30 minute incubation with Vector ABC kit (PK-4005, Vector Labs) as detailed in the manufacturer's instructions. All sections were then applied with Liquid DAB (K3468, Agilent) for 10 minutes and were then washed in water and counterstained with haematoxylin z (CellPath, UK).

2.4.3 Lecia Bond Rx Autostainer

The following antibodies were stained on Lecia Bond Rx Autostainer; cleaved Caspase 3 (9661, Cell Signalling), CD3 (ab16669, Abcam), M-CSFR (ab18836, Abcam), F4/80 (ab6640, Abcam), Ki67 (12202, Cell Signalling), Ly6G (BE0075-1, BioXcell) and pSmad3 (ab52903, Abcam). All 4μM FFPE sections were dewaxed according to manufacturer's instructions (AR9222, Leica). For antigen retrieval, sections to be stained for F4/80 were incubated in enzyme 1 solution at 37℃ for 10 minutes, and sections for Caspase 3, CD3, M-CSFR, Ki67, Ly6G and pSMAD3 were incubated in enzyme solution 2 (AR9640, Leica) for 20 minutes at 95℃. Sections were then washed with Leica wash buffer (AR9590, Leica) prior to peroxidase block using the Intense R kit (DS9263, Leica). F4/80 and Ly6G sections were incubated with blocking solution from Rat ImmPRESS kit (MP-7404, Wector Labs) for 20 minutes at room temperature. Sectons were then rinsed with wash buffer before application of primary antibodies targeting Caspase 3, CD3, M-CSFR, F4/80, Ki67, Ly6G and pSMAD3 (optimised dilutions and relevant information can be found in Table 2) and were incubated for 30 minutes. Following primary antibody incubation, sections were rinsed with wash buffer and secondary antibodies were applied and incubated for 30 minutes; Caspase 3, M-CSFR, Ki67 and pSMAD3 incubated with Rabbit EnVision (K4003, Agilent), and F4/80 and Ly6G sections were incubated with Rat ImmPRESS (MP-7404, Vector Labs). All sections were then rinsed with wash buffer, and applied with Liquid

DAB (K3468, Agilent) and counterstained with Haematoxylin from Intense R kit (DS9263, Leica).

2.4.4 Haematoxylin & Eosin staining (H&E)

All H&E staining was performed on Leica Autostainer (ST5020). 4μm sections were cut from FFPE blocks and were dewaxed with 3x5 minute washes in Xylene and followed by graded alcohol washes — 2x 3 minute washes in 100% alcohol and 1x 3 minute wash in 70% alcohol and then stained for 13 minutes with Haem Z (RBA-4201-00A, Cell Path). Sections were then rinsed with water, transferred to 1% acid alcohol, rinsed with water again before being transferred to Scott's Tap Water Substitute, which applies a blue stain specifically to nuclear components such as chromatin. Sections were then rinsed with water and transferred to Putt's Eosin solution for 3 minutes. Metastatic scoring was visualised through H&E and quantified based on the absence (NO) or presence (YES) of metastatic lesions and visualised as a % incidence.

2.4.5 Pico-Sirius Red staining

Staining for Pico-Sirius Red was performed manually. 4μm sections were cut from FFPE blocks and were dewaxed with 3x5 minute washes in Xylene and followed by graded alcohol washes — 2x 1 minute washes in 100% alcohol and 1x 1 minute wash in 70% alcohol, and then rinsed in water for 5 minutes. Slides were then stained for 2 hours in Pico-Sirius Red solution. Working solution of Pico-Sirius Red contains equal volumes of 0.1% Direct red 80 in distilled water (Sigma Aldrich) and 0.1% Fast green in distilled water (Raymon A Lamb), this was then diluted 1:9 with Aqueous Picric acid solution (VWR). Pico-Sirius Red quantification was performed on the HALO® image analysis platform, where % positive stain was quantified on annotated tumour areas.

2.4.6 RNAscope ISH

RNAScope ISH targeting γδ T cell mRNA was performed using Mm-Trdc probe (449358) along with MmPPIB positive control (313918) and dapß negative control (312038, Advanced Cell Diagnostics, Hayward, CA), using RNAScope 2.5 LS detection kit (Brown, 322100, Advanced Cell Diagnostics, Hayward, CA). Performed on Leica Bond Rx Autostainer as per manufacturer's instructions. All

RNAscope ISH was quantified manually through randomly selected fields of view (FOV) at x2.5 magnification, and these were then quantified at x20 magnification.

2.5 Bulk RNA Sequencing (RNASeq)

2.5.1 γδ T cell sorting protocol

Immune cell isolation from spleen and liver tissue from WT and KPC mice and with liver tissue underwent percoll gradient centrifugation, as previously described. Spleen samples underwent an additional CD3 enrichment step using MojoSort™ Mouse CD3 Selection Kit (480100, Biolegend). MojoSort™ Buffer (5X) (480017, Biolegend) contains 5X PBS (ph7.2), 2.5% BSA and 10mM ethylene diamine tetra-acetic acid (EDTA) and was diluted to a working 1X solution by the addition of sterile distilled water. Spleen suspensions were resuspended in 100μL of 1X MojoSort™ Buffer for every $10x10^6$ cells. 10μL of Biotin Antibody Cocktail was then added and incubated on ice for 15 minutes (scaled up appropriately if samples contained >$10x10^6$ cells). Samples were then vortexed briefly and 10μL of Streptavidin Nanobeads were added and incubated on ice for 15 minutes (scaled up appropriately if samples contained >$10x10^6$ cells). Following incubation, 1X MojoSort™ Buffer was added to make a final volume of 2.5mL and sample tubes were then place into MojoSort™ Magnet (480019, Biolegend) for 5 minutes at room temperature. CD3$^-$ cells are magnetically labelled and so CD3$^+$ cells remain in suspension. After 5 minutes, with the sample tube retained within the magnet, the liquid was poured out and CD3$^+$ T cells were collected. Samples were then centrifuged at 2000rpm for 2 minutes at 4℃ and cell counts were repeated to obtain a suspension concentration for subsequent antibody staining.

Staining was then performed in 5mL round bottom polystyrene tubes. Samples were centrifuged at 2000rpm for 2 minutes at 4℃, resuspended in 50μL Fc Block (50μl per $4x10^6$ cells) and incubated for 20 minutes on ice. 50μl of 2X antibody mix with CD3 (FITC) and γδ TCR (PE) was then added, and cells were incubated for 30 minutes on ice. Samples were then centrifuged at 2000rpm for 2 min at 4℃, washed with FACS Buffer and centrifuged at 2000rpm for 2 min at 4℃. Samples were then resuspended in an appropriate volume of FACS sorting buffer,

with a max concentration of 10^6 cells/mL. FACS Sorting Buffer contained 2% FCS, 2.5% 1M HEPES and 0.4% 0.5M EDTA in 1X PBS. DAPI (422801, Biolegend) was used as a live/dead marker with 1μL (1mg/mL) added to samples immediately prior to sorting. Unstained cells, DAPI only cells and CD3 FMO and γδ TCR FMO on cells were also prepared, along with unstained compensation beads and single stain compensation beads (as previously described). Sorting was performed by Tom Gilbey (Y61, Flow Technician) on Aria Sorter Z6001 (BD Biosciences), and samples were collected in 300-500μL RLT buffer depending on starting concentration.

2.5.2 RNA isolation from sorted γδ T cells

Following sorting, collected cells in RLT buffer were processed the same day. RNA isolation was performed using the RNeasy® Micro Kit (74004, Qiagen), and was performed as per manufacturer's instructions. Collected cells were lysed by vortexing in the collection liquid, and an equal volume of 70% ethanol was added to the lysate and mixed well by pipetting. Samples were then transferred to an RNeasy MinElute spin column placed in a 2mL collection tube. Samples were centrifuged at 8000g for 15 seconds, and the flow-through was discarded. 350μL of Buffer RW1 Wash Buffer was added to the MinElute spin column, samples were then centrifuged at 8000g for 15 seconds and the flow-through discarded. Each sample was then incubated with DNAse1 mix (10μL of DNase 1 stock solution was then added to 70μl of Buffer RDD) (79254Qiagen) for 15 minutes at room temperature. 350μl of Buffer RW1 was added to the MinElute spin column, and samples were centrifuged at 8000g for 15 seconds and the flow-through was discarded along with the collection tube. The MinElute columns containing sample material were then transferred to a new 2mL collection tube, and 500μL Buffer RPE was added to the spin column. Samples were then centrifuged at 8000g for 15 seconds and the flow-through was discarded. 500μL of 80% ethanol was then added to the MinElute column, samples were centrifuged at 8000g for 2 minutes and the flow-through and collection tube were discarded. RNeasy MinElute spin columns containing sample material were then transferred to a new 2mL collection tube and centrifuged at full speed (16,000g) for 5 minutes with the column lid open to dry the membrane. MinElute columns were then placed onto a 1.5mL RNase-free Eppendorf collection tube. 14μL of RNase-free

water was pipetted directly onto the MinElute column membrane and were centrifuged at full speed for 1 minute to elute the RNA.

2.5.3 RNA isolation from PDAC tumour tissue

KPC and KPC;Tcrd$^{-/-}$ mice were aged to humane clinical endpoint, and 2mm PDAC tumour pieces were snap frozen in RNAlater (R0901, Sigma Aldrich) and stored at -80℃. Prior to RNA extraction, tumour samples were removed from the -80℃ freezer and defrosted on ice. Tissue homogenisation was performed on Precellys Evolution Homogenizer (Bertin Technologies) at 4℃. PDAC tumour pieces were transferred to pre-cooled Precellys Hard Tissue Tubes (PHT) (CK28R, P000916-LYSK0-A) which contain ceramic beads for hard tissue dissociation. 350μL RLT buffer was added to PHT tubes with tumour pieces and were transferred to Precellys Homogenizer. Tumour pieces were dissociated through "Hard" program at 5000rpm for 3x 20 seconds with 20 second pauses.

RNA isolation was the performed using RNeasy® Mini Kit (7410, Qiagen). PHT tubes were first centrifuged at 13,000rpm for 3 minutes at 4℃, and RLT homogenate was transferred to Qiashredder columns (79654, Qiagen). Samples were centrifuged at 13,000rpm for 3 minutes at 4℃ and 70% ethanol was added to flow-through. The RLT homogenate/70% ethanol mixes were then transferred to RNeasy Spin Column and centrifuged at 13,000rpm for 1 minute at 4℃, and flow-through was discarded. RNeasy columns were then washed with 350μL RW1 buffer, centrifuged at 13,000rpm for 1 minute at 4℃ and the flow-through was discarded. DNase 1 digestion was then performed on each column (10μL DNase 1 and 70μl RDD buffer per column) (79254Qiagen) for 15 minutes at room temperature. Columns were then washed with 350μL RW1 buffer, centrifuged at 13,000rpm for 1 minute at 4℃ and the flow-through was discarded. 500μL of RPE buffer was then added to columns, and samples were then centrifuged at 13,000rpm for 2 minutes at 4℃. RNeasy columns were then transferred to a fresh 2mL collection tube and were centrifuged at 13,000rpm for 1 minute at 4℃. RNeasy columns were then transferred to 1.5mL RNase-free Eppendorf tubes. Samples were then eluted in 350-500μL RNase-free water by centrifugation at 13,000rpm for 1 minute at 4℃. RNA quality and concentrations was measured on NanoDrop Spectrophotometer (ThermoFisher)

2.5.4 RNA sequencing

All RNA sequencing was performed by William Clark at the CRUK Beatson Institute Molecular Technology Services. RNA quality was determined through Agilent 2200 Tapestation with RNA Screentape (Agilent, ThermoFisher). RNAseq libraries were generated as per manufacturer's instructions using the TruSeq Stranded mRNA Library Prep Kit (20020594, Illumina). TruSeq library preparation used PolyA selection by OligodT coated beads to extract mRNA from 100ng of sample RNA, this was then followed by heat fragmentation to generate fragment sizes between 120-200 base pairs. cDNA synthesis was then performed using the SuperScript III Reverse Transcriptase kit (18080-044, Invitrogen) using random primers, which were then subjected to 13 cycles of PCR. RNAseq libraries were quantified using the Qubit v2.0 HS DNA assay (Q32854, Invitrogen), and libraries were then sequenced through 2x 36 cycle pair-end sequencing using the NextSeq500 sequencer (Illumina).

2.5.5 Bioinformatics analysis.

Data analysis was performed by Robin Shaw. Quality checks on raw RNA-Seq data files were performed using FastQC v0.11.7, FastP and FastQ Screen v0.12.0. RNA-Seq paired ends aligned to the GRCm38 version of the human genome and annotated using HiSat2 v2.1.0. Expression levels were analysed using HTSeq v0.9.1 and R environment v4.1 using packages from the Bioconductor data analysis suite. Differential gene expression analysis was based on negative binomial distribution with DESeq2 package v1.32.0.

2.6 Luminex

2.6.1 Serum preparation

KPC and KPC;Tcrd$^{-/-}$ mice were aged to human clinical endpoint, and WT and Tcrd$^{-/-}$ age-matched controls were also sacrificed. Blood was harvested via cardiac puncture and transferred into 1.5mL Eppendorf tube, then allowed to coagulate at room temperature. Serum was separated by centrifugation at 10,000rpm for 10 minutes at 4°C. Serum was then transferred to a new 1.5mL Eppendorf tube, snap frozen and stored at -80°C until required.

2.6.2 Reagent preparation

Luminex assay (LZSAMSM-34, R&D) was constructed to target 33 mouse chemokines and cytokines. Full list of targeted analytes are as follows: CCL2, CCL3, CCL4, CCL5, CCL7, CCL11, CCL12, CCL20, CCL21, CCL22, CXCL1, CXCL2, CXCL10, CXCL12, CXCL13, GM-CSF, IFN-γ, IL-1α, IL-2, IL-3, IL-4, IL-5, IL-6, IL-10, IL12p70, IL-13, IL-16, 1IL-17A, IL-17E, IL-27, IL-33, M-CSF and TNF-α. All reagents were brought to room temperature prior to use and prepared according to manufacturer's instructions. Standard Cocktails were reconstituted as determined in the Certificate of Analysis with Calibrator Diluent RD6-52 and were gently agitated for 15 minutes on a plate shaker at room temperature. Standards A (1497050) and C (1487157) were reconstituted in 0.275mL; Standard B (149776) was reconstituted in 0.225mL; Standards D (1482316), E (1515954) and F (1528211) were reconstituted in 0.25mL, reconstituted in 0.25mL; and Standard K (1509513) was reconstituted in 0.2mL. 100µL of each Standard Cocktail was then combined with 300µL of Calibrator Diluent to create Standard 1 with a total volume of 1000µL. A 3-fold serial dilution was then performed by the addition of 100µL of Standard 1 into 200µL of Standard 2, and repeated until Standard 6.

Microparticle Cocktail was centrifuged at 1000g for 30 seconds and then gently vortexed to resuspend the microparticles. 500µL of the Microparticle Cocktail was then diluted in 5mL of Assay Diluent RD1W into a separate mixing bottle. Biotin-Antibody cocktail was centrifuged at 1000g for 30 seconds and then gently vortexed, and 500µl of Biotin-Antibody Cocktail was diluted in 5.0mL Assay Diluent RD1W. Streptavidin-PE was centrifuged at 1000g for 30 seconds and then gently vortexed, and 220µL Streptavidin-PE concentrate was diluted in 5.35mL Wash Buffer, all according to manufacturer's instructions on the Certificate of Analysis.

2.6.3 Assay procedure

First, 50µL of each standard dilution (S1 → S6), 50µL of diluted serum and 50µL of calibrator diluent (blank) were added to the microplate, with all standards and serum samples plated in duplicate. The prepared Microparticle Cocktail was vortexed briefly, and 50µL was then added to the wells containing standards,

serum and blanks. This was then covered with a foil plate sealer and incubate for 2 hours at room temperature on a plate shaker set to 880rpm. The microplate was then secured into a magnetic 96 well separator, and liquid was removed after 1 minute. The microplate was then washed with 100μL of Wash Buffer in each well, allowed to sit for 1 minute and then the liquid was removed. Wash procedure was then repeated x2 times. The prepared Biotin-Antibody Cocktail was vortexed briefly, and 50μL was added to each well. Microplate was then sealed with a foil cover and incubated for 1 hour at room temperature on a plate shaker set to 800rpm. Wash procedure was then performed x3 times, as described above. The prepared Streptavidin-PE mix was vortexed briefly and 50μL was added to each well, and the microplate was the sealed with a foil cover and incubated for 30 minutes at room temperature on a plate shaker set to 800rpm. Wash procedure was then performed x3 times, as described above. Microparticles within the wells were then resuspended in 100μL Wash Buffer and incubated for 2 minutes at room temperature on a plate shaker set to 800rpm.

2.6.4 Luminex settings

Acquisition of Luminex assay was performed on Luminex® 200 (Institute of Infection, Immunity and Inflammation, University of Glasgow), set to an instrument flow rate of 60μL/minute, sample volume of 50μL, and doublet discriminator gates were set to 8000 and 16,500. Microparticle regions were set for each target analyte: CCL2 (18), CCL3 (46), CCL4 (51), CCL5 (38), CCL7 (39), CCL11 (74), CCL12 (42), CCL20 (48), CCL21 (72), CCL22 (75), CXCL1 (13), CXCL2 (20), CXCL10 (37), CXCL12 (54), CXCL13 (21), GM-CSF (12), IFN-γ (33), IL-1α (47), IL-2 (22), IL-3 (34), IL-4 (25), IL-5 (26), IL-6 (27), IL-10 (28), IL12p70 (15), IL-13 (29), IL-16 (35), 1IL-17A (30), IL-17E (55), IL-27 (56), IL-33 (43), M-CSF (45) and TNF-α (14). The count per region was set to 50, and the MFI was the recorded for each analyte region in each well. Using the standard concentrations on the Certificate of Analysis, the concentrations of the 3-fold standard dilutions were calculated. The duplicate readings from each standard and samples were averaged and the MFI from blank wells then subtracted. Analyte concentrations were determined by extrapolation from standard curves and multiplied by the dilution factor.

2.7 Western Blot

2.7.1 Protein extraction

PDAC tumour pieces frozen in RNAlater (described previously) were removed from -80℃ freezer, thawed on ice and Precellys Evolution Homogenizer (Bertin Technologies) prepared as previously described. 1X Lysis Buffer was prepared using 100X HALT™ Protease and Phosphatase (1861281, Thermo Scientific), 100X 0.5M EDTA (1861274, Thermo Scientific) and RIPA Buffer (89901, Thermo Scientific), and 200μl lysis buffer was added to PHT tube containing PDAC tumour tissue. Samples were then processed by Hard program at 5000rpm for 3x 20 seconds with 20 second pauses. PHT tubes were then centrifuged at 4000rpm for 5 minutes at 4℃. Supernatants were then transferred to ice cold 1.5mL Eppendorf tubes. Debris was then removed through centrifugation at 13,000rpm for 30 minutes at 4℃, and supernatants were then collected in ice cold 1.5mL Eppendorf tubes and transferred to -80℃ freezer for storage.

Extracted protein supernatants were then measured for protein levels by Microplate BCA™ Protein Assay Kit (23252, ThermoFisher). BCA standards were prepared from 2mg/mL albumin standard (23209, Thermo Scientific) at the following concentrations: 2000μg/mL (neat); 1000μg/mL, 400μg/mL, 200μg/mL, 100μg/mL and 80μg/mL and were loaded onto the 96 well plate (1825310, Thermo Scientific) along with neat protein samples and protein samples diluted 1:5 and 1:10 in distilled water. BCA/Cu(II) sulphate solution was prepared by combining 5mL Solution A (BCA)(23221, Thermo Scientific) with 100μL Solution B (Cu(II) Sulphate Pentahydrate 4%w/v (1859078, Thermo Scientific). 200μL of BCA/Cu(II) Sulphate solution was then to each well, and incubated for 30 mins at 37℃. Following incubation, plate was read on SpectraMax® ABS Plus with SoftMax Pro software to determine protein concentration.

2.7.2 Western blot

After determination of the protein concentration, 30μL of reaction mixture was prepared as follows: 20ng of protein sample in distilled water (19.5μl), 3μL 10X Sample Reducing Agent (B0009, Life Technologies) and 7.5μL 4X LDS Sample Buffer (B0007, Life Technologies). 1000mL of Running Buffer was then prepared

as follows: 950mL distilled water, 50mL 20X MES SDS Running Buffer (B0002, Life Technologies) and 2mL Antioxidant (BT0005, Invitrogen). Gel apparatus was prepared and filled with 800mL running buffer. Protein samples were retrieved from -80℃ freezer and placed in heat block for 10 minutes at 95℃, vortexed and then centrifuged briefly at 13,000rpm. 6μL of protein reference ladder (SM1163, ThermoFisher), 25μL of protein sample and 25μL of recombinant IL-33 (210-33, Peprotech) were loaded into a pre-cast gel (4-12% Bis-Tris Plus, NW04122BOX, Invitrogen), which was then run at 100V for 1hr 15 minutes. Samples were then transferred to iBlot 2 NC Mini Stacks (IB23002, Invitrogen) and placed in iBlot 2 Gel Transfer Device (IB21001, Invitrogen) for membrane transfer. Membranes were then blocked with blocking buffer (1X TBST with 5% milk) and incubated for 1hr at room temperature with gentle agitation. Membranes were then washed in TBST for 1x 15 minutes and 3x 5 minutes, and then incubated with goat anti-mIL-33 primary antibody (AF3626, R&D Systems, 1:3000) and anti-mβ-actin (A5316, Sigma, 1:5000) overnight at 4℃ with gentle agitation. Membranes were then washed in TBST for 1x 15 minutes and 3x 5 minutes at room temperature, and then incubated with anti-goat HRP-linked secondary antibody (ab6741, abcam, 1:20,000) or anti-mouse HRP-linked secondary antibody (12.2015, Cell Signalling, 1:3000) for 1hr at room temperature with gentle agitation. Membranes were washed in TBST for 1x 20 minutes and 4x 5 minutes, transferred to Wahtmann paper and then coated in luminol solution (Reagent 1 – Peroxide solution, Reagent 2 – Luminol Enhancer Solution) (Pierce™ ECL Western, 32209, Thermo Scientific). Membranes were then exposed on ChemiDoc Imager (Bio-Rad). Membranes were stripped with stripping buffer (10mL 1% SDS, 10mL 2M Glycine and 80mL distilled water) for 1 hour at room temperature with gentle agitation then rinsed 3x with TBST. Membranes were washed in TBST for 1x 15 minutes and 2x 5 minutes, and then blocked overnight in blocking buffer at 4℃.

2.8 Statistics

All statistical analyses were performed on GraphPad Prism (v9.0.2). For metastasis scoring, Fisher's exact test was used. Fisher's test is used to determine if the proportions of one variable are significantly different on the proportions of another variable. In this case, it was used to determine if the proportions of metastatic incidence in KPC mice are significantly different from

the proportions of metastatic incidence in KPC;Tcrd$^{-/-}$ mice. Power calculation was performed to determine appropriate sample size and was compared to previously published studies of metastasis incidence in spontaneous breast cancer models. It was determined that a minimum of 30 mice would be required in each cohort to reach statistical significance. To compare two groups the Mann Whitney test was used for a non-paired, non-parametric analysis. Non-paired due to the sample groups (ie KPC and KPC;Tcrd$^{-/-}$) do not naturally pair together, and non-parametric owing to the small sample size and the abnormal distribution of the data. The Kruskal-Wallis test is an extension of the Mann-Whitney test, as it performs non-paired and non-parametric analysis in more than two groups. Both Mann-Whitney and Kruskal-Wallis tests do not assume normal distribution. P values shown as * P < 0.05, ** P<0.01 and *** P<0.005.

Chapter 3   Phenotyping γδ T cells in KPC mice.

3.1 Introduction and Aim.

Immune cell paucity is a defining characteristic of PDAC, but there is a growing appreciation that γδ T cells play an important role in driving tumourigenesis and subverting anti-tumour immunity. As previously mentioned, pro-tumour γδ T cells can be identified through surface marker expression (CCR6$^+$CD27$^-$) and TCR usage (Vγ4$^+$/Vγ6$^+$), but mainly through their expression of the pro-tumour cytokine IL-17A, which is demonstrated in various tumour settings.(Rei et al., 2014) (Ma et al., 2014) (Coffelt et al., 2015) It has been shown that γδ T cells (RORγt$^+$) are rarely observed in normal pancreas but are found to increase by roughly 50-fold in precursor PanIN lesions. (McAllister et al., 2014) Additionally, the expression of oncogenic Kras^{G12D} leads to increased expression of IL-17A receptors (IL-17R) in PanINs, which sensitises them to IL-17A signalling, and the loss of IL-17A delays PanIN progression and reduces fibrosis.(McAllister et al., 2014) In the *Mist1$^{CreERT2/+}$;LSL-Kras^{G12D}* (KC^{iMist1}) model, the synergistic influence of Kras^{G12D} and pancreatitis was found to increase the production of IL-17A from both CD4$^+$ (Th17) and γδ T cells, but leaves anti-tumour IFN-γ and TNF-α production unchanged. (McAllister et al., 2014) Additionally, the production of IL-17A in the early TME has been found to promote stemness-related genes such as DCLK1 in PanIN lesions, associated with poorer prognosis in human PDAC patients. (Zhang et al., 2018) Given that γδ T cells are major sources of IL-17A and are significantly increased in early PDAC, this evidence suggests they may play an important role in driving early tumourigenesis.

PDAC is considered an immunologically cold tumour, and very little is known about the pro-tumour functions of infiltrating γδ T cells despite their presence in early tumourigenesis. However, Daley et al. suggest that γδ T cells constitute a significant portion of the TIL population in human PDAC, making up an average of 40%. (Daley et al., 2016) Interestingly, PDAC-infiltrated Vγ4$^+$ cells are enriched compared to the spleen; they produce significant levels of IL-10 and IL-17A; and they display increased expression of CCR2, CCR5 and CCR6 which is indicative of pro-tumour function in mice. (Daley et al., 2016) The loss of γδ T cells in *Pdx1-Cre;Kras^{G12D}* (KC) mice also reduced fibrosis, increased survival, and depletion of Vγ4 cells in orthotopic KPC mice was tumour-protective and

extended survival. (Daley et al., 2016) The protumour γδ T cell function in orthotopic KPC mice was mainly driven through the expression of exhaustion ligands PD-L1 and Galectin-9, which directly inhibited αß T cell (CD4$^+$/CD8$^+$) activation through checkpoint ligation.(Daley et al., 2016) These findings indicate that PDAC-infiltrating γδ T cells have potent immune-suppressive function, contribute to tumourigenesis through promoting stromal deposition, and that deletion of γδ T cell populations may be beneficial. Finally, there is also evidence that tumour-infiltrating γδ T cells in human PDAC are located proximally to *pancreatic stellate cells* (PSCs) within the TME and drive the production of pro-tumour IL-6 from PSCs — mediating protumour function through cellular crosstalk within the stromal compartment. (Seifert et al., 2020)

The above study by Daley et al. is one of the few examples within the literature of γδ T cell phenotyping in PDAC, however, there still exists a significant knowledge gap in the literature in both murine and human PDAC. Whilst informative, the study by Daley et al. has limitations, namely the use of different PDAC models. Firstly, the use of the KC model crossed with γδ-deficient (Tcrδ$^{-/-}$) mice; as the KC model has very long latency and does not always result in invasive PDAC when compared to the gold standard KPC.(Westphalen and Olive, 2012) Additionally, the use of orthotopic KPC models in place of spontaneous KPC mice is not a faithful recapitulation of human PDAC due to reduced tumour cell heterogeneity from *in vitro* passaging, and also the peri- and post-operative inflammatory insults that may alter immune responses. (Lee et al., 2016) Finally, given γδ T cell rarity, the finding that they constitute an average of 40% of the PDAC TILs is astonishingly high and deserves greater investigation.

I aimed to address these shortcomings by phenotyping γδ T cells in spontaneous endpoint KPC mice, confirming their pro-tumour function and determining their infiltration at various timepoints, all of which will enhance our understanding of γδ T cell kinetics and phenotype in murine PDAC.

3.2 γδ T cell kinetics in PDAC progression.

3.2.1 γδ T cells are abundant in late stage KPC PDAC tissue.

In the first set of experiments, I set out to comprehensively define γδ T cell infiltration in normal pancreas tissue, PanIN lesions and advanced PDAC. The first step was to visualise γδ T cells in the primary tumour (PDAC), main metastatic site (liver) and in lymphoid organs (spleen), and to achieve this I utilised RNAscope targeting the γδ T cell receptor (TCR). RNAscope is a form of *in situ hybridisation* (ISH) that uses RNA-specific probes that bind target RNA, in this case the delta chain constant region (Trdc) of the γδ TCR. These probes then hybridise together and enable the amplification of RNA-specific signals with very little background contamination. When quantifying RNAScope by random fields of view (FOV), I found no observable evidence of γδ T cells in the pancreas of tumour-free mice but found them to be relatively abundant in endpoint PDAC tumours (Figure 3-1A). The opposite trend occurred in liver tissue, where there were fewer γδ T cells found in livers from KPC mice when compared to WT controls (Figure 3-1B). I initially hypothesised that γδ T cells might be migrating to initiate the formation of, or in response to, PDAC tumours. In support of this I found significantly fewer γδ T cells in the spleen of KPC mice compared to WT controls (Figure 3-1C). This early data suggests that γδ T cells may be migrating from the liver and exiting circulation into PDAC tissue in late stage KPC mice.

3.2.2 γδ T cells accumulate in late-stage PDAC tissue, but not in early tumour progression.

I next sought to determine the kinetics of γδ T cell infiltration throughout pancreatic tumour progression and performed additional Trdc RNAScope at 6wk and 10wk timepoints. In 6wk KPC mice, PanIN lesions are typically well established, and at 10 weeks advanced PanINs can be found — the 10wk timepoint can be regarded as the halfway stage based on median KPC survival of roughly 5 months. (Herreros-Villanueva et al., 2012) In 6-week pancreas, γδ T cells were not significantly infiltrated as observed in endpoint PDAC tissue (Figure 3-2A). Conversely, in 6wk KPC livers there is a similar reduction in γδ T cells that was observed in endpoint tissue (Figure 3-2B). Finally, no differences were observed in γδ populations in 6wk spleen compared to WT (Figure 3-2C). Results from 10wk RNAscope reveal a similar trend in all tissues, and so these

data suggest that γδ T cells do not infiltrate the PDAC TME until late stage tumourigenesis. Despite the decrease in 6wk KPC liver, I did not see a corresponding change in either spleen or pancreas, suggesting my hypothesis that γδ T cells migrate to PDAC tissue may not apply to early tumourigenesis. This reduction could also be due to increased cell death or reduced proliferation of local γδ T cell populations and requires further investigation. Regardless, these data show that γδ T cells infiltrate endpoint PDAC tissue but are not found at any significant levels in early stage tumourigenesis.
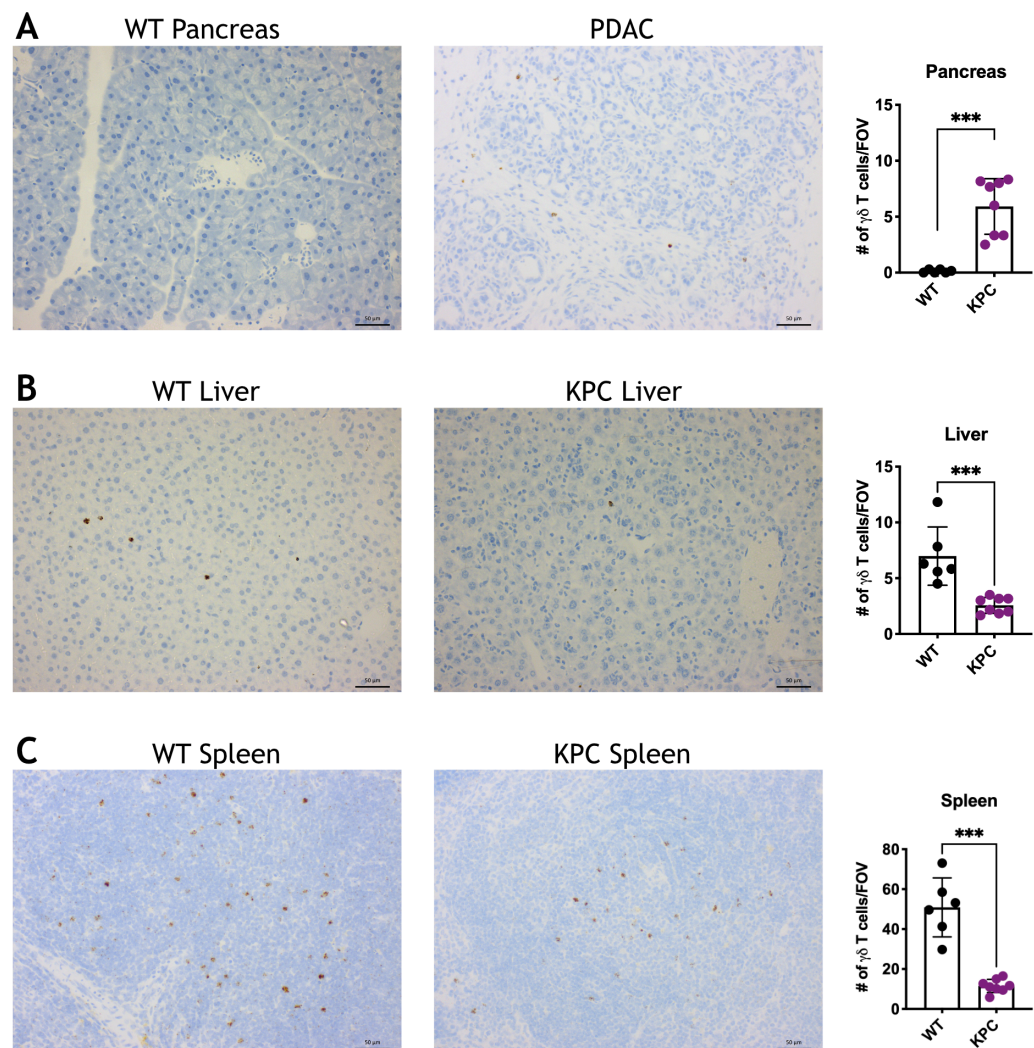
Figure 3-1 γδ T cells infiltrate endpoint PDAC tissue, but not tumour-free pancreas.
RNAScope *in situ hybridisation* (RNA-ISH) was performed to visualise and quantify γδ T cells within PDAC (A), liver (B) and spleen (C) tissue in clinical endpoint KPC mice and age-matched controls. RNAScope probes were specific for the delta chain constant region of the TCR. Representative images are shown at x20 magnification and subsequent quantification is also shown. γδ T cell numbers in WT (n=6) and KPC tumour-bearing mice (n=8) were obtained through random fields of view (FOV), and each data point represents the average of 6 FOVs per mouse. Scale bars represent 50μm. *** P < 0.005 determined by Mann-Whitney U-Test.
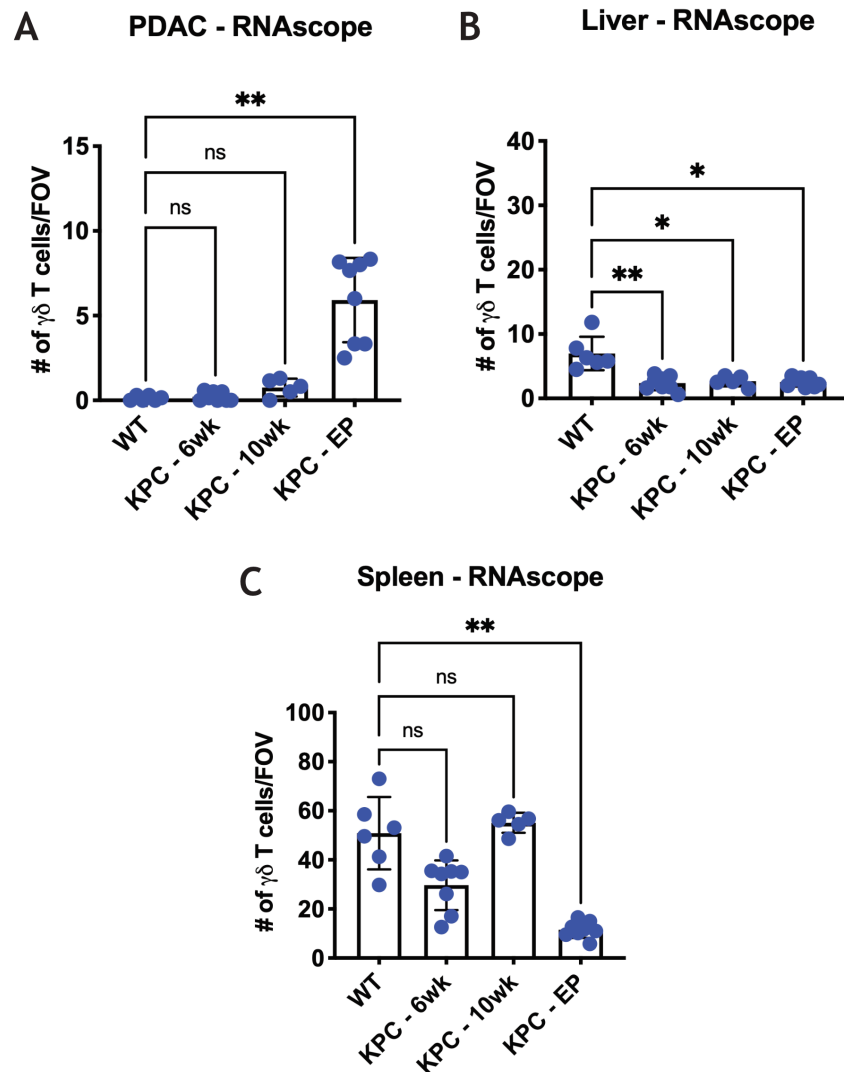
Figure 3-2 γδ T cells infiltrate KPC PDAC tumours in late stage tumourigenesis, and not during early-stage tumourigenesis.
KPC mice were taken at 6 weeks (n=8), 10 weeks (n=5) and humane clinical endpoint (n=8). Trdc RNA-ISH was then performed in pancreas (A), liver (B) and spleen (C). WT mice (n=6) were age-matched to clinical endpoint mice. γδ T cell numbers were obtained through random field of views (FOVs), and each data point represents the average of 6 FOVs per mouse. * $P < 0.05$ and ** $P < 0.01$ as determined by Kruskal-Wallis test.

3.3 Phenotyping of γδ T cells in KPC mice.

3.3.1 Flow cytometry confirms γδ T cells infiltrate KPC PDAC tumours.

Given the evidence in established literature that PDAC-infiltrated γδ T cells are sources of IL-17A, I aimed to confirm this in my spontaneous KPC model. To achieve this, I designed a flow cytometry panel that identified γδ T cells, and targeted IFN-γ, Granzyme B and IL-17A production through intracellular staining. The representative image below demonstrates the gating strategy I used to identify bulk γδ T cells, delineate pro- and anti-tumour subsets based on CD27

status, and their IL-17A/IFN-γ status (Figure 3-3A). Identification of bulk γδ T cells (CD3+γδ TCR+) by flow cytometry revealed that proportions of γδ T cells in PDAC tumours from KPC mice are increased compared to tumour free-pancreas, which corroborates my RNAScope data (Figure 3-1B). However, bulk γδ T cells remain unchanged in KPC liver and spleen when compared to WT controls (Figure 3-3B).
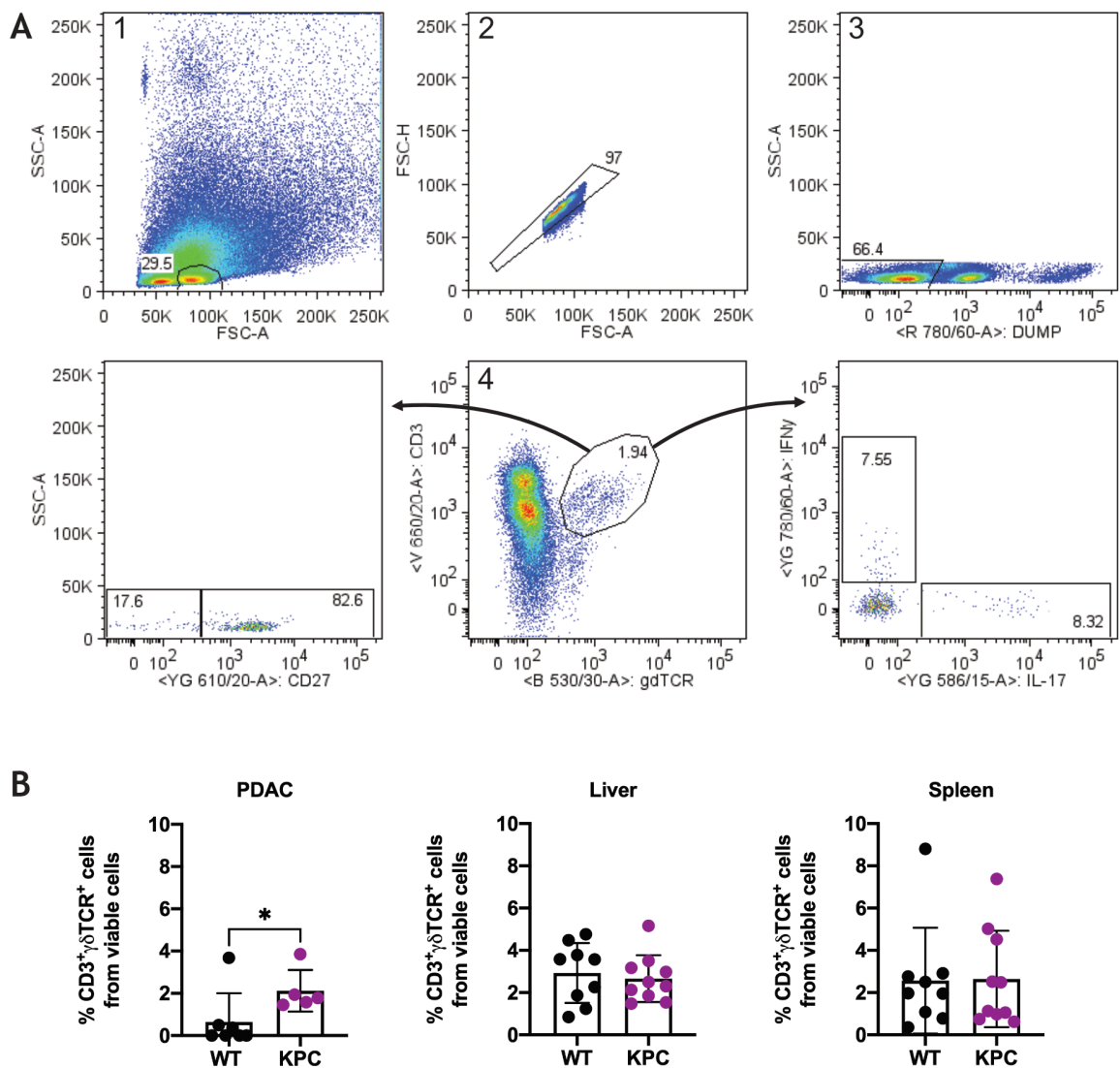
Figure 3-3 Flow cytometry confirms γδ T cells infiltrate endpoint PDAC tissue.
KPC mice were aged to clinical endpoint, and γδ T cells were isolated from primary PDAC, liver and spleen. Representative image illustrating the gating strategy used to identify γδ T cells – bulk lymphocytes (1), doublet exclusion (2), dump channel exclusion (3) and CD3+ γδ TCR+ cells (4), followed by CD27 subset delineation and cytokine production (A). Quantification of bulk γδ T cell populations shown as a proportion of viable cells that are CD3+γδ TCR+ (B). * P < 0.05 determined by Mann-Whitney U-Test.

3.3.2 PDAC-infiltrated γδ T cells display a pro-tumour phenotype through IL-17A production.

γδ T cells are a heterogenous population with different effector functions, and so I aimed to phenotype γδ T cells in PDAC, liver and spleen tissue to determine if a specific population is preferentially expanded in KPC mice. More specifically, I looked to assess the changes in anti-tumour (CD27$^+$IFN-γ$^+$) and pro-tumour (CD27$^-$IL-17A$^+$) γδ T cells, as CD27 status and production of IFN-γ and IL-17A delineates γδ T cells into two mutually exclusive populations. In PDAC tissue, I found a significant increase in IL-17A production by γδ T cells compared to WT pancreas, but IFN-γ production remained unchanged, suggesting a predominately pro-tumour function in PDAC tissue (Figure 3-4A). Given that pro-tumour γδ T cells are also defined as CD27$^-$, I looked to determine if the CD27$^-$ γδ T cell subset expands in PDAC tissue from KPC mice. However, there was no corresponding expansion of the CD27$^-$ (pro-tumour) subset and the CD27$^+$ (anti-tumour) subset also remained unchanged in PDAC tissue, this finding was unexpected and cannot be explained by any current defined literature (Figure 3-4A). In KPC livers, IL-17A production from γδ T cells was significantly reduced but IFN-γ production and the CD27 subsets remained unchanged compared to WT controls (Figure 3-4B). I also investigated γδ T cell phenotypes in spleen tissue to determine if the phenotype of circulating γδ T cells in KPC mice is different from primary PDAC tissue and the metastatic niche. I found that γδ T cells in the spleen of KPC mice had no changes to IL-17A production but produced significantly less IFN-γ compared to WT controls (Figure 3-4C). Unlike PDAC and liver tissue from KPC mice, the pro-tumour CD27$^-$ γδ T cells in the spleen from KPC mice significantly expands at the expense of the anti-tumour CD27$^+$ population (Figure 3-4C).

These data show that bulk γδ T cell populations in KPC PDAC tissue display a predominately pro-tumour function, owing to the significant production of IL-17A. Conversely, the significant reduction of IL-17A production by γδ T cells in KPC liver tissue shows that γδ T cell phenotype within the metastatic niche of KPC mice is distinct from primary PDAC tissue. The reduction of IL-17A produced by liver γδ T cells indicates a less potent pro-tumour function; however, the lack of increased IFN-γ production by liver γδ T cells indicates this does not translate into enhanced anti-tumour function. To summarise, I have shown that γδ T cells

in primary PDAC and the liver metastatic niche of KPC mice have distinct phenotypes, demonstrated through differential production of IL-17A. The expansion of CD27⁻ γδ T cells in KPC spleen indicates a systemic signal might be driving the expansion of circulating pro-tumour γδ T cells, but that an additional PDAC TME-specific signal is needed to elicit IL-17A production by γδ T cells following infiltration into the PDAC TME.
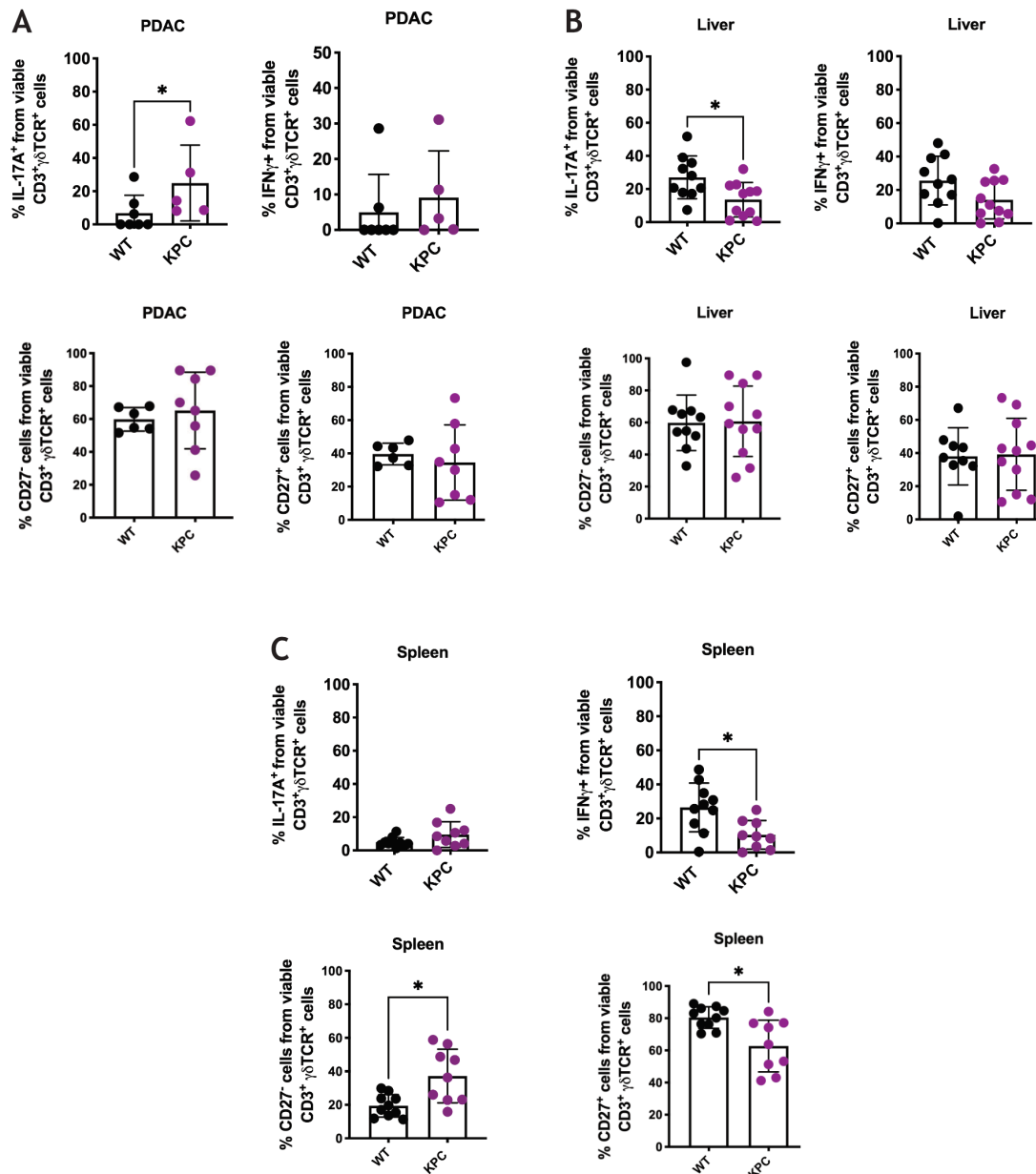
Figure 3-4 γδ T cells in PDAC tissue display a pro-tumour IL-17A⁺ phenotype.
KPC mice were aged to clinical endpoint and γδ T cells were isolated from PDAC, liver and spleen. Quantifications of PDAC-derived γδ T cell cytokine production (WT n=7, KPC n=5) along with CD27 subset proportions (WT n=6, KPC n=8) from PDAC tissue (A). Quantifications of liver-derived γδ T cell cytokine production (WT n=10, KPC=11) and CD27 subset proportions (B). Quantifications of spleen-derived γδ T cell cytokine production and CD27 subset proportions (WT n=10, KPC n=9) (C). * P < 0.05 determined by Mann-Whitney U-Test.

3.3.3 The expansion of CD27⁻ γδ T cells in KPC spleen is attributable to the Vγ6⁺Vδ6.3⁺ subset.

Following my finding that circulating pro-tumour CD27⁻ γδ T cells are significantly expanded in the spleen of KPC mice, I sought to further characterise γδ T cell phenotype in my KPC model and determine if this expansion is driven by a particular subset of γδ T cells. As previously mentioned, murine γδ T cells arise in developmental waves with divergent TCR γ chains, differential effector function and distinct tissue-homing capacity. (Parker and Ciofani, 2020) (Prinz et al., 2013) (Silva-Santos et al., 2015) To investigate this, I designed a flow cytometry panel that identified γδ T cells and further stratified them into distinct subgroups based on γ chain TCR usage (Figure 3-5). More specifically, I targeted the Vγ1⁺, Vγ4⁺ and Vγ6⁺ γδ T cell subsets, as the established literature identifies Vγ1⁺ and Vγ4⁺ cells as sources of IFN-γ, with Vγ4⁺ and Vγ6⁺ cells the main IL-17A producers. (Prinz et al., 2013) The anatomical locations also directed my focus towards these subsets; Vγ1⁺cells are found in the liver, spleen, lymphoid tissue and blood; Vγ4⁺ cells are found in liver, lungs, lymphoid tissue and dermis; and Vγ6⁺ cells are located in the uterus, liver, lungs and tongue. (Parker and Ciofani, 2020) I did not include the Vγ5⁺ or Vγ7⁺ subsets due to their specific anatomical locations in the skin and small intestine epithelium, respectively. (Parker and Ciofani, 2020) However, one technical limitation was a complete lack of available fluorophore conjugated anti-Vγ6 antibodies. Our lab has recently conjugated an anti-Vγ6 antibody from a hybridoma cell line, but this requires additional labelling with a conjugation kit and was not available when I designed this flow cytometry panel. As a result, I could only define the Vγ6⁺ γδ T cell population as Vγ1⁻/Vγ4⁻, however, given the distinct anatomical locations of the Vγ subsets and the clear distinction between Vγ1⁺ and Vγ4⁺ subsets, this was not considered a major obstacle. (Figure 3-5). Thus, I aimed to determine if a specific Vγ TCR subset is expanded in KPC mice, and to ascertain if the current literature regarding Vγ subset compartmentalisation is applicable to the KPC model.

I also looked to investigate additional cytokines produced by γδ T cells in the KPC model, as I have already confirmed that γδ T cells are major sources of IL-17A in the primary tumour (Figure 3-4A). Established literature has already detailed that γδ T cells exert pro-metastatic function by systemic IL-17A

production, leading to increased granulocyte-colony stimulating factor (G-CSF) expression and the expansion of immune-suppressive neutrophils that promote breast cancer metastasis.(Coffelt et al., 2015) Thus, I looked to determine if γδ T cells from KPC mice can produce cytokines that direct crosstalk between other innate immune cell populations, and so focussed on M-CSF and GM-CSF, which both drive the mobilisation and differentiation of innate immune cells from bone marrow. There is published evidence that γδ T cells expand in response to plasmodium infection and produce M-CSF to direct myeloid cell differentiation.(Mamedov et al., 2018) Furthermore, the production of M-CSF was found to occur in a TCR-restricted manner, with nearly 75% of expanded γδ T cells expressing the V-segment TRAV15N-1 (Vδ6.3$^+$) during plasmodium infection. Finally, the expansion of Vδ6.3$^+$ γδ T cells is also associated with significant expression of M-CSF by γδ T cells in the spleen (>90%) and in the liver.(Mamedov et al., 2018) Therefore, published data shows that γδ T cells can directly shape the myeloid compartment through the systemic production of M-CSF. Thus, I aimed to determine if a particular subset of splenic γδ T cells is expanded in my KPC model, and if they can produce M-CSF or GM-CSF which may indicate γδ T cell-myeloid cell crosstalk.
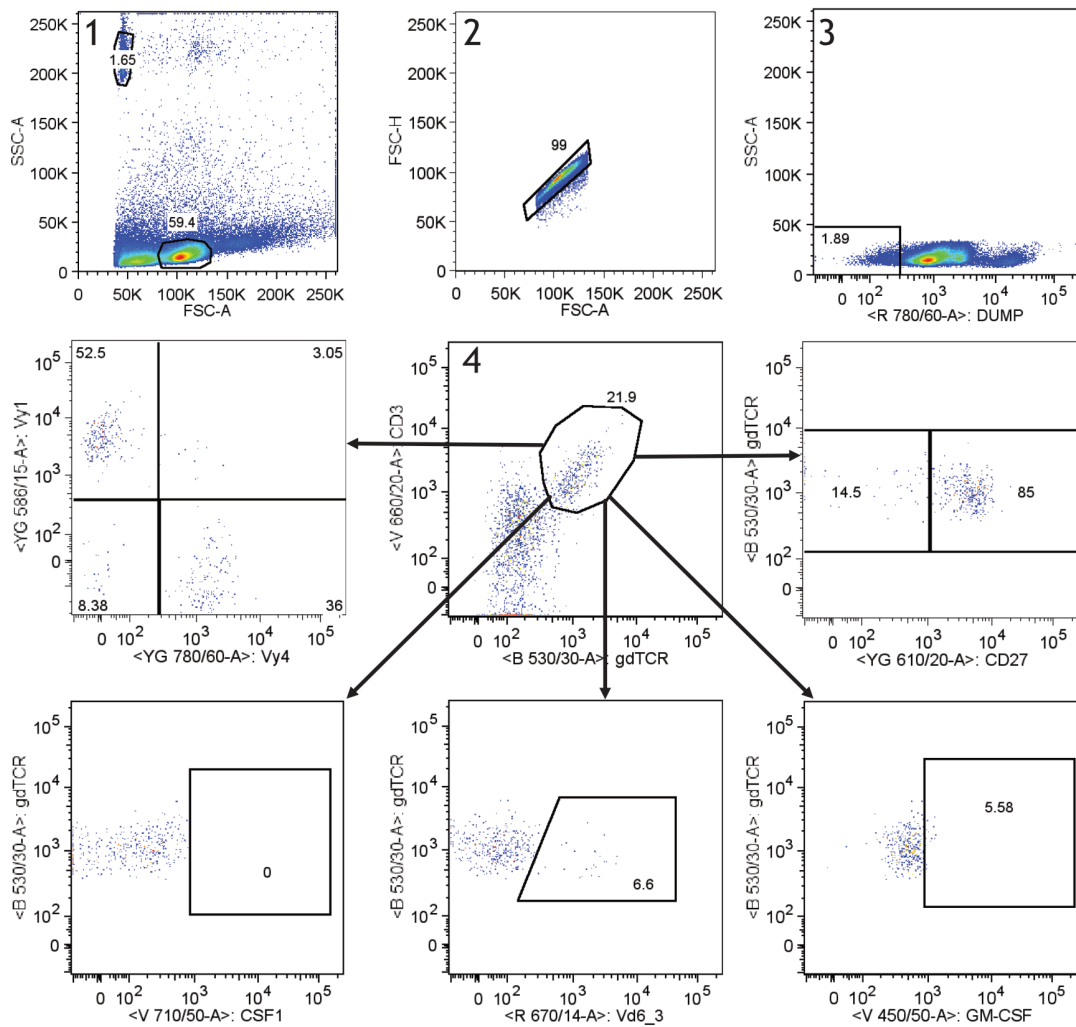
Figure 3-5 γδ T cell subsets are primarily Vγ1⁺ or Vγ4⁺ in WT tissue.
KPC mice were aged to clinical endpoint, but representative plots are of γδ T cells isolated from WT mice, which were aged alongside KPC mice. Representative image from WT liver illustrating the gating strategy used to identify γδ T cells – bulk lymphocytes (1), doublet exclusion (2), dump channel exclusion (3) and CD3⁺ γδ TCR⁺ cells (4), followed by identification of Vγ1⁺, Vγ4⁺ and Vδ6.3⁺ subsets, CD27 status and production of M-CSF (CSF1) and GM-CSF.

The first step in assessing the TCR usage in KPC spleen was to confirm my previous observation that CD27⁻ γδ T cells are expanded in the spleen of KPC mice (Figure 3-4C), which I was able to confirm (Figure 3-6A). Since γδ T cells produce significant levels of M-CSF during plasmodium infection, I then looked to see if bulk γδ T cells (CD3⁺γδ TCR⁺) from KPC spleen can produce M-CSF. I found no evidence of M-CSF production by splenic γδ T cells in either KPC mice or WT controls, but instead found that GM-CSF production in γδ T cells from KPC spleens is significantly increased compared to WT controls (Figure 3-6B). Additionally, I discovered that the Vγ1⁺ subset was significantly reduced and there was no change to the Vγ4⁺ subset in KPC spleen when compared to WT mice; however, the Vγ1⁻/Vγ4⁻ subset was significantly increased along with the

Vδ6.3$^+$ subset (Figure 3-6C). I then investigated if Vγ1$^+$, Vγ4$^+$, Vγ1$^-$/Vγ4$^-$ and Vδ6.3$^+$ subsets could produce M-CSF and GM-CSF. The production of M-CSF by bulk γδ T cells and individual subsets was negligible due to sub-optimal staining. However, I found that the Vγ1$^+$ and Vγ4$^+$ subsets displayed no significant production of GM-CSF, but that the Vγ1$^-$/Vγ4$^-$ and Vδ6.3$^+$ subsets in the spleen of KPC mice both produced significant levels of GM-CSF compared to WT controls (Figure 3-6D). Finally, I found that the expansion of the Vδ6.3$^+$ subset associates with the Vγ1$^-$/Vγ4$^-$ subset, but not the Vγ1$^+$ or the Vγ4$^+$ subsets (Figure 3-6E). To summarise, in KPC tumour-bearing mice, the Vγ6$^+$Vδ6.3$^+$ subset is significantly expanded in the spleen tissue compared to WT mice, and they produce significant levels of GM-CSF, an important granulocyte-stimulating cytokine.

Finally, I also looked to further phenotype γδ T cell cells in the liver metastatic niche, so I performed identical analyses as above in the livers of endpoint KPC mice. In short, both CD27 subsets remained unchanged (Figure 3-7A) and I observed no significant production of M-CSF or GM-CSF by liver γδ T cells (Figure 3-7B). Additionally, there was no expansion of any γ chain subset (Vγ1$^+$, Vγ4$^+$, Vγ1$^-$/Vγ4$^-$), the Vδ6.3$^+$ subset (Figure 3-7C/E) or any change to subset-specific cytokine production (Figure 3-7D). These findings suggest that the expansion of the Vγ6$^+$Vδ6.3$^+$ subset is restricted to the spleen, and that tissue tropism may impact γδ T cell phenotype in KPC tumour-bearing mice.
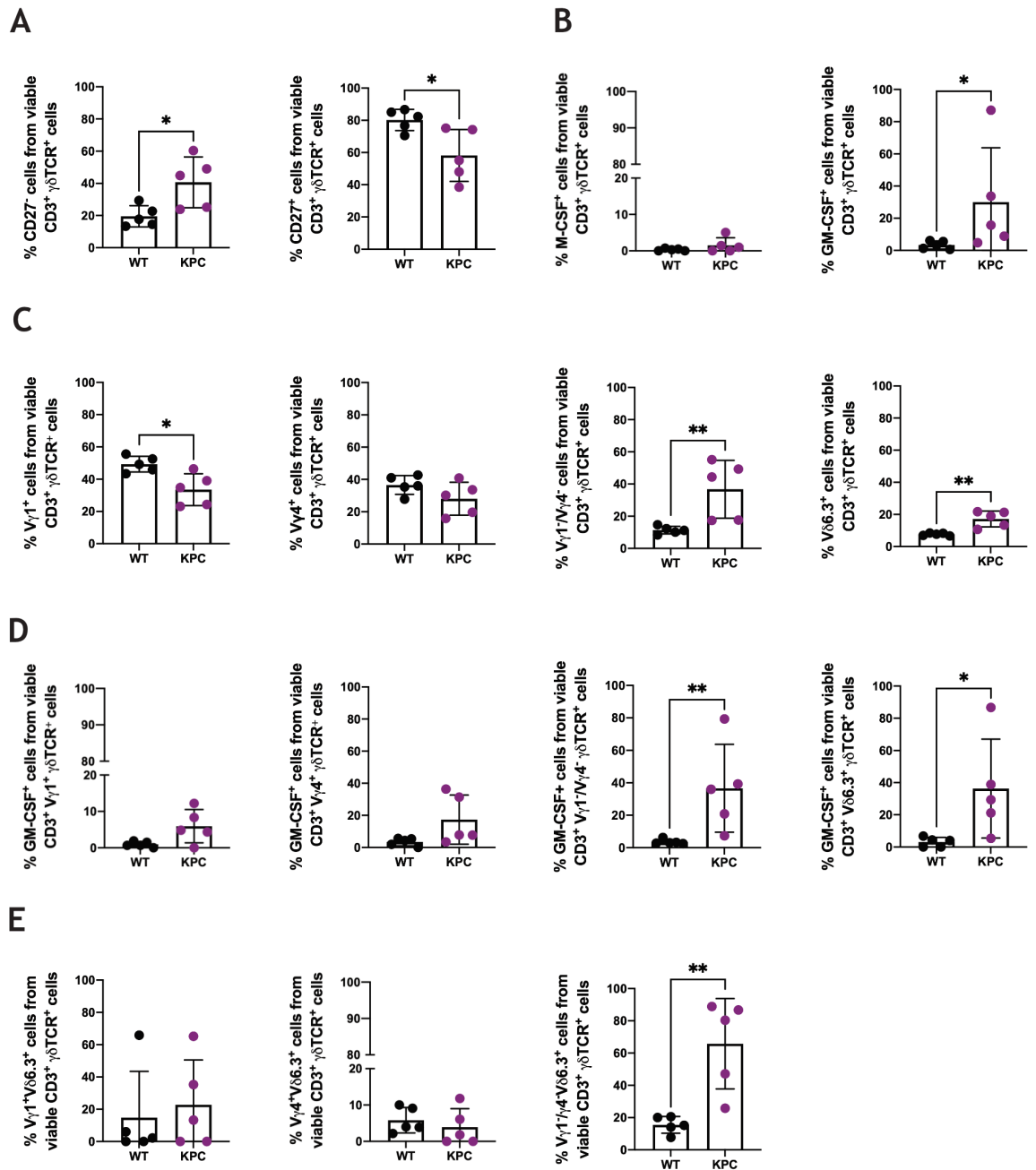
Figure 3-6 Vγ6+Vδ6.3+ cells are expanded in KPC spleen and produce GM-CSF.
KPC mice were aged to clinical endpoint and γδ T cells were isolated from spleen of KPC mice (n=5) and age-matched WT controls (n=5). Proportions of pro-tumour CD27− and anti-tumour CD27+ subsets from bulk γδ T cells (CD3+γδ TCR+) (A). Proportions of M-CSF+ and GM-CSF+ cells from bulk γδ T cells (B). Proportions of Vγ1+, Vγ4+, Vγ1−/Vγ4− and Vδ6.3+ subsets from bulk γδ T cells (C). Proportions of GM-CSF+ cells from Vγ1+, Vγ4+, Vγ1−/Vγ4− and Vδ6.3+ γδ T cells (D). Proportions of Vγ1+, Vγ4+ and Vγ1−/Vγ4− cells from Vδ6.3+ γδ T cells (E). * P < 0.05 ** P < 0.01 determined by Mann-Whitney U-Test.
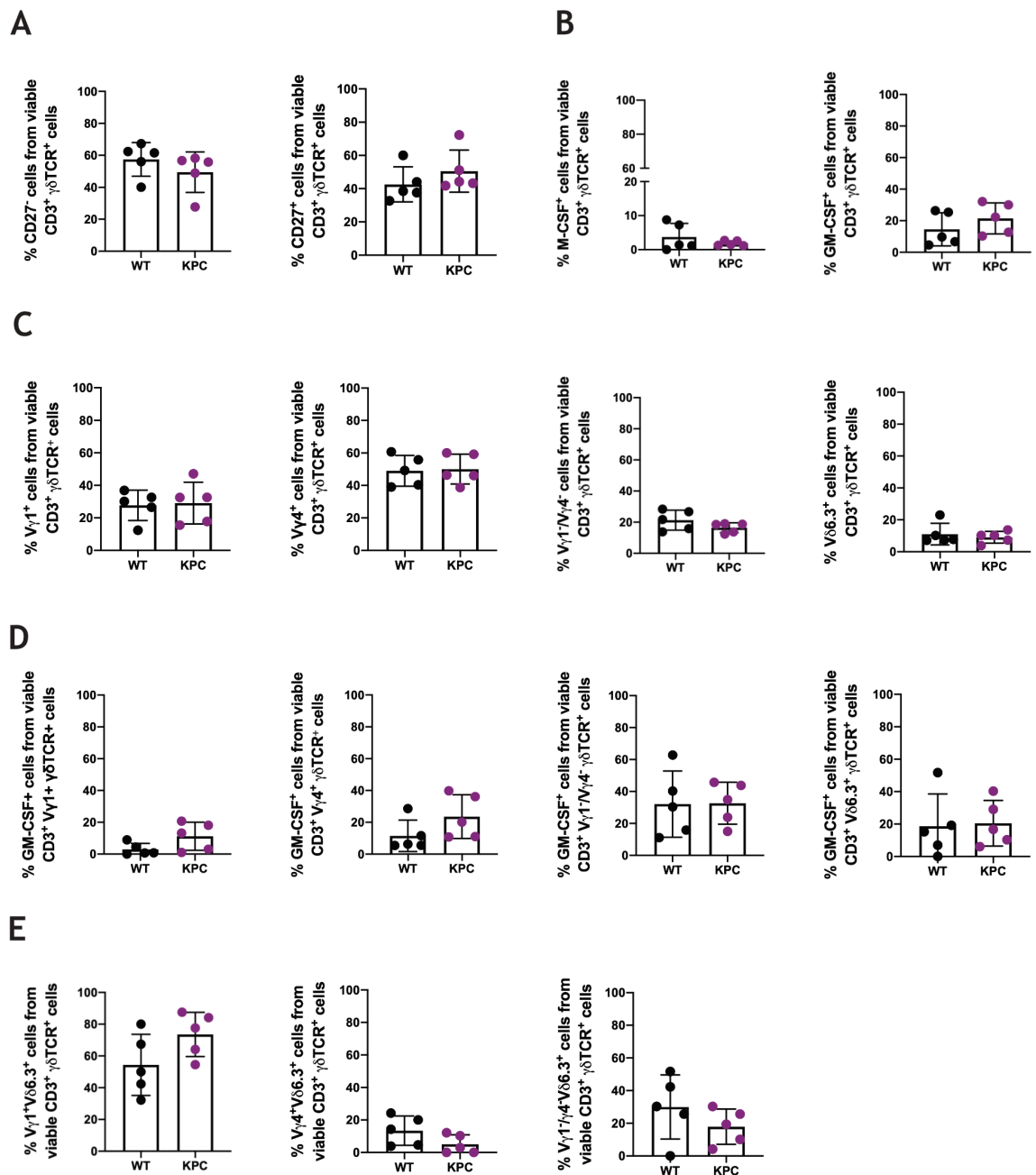
Figure 3-7 Vγ6⁺Vδ6.3⁺ cells are not expanded in KPC livers and do not produce GM-CSF.
KPC mice were aged to clinical endpoint and γδ T cells were isolated from livers of KPC mice (n=5) and age-matched WT controls (n=5). Proportions of pro-tumour CD27⁻ and anti-tumour CD27⁺ subsets from bulk γδ T cells (CD3⁺γδ TCR⁺) (A). Proportions of M-CSF⁺ and GM-CSF⁺ cells from bulk γδ T cells (B). Proportions of Vγ1⁺, Vγ4⁺, Vγ1⁻/Vγ4⁻ and Vδ6.3⁺ subsets from bulk γδ T cells (C). Proportions of GM-CSF⁺ cells from Vγ1⁺, Vγ4⁺, Vγ1⁻/Vγ4⁻ and Vδ6.3⁺ γδ T cells (D). Proportions of Vγ1⁺, Vγ4⁺ and Vγ1⁻/Vγ4⁻ cells from Vδ6.3⁺ γδ T cells (E).

3.4 Bulk RNA-seq analysis of γδ T cells from KPC tumour-bearing mice and WT mice.

Phenotypic analysis by flow cytometry has revealed differential cytokine production by γδ T cells in different tissues; for example, γδ T cells from PDAC tissue produce significant levels of IL-17A, and Vγ6⁺ γδ T cells from spleen tissue

produce significant levels of GM-CSF. This heterogeneous function suggests that γδ T cells in KPC mice display tissue tropism and may direct different effector functions in a context- and tissue-dependent manner. To further phenotype γδ T cells in KPC mice, I utilised the Molecular Technology Service available at the Beatson Institute for Cancer Research to perform bulk RNA-Seq analysis on sorted γδ T cells to further elucidate their phenotype and cytokine production. Given I have shown that IL-17A-producing γδ T cells are found in the PDAC TME, I would ideally have performed bulk RNA-seq analysis on sorted γδ T cells from the PDAC TME. However, as shown by RNAScope field-of-view and flow cytometric analysis, the numbers of γδ T cells in WT pancreas is very low and therefore could not act as an adequate control population. Additionally, although γδ T cells do infiltrate primary PDAC tissue, they are still a minor component of the TME, and the methods of extraction used would not provide sufficient yield for effective bulk RNA-seq analysis. Therefore, I chose to sort γδ T cells from the liver and the spleen of WT and KPC tumour-bearing mice, with the aim of phenotyping γδ T cells in the main metastatic site (liver) and in secondary lymphoid organs (spleen).

The gating strategy used to identify γδ T cells is shown below (Figure 3-8), where the aim was to sort γδ T cells based on their expression of CD3 (FITC, B530/30) and γδTCR (PE, YG582/15) and lack of DAPI (live/dead marker, V450/40) uptake. Prior to labelling with conjugated antibodies, the cell suspension for sorting underwent a purification step and was pre-treated with MojoSort^{TM} Mouse CD3 Positive Selection Kit (Biolegend) to remove all CD3$^-$ cells from the suspension. The subsequent suspension was then used to isolate γδ T cells (CD3$^+$γδTCR$^+$), represented by the colour magenta in the P4 gate (Figure 3-8D). The location of γδ T cells can be retrospectively view throughout the preceding gates, and as seen below, the gating inaccuracy in the doublet exclusion gate (FSC-W vs FSC-A) resulted in the inclusion of unwanted doublet populations in the analysis (Figure 3-8B). Differentially expressed gene analysis (DEGA) revealed this contamination is mostly from neutrophils, as *Lcn2* (lipocalin-2), *Mpo* (myeloperoxidase), *Ngp* (neutrophilic granule protein), *S100a9* and *Padi4* (peptidyl arginine deaminase 4) are all genes strongly associated with neutrophil biology; the expression of *Msr1* (macrophage scavenging receptor 1) also indicates contamination by macrophages (Figure 3-8E). Whilst this

contamination is not optimal, it could have arisen through a failure of the positive enrichment step for CD3$^+$ cells. Additionally, it could have occurred through potential direct cell-cell interactions between γδ T cells and neutrophils to create doublet populations that would otherwise have been excluded by more accurate doublet gating.
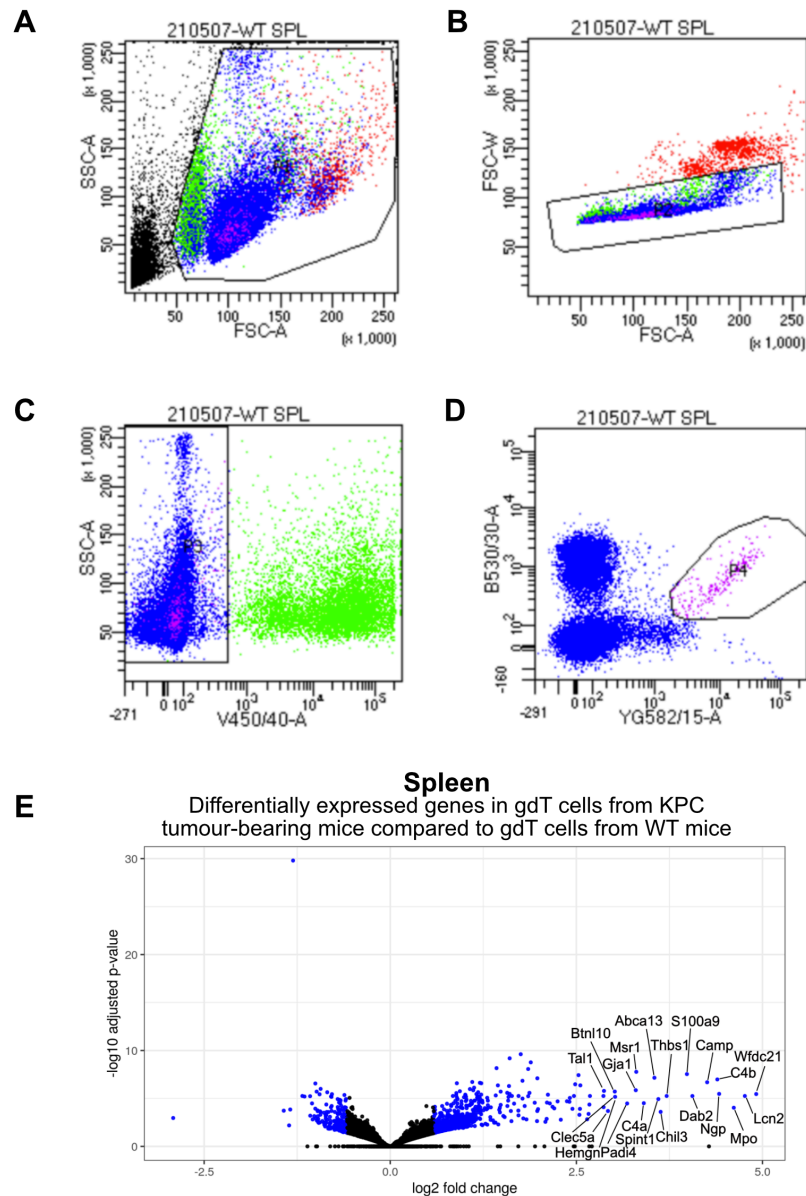
Figure 3-8 Inaccuracy of doublet exclusion gate resulted in contamination by myeloid cells. γδ T cells were isolated from single cell suspensions through the gating strategy shown above. DAPI live/dead marker was in the V450/40 channel, CD3$^+$ cells were identified by FITC conjugated antibody in the B530/30 channel and γδTCR$^+$ cells were identified by PE conjugated antibody in the YG582/15 channel. γδ T cells were sorted from SSC-A vs FSC-A plots (A), followed by doublet exclusion on FSC-W vs FSC-A plots (B), then dump channel exclusion on SSC-A vs V450/40 plots (DAPI) (C) and finally the selection of CD3$^+$γδ TCR$^+$ cells on B530/30 vs YG582/15 plots (D).Volcano plot illustrating the top 20 upregulated genes in γδ T cells sorted from KPC spleen compared to γδ T cells from WT spleen (E). Sorting performed by Tom Gilbey.

3.4.1 γδ T cells from KPC liver have few differentially expressed genes compared to γδ T cells from WT liver.

Following the analysis of splenic γδ T cells, I looked to determine if there were any differentially expressed genes in γδ T cells from KPC tumour-bearing liver compared to WT liver. In doing so I aimed to identify potential gene candidates that may indicate a γδ T cell-derived product that may locally influence the development of metastatic lesions. Following sequencing, it was discovered that one of the γδ T cell RNA samples from KPC tumour-bearing liver had significantly lower read depth compared to the other 15 samples, and so was excluded from the analysis. I found that γδ T cells from KPC tumour-bearing liver display 13 significantly upregulated genes when compared to γδ T cells from WT liver. These 13 genes include *Fn1* (fibronectin-1), *Igkv1-135*, *Thbs1* (thrombospondin-1), *Saa3* (serum amyloid A3), *Vcan* (versican), *Bst1* (bone marrow stromal cell antigen 1), *Arg1* (arginase 1), *F13a1* (coagulation factor XIII), *Ccl6*, *F10* (coagulation factor X), *Ccl9*, *Eps8* (epidermal growth factor receptor pathway substrate) and *Gda* (guanine deaminase) (Figure 3-9A). To better visualise hierarchical clustering and provide a clearer visualisation of differential gene expression between γδ T cells from WT and KPC-tumour-bearing spleen, I then used heatmaps to highlight the differentially expressed genes between the two cohorts (Figure 3-9B). Due to variable gene expression within the KPC samples, supervised analysis was performed to group WT γδ T cell and KPC γδ T cell samples together. However, as can be seen below the differentially expressed gene signatures appear to be driven by one KPC sample. Due to the exclusion of another KPC liver sample because of low read depth, significant variation between this sample and other KPC samples dominates the DEGA analysis.

A

Liver
Differentially expressed genes in gdT cells from KPC
tumour-bearing mice compared to gdT cells from WT mice

B
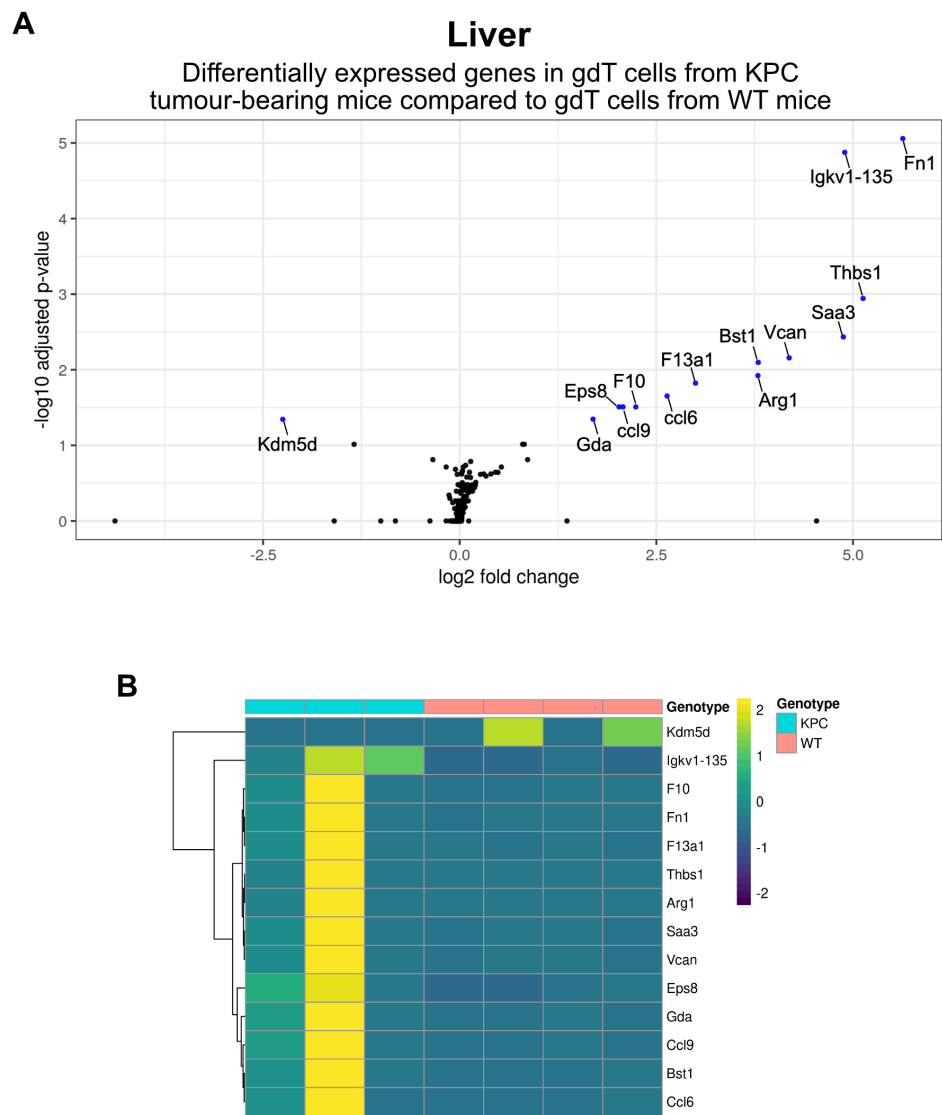
Figure 3-9 γδ T cells from KPC tumour-bearing liver have 14 significant differentially expressed genes compared to γδ T cells from WT liver.
γδ T cells from KPC (n=3) and WT (n=4) liver were sorted, and isolated RNA was sequenced. Unsupervised differentially expressed gene analysis (DEGA) was performed to identify differences in gene expression between γδ T cells from WT and KPC liver tissue. Annotated volcano plots showing all significantly differentially expressed genes in γδ T cells from KPC tumour-bearing liver (A). Heatmap plot to visualise hierarchical clustering and differential gene expression between γδ T cells from WT and KPC tumour-bearing liver (supervised analysis) (B). RNA sequencing performed by Billy Clarke and bioinformatics analysis was performed by Robin Shaw.

3.4.2 γδ T cells from KPC tumour-bearing spleen form distinct clusters from γδ T cells in WT spleen.

Given the extent of neutrophil contamination in the spleen tissue, and that the majority of the top 20 upregulated genes found in DEGA analysis are most likely neutrophil products, I looked to confirm if the upregulated genes observed in KPC liver γδ T cells (Figure 3-9) are also found in γδ T cells isolated from KPC spleen (Figure 3-10). Of the genes significantly increased in γδ T cells from KPC-

tumour-bearing liver, *Thbs1, Vcan, Gda, F10, Bst1, Ccl6, Saa3, Fn1* and *Ccl9* were also significantly upregulated in γδ T cells from KPC tumour-bearing spleen (Figure 3-10A). It should be noted that *Cd27* (CD27) is one of the gene hits that is significantly downregulated in γδ T cells from KPC tumour-bearing spleen when compared to WT γδ T cells (Figure 3-10A). This matches with my flow cytometry data where CD27⁻ γδ T cells expand in KPC spleen at the expense of the CD27⁺ γδ T cell subset (Figure 3-4C). Thus, the downregulation of *Cd27* acts as an internal control and confirms that the changes in gene expression, unless directly linked to myeloid cell biology, are likely attributable to γδ T cells. As shown through heatmaps, the gene expression profile of γδ T cells from WT spleen are distinct from the profiles of γδ T cells from KPC-tumour-bearing spleen (Figure 3-10B). Gene expression levels within the KPC cohort also displays an inherent heterogeneity, but some of the most differentially expressed genes within the heatmaps analysis are neutrophil-associated genes, including *Mmp9, Mpo and Clec5a* (Figure 3-10B).

To summarise, bulk RNAseq of sorted γδ T cells from both liver and spleen in KPC tumour-bearing mice have raised interesting results, particularly the expression of extracellular matrix-associated products (*Thbs1, Vcan* and *Fn1*) and chemokines (*Ccl6* and *Ccl9*). However, the expression of numerous neutrophil-associated genes suggests significant myeloid cell contamination. Thus, the overtly expressed neutrophil genes may be concealing differentially expressed genes within γδ T cells, which would otherwise have potentially identified γδ T cell-derived products that would have further clarified their phenotype and function in KPC mice.

A Spleen
Differentially expressed genes in gdT cells from KPC
tumour-bearing mice compared to gdT cells from WT mice

B
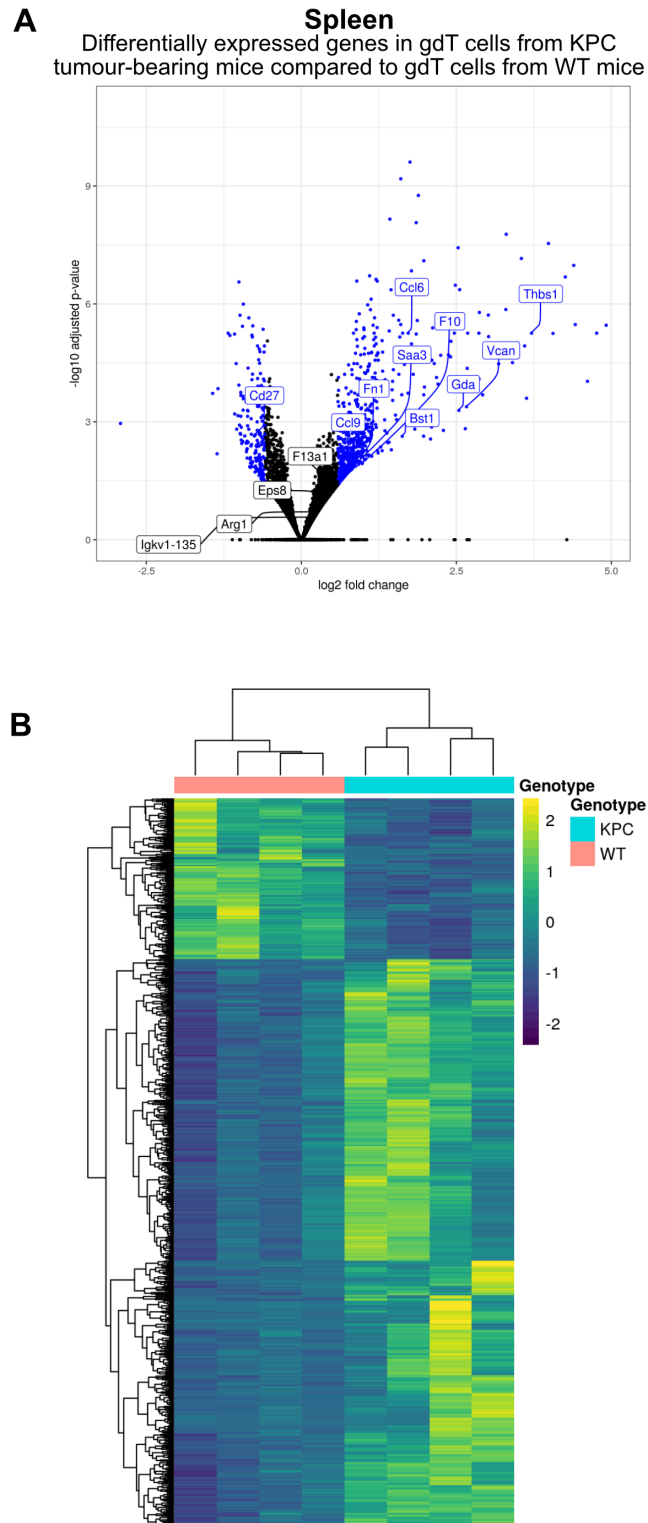
Figure 3-10 γδ T cells from KPC tumour-bearing spleen have distinct gene expression profiles when compared to γδ T cells from WT spleen.
γδ T cells from KPC (n=4) and WT (n=4) and spleen were sorted, and isolated RNA was sequenced. Unsupervised differentially expressed gene analysis (DEGA) was performed to identify differences in gene expression between γδ T cells from WT and KPC spleen tissue. Top differentially expressed genes from liver analysis are highlighted in volcano plot of differentially expressed genes in spleen γδ T cells (A). Heatmap plot to visualise hierarchical clustering and differential gene expression between γδ T cells from WT and KPC tumour-bearing spleen (B).

3.5 Discussion.

In this chapter, I aimed to confirm γδ T cell infiltration in PDAC tumours, determine γδ T cell kinetics throughout tumour progression, and phenotype γδ T cells in PDAC, liver and spleen tissue in KPC mice.

Firstly, I found that γδ T cells are not present in WT pancreas but are significantly increased in endpoint PDAC tissue. This confirms the established literature that γδ T cells can infiltrate the PDAC TME in the KPC model. (Daley et al., 2016) One caveat of endpoint RNAScope is the inability to determine if γδ T cell infiltration results from a response to tumourigenesis, or directs early neoplastic transformation, as γδ T cells have been implicated in both early and late stage PDAC. (McAllister et al., 2014, Daley et al., 2016) By identifying γδ T cell infiltration into PDAC tumour tissue, my data confirms that γδ T cell kinetics are distinct from other cancer types, particularly breast cancer. In the KEP model of metastatic breast cancer, γδ T cells exert their function through the systemic production of IL-17A and do not infiltrate KEP tumours. (Coffelt et al., 2015) Additionally, depletion of γδ T cells in early disease did not impact progression of KEP mice, suggesting a more important role in late-stage disease in breast cancer.(Coffelt et al., 2015) This contrasts to the literature surrounding PDAC, where the expansion of IL-17A$^+$ CD4$^+$ T cells and γδ T cells at 9 weeks in KC^{iMist1} mice suggests that γδ IL-17A production is prevalent even in early stage PDAC.(McAllister et al., 2014) However, my preliminary findings show that γδ T cells are not significantly increased in 6wk or 10wk KPC pancreas, which suggests a more important role in late stage tumourigenesis.

My phenotypic analysis of γδ T cells in KPC mice yielded very informative results that both support and contradict the current literature. Unlike in metastatic breast cancer, I have shown that γδ T cells infiltrate primary PDAC tissue and are significant sources of IL-17A, which corroborates established KPC data. (Daley et al., 2016) This shows that γδ T cell infiltration may subsequently drive effector functions in a TME specific manner, which contradicts the observations seen in breast cancer. I also found that PDAC-infiltrated γδ T cells are consistently <5% of the TILs, so my findings demonstrate that whilst they are capable of infiltrating PDAC tissue, γδ T cells remain a minor component of the TILs, similar to the the ID8 model of ovarian cancer and orthotopic KPC models.

(Rei et al., 2014, Daley et al., 2016) Furthermore, γδ T cells in orthotopic KPC models have previously been shown to produce IFN-γ, suggesting a highly heterogeneous population that can also promote Th1 function. (Daley et al., 2016) My findings from the spontaneous KPC model shows no evidence of systemic, or PDAC-specific, IFN-γ production by γδ T cells. Finally, despite the lack of CD27⁻ subset expansion in PDAC tissue, the significant production of IL-17A by γδ T cells confirms γδ T cells display a strong pro-tumour phenotype in endpoint PDAC tissue.

I have also shown that in KPC spleen, the expansion of the CD27⁻ subset occurs concurrently with an expansion of the Vγ6⁺Vδ6.3⁺ subset, which also produces significant levels of GM-CSF. Current literature of Vγ6⁺ γδ T cells shows they are generally restricted to the uterus, lungs and tongue, produce IL-17A and IL-22, and have an invariant Vγ6⁺Vδ1⁺ TCR configuration.(Parker and Ciofani, 2020) Furthermore, Vγ6⁺ cells are rarely observed in the spleen under steady state conditions, and their development is restricted to the second embryonic wave after the Vγ5⁺ subset — unlike the Vγ4⁺ subset which is maintained throughout adult life.(Roark et al., 2004) (Parker and Ciofani, 2020) The restriction of the Vγ6⁺ subset to the second embryonic wave also means they are found less frequently Vγ4⁺ subset. (Parker and Ciofani, 2020) However, the Vγ6⁺Vδ1⁺ subset display a greater capacity for expansion than Vγ1⁺ and Vγ4⁺ subsets in response to inflammation. (Roark et al., 2004) More specifically, following listeria infection, Vγ6⁺Vδ1⁺ cells in liver and spleen increase 24-fold and 18-fold, respectively, showing that Vγ6⁺ γδ T cells can readily expand in response to an inflammatory insult. (Roark et al., 2004) My finding that Vγ6⁺ γδ T cells increase nearly 4-fold corroborates this data, and suggests that the presence of KPC tumours acts as an inflammatory insult to drive Vγ6⁺ cell expansion. I also show that the Vγ6⁺ subset expansion is associated with an expansion of the Vδ6.3⁺ subset in KPC spleen. During embryogenesis, the Vγ6⁺ subset normally has an invariant Vγ6⁺Vδ1⁺ configuration, with Vγ1⁺ cells normally expressing the Vδ6.3⁺ chain; and they are producers of IL-17A and IFN-γ, respectively.(Dalton et al., 2004, Silva-Santos et al., 2015) My findings show that splenic γδ T cells in KPC mice undergo a phenotypic switch of the Vδ6.3⁺ TCR chain from the Vγ1⁺ subset to the Vγ6⁺. This switch also appears to be restricted to the spleen, as the liver γδ T cells remain unchanged in KPC mice. Due to the primary PDAC tissue being

used for other experiments at the time, I have been unable to perform this analysis in primary PDAC tissue, so cannot determine if this phenotypic switch is occurring within PDAC tissue. This would be very informative, as Daley et al. have shown that the Vγ4+ subset is the dominant γδ T cell subset in KPC mice.

I also discovered that γδ T cells from KPC spleen are significant sources of GM-CSF, an important granulocyte-stimulating cytokine. In experimental autoimmune encephalomyelitis (EAE), the production of IL-23 by DCs stimulates the production of GM-CSF from γδ T cells along with IL-17A, IL-21 and IL-22. (Malik et al., 2016) GM-CSF production by autoreactive RORγt+ T cells drives EAE disease severity through the activation of microglial cells, but also through the accumulation of peripheral macrophages. (Ponomarev et al., 2007, Codarri et al., 2011) In particular, CCR2+Ly6Chi monocytes in EAE are the main responders to γδ T cell-derived GM-CSF and are critical for driving EAE pathology. (Croxford et al., 2015) This has implications for my findings, as the expanded Vγ6+Vδ6.3+ γδ T cells in KPC spleen are significant sources of GM-CSF, and so may have the capacity to direct immune crosstalk to influence myeloid populations in PDAC.

Finally, I performed bulk RNAseq on sorted γδ T cells from liver and spleen of WT and KPC tumour-bearing mice, with the aim of further elucidating the phenotype of γδ T cells in the metastatic niche and in secondary lymphoid organs, such as the spleen. I found that 13 genes were significantly upregulated in γδ T cells from KPC tumour bearing liver, and that 9 of these were also significantly upregulated in γδ T cells in KPC tumour-bearing spleen (*Thbs1, Vcan, Gda, F10, Bst1, Ccl6, Saa3, Fn1* and *Ccl9)*. Of these genes there a several that relate to extracellular matrix function (*Thbs1, Vcan and Fn1*), chemokine function (*Ccl6 and Ccl9*) and IL-17A biology (*Saa3*). *Ccl9* may be of interest for future study, as the CCL9-CCR1 axis has been implicated in tumour invasion, where expression of CCL9 by tumour epithelial cells recruits CCR1+ immature myeloid cells to promote tumour invasion. (Kitamura et al., 2007) Additionally, disrupted CCL9-CCR1 signalling has also been shown to block metastatic dissemination and improve survival in mouse models of colorectal liver metastasis. (Kitamura et al., 2010) Thus, this indicates γδ T cells might produce chemokines associated with myeloid cell crosstalk, which may have implications in PDAC metastatic disease.

Chapter 4   The role of γδ T cells in PDAC progression.

4.1 Introduction and Aim.

In this chapter, I aim to address the role of γδ T cells in early PDAC tumourigenesis, throughout PDAC progression and their role in metastatic disease. To better understand the role of γδ T cells it was important to explore all aspects of tumourigenesis, particularly the precursor PanIN stage, as IL-17A and γδ T cells have previously been implicated in early-stage disease. (McAllister et al., 2014, Zhang et al., 2018)

During acute pancreatitis, IL-1ß is released by damaged acinar cells to mediate the recruitment of macrophages and CD4⁺ T cells. CD4⁺ T cells then differentiate into IL-17A⁺ Th17 cells, which are the main source of IL-17A in acute pancreatitis along with Vγ4⁺ γδ T cells.(Hu et al., 2020) Similarly, following neoplastic transformation, which is driven by oncogenic Kras signalling in the presence of chronic pancreatitis, both CD4⁺ Th17 and γδ T cells produce IL-17A. (McAllister et al., 2014) IL-17A plays a central role in early tumourigenesis, as over-expression of IL-17A dramatically accelerates ADM, PanIN formation and also enhances stromal deposition; and the loss of IL-17A through genetic depletion and pharmacological inhibition results in delayed PanIN formation and an impaired stromal reaction. Furthermore, the induction of oncogenic Kras signalling increases the expression of the IL-17 receptor (IL-17R) on PanIN epithelium, which is further augmented by chronic pancreatitis.(McAllister et al., 2014) Thus, the transformation of PanIN cells by Kras signalling upregulates IL-17R, which enhances their ability to respond to IL-17A.

One of the major functional responses of PanIN lesions to IL-17R signalling is through the promotion of cancer cell stemness. This has previously been observed in other cancer models, where IL-17B produced by immune cells in gastric cancer promotes AKT\ß-catenin signalling and cancer cell stemness.(Bie et al., 2016) In early pancreatic tumourigenesis, IL-17R signalling through NF-κB expands DCLK1⁺ tuft cells within the PanIN epithelium — DCLK1 is a marker for tuft cells but is also considered to be an embryonic stem cell (ESC) signature gene.(Zhang et al., 2018) Increased expression of ECS gene signatures indicates a

more stem cell-like population, which can confer greater capacity to initiate tumour formation and drive ADM progression to PanIN lesions, and then to fully invasive carcinoma. Pharmacological inhibition of IL-17A significantly reduces DCLK1$^+$ cells within PanINs, indicating that IL-17A promotes a cancer stem cell gene signature. Therefore, the production of IL-17A in early neoplasia is pro-tumourigenic, drives PanIN formation, contributes to stromal deposition and promotes cancer cell stemness in PDAC precursor lesions.

The findings from McAllister et al. and Zhang et al. are important, as there are few studies that implicate IL-17A as a driver of early PDAC tumourigenesis. Additionally, McAllister et al. show that γδ T cells and CD4$^+$ Th17 cells are major sources of IL-17A in early PDAC. Interestingly, in the *Mist1$^{CreERT2/+}$;LSL-Kras^{G12D}* (KC^{iMist1}) model with chronic pancreatitis, although CD4$^+$ Th17 cells are five times more abundant than γδ T cells, only 10% of CD4$^+$ T cells produce IL-17A compared to 50% of γδ T cells. (McAllister et al., 2014) Given the differential secretion patterns and levels of infiltration between these cell populations, McAllister et al. concluded that IL-17A production by each cell type provide a similar contribution within the early TME. This suggests that between γδ T cells and CD4$^+$ Th17 cells, there exists a possible redundancy in early PDAC, however, there is no current data confirming any synergism between CD4$^+$ Th17 cells and IL-17A$^+$ γδ T cells in PDAC. Most studies have therefore focussed on the function of IL-17A itself, opposed to determining if there is a dominant IL-17A-producing population that drives tumorigenesis. There exists some data from studies in viral pancreatitis showing that IL-23 production from DCs activates Vγ4$^+$ γδ T cells to produce more IL-17A than CD4$^+$ Th17 cells; and that specifically Vγ4$^+$ γδ T cell-derived IL-17A is pathogenic and promotes pancreatitis through neutrophil influx. (Yan et al., 2019) Therefore, this evidence suggests that pancreatitis could be driven preferentially by IL-17A from γδ T cells, rather than Th17 cells in PDAC.

Despite the well published pro-tumour function of IL-17A$^+$ γδ T cells in numerous cancer settings, there have been very few studies that have investigated this in PDAC. Since the loss of IL-17A has been shown to impair the development of precursor PanIN lesions, I hypothesise that the loss of γδ T cells will lead to a delay in PanIN and PDAC progression, as Daley et al have shown that the loss of γδ T cells in KC mice (KC;Tcrδ$^{-/-}$) delays PanIN progression, and also translates

into significantly increased survival. (Daley et al., 2016) However, the KC model displays a low frequency of penetrance from PanIN lesions to fully invasive carcinoma and metastatic disease.(Ariston Gabriel et al., 2020) Since the loss of γδ T cells has not been investigated in the gold standard spontaneous KPC model, one could argue that the impact of γδ T cell loss on PDAC progression and metastatic disease has not yet been properly investigated. However, the cumulative evidence within the literature surrounding γδ T cell function in early tumourigenesis suggests an important protumour function that may be central to the progression of metastatic PDAC.

Thus, the aim of this chapter is to determine the role of γδ T cells in early tumourigenesis, determine their function in directing PDAC progression, and to ascertain if they play a role in driving metastatic disease in PDAC.

4.2 Loss of γδ T cells in early tumourigenesis delays PanIN development at 6 weeks, but PanIN progression at 10 weeks is unchanged.

The first step in determining the role of γδ T cells in PDAC was to investigate the impact of γδ T cell loss on precursor PanIN lesions. As previously mentioned, prior to the development of fully invasive carcinoma, PDAC develops from non-invasive precursor lesions known as PanINs. PanIN lesions develop asymptomatically within the pancreatic epithelium and progress sequentially through distinct stages, with each PanIN stage identifiable through the acquisition of mutations and distinct histological changes. PanIN lesions are non-invasive as they do not breach the basement membrane and can be separated into low (PanIN-1A/B) intermediate (PanIN-2) and high grade (PanIN-3) lesions (Figure 4-1). The morphological changes that identify each PanIN grade are as follows: PanIN-1A display expanded cytoplasm, cellular elongation, and basal polarity; PanIN-1B maintain the basal polarity but also display invaginations; PanIN-2 lose basal polarity, have clear invaginations and begin to show nuclear atypia such as nuclear crowding; finally, PanIN-3 lesions have severe nuclear atypia including nuclear crowding, mitosis and budding of proliferating cells into the lumen. (Hruban et al., 2000, Distler et al., 2014) PanIN-3 cells are regarded as *carcinoma in situ* as they are the preceding step to fully invasive carcinoma.
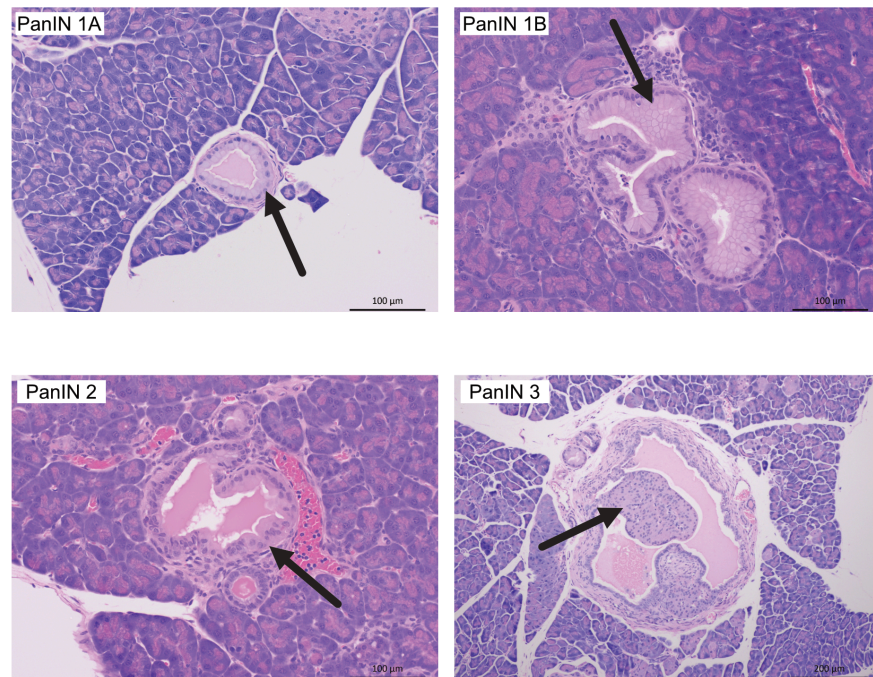
Figure 4-1 PanIN lesions develop sequentially with distinct histological features.
Low grade lesions (PanIN-1A) are identifiable through cytoplasmic expansion, cellular elongation, papillary growth pattern and they maintain basal polarity (top left). PanIN-1B lesions are distinct from PanIN-1A due to the development of invaginations (top right). Intermediate grade (PanIN-2) lesions display invaginations along with a loss basal nuclear polarity and nuclear crowding (bottom left). High grade (PanIN-3) lesions are identifiable through luminal budding and the presence of cellular islands within the lumen (bottom right). Representative images of H&E staining of 6wk pancreas, PanIN-1A/B and PanIN-2 imaged at 20x magnification, with PanIN-3 imaged at 10x magnification, scale bar representing 100μm and 200μm, respectively.

I then sought to quantify the number of PanIN lesions at different timepoints to determine if the absence of γδ T cells in KPC mice (KPC;Tcrd$^{-/-}$) delays the development of PanINs. KPC and KPC;Tcrd$^{-/-}$ mice were aged to 6 weeks and 10 weeks of age, and pancreas tissue was stained with haematoxylin and eosin (H&E) to visualise the cellular architecture — haematoxylin stains nuclear components and eosin stains the cytoplasm (Figure 4-1 & Figure 4-3A).(Fischer et al., 2008) KPC mice at 6 weeks are considered to have early-stage PanIN lesions, and KPC mice at 10 weeks have late-stage PanINs, so are ideal timepoints to assess early PDAC progression.(Keenan et al., 2014) In both 6wk and 10wk pancreas from KPC mice, I recorded the total number of PanIN lesions and sub-categorised them based on their grade (PanIN-1/2/3). Firstly, I found that pancreas from 6wk KPC;Tcrd$^{-/-}$ mice had no significant differences in the number of low grade (PanIN-1) or high grade (PanIN-3) lesions when compared to KPC mice (Figure 4-2A). However, there was a significant reduction in the number of intermediate (PanIN-2) lesions in pancreas from 6wk KPC;Tcrd$^{-/-}$

mice (Figure 4-2A). Furthermore, I also found there was a significant reduction in the total number of PanIN lesions in 6wk KPC;Tcrd$^{-/-}$ pancreas compared to 6wk KPC mice (Figure 4-2B), which is attributable to the reduction in PanIN-2 lesions. When the quantifications of the PanIN lesions are represented as proportions, the differences between KPC and KPC;Tcrd$^{-/-}$ pancreas at 6wk are more apparent, with the majority of PanIN lesions in 6wk KPC;Tcrd$^{-/-}$ pancreas consisting of PanIN-1 lesions compared to greater numbers of PanIN-2 and PanIN-3 lesions found in 6wk KPC pancreas (Figure 4-2B). This data indicates that γδ T cells play an important role in promoting the progression of early stage PanIN lesions.
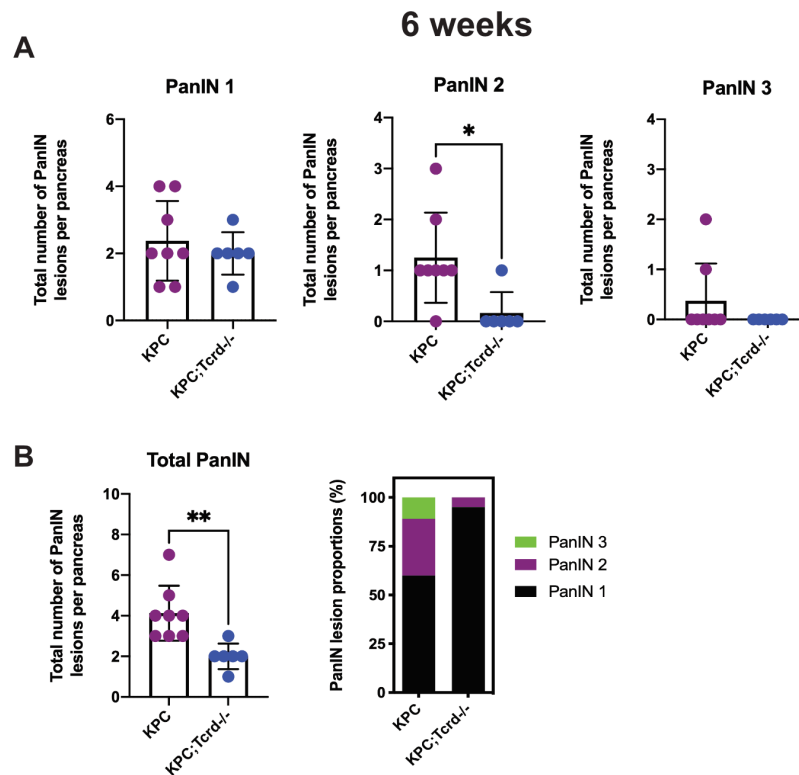
Figure 4-2 Genetic ablation of γδ T cells delays the progression of early stage PanIN lesions in 6wk KPC;Tcrd$^{-/-}$ pancreas.
KPC (n=8) and KPC;Tcrd$^{-/-}$ (n=6)mice were aged to 6 weeks, sacrificed and pancreas tissue was stained using H&E IHC. Quantification of low (PanIN-1A/B), intermediate (PanIN-2) and high grade (PanIN-3) lesions was performed, each data point represents the number of lesions from an individual mouse (A). The total number of PanIN lesions was quantified and is shown as the "*total number of PanIN lesions per pancreas*" and as a proportion (%) of PanIN grades, each dot represents an individual mouse (B). ** $P < 0.01$ and * $P < 0.05$ as determined by Mann-Whitney U-Test.
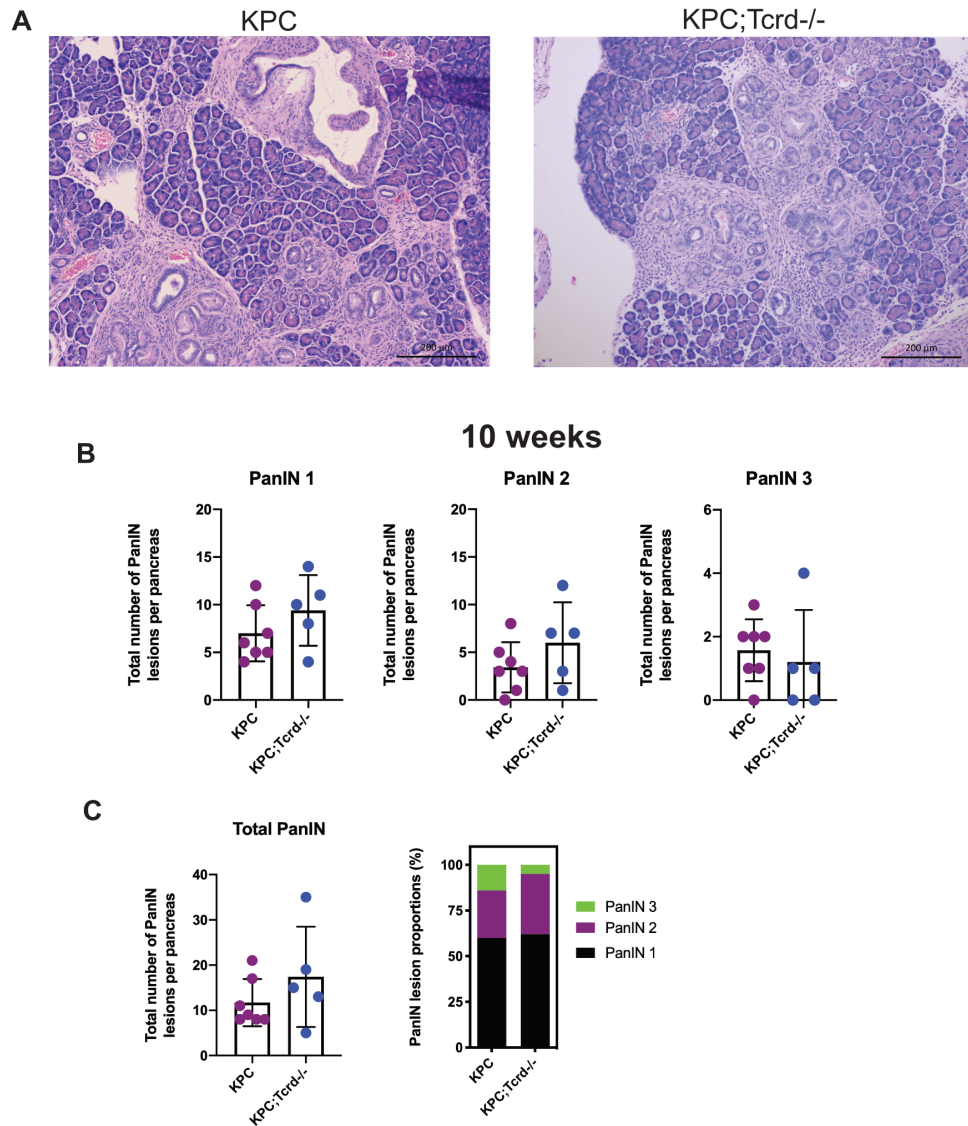
Figure 4-3 Genetic ablation of γδ T cells does not delay the progression of late-stage PanIN lesions in 10wk KPC;Tcrd$^{-/-}$ pancreas.
Representative images of H&E staining from 10wk pancreas, imaged at 10x magnification with scale bar representing 200μm (A). Quantification of low (PanIN-1A/B), intermediate (PanIN-2) and high grade (PanIN-3) lesions was performed in 10wk KPC (n=7) and KPC;Tcrd$^{-/-}$ (n=5) mice, each data point represents the number of lesions from an individual mouse (B). The total number of PanIN lesions was quantified and is shown as the "*total number of PanIN lesions per pancreas*", and as a proportion (%) of PanIN grades, each dot represents an individual mouse (C).

However, I found that 10wk KPC;Tcrd$^{-/-}$ pancreas displayed no delayed PanIN progression when compared to 10wk KPC mice, as there were no differences to individual PanIN grades or in the total number of PanIN lesions (Figure 4-3B/C). These data indicate that whilst loss of γδ T cells in early-stage (6wk) PanIN lesions is protective and delays progression, this benefit is largely lost by late-stage (10wk) PanIN lesions. This indicates there is some redundancy within the early PDAC TME, and that PanIN progression in 10wk KPC;Tcrd$^{-/-}$ pancreas can be driven by another pro-tumour mechanism.

4.3 Genetic depletion of γδ T cells does not change KPC survival.

Following on from my finding that the loss of γδ T cells specifically delays early-stage (6wk) but not late-stage (10wk) PanIN lesion progression, the next step was to ascertain if the absence of γδ T cells impacts the survival of KPC mice. KPC mice reach clinical endpoint due to primary tumour growth, or through the development of off-target pathologies such as thymic lymphoma and lung fibrosis. I first examined PDAC-specific survival in KPC, KPC;Tcrd$^{+/-}$ and KPC;Tcrd$^{-/-}$ mice, and censored any cases where KPC mice reached humane clinical endpoint due to off-target pathologies. I found there were no significant changes to PDAC-specific survival regardless of γδ T cell status; KPC median survival was 150 days and KPC;Tcrd$^{+/-}$ and KPC;Tcrd$^{-/-}$ median survival were 161 and 163 days, respectively (Figure 4-4A). When off-target pathologies were included in survival analysis, there were again no significant differences in survival between γδ T cell cohorts — the median survival of KPC mice was 125 days and KPC;Tcrd$^{+/-}$ and KPC;Tcrd$^{-/-}$ median survival was 133 and 129 days, respectively (Figure 4-4B). These data indicate that loss of γδ T cells does not impact survival in KPC mice, and does not render them more susceptible to off-target pathologies such as thymic lymphoma.

Given that there was no survival benefit to KPC;Tcrd$^{-/-}$ mice, this suggests that progression of primary PDAC is not driven by γδ T cells in KPC mice. To confirm, I also assessed the pathological features of KPC and KPC;Tcrd$^{-/-}$ PDAC to determine if there were any differences regarding tumour differentiation status. I found no change in the differentiation status between KPC and KPC;Tcrd$^{-/-}$ PDAC tissue, with tumours from both cohorts exhibiting a range of differentiation states, and still demonstrating the ability to become well-differentiated. (Figure 4-4C). Thus, whilst γδ T cell function may be redundant in early tumourigenesis; the absence of a survival benefit in KPC;Tcrd$^{-/-}$ mice; and the similar pathology between KPC and KPC;Tcrd$^{-/-}$ PDAC tissue indicates that γδ T cells do promote the progression of primary PDAC tumours.
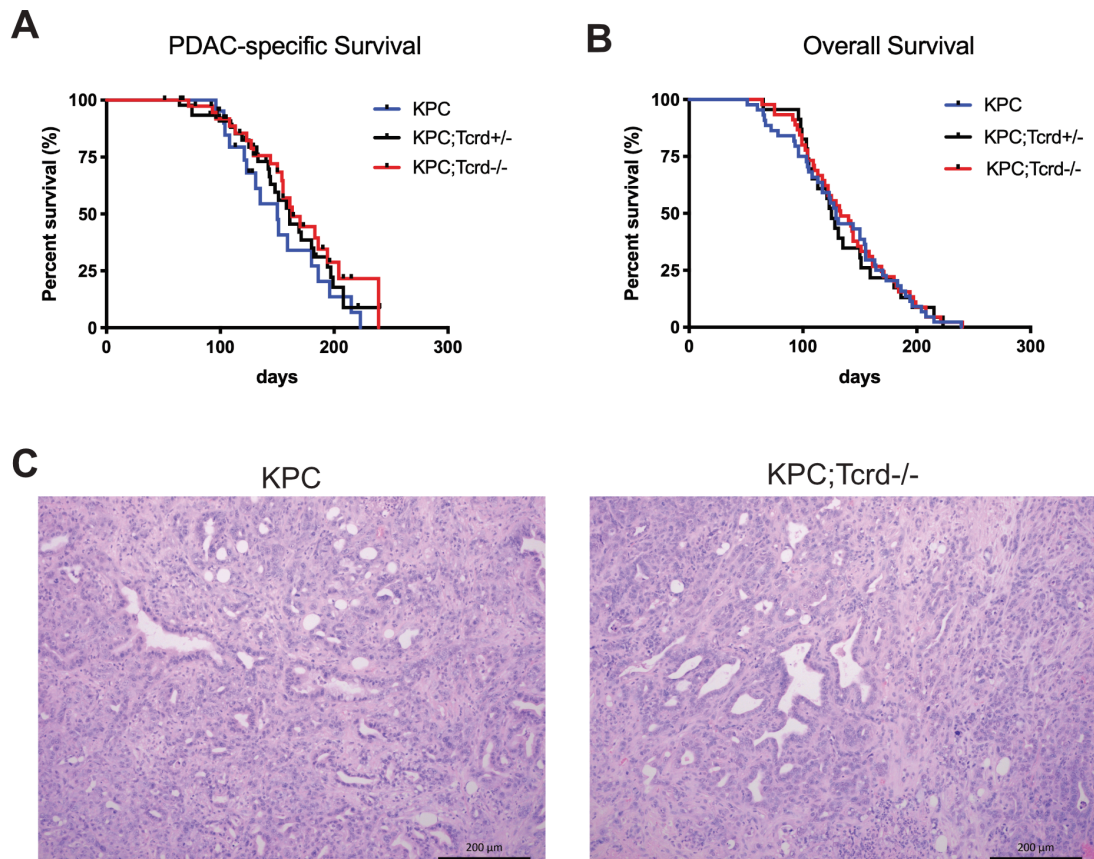
Figure 4-4 Loss of γδ T cells does not extend the survival of KPC mice.
Mice were aged to clinical endpoint and Kaplan-Meyer survival analysis was performed. PDAC-specific survival was analysed in KPC (n=16) KPC;Tcrd$^{+/-}$ (n=27) and KPC$^{-/-}$ (n=21) mice, and median survival was determined — KPC (150 days), KPC;Tcrd$^{+/-}$ (161 days) and KPC;Tcrd$^{-/-}$ (163 days) (A).Overall survival of KPC (n=23), KPC;Tcrd$^{+/-}$ (n=45) and KPC$^{-/-}$ (n=44) was analysed to determine if loss of γδ T cells increased susceptibility to off-target effects (B). Tumour differentiation status of KPC and KPC;Tcrd$^{-/-}$ was compared, representative images of PDAC tumour from KPC (left) and KPC;Tcrd$^{-/-}$ (right), images are shown at 10x magnification with scale bar representing 200μm (C).

4.4 The PDAC TME remains largely unchanged in the absence of γδ T cells throughout tumourigenesis.

Following on from my discovery that late-stage PanIN progression, KPC survival and PDAC differentiation status are all unchanged in KPC;Tcrd$^{-/-}$ mice, I then looked to ascertain if there are any other changes to the TME during KPC;Tcrd$^{-/-}$ tumour development. To investigate this, immunohistochemistry (IHC) staining targeting Ki67, Sirius Red and Caspase 3 was performed on 6wk, 10wk and endpoint pancreas tissue from KPC and KPC;Tcrd$^{-/-}$ mice. This enabled me to investigate the impact of γδ T cell absence on cellular proliferation, collagen deposition and apoptosis in the TME throughout progression (Figure 4-5, Figure 4-6 & Figure 4-7).

6 weeks

	KPC	KPC;Tcrd-/-

A

Ki67

100 μm

B

Sirius Red

100 μm

C

Caspase 3

100 μm
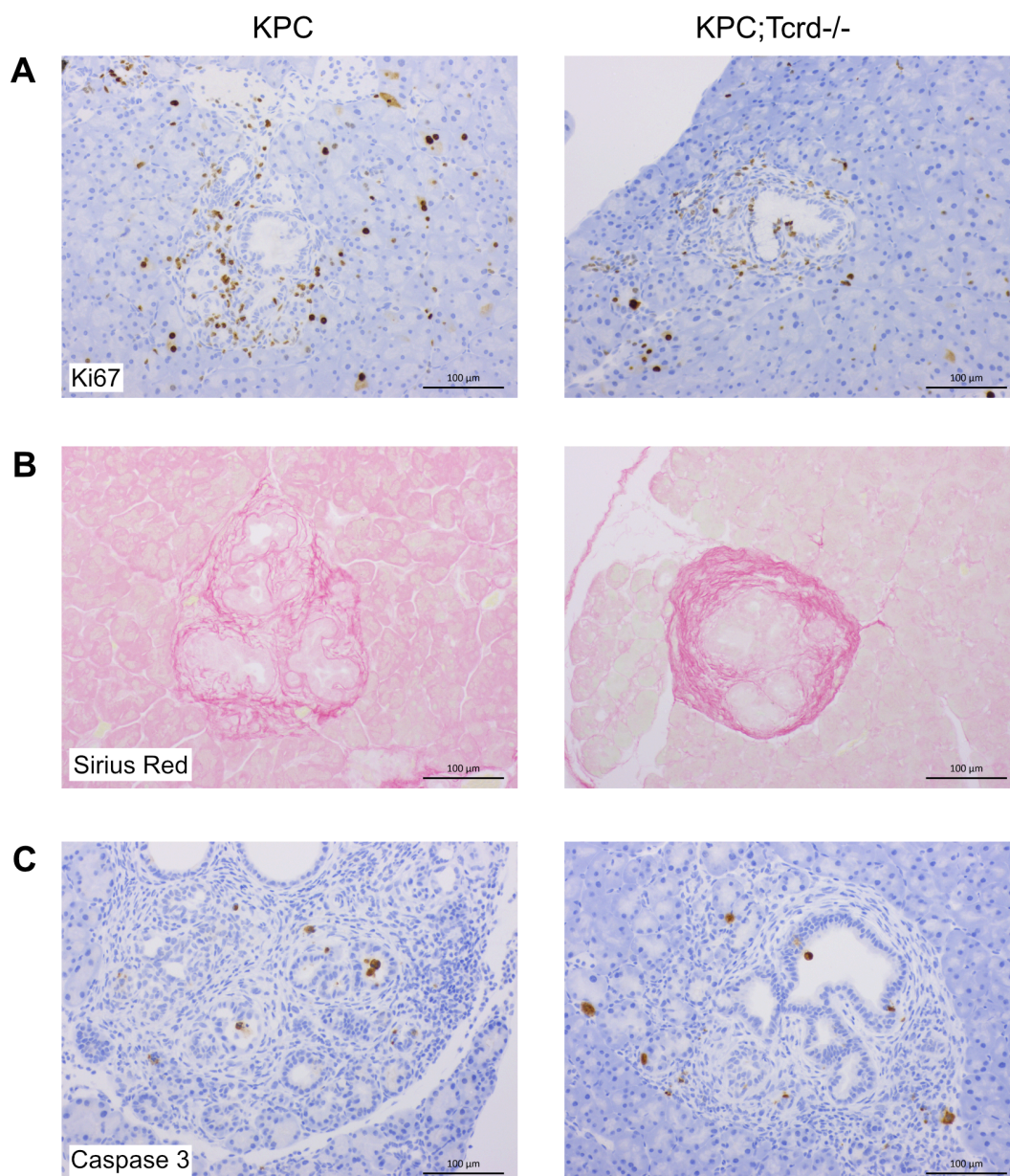
Figure 4-5 PDAC TME components are apparent with early-stage (6wk) PanIN lesions.
Representative images of IHC staining in KPC and KPC;Tcrd$^{-/-}$ pancreas aged to 6wk. IHC staining was performed to target cellular proliferation (Ki67) (A), collagen deposition (Sirius Red) (B) and apoptosis (Caspase 3) (C). Representative images shown at 20x magnification with scale bar representing 100μm.

10 weeks

KPC   KPC;Tcrd-/-
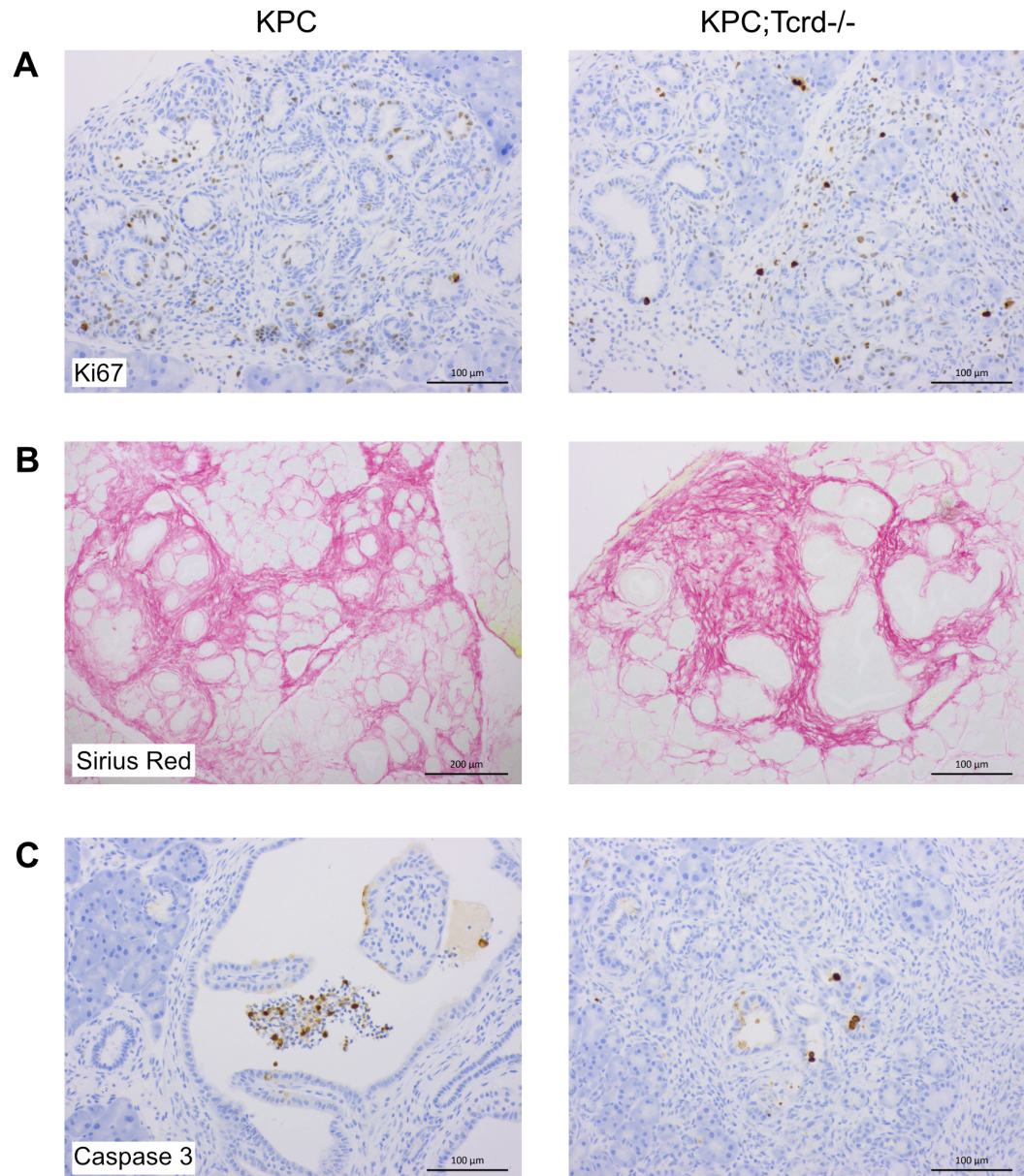
Figure 4-6 TME components become more prevalent in late-stage (10wk) PanIN lesions.
Representative images of IHC staining in KPC and KPC;Tcrd$^{-/-}$ pancreas aged to 10wk. IHC
staining was performed to target cellular proliferation (Ki67) (A), collagen deposition (Sirius Red)
(B) and apoptosis (Caspase 3) (C). Sirius Red from KPC pancreas (B) imaged at 10x magnification
with scale bar representing 200μm, all other images shown at 20x magnification with scale bar
representing 100μm.

Endpoint

	KPC	KPC;Tcrd-/-
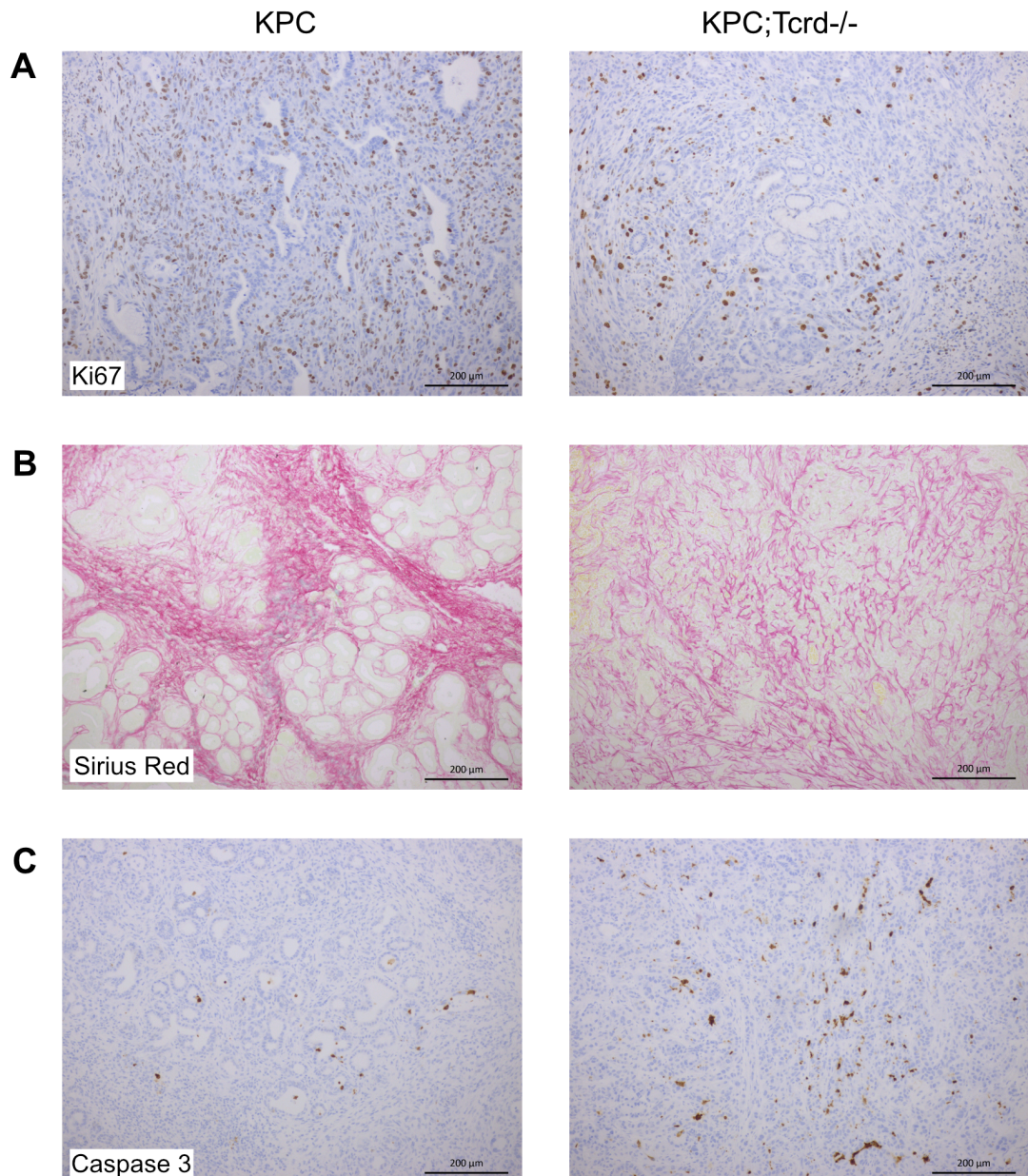
Figure 4-7 Endpoint PDAC TME has extensive collagen deposition, cellular proliferation and apoptotic cell death.
Representative images of IHC staining in KPC and KPC;Tcrd$^{-/-}$ pancreas aged to humane clinical endpoint. IHC staining was performed to target cellular proliferation (Ki67) (A), collagen deposition (Sirius Red) (B) and apoptosis (Caspase 3) (C). Representative images shown at 10x magnification with scale bar representing 200μm.

I found no changes to Ki67 or Caspase 3 status in 6wk KPC;Tcrd$^{-/-}$ pancreas, indicating that γδ T cells do not direct cellular proliferation or apoptosis in early-stage PanINs, despite being implicated in their progression (Figure 4-8A). There was a significant reduction in Sirius Red staining, indicating a marked reduction in collagen deposition (Figure 4-8A), corroborating the reduction in

the total number of PanIN lesions in 6wk KPC;Tcrd$^{-/-}$ pancreas (Figure 4-2B), as PanIN lesion development accounts for the majority of collagen deposition in 6wk pancreas. I found no changes to Ki67, Sirius Red and Caspase 3 staining in 10wk KPC;Tcrd$^{-/-}$ pancreas, further confirming that the delay to PanIN progression is lost by late-stage (10wk) PanINs in KPC;Tcrd$^{-/-}$ mice (Figure 4-8B). Finally, endpoint PDAC from KPC;Tcrd$^{-/-}$ mice showed no changes to Ki67 or Sirius Red staining, indicating that γδ T cells do not impact on cellular proliferation or collagen deposition in late-stage PDAC (Figure 4-8C). Interestingly, there is a significant increase in Caspase 3 staining in endpoint KPC;Tcrd$^{-/-}$ PDAC, suggesting that γδ T cells may restrict apoptotic cell death (Figure 4-8C). This indicates a potential protumour function, but this does not translate into any significant survival benefit. To summarise, γδ T cells play an important role in directing early-stage PanIN progression, evident through the reduced total number of PanIN lesions and collagen deposition in 6wk KPC;Tcrd$^{-/-}$ pancreas. However, this benefit is largely lost by late-stage (10wk) PanINs and in end-stage PDAC, where loss of γδ T cells is not associated with any significant changes to the TME, PDAC differentiation status or enhanced survival in KPC mice. Thus, γδ T cells do not play a significant role in the promotion of PDAC tumour progression.
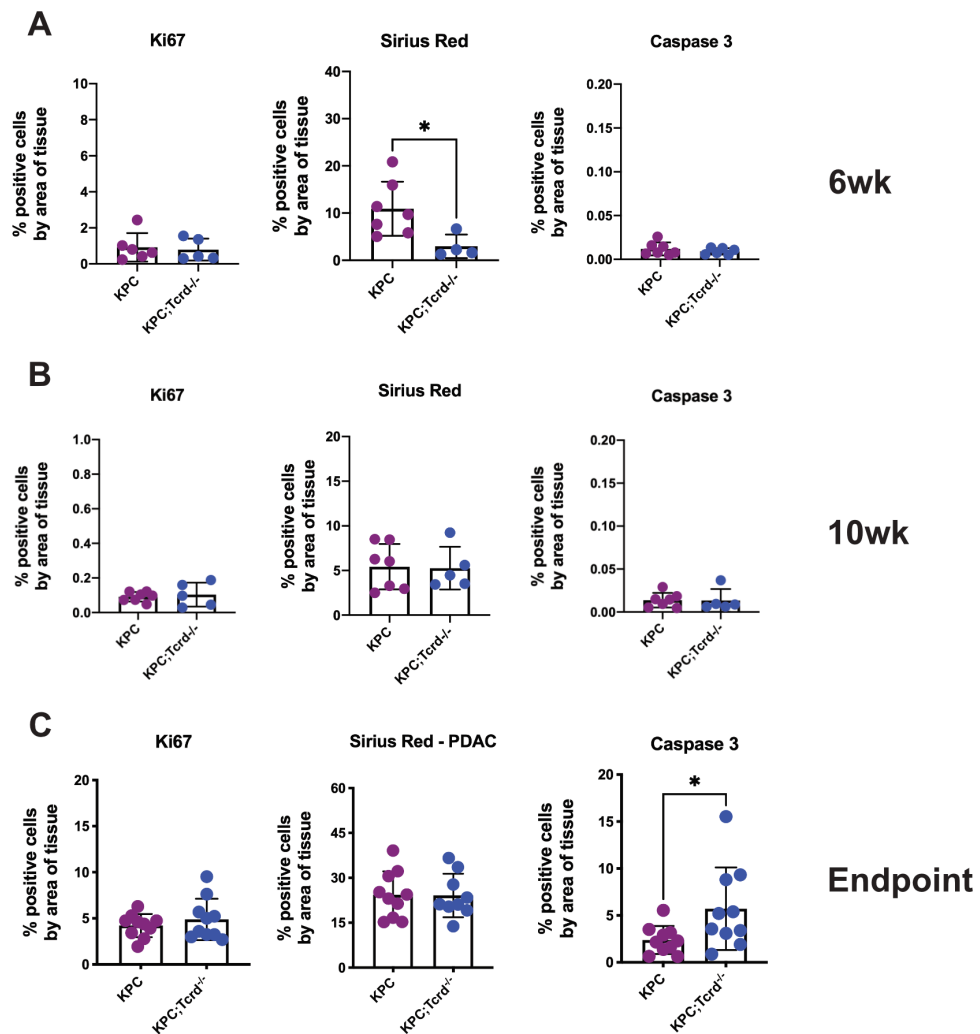
Figure 4-8 Early-stage TME in KPC;Tcrd⁻/⁻ mice display reduced collagen deposition, but the absence of γδ T cells does not significantly alter the TME through PDAC progression. KPC and KPC;Tcrd⁻/⁻ mice were aged to 6wk (KPC n=7; KPC;Tcrd⁻/⁻ n=6) (A), 10wk (KPC n=7; KPC;Tcrd⁻/⁻ n=5) (B) and clinical endpoint (KPC n=10; KPC;Tcrd⁻/⁻ n=10) (C), and IHC staining was performed targeting Ki67, Sirius Red and Caspase 3. Quantification was performed on HALO® image analysis platform and is shown as "*% positive cells by area of tissue*". * P < 0.05 as determined by Mann-Whitney U-Test.

4.5 Absence of γδ T cells in KPC mice reduces the incidence of spontaneous liver metastasis.

Finally, in this chapter I aimed to determine the role of γδ T cells in PDAC metastasis. To achieve this, I aged KPC and KPC;Tcrd⁻/⁻ mice to clinical endpoint, performed H&E staining on liver tissue and examined liver tissue sections for the presence of metastasis. KPC mice develop metastasis in a similar manner to human disease, with most common spread found within the liver and lungs. This KPC model has been maintained on a C57BL/6J background, which is more resistant to metastatic dissemination, as they elicit a strong Th1 response. (Song and Hwang, 2017) This includes higher NK cell activity, which are known to

be important anti-metastatic cells. (López-Soto et al., 2017) However, I was able to confirm that both KPC and KPC;Tcrd$^{-/-}$ cohorts were capable of developing overt metastatic liver lesions (Figure 4-9A/B). The scoring of metastatic incidence was based on the presence (YES) or absence (NO) of metastatic lesions, regardless of size or number. Whilst determining lesion size or the number of metastatic foci can more accurately reflect metastatic progression, this cannot be accurately determined without the use of serial sections — we deemed this was not in line with the 3Rs (replace, reduce and refine) and so employed the aforementioned scoring strategy. I discovered that KPC mice had a 38.46% incidence of spontaneous liver metastasis, but that KPC;Tcrd$^{-/-}$ mice had a significantly lower incidence rate, only 16.2% (Figure 4-9C). These data indicate that γδ T cells play a crucial role in driving metastatic disease, and their absence results in a significantly lower metastatic burden.
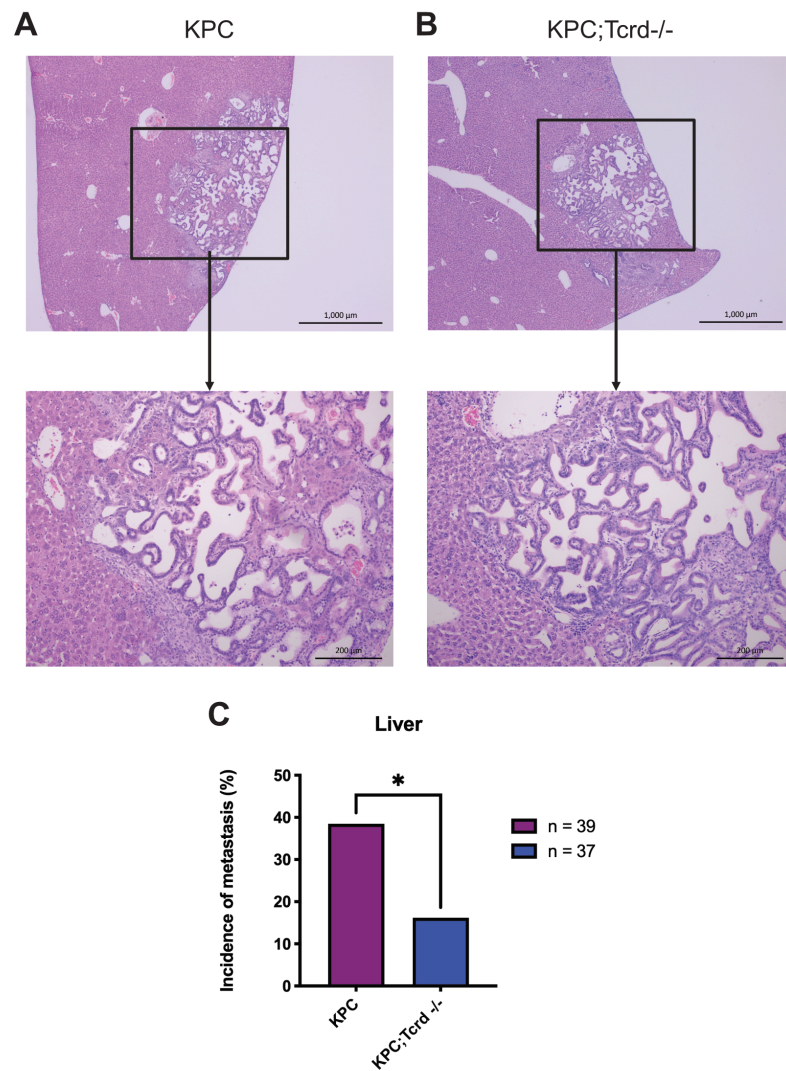
Figure 4-9 Absence of γδ T cells in KPC mice significantly reduces the incidence of spontaneous liver metastasis.
KPC (n=39) and KPC;Tcrd$^{-/-}$ (n=37) mice were aged to clinical endpoint and livers were stained through H&E IHC. Representative images of metastatic lesions from KPC (A) and KPC;Tcrd$^{-/-}$ (B) liver tissue — 2.5x magnification shown in top panel with insert shown below at 10x magnification, and scale bars represent 1,000 μm and 200μm, respectively. Metastatic scoring was based on the presence (YES) or absence (NO) of spontaneous metastatic lesions, and is shown as a percentage (%) incidence of metastatic lesions (C). * P < 0.05 as determined by Fisher's exact test.

4.6 Discussion.

In this chapter I aimed to elucidate the role of γδ T cells in PDAC progression and investigated the impact of γδ T cell absence in KPC mice at various timepoints. Firstly, I found that loss of γδ T cells significantly delays early-stage PanIN lesion development at 6 weeks, specifically impairing the progression of intermediate grade PanIN-2 lesions. The delay in PanIN progression initially supported my hypothesis that γδ T cells play an important pro-tumour function in early tumourigenesis. Given that IL-17A, of which γδ T cells are major

sources, has been shown to promote PanIN progression in KC[iMist1] mice; and loss of γδ T cells in KC;Tcrδ$^{-/-}$ mice significantly delays the progression of PanIN lesions, my data initially confirmed these findings from the literature.(McAllister et al., 2014, Daley et al., 2016) However, I found the delay in PanIN progression in 6wk KPC;Tcrd$^{-/-}$ pancreas is lost in 10wk KPC;Tcrd$^{-/-}$ mice. An explanation for this could be due to the existence of redundancy within the TME, as there is evidence from McAllister et al. that shows CD4$^+$ Th17 cells are far more numerous within the early TME, and may contribute similar amounts of IL-17A to γδ T cells. (McAllister et al., 2014) Therefore, given that IL-17A is a major driver of PanIN lesions, and that γδ T cells are not the sole source of IL-17A within the TME, it is entirely possible that this niche has been filled by other pro-tumour IL-17A-producing cells in the absence of γδ T cells.

The next major finding of this chapter was the lack of any survival benefit in the KPC;Tcrd$^{-/-}$ mice. The most striking findings in the study conducted by Daley et al. demonstrated increased survival in spontaneous KC;Tcrδ$^{-/-}$ mice, and in orthotopic KPC tumours transplanted into γδ T cell-deficient hosts.(Daley et al., 2016) In the KC;Tcrδ$^{-/-}$ model, this was also in conjunction with significantly delayed PanIN lesions, suggesting that γδ T cells play a central role in driving tumour progression in early- and late-stage PDAC.(Daley et al., 2016) As previously mentioned, the spontaneous KPC model is a more faithful recapitulation of human disease when compared to the spontaneous KC model. With the addition of Trp53^{R17H} point mutation, KPC mice are more representative of human disease, as the expression of oncogenic Kras^{G12D} alone often results in restricted tumour growth due to senescence and growth arrest.(Morton et al., 2010) The addition of mutant p53^{R172H} results in more rapid progression of PDAC where median onset is 130 days, contrasting with KC mice which develop PanIN lesions by 2 months but rarely develop carcinoma.(Morton et al., 2010) Crucially, mutant p53^{R172H} results in frequent liver metastases, indicating that mutant p53 in KPC mice drives invasive carcinoma by overcoming senescence and growth arrest, and also plays a fundamental role in promoting metastasis.(Morton et al., 2010). Thus, the KPC model is an ideal GEMM to assess the impact of γδ loss more accurately in PDAC. However, my data contradicts the findings from Daley et al., as loss of γδ T cells in KPC mice does not significantly impact PDAC survival. It should be noted that the KPC;Tcrd$^{-/-}$model is deficient for all γδ T

cells, meaning the pro-tumour (CD27$^-$) IL-17-producing Vγ4$^+$ and Vγ6$^+$ cells, along with the anti-tumour (CD27$^+$) IFN-γ-producing Vγ1$^+$ cells, are all absent. Thus, the global deficiency of γδ T cells in the KPC;Tcrd$^{-/-}$ model is a blunt tool, and the loss of important anti-tumour cell populations may explain the lack of survival benefit. Daley et al. demonstrated that specific depletion of Vγ4$^+$ cells provided significant protection, and so genetic ablation of specifically the IL-17-producing populations would be a more refined approach to determine the function of pro-tumour γδ T cells in the KPC model.

Furthermore, there is evidence in the literature that confirms IL-17A production in PDAC is a crucial factor that determines survival in KPC mice. A recent study by Mucciolo et al shows that genetic ablation of IL-17A in the autochthonous KPC model (KPC;IL-17A$^{-/-}$) was associated with a significant extension of survival, but also increased fibrotic deposition.(Mucciolo et al., 2021) This extension of survival matches with data from Daley et al., who show in orthotopic KPC models that depletion of Vγ4$^+$ (IL-17A$^+$) γδ T cells confers a significant survival benefit. (Daley et al., 2016) In KPC;IL-17A$^{-/-}$ mice, although the changes in survival were associated with increased deposition, the collagen fibres were found to be less compact and had reduced stiffness compared to KPC mice. (Mucciolo et al., 2021) The reduced collagen stiffness in KPC;IL-17A$^{-/-}$ mice was found to promote greater matrix remodelling and release of effector molecules such a IL-12 and IFN-γ by CAFs; and is also associated with increased inflammatory infiltrate with significantly fewer FOXP3$^+$ Tregs and increased cytotoxic CD8$^+$ T cells. (Mucciolo et al., 2021) Whilst the evidence from Daley et al. suggests that γδ T cells do contribute to the stromal reaction in KC;Tcrδ$^{-/-}$ mice, I found no evidence of this in KPC;Tcrd$^{-/-}$ mice as Sirius Red deposition is unchanged in late-stage PDAC along with survival. Given these findings, I would conclude that the production of IL-17A by γδ T cells alone is insufficient to drive collagen deposition as observed in Mucciolo et al.; that the loss of the anti-tumour IFN-γ$^+$ γδ T cell population in KPC;Tcrd$^{-/-}$ mice may negate the beneficial impact of losing pro-tumour IL-17A$^+$ γδ T cells; and that possible redundancy within the TME exists due to other cellular sources of IL-17A negating the loss of IL-17A$^+$ γδ T cells.

Finally, I discovered that the absence of γδ T cells in KPC mice reduces spontaneous metastatic incidence by >50% − 38.46% in KPC mice to 16.2% in

KPC;Tcrd$^{-/-}$ mice. Currently in the literature, there have been no studies that describe γδ T cells as drivers of metastasis in PDAC, so my study is the first to identify that γδ T cells are important drivers of PDAC metastatic disease. Furthermore, given that PanIN progression and PDAC-specific survival, are largely unchanged in KPC;Tcrd$^{-/-}$ mice, these data indicate that the promotion of PDAC metastasis is a distinct mechanism from those that direct primary tumour growth, and that γδ T cells play a more prominent role in directing metastatic disease.

Chapter 5   The impact of γδ T cells in the tumour TME and metastatic niche.

5.1 Introduction and Aim.

The aim of this chapter is to further investigate the impact of γδ T cells in the primary tumour TME and in the liver metastatic niche. Thus far, I have demonstrated that pro-tumour IL-17A⁺ γδ T cells infiltrate primary PDAC tissue, and that the absence of γδ T cells reduces the incidence of spontaneous liver metastasis more than two-fold. However, the absence of γδ T cells does not confer a survival benefit in KPC;Tcrd$^{-/-}$ mice, and so γδ T cells therefore do not promote the progression of primary PDAC tumours. Instead, γδ T cells exert a clear pro-metastatic function either in a local manner within the metastatic niche, or distally within the primary PDAC tumour. Thus, the aim of this chapter is to investigate the impact of γδ T cells in the primary tumour and the metastatic niche, and to identify any potential pro-metastatic mechanisms that are directed through γδ T cells.

The function of γδ T cells in different cancer settings is diverse with numerous effector mechanisms, but the pro-tumour function of γδ T cells centres around the production of IL-17A. (Rei et al., 2014, Coffelt et al., 2015, Daley et al., 2016) However, IL-17A-producing γδ T cells are not simply pro-tumour cells, as they play an important role in a variety of immune settings; a notable example is their role in adipose tissue homeostasis where they are indispensable for the regulation of thermogenesis. (Kohlgruber et al., 2018) γδ T cells are enriched within adipose tissue and are primarily PLZF⁺CD27⁻, which is indicative of IL-17A production.(Kohlgruber et al., 2018) The function of IL-17A⁺ γδ T cells in adipose tissue is to regulate immune cell populations, initiated by IL-17A⁺ γδ T cells that promote the production of IL-33 from PDPN⁺ stromal cells; IL-33 binds to the ST2 receptor on FOXP3⁺ Tregs and provides transcriptional stability and promotes their expansion within adipose tissue.(Kohlgruber et al., 2018) The loss of γδ T cells negatively impacts thermogenesis, as Vγ4/6$^{-/-}$ and IL-17A$^{-/-}$ mice display impaired body temperature regulation.(Kohlgruber et al., 2018) Thus, IL-17A⁺ γδ T cells not only drive tumourigenesis, but also have indispensable homeostatic function, further highlighting the diverse nature of γδ T cells.

Given the enrichment of CD27⁻IL-17A⁺ γδ T cells in adipose tissue and their non-redundant function in thermogenesis, understanding how PDAC tumourigenesis affects their behaviour within this niche is important. In humans, cancer-associated cachexia is a major disease co-morbidity, with 80% of PDAC patients suffering from cachexia, which is characterised by the progressive loss of muscle and adipose tissue mass.(Narasimhan et al., 2021) Additionally, cachexia is also characterised through systemic inflammation and significantly altered adipose tissue metabolism — adipose tissue wastage often precedes and is more pronounced than muscle wastage.(Henriques et al., 2018, Tsoli et al., 2016) Therefore, despite the regulatory role of IL-17A⁺ γδ T cells in homeostatic conditions, the systemic inflammation associated with PDAC tumourigenesis may alter the function of adipose tissue γδ T cells, disrupt their homeostatic function and contribute to cachexia.

Another characteristic of PDAC biology is the immune-suppressive tumour microenvironment (TME), which restricts anti-tumour immune responses and is central to tumour outgrowth. The extensive desmoplastic stroma has resulted in PDAC tumours being described as immunologically cold, as the dense stroma acts as a barrier to infiltration of anti-tumour immune cells.(Wachsmann et al., 2012) Reductions in matrix stiffness enables greater inflammatory infiltrate into tumours that is characterised by increased CD8⁺ T cells, reduced Tregs and significantly increased survival. (Mucciolo et al., 2021) Furthermore, a study into the spatial distribution of TME components confirmed that CD8⁺ T cell proximity to cancer cells influences survival, but that CD8⁺ T cell proximity to components such as α-SMA⁺ fibroblasts and collagen does not directly associate with impaired CD8⁺ T cell function. (Carstens et al., 2017) Thus, whilst the barrier function of the PDAC TME is crucial to limit anti-tumour immune cell infiltration, it is not the only factor within the TME capable of subverting anti-tumour immunity. The description of PDAC tumours as immunologically cold is an oxymoron, as the TME is dominated by the presence of immune-suppressive cells, particularly myeloid cells such as macrophages (TAMs) and neutrophils, and also by cancer-associated fibroblasts (CAFs).(Candido et al., 2018, Steele et al., 2016, Öhlund et al., 2017)

Neutrophil function is controlled through CXCR2 signalling, which regulates neutrophil migration, and is significantly increased in human PDAC and

associates with poor survival.(Reid et al., 2011) Furthermore, loss of neutrophil homing by genetic ablation (*KPC;Cxcr2$^{-/-}$*) and pharmacological inhibition of CXCR2 significantly reduces metastasis and prolongs survival. (Steele et al., 2016) The reduction of metastasis (50% in KPC to 5% in *KPC;Cxcr2$^{-/-}$* mice) demonstrates the confounding nature of PDAC tumours, as crucial pro-metastatic functions are driven through infiltrated immune-suppressive myeloid cells. (Steele et al., 2016) γδ T cells significantly infiltrate PDAC tumours; but they also drive metastatic dissemination in breast cancer through expanding pro-metastatic neutrophil populations. (Daley et al., 2016, Coffelt et al., 2015) Additionally, they also promote ovarian cancer tumourigenesis through mobilisation of macrophages.(Rei et al., 2014) Thus, in this chapter, I aim to investigate the cross-talk between γδ T cells and the myeloid compartment of the TME, and also determine if a γδ T cell-myeloid cell axis promotes PDAC metastatic disease.

In addition to neutrophils, TAMs are another dominant myeloid cell population within PDAC, and are associated with increased metastasis and poor prognosis.(Kurahara et al., 2011) Inhibition of TAM populations through M-CSFR blockade leads to improved survival through reductions in primary tumour weight, reduced collagen deposition and α-SMA$^+$ stromal cells; but loss of macrophages also enables greater production of IFN-γ, Granzyme B and perforin from CD8$^+$ T cells. (Candido et al., 2018) Thus, TAMs are central to PDAC tumour growth, the subversion of anti-tumour cytolytic CD8$^+$ T cells and they significantly contribute to the desmoplastic reaction. Despite this clear pro-tumour function of PDAC TAMs, there remains a lack of consensus as to which macrophage population drives PDAC progression. Numerous sources within the literature point to monocyte-derived macrophages as the main drivers of PDAC tumourigenesis, particularly through CCR2-mediated monocyte recruitment followed by polarisation to TAM phenotype through M-CSF, IL-4, IL-10, IL-13 and TGF-β present within the PDAC TME. (Yang et al., 2020, Arango Duque and Descoteaux, 2014) However, Zhu et al. detail that orthotopic KPC transplantation into *Ccr2$^{-/-}$* mice did not affect tumour growth; but instead the depletion of embryonic-derived (tissue-resident) macrophages preferentially promote PDAC tumourigenesis.(Zhu et al., 2017) Conversely, a recent paper has detailed that BRD4 expression by PDAC cells results in the production of CCL2 to

recruit TNF-α+ macrophages, which promote the development of the basal-like PDAC subtype associated with poorer prognosis.(Mengyu Tu, 2021) Thus, despite the consensus that PDAC TAMs are potently pro-tumour, there is contradicting evidence as to which population of macrophages are more important. Thus, in this chapter I will further investigate PDAC TAM populations, and specifically uncover if γδ T cells preferentially promote specific macrophage populations in murine PDAC.

As mentioned above, there is also a growing appreciation of the heterogeneity of CAF sub-populations within the PDAC TME. Previously, it was thought that the activation of pancreatic stellate cells (PSCs) promotes a myofibroblastic phenotype through α-SMA upregulation, which associated with the production of ECM remodelling products such as collagen, fibronectin, and matrix metalloproteinases (MMPs).(Öhlund et al., 2014) Instead, CAFs can now be sub-categorised into three distinct sub-populations with distinct effector functions; myofibroblastic CAFs (myCAFs), inflammatory CAFs (iCAFs) and antigen-presenting CAFs (apCAFs). (Biffi et al., 2019, Elyada et al., 2019) More specifically, TGF-β signalling in the TME acts on PSCs close to PDAC cells which become collagen-producing α-SMA^{hi} IL-6^{lo} myCAFs; IL-1α acts on more distal PSCs to become α-SMA^{lo} IL-6^{hi} iCAFs through NF-κB signalling, which produce inflammatory mediators such as IL-1α, IL-6, G-CSF and CXCL1; and finally IFN-γ promotes MHC II^{hi} apCAF formation which promote CD4+ T cell activation. (Biffi et al., 2019, Elyada et al., 2019) Given the heterogeneous function of CAF sub-populations and their contribution to the TME, I aim to investigate the impact of γδ T cell absence on CAF populations, with the aim of identifying potential links to γδ T cells and the promotion of PDAC desmoplasia.

The final aim of this chapter is to explore the influence that γδ T cells have on other immune cell populations within the primary tumour and metastatic niche. Pro-tumour γδ T cells exert heterogeneous effector functions, but this centres around the production of IL-17A. IL-17A+ γδ T cells promote expansion of immune-suppressive neutrophils to impair anti-metastatic CD8+ T cells in breast cancer; mobilise pro-tumour macrophages in ovarian cancer; and IL-17A signalling inhibits the CXCL9/10-mediated recruitment of anti-tumour CD8+ T cells in colorectal cancer. (Coffelt et al., 2015, Rei et al., 2014, Chen et al.,

2019b) The protumour function of γδ T cells in PDAC is largely unknown; however, Daley et al. show that γδ T cells are pathogenic in PDAC as they impair CD4$^+$/CD8$^+$ T cells through immune checkpoint ligation.(Daley et al., 2016) More specifically, this function is driven through the Vγ4$^+$ subset that produce significant levels of IL-17A and IL-10, both potent immune-suppressive cytokines, and that the presence of CD4$^+$ and CD8$^+$ T cells increases 10-fold in the absence of γδ T cells. Finally, tumour-infiltrating γδ T cells express high levels of PD-L1 and Galectin-9, and pharmacological blockade of PD-L1 and Galectin-9 enhances the infiltration of activated (CD44$^+$CD62L$^-$) αβ T cells.(Daley et al., 2016) This evidence, in orthotopic KPC models, indicates that γδ T cells in murine PDAC may have potent immune-modulatory function and directly contribute to immune suppression. Therefore, in this chapter I aim to interrogate the ability of γδ T cells to influence immune cell activation in the PDAC TME and metastatic niche of KPC mice.

To summarise, in this chapter I aim to determine the impact of γδ T cells on the primary tumour and metastatic niche. To achieve this, I will first determine if γδ T cells play a role in cancer cachexia and will assess their immune-modulating capabilities in adipose tissue. Secondly, I aim to investigate the immune-modulating capacity of γδ T cells in primary tumour and metastatic niche through assessing immune cell activation states. Additionally, I will also address the impact of γδ T cell absence on components of the primary tumour and metastatic niche. Finally, I also aim to determine if γδ T cells can mediate crosstalk with pro-tumour myeloid cells in KPC mice.

5.2 Contribution of γδ T cells to cancer cachexia.

Given the published evidence that IL-17A$^+$CD27$^-$ γδ T cells have been shown to play a central role in the maintenance of adipose tissue homeostasis, I aimed to assess their role the adipose tissue of KPC mice and determine if they contribute to cachexia in KPC mice. I also investigated if the loss of γδ T cells in KPC;Tcrd$^{-/-}$ adipose tissue leads to significant changes to other immune cell populations, given that γδ T cells promote Treg expansion. I investigated this in brown (BrAT), subcutaneous (SubAT) and epididymal (EpiAT) adipose tissue. BrAT plays a central role in murine thermogenesis and metabolism owing to the large proportion of mitochondria, and the loss of white adipose tissue deposits such as SubAT and EpiAT is a major aspect of cancer cachexia.(Han et al., 2018) Furthermore, IL-17A$^+$ γδ T cells are significantly enriched in BrAT, SubAT and EpiAT compared to peripheral tissues, and so are ideal tissues to investigate γδ T cell function. (Kohlgruber et al., 2018)

5.2.1 γδ T cells do not contribute to adipose tissue wastage in KPC mice.

The first stage in investigating the role of γδ T cells in cancer cachexia was to compare the weights of SubAT, EpiAT and BrAT in KPC mice, and determine if the loss of γδ T cells impacts their weight at humane clinical endpoint. I found that SubAT weights from KPC and KPC;Tcrd$^{-/-}$ mice are significantly reduced compared to their respective controls, but that there is no significant difference between the weights of KPC and KPC;Tcrd$^{-/-}$ mice (Figure 5-1A). I observed a similar trend in EpiAT (Figure 5-1B), but there were no differences in BrAT weights in any cohorts (Figure 5-1C). However, the significant reductions in the SubAT and EpiAT depots in KPC and KPC;Tcrd$^{-/-}$ mice confirms that cancer-induced cachexia is a phenotype of KPC mice. However, the lack of any discernible difference between the weights of adipose tissue depots between KPC and KPC;Tcrd$^{-/-}$ mice indicates that γδ T cells do not contribute to cachexia, or at least the wasting of adipose tissue depots in KPC mice.
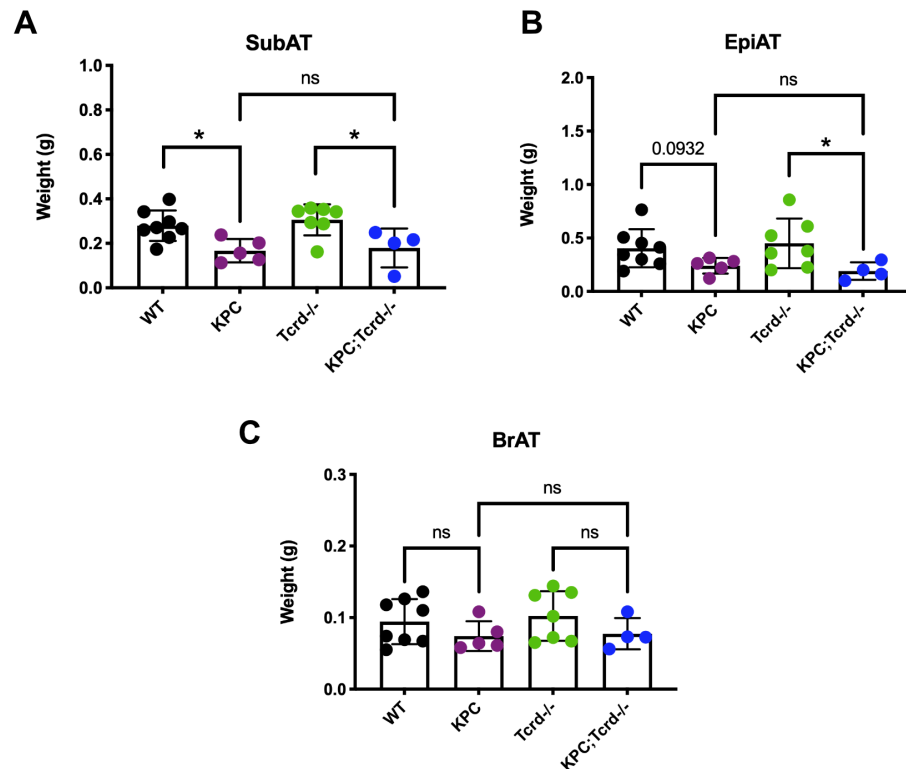
Figure 5-1 γδ T cells do not contribute to adipose tissue wastage in KPC mice.
KPC (n=5) and KPC;Tcrd$^{-/-}$ (n=4) mice were aged to humane clinical endpoint and WT (n=8) and Tcrd$^{-/-}$ (n=7) mice were aged-matched to provide suitable controls, respectively. Adipose tissue was dissected and fat deposits from subcutaneous (SubAT) (A), epididymal (EpiAT) (B) and brown (BrAT) (C) adipose tissue were weighed. * P < 0.05 as determined by Mann-Whitney U-Test.

5.2.2 Loss of γδ T cells does not change immune cell activation state in adipose tissue from KPC;Tcrd$^{-/-}$ mice.

Despite the evidence showing that γδ T cells do not play a significant role in adipose tissue cachexia, I sought to further characterise their impact on other adipose tissue immune cells, as IL-17A^{+} γδ T cells have been shown to maintain certain immune cell niches in adipose tissue. (Kohlgruber et al., 2018) Therefore, I performed flow cytometry to phenotype the γδ T cell populations in adipose tissue; elucidate the effect of γδ T cell loss on the activation status of CD4^{+}/CD8^{+} T cells and their cytokine production; and finally, determine the impact of γδ T cell loss on NK cell maturation and cytokine production in KPC;Tcrd$^{-/-}$ adipose tissue (Figure 5-2).
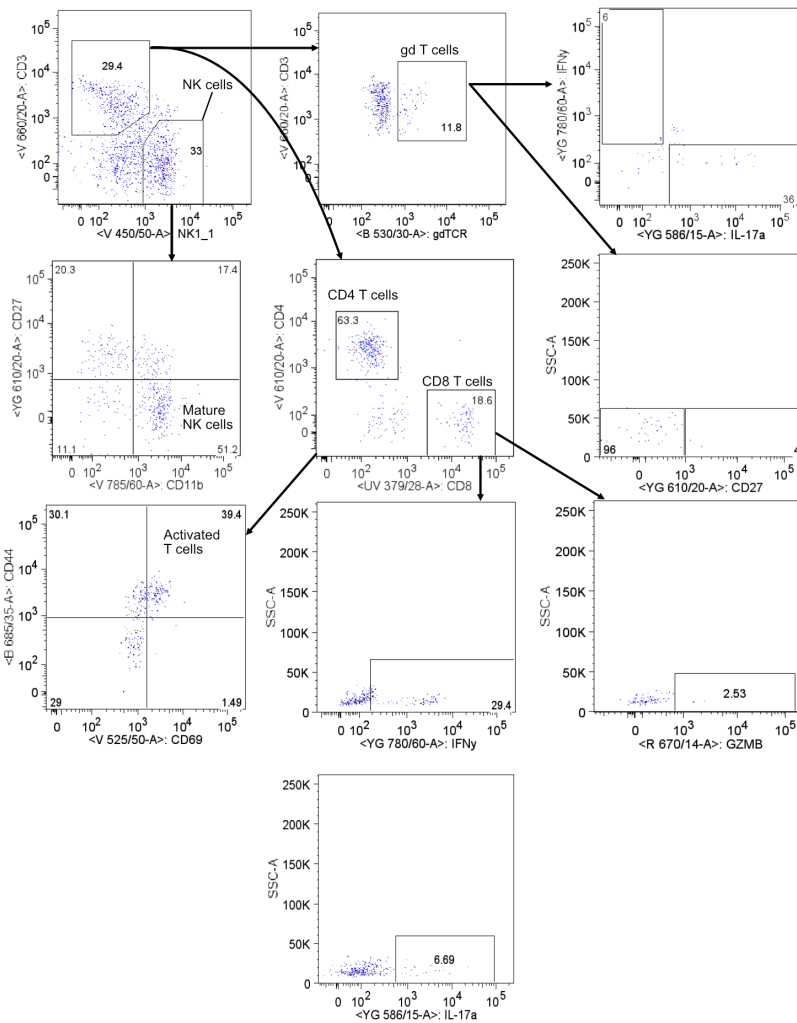
Figure 5-2 Adipose tissue contains significant populations of γδ T, αβ T and NK cells.
Representative image of the gating strategy implemented to identify γδ T cells, CD4⁺/CD8⁺ T cells and NK cells, and to interrogate T cell activation status (CD44⁺CD69⁺), NK cell maturity (CD11b⁺CD27⁻) and cytokine production (IFN-γ, IL-17A and Granzyme B). Representative flow plots taken from KPC EpiAT.

I observed no significant changes to any immune cell populations between KPC and KPC;Tcrd$^{-/-}$ mice or when compared to respective controls in EpiAT (Figure 5-3). Firstly, bulk γδ T cells are not expanded in EpiAT from KPC mice compared to WT controls; they display no significant differences in the production of IL-17A or IFN-γ; and there is no preferential expansion of either CD27⁻ or CD27⁺ γδ T cell subsets (Figure 5-3A). Bulk CD4⁺ T cells (CD3⁺CD4⁺) are also unaffected by γδ T cell loss, with no significant changes to the production of IFN-γ and IL-17A or to their activation state (CD44⁺CD69⁺) (Figure 5-3B), a trend that is mirrored in the CD8⁺ T cell populations (Figure 5-3C). Finally, the bulk NK cell population in EpiAT also remained unchanged between the cohorts along with mature NK cell populations (Figure 5-3D). NK cells develop through a four-stage process which can be delineated through the two surface molecules CD27 and CD11b —

CD11b^{lo}CD27^{lo} → CD11b^{lo}CD27^{hi} →CD11b^{hi}CD27^{hi} → CD11b^{hi}CD27^{lo}. (Chiossone et al., 2009) I focussed upon the CD11b^{hi}CD27^{lo} (mature) NK cell subset, as they display greater cytotoxic function with increased Granzyme B and perforin gene signatures and higher capacity for inflammation induction. (Chiossone et al., 2009) However, there was also no significant changes to the mature NK cell population or their production of IFN-γ or Granzyme B (Figure 5-3D).

Similar to EpiAT, the γδ T cell populations remain largely unchanged in SubAT from KPC mice compared to WT controls, as there were no observable differences between bulk γδ T cells, IL-17A and IFN-γ production and CD27 subset status (Figure 5-4A). As with EpiAT, bulk CD4$^+$ T cells remained unchanged along with their cytokine production (IFN-γ and IL-17A); however, CD4$^+$ activation state (CD44$^+$CD69$^+$) appeared to increase in KPC;Tcrd$^{-/-}$ SubAT when compared to KPC mice, but this did not achieve statistical significance (Figure 5-4B). There was a similar trend in the CD8$^+$ T cells, where bulk CD8$^+$ T cells and their production of IFN-γ and Granzyme B remained unchanged; but CD8$^+$ T cells from KPC;Tcrd$^{-/-}$ SubAT display a significantly increased activation state when compared to KPC mice (Figure 5-4C). Furthermore, bulk NK cells in SubAT remain unchanged in all cohorts; there is a near significant increase in mature (CD11b$^+$CD27$^-$) NK cells in KPC;Tcrd$^{-/-}$ SubAT, but this does not translate to any significant differences in cytokine production (Figure 5-4D). Finally, BrAT displays no significant differences to bulk γδ T cells or in their IL-17A and IFN-γ cytokine production, but there appears to be significantly increased CD27$^-$ and decreased CD27$^+$ γδ T cells (Figure 5-5A). Similarly, BrAT from KPC;Tcrd$^{-/-}$ shows no changes to bulk CD4$^+$/CD8$^+$ T cell populations, their cytokine production or to their activation state (CD44$^+$CD69$^+$) (Figure 5-5B/C). Bulk NK cells and mature (CD11b$^+$CD27$^-$) NK cells also remain unchanged along with mature NK cell cytokine production (Figure 5-5D), further indicating that γδ T cells do not influence immune cell activation status in the adipose tissue niche.
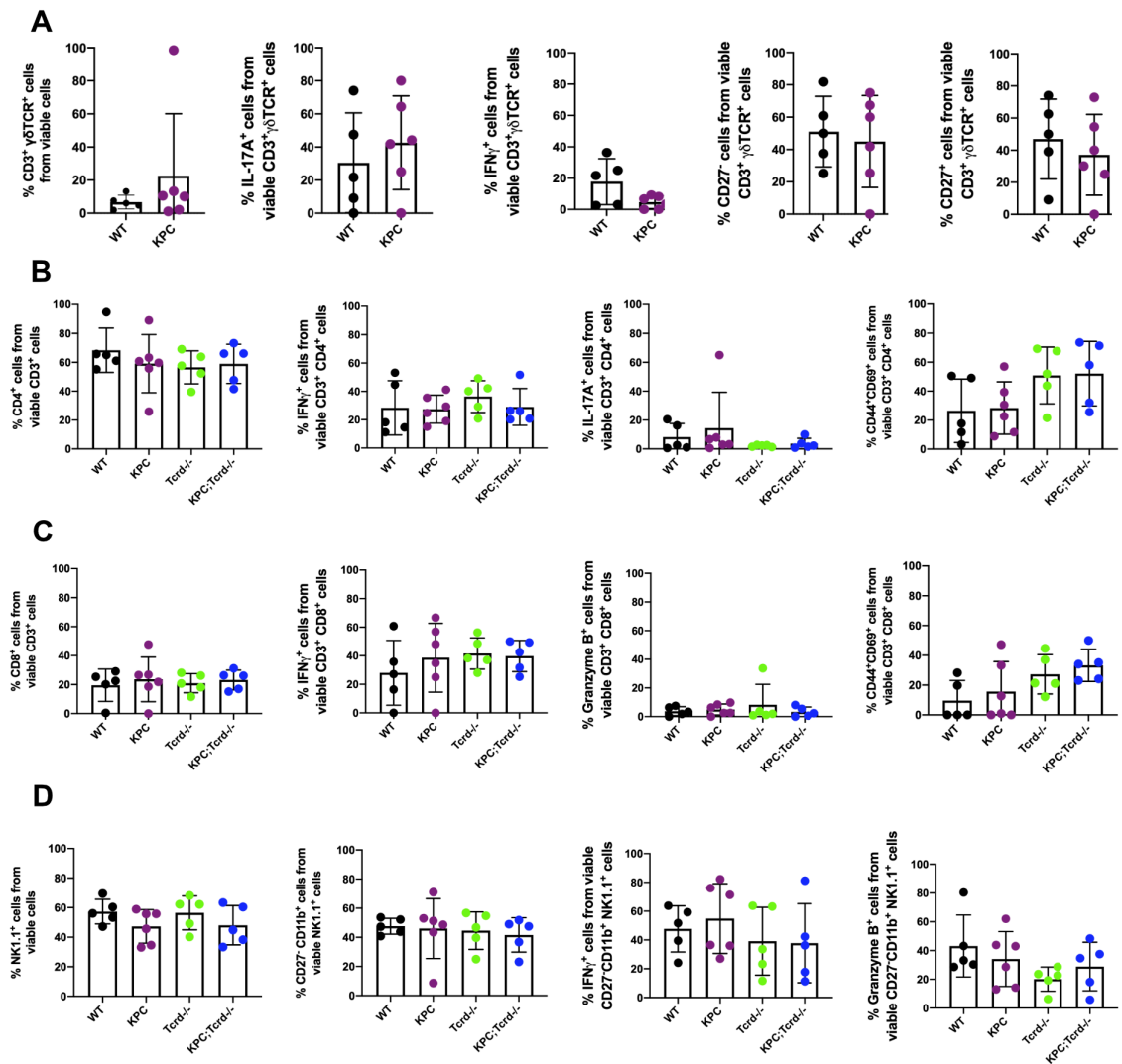
Figure 5-3 CD4⁺/CD8⁺ T and NK cell populations are unaffected by the absence of γδ T cells in EpiAT from KPC;Tcrd$^{-/-}$ mice.
EpiAT was harvested from KPC (n=6) and KPC;Tcrd$^{-/-}$ (n=5) mice aged to humane clinical endpoint, and EpiAT from also harvested from aged-matched WT (n=5) and Tcrd$^{-/-}$ (n=5) controls. Bulk γδ T cell (CD3⁺γδTCR⁺) populations were assessed along with IL-17A and IFN-γ production and CD27 subset expansion (A). Bulk CD4⁺ T cells were assessed along with IFN-γ and IL-17A production and activation state (CD44⁺CD69⁺) (B). Bulk CD8⁺ T cells were also assessed along with IFN-γ and Granzyme B production and activation state (CD44⁺CD69⁺) (C). Bulk NK cells (NK1.1⁺) cells were assessed along with CD11b⁺CD27⁻ (mature) NK cells and mature NK cell cytokine production (IFN-γ and Granzyme B) (D).

Figure 5-4 CD8+ T cells are more activated in SubAT from KPC;Tcrd−/− mice, but other immune cell populations remain unchanged.
SubAT was harvested from KPC (n=5) and KPC;Tcrd−/− (n=5) mice aged to humane clinical endpoint, and SubAT from also harvested from aged-matched WT (n=5) and Tcrd−/− (n=5) controls. Bulk γδ T cell (CD3+γδTCR+) populations were assessed along with IL-17A and IFN-γ production and CD27 subset expansion (A). Bulk CD4+ T cells were assessed along with IFN-γ and IL-17A production and activation state (CD44+CD69+) (B). Bulk CD8+ T cells were also assessed along with IFN-γ and Granzyme B production and activation state (CD44+CD69+) (C) Bulk NK cells (NK1.1+) cells were assessed along with CD11b+CD27− (mature) NK cells and mature NK cell cytokine production (IFN-γ and Granzyme B) (D). * P < 0.05 as determined by Kruskal-Wallis test.

Figure 5-5 CD27⁻ γδ T cells are significantly expanded in BrAT in KPC mice.
BrAT was harvested from KPC (n=6) and KPC;Tcrd$^{-/-}$ (n=5) mice aged to humane clinical endpoint, and BrAT from also harvested from aged-matched WT (n=5) and Tcrd$^{-/-}$ (n=5) controls. Bulk γδ T cell (CD3$^+$γδTCR$^+$) populations were assessed along with IL-17A and IFN-γ production and CD27 subset expansion (A). Bulk CD4$^+$ T cells were assessed along with IFN-γ and IL-17A production and activation state (CD44$^+$CD69$^+$) (B). Bulk CD8$^+$ T cells were also assessed along with IFN-γ and Granzyme B production and activation state (CD44$^+$CD69$^+$) (C) Bulk NK cells (NK1.1$^+$) cells were assessed along with CD11b$^+$CD27$^-$ (mature) NK cells and mature NK cell cytokine production (IFN-γ and Granzyme B) (D). * P < 0.05 as determined by Mann-Whitney test.

Thus, other than significantly increased CD8$^+$ T cell activation in SubAT in KPC;Tcrd$^{-/-}$ mice, the loss of γδ T cells does not appear to have an significant impact on immune cell populations in EpiAT, SubAT. Finally, BrAT from KPC mice has significantly increased CD27$^-$ γδ T cells compared to WT mice and indicates that pro-tumour γδ T cells may be enriched in BrAT, which could impact on BrAT metabolism. Overall, γδ T cells do not promote cancer-associated cachexia in KPC mice, and do not alter the activation state of major immune cell populations in adipose tissue.

5.3 The impact of γδ T cells on immune cell populations in KPC mice.

5.3.1 γδ T cells do not enhance the activation state or cytokine production of CD4/CD8 T cells in KPC mice.

I have previously shown that γδ T cells infiltrate KPC PDAC tissue and display a pro-tumour phenotype through the production of IL-17A. Given that published literature details the function of γδ T cells in orthotopic KPC models is immune-suppressive and restrains αß ($CD4^+$/$CD8^+$) T cell activation, I sought to investigate if γδ T cells exert similar control over αß T cells and NK cells in autochthonous KPC mice. To investigate this, I performed flow cytometric analysis to identify $CD4^+$ T cells, $CD8^+$ T cells and NK cells (Figure 5-6). To determine the activation state of $CD4^+$ and $CD8^+$ T cells, I assessed the expression of CD44 and CD69, as the combined expression of these surface markers indicates an activated phenotype.(Lindell et al., 2006) I then also interrogated the cytokine production of $CD4^+$ and $CD8^+$ T cells and assessed the extent to which IFN-γ ($CD4^+$/$CD8^+$), IL-17A ($CD4^+$) and Granzyme B ($CD8^+$) were produced by these cells. Additionally, I also investigated NK cell maturation as previously described, and the cytokine production from mature NK cells. Finally, I then also looked to assess how the loss of γδ T cells would impact on the activation state of CD4/CD8 T cells and their cytokine production; and how the loss of γδ T cells impacted NK cell maturation and mature NK cell cytokine production.
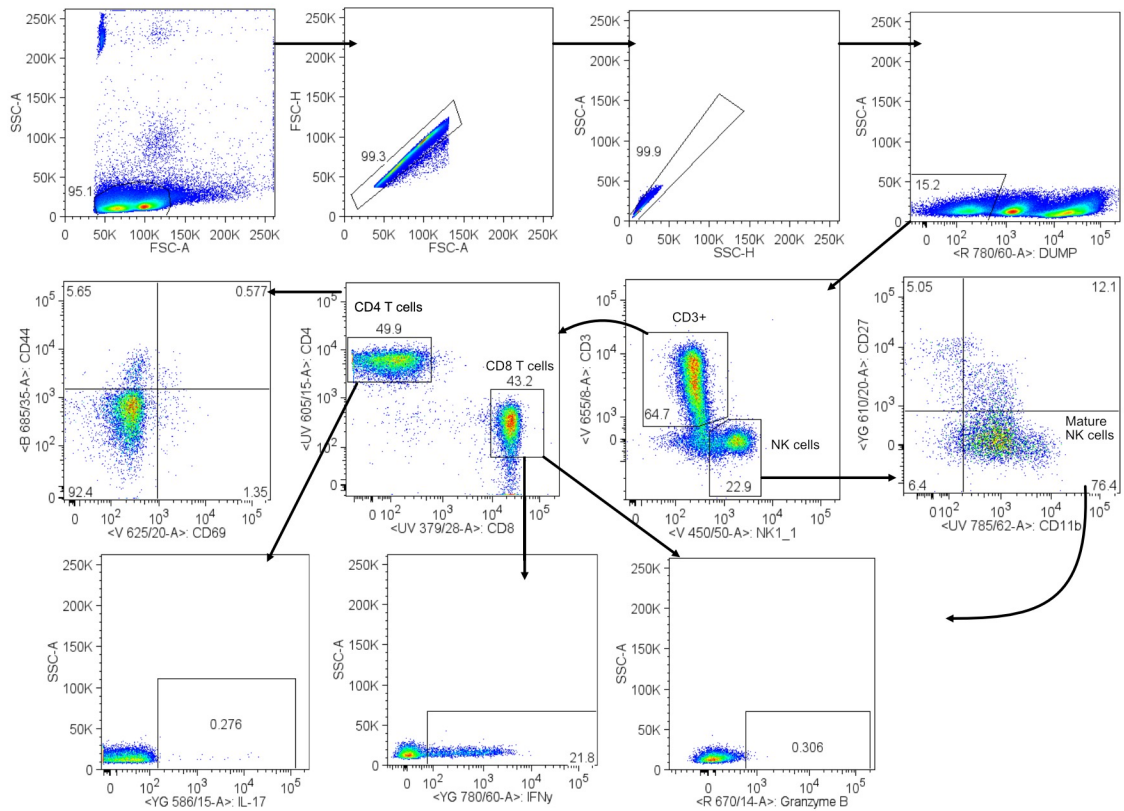
Figure 5-6 CD4/CD8 T and NK cells are form distinct populations within peripheral tissues. Representative flow cytometry plots illustrating the gating strategy implemented to identify CD4$^+$ T cells, CD8$^+$ T cells and NK (NK1.1$^+$) cells. Cytokine production of CD4$^+$ (IFN-γ and IL-17A) and CD8$^+$ (IFN-γ and Granzyme B) T cells and their activation state (CD44$^+$CD69$^+$) were assessed. Mature NK cells (NK1.1$^+$CD11b$^+$CD27$^-$) and their cytokine production (IFN-γ and Granzyme B) were assessed. Representative plots obtained from KPC spleen.

The first step in characterising the impact of γδ T cells on the activation state of immune cells was to investigate the primary PDAC tumour, as Daley et al. detailed that tumour-infiltrating γδ T cells in orthotopic KPC directly impair CD4$^+$/CD8$^+$ T cells via checkpoint receptor ligation. (Daley et al., 2016) In primary PDAC tissue, I found that KPC mice have no changes to bulk CD4$^+$ T cells (Figure 5-7A), CD4$^+$ T cell activation state (Figure 5-7B) or in the production of IFN-γ or IL-17A (Figure 5-7C) when compared to WT controls. I found identical findings in the CD8$^+$ T cells, which had no changes to bulk CD8$^+$ populations (Figure 5-7D), activation state (Figure 5-7E) or production of IFN-γ or Granzyme B (Figure 5-7F) compared to WT controls. When I assessed the impact of γδ T cells, I found no change to the activation state of CD4$^+$/CD8$^+$ T cells, and no differences in cytokine production between KPC and KPC;Tcrd$^{-/-}$ PDAC tissue. Thus, these data suggest that γδ T cells do not impact the activation state of αβ T cells in PDAC tumours of spontaneous KPC mice.
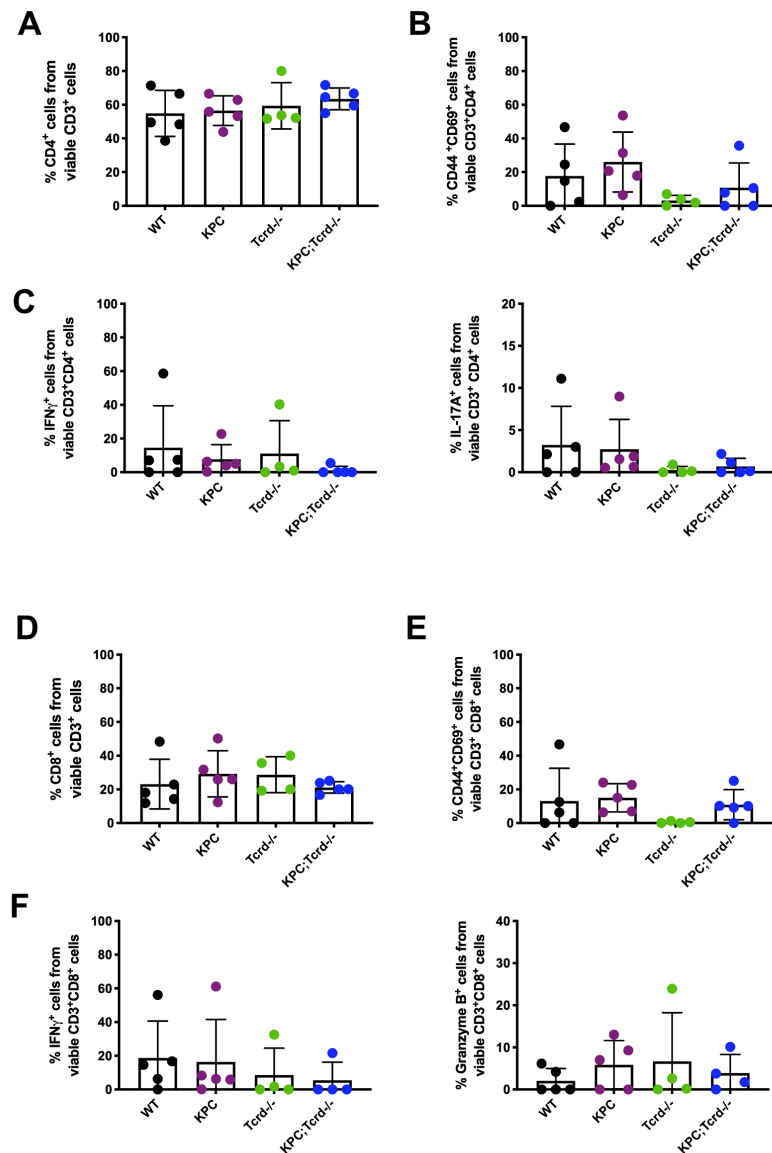
Figure 5-7 CD4⁺ and CD8⁺ T cell activation state in primary PDAC tissue is unaffected by the absence of γδ T cells in KPC;Tcrd⁻/⁻ mice.
KPC (n=5) and KPC;Tcrd⁻/⁻ (n=5) mice were aged to humane clinical endpoint, with WT (n=5) and Tcrd⁻/⁻(n=4) aged matched controls taken. Primary PDAC or WT pancreas tissue was harvested and flow cytometry was performed on isolated immune cells. Bulk CD4⁺ T cell (A), activated CD4⁺ T cells (CD44⁺CD69⁺) (B) and production of IFN-γ and IL-17A from CD4⁺ T cells (C) was assessed. Bulk CD8⁺ T cell (D), activated CD8⁺ T cells (CD44⁺CD69⁺) (E) and production of IFN-γ and Granzyme B from CD8⁺ T cells (F) was assessed.

Continuing on from this, I then assessed if γδ T cells played a role in restraining αß T cell activity in the liver metastatic niche, as a greater level of T cell activation and anti-tumour cytokine production may explain the observed reduction of liver metastasis found in KPC;Tcrd⁻/⁻ mice. However, I found identical results from the KPC PDAC tissue; bulk CD4⁺ T cells (Figure 5-8A), CD4⁺ T cell activation state (Figure 5-8B) and CD4⁺ T cell production of IFN-γ and IL-17A (Figure 5-8C) were not significantly reduced in KPC mice compared to WT

mice, and was unaffected by the absence of γδ T cells. Similarly, bulk CD8⁺(Figure 5-8D), CD8⁺ T cell activation (Figure 5-8E) and CD8⁺ T cell production of IFN-γ and Granzyme B (Figure 5-8F) were not significantly impaired in KPC mice compared to WT mice, and were also unchanged by the loss of γδ T cells in KPC;Tcrd$^{-/-}$ mice.
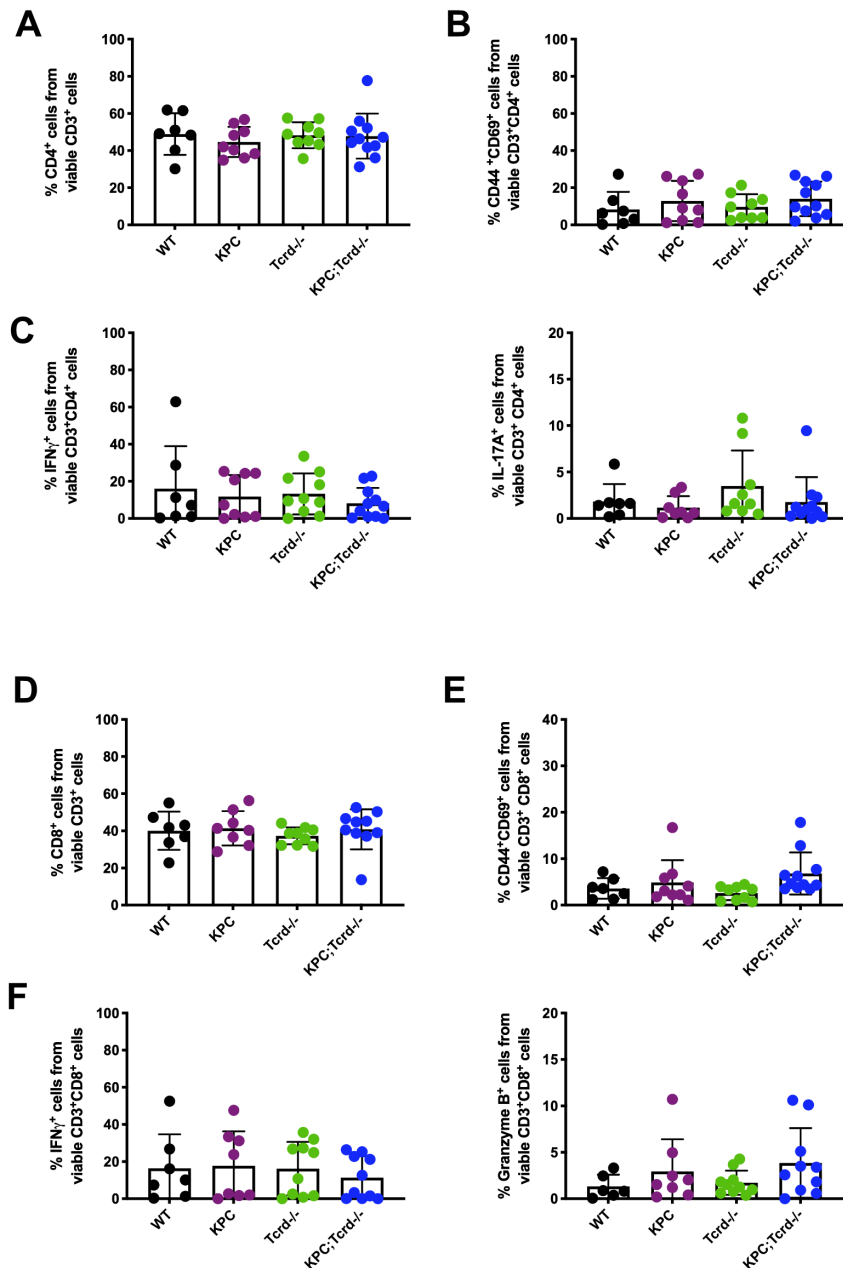
Figure 5-8 CD4⁺ and CD8⁺ T cell activation state is unaffected by the absence of γδ T cells in the liver metastatic niche of KPC;Tcrd$^{-/-}$ mice.

KPC (n=9) and KPC;Tcrd$^{-/-}$ (n=11) mice were aged to humane clinical endpoint, with WT (n=7) and Tcrd$^{-/-}$(n=10) aged matched controls taken. Liver tissue was harvested and flow cytometry was performed on isolated immune cells. Bulk CD4⁺ T cell (A), activated CD4⁺ T cells (CD44⁺CD69⁺) (B) and production of IFN-γ and IL-17A from CD4⁺ T cells (C) were assessed. Bulk CD8⁺ T cell (D), activated CD8⁺ T cells (CD44⁺CD69⁺) (E) and production of IFN-γ and Granzyme B from CD8⁺ T cells (F) were assessed.

Finally, I then determined whether γδ T cells influence populations of circulating CD4$^+$ and CD8$^+$ T cells in KPC spleen tissue, but I found no significant changes to CD4$^+$ T cell activation state (Figure 5-9B) and no significant changes in IFN-γ and IL-17A cytokine production (Figure 5-9C) in CD4$^+$ T cells in KPC spleen compared to WT controls. Interestingly, I observed a significant increase in the proportions of bulk CD4$^+$ T cells in KPC;Tcrd$^{-/-}$ compared to KPC spleen (Figure 5-9A), but this did not translate into any significant changes to activation state or cytokine production. Finally, there were no changes to bulk CD8$^+$ T cells (Figure 5-9D), CD8$^+$ T cell activation state (Figure 5-9E) or CD8$^+$ T cell cytokine production (Figure 5-9F) in KPC spleen compared to WT controls, and these were unaffected by the absence of γδ T cells.

In summary, I aimed to determine the role of γδ T cells in controlling immune cell activation in autochthonous KPC mice. I found no evidence in PDAC, liver and spleen tissue that CD4$^+$ or CD8$^+$ T cells displayed increased activation or had any significant differences in cytokine production compared to WT controls. There was also no evidence of improved CD4$^+$/CD8$^+$ activation or cytokine production in PDAC, liver and spleen tissue of KPC;Tcrd$^{-/-}$ mice, suggesting that γδ T cells do not restrain αβ T cell activation in KPC mice, contrary to published evidence. Crucially, this also indicates the reduction in metastatic incidence is not due to changes in impaired anti-tumour cytolytic CD8$^+$ T cells, as seen in breast cancer.
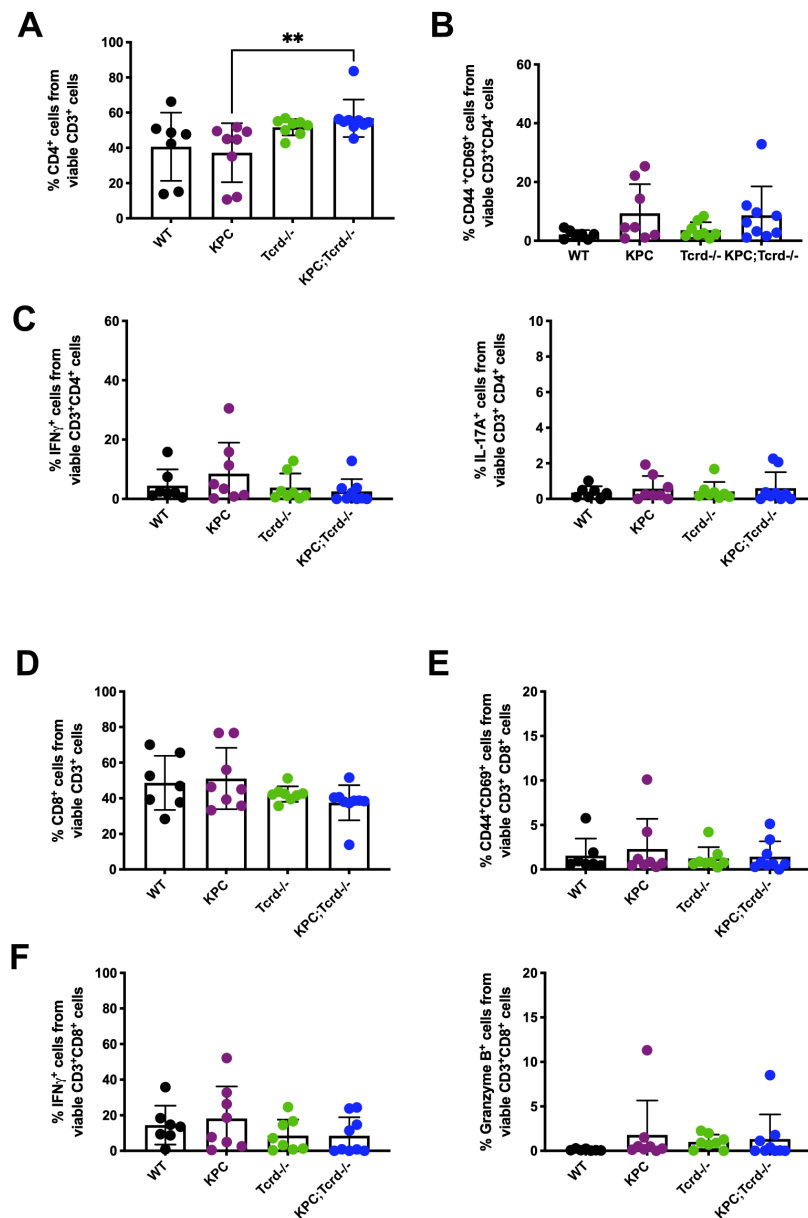
Figure 5-9 Bulk CD4⁺ T cells are significantly increased, but CD8⁺ T cells remain unchanged, in the absence of γδ T cells in KPC;Tcrd⁻/⁻ spleens.
KPC (n=8) and KPC;Tcrd⁻/⁻ (n=9) mice were aged to humane clinical endpoint, with WT (n=7) and Tcrd⁻/⁻(n=8) aged matched controls taken. Spleen tissue was harvested, and flow cytometry was performed on isolated immune cells. Bulk CD4⁺ T cell (A), activated CD4⁺ T cells (CD44⁺CD69⁺) (B) and production of IFN-γ and IL-17A from CD4⁺ T cells (C) was assessed. Bulk CD8⁺ T cell (D), activated CD8⁺ T cells (CD44⁺CD69⁺) (E) and production of IFN-γ and Granzyme B from CD8⁺ T cells (F) was assessed. ** $P < 0.01$ as determined by Kruskal-Wallis Test.

5.3.2 γδ T cells restrain the production of IFN-γ from mature (CD11b⁺CD27⁻) NK cells in KPC liver tissue.

Following on from the finding that CD4⁺ and CD8⁺ T cells from KPC mice have no significant differences activation state or cytokine production when compared to WT controls, or in the absence of γδ T cells, I changed my focus towards NK cells which are another important immune cell with potent anti-metastatic

properties. In this instance, I aimed to determine if NK cells in KPC mice have impaired cytokine production compared to WT mice and if γδ T cells can influence their activity. Firstly, I found that NK cells in KPC PDAC tissue have no significant differences in bulk NK cells (NK1.1$^+$), NK cell maturation state (CD11b$^+$CD27$^-$) or in IFN-γ and Granzyme B production (Figure 5-10A). Similarly, proportions of bulk and mature (CD11b$^+$CD27$^-$) NK cells in KPC liver remain unchanged compared to WT controls; however, IFN-γ and Granzyme B production in mature NK cells from KPC livers was significantly reduced compared to WT controls (Figure 5-10B). Furthermore, the absence of γδ T cells restored the IFN-γ producing capacity of mature NK cells in KPC;Tcrd$^{-/-}$ liver but not Granzyme B production (Figure 5-10B). Finally, I observed no impairment to bulk NK cells, NK cell maturation or cytokine production in KPC spleens compared to WT controls, and the absence of γδ T cells in KPC;Tcrd$^{-/-}$ spleen had no impact (Figure 5-10C). This increased IFN-γ production in mature NK cells from KPC;Tcrd$^{-/-}$ livers may indicate a possible anti-tumour mechanism that is suppressed by γδ T cells in KPC mice; as IFN-γ production by NK cell contributes to metastasis clearance through augmented NK cell activation and the induction of Th1 immunity. (Lin et al, 2021) Thus, the increased production of IFN-γ by NK cells in KPC;Tcrd$^{-/-}$ liver tissue indicates a potential link between γδ T cells and liver metastasis, but this requires further investigation to fully define this phenotype. Future areas of study could be focussed on FasL and TRAIL, which are expressed on the surface of NK cells and direct NK cell cytotoxicity through binding of their cognate receptor (Fas and TRAILR) on cancer cells to induce apoptosis. (Paul and Lal, 2017) Thus, the exploration of additional NK cell cytotoxic mechanisms is required to elucidate if liver NK cell dysfunction is a phenotype of KPC mice.

PDAC
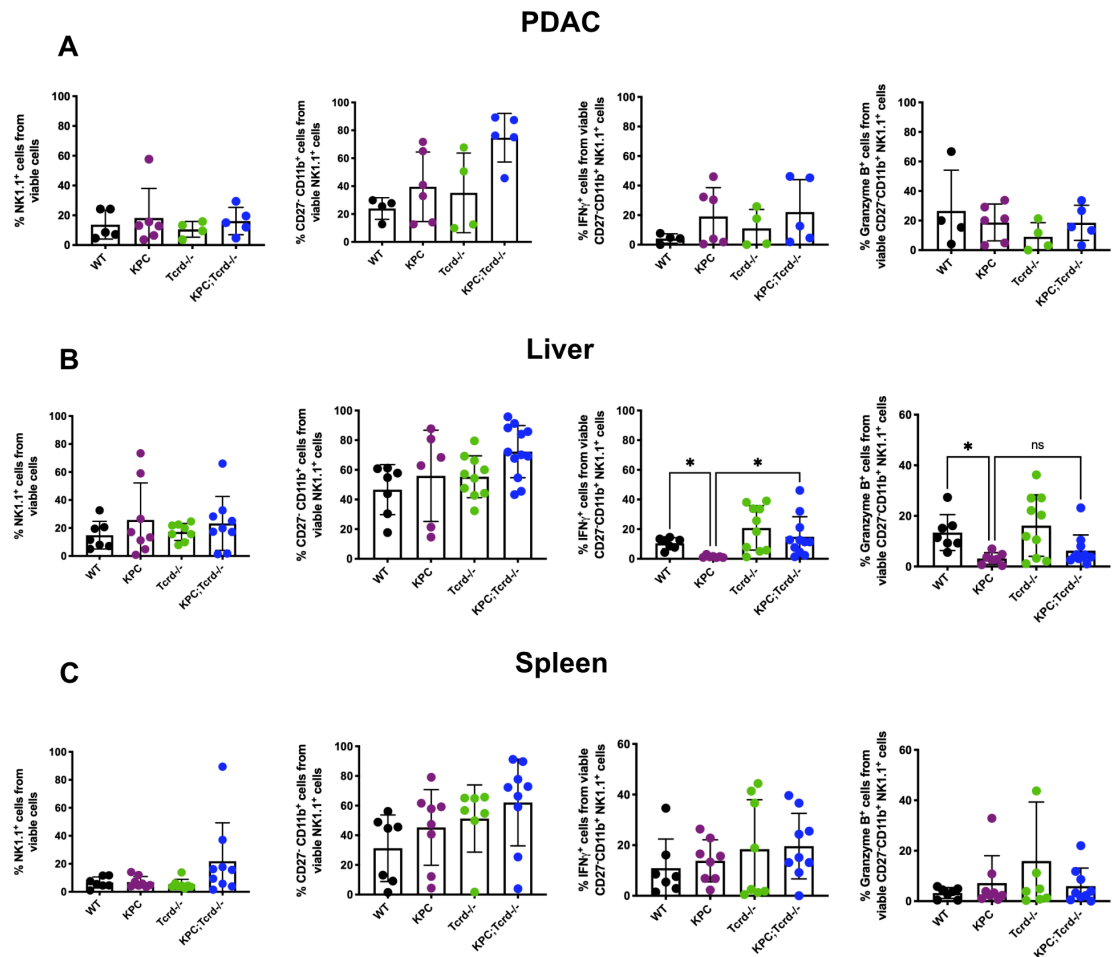
Liver

Spleen

Figure 5-10 Loss of γδ T cells increases the production of IFN-γ from mature CD11b⁺CD27⁻ NK cells, but not Granzyme B.

KPC and KPC;Tcrd$^{-/-}$ mice were aged to humane clinical endpoint and PDAC, liver and spleen were harvested. Pancreas, liver and spleen tissue were also taken from age-matched controls. Bulk NK cells, mature (CD11b⁺CD27⁻) and mature NK cell cytokine production was assessed in PDAC (WT n=5, KPC n=6, Tcrd$^{-/-}$ n=4 and KPC;Tcrd$^{-/-}$ n=5) liver (WT n=7, KPC n=8, Tcrd$^{-/-}$ n=10 and KPC;Tcrd$^{-/-}$ n=12) and spleen (WT n=7, KPC n=8, Tcrd$^{-/-}$ n=8 and KPC;Tcrd$^{-/-}$ n=9). ** P < 0.01 and * P < 0.05 as determined by Kruskal-Wallis Test.

5.3.3 Liver NK cells can be further sub-categorised into tissue-resident NK vs circulating NK cells.

As previously described, NK cell activity is tightly regulated by a combination of activating and inhibitory receptors. Activating receptors include NKG2D which binds to MICA, MICB and ULBP1-6 proteins which are upregulated during cellular stress, and CD226 (DNAM-1) which binds to CD155.(Huntington et al., 2020, Paul and Lal, 2017, Kumar, 2018) Inhibitory receptors that restrain NK cell activity include *T-cell Ig and ITIM domain* (TIGIT) and CD96 (TACTILE). (Yin et al., 2018) Thus, NK cells can become activated through CD226 (DNAM-1) ligation upon binding to CD112 and CD155 ligands expressed on antigen-presenting cells or

transformed tumour cells.(Dougall et al., 2017) Inhibitory receptors TIGIT and CD96 also bind to CD112 and CD155, and directly compete with CD226 by binding to CD155 with higher affinity to impair NK cell activation. Given this information, I aimed to assess if the impaired IFN-γ production observed in NK cells in KPC mice is due to increased inhibitory receptor expression on NK cells. To investigate this, I designed a flow cytometry panel to identify the expression of inhibitory (TIGIT and CD96) and activating (CD226) receptors, and the production of IFN-γ, Granzyme B and TNF-α (Figure 5-11). Furthermore, murine NK cells can be sub-categorised into tissue-resident (CD49a$^+$DX5$^-$) and circulating NK cells (CD49a$^-$DX5$^+$), and so I aimed to assess if γδ T cells preferentially suppress or promote a specific population of NK cells (Figure 5-11).(Jewett et al., 2020, Sojka et al., 2014)

5.3.4 Circulating NK cells may express higher levels of TIGIT inhibitory receptor in KPC;Tcrd$^{-/-}$ mice.

First, I looked to find if either circulating (CD49a$^-$DX5$^+$) or tissue-resident (CD49a$^+$DX5$^-$) NK cells are preferentially expanded or suppressed in KPC mice, and looked to determine the impact that loss of γδ T cells has on both populations. I found that both circulating NK cells (Figure 5-12A) and tissue-resident NK cells (Figure 5-12B) were not changed in KPC liver compared to WT controls, and the absence of γδ T cells in KPC;Tcrd$^{-/-}$ had no additional effect. I then looked to assess the expression profiles of activating (CD226) and inhibitory (CD96 and TIGIT) receptors within each population. In circulating NK cells, I observed very low expression of CD96 and found no observable differences between the experimental groups (Figure 5-12C); and CD226 expression appears lower in both the KPC and KPC;Tcrd$^{-/-}$ cohorts compared to respective controls, but there are no changes between KPC and KPC;Tcrd$^{-/-}$ mice (Figure 5-12C). Interestingly, there appears to be slightly higher expression of the inhibitory TIGIT receptor in circulating NK cells from KPC;Tcrd$^{-/-}$ liver, although the expression levels remain low (Figure 5-12C). Additionally, there appears to be no changes to IFN-γ and Granzyme B production between all experimental groups; however, expression of TNF-α may be increased in circulating NK cells from KPC;Tcrd$^{-/-}$ livers (Figure 5-12C). In tissue-resident NK cells, the expression of CD96, CD226 and TIGIT remains unchanged between KPC and KPC;Tcrd$^{-/-}$ groups, with similar trends observed in the production of IFN-γ and Granzyme B

(Figure 5-12D). Similar to circulating NK cells, tissue-resident NK cells may have higher expression of TNF-α in KPC;Tcrd$^{-/-}$ livers. However, more experimental repeats are required before meaningful conclusions can be drawn from this data.
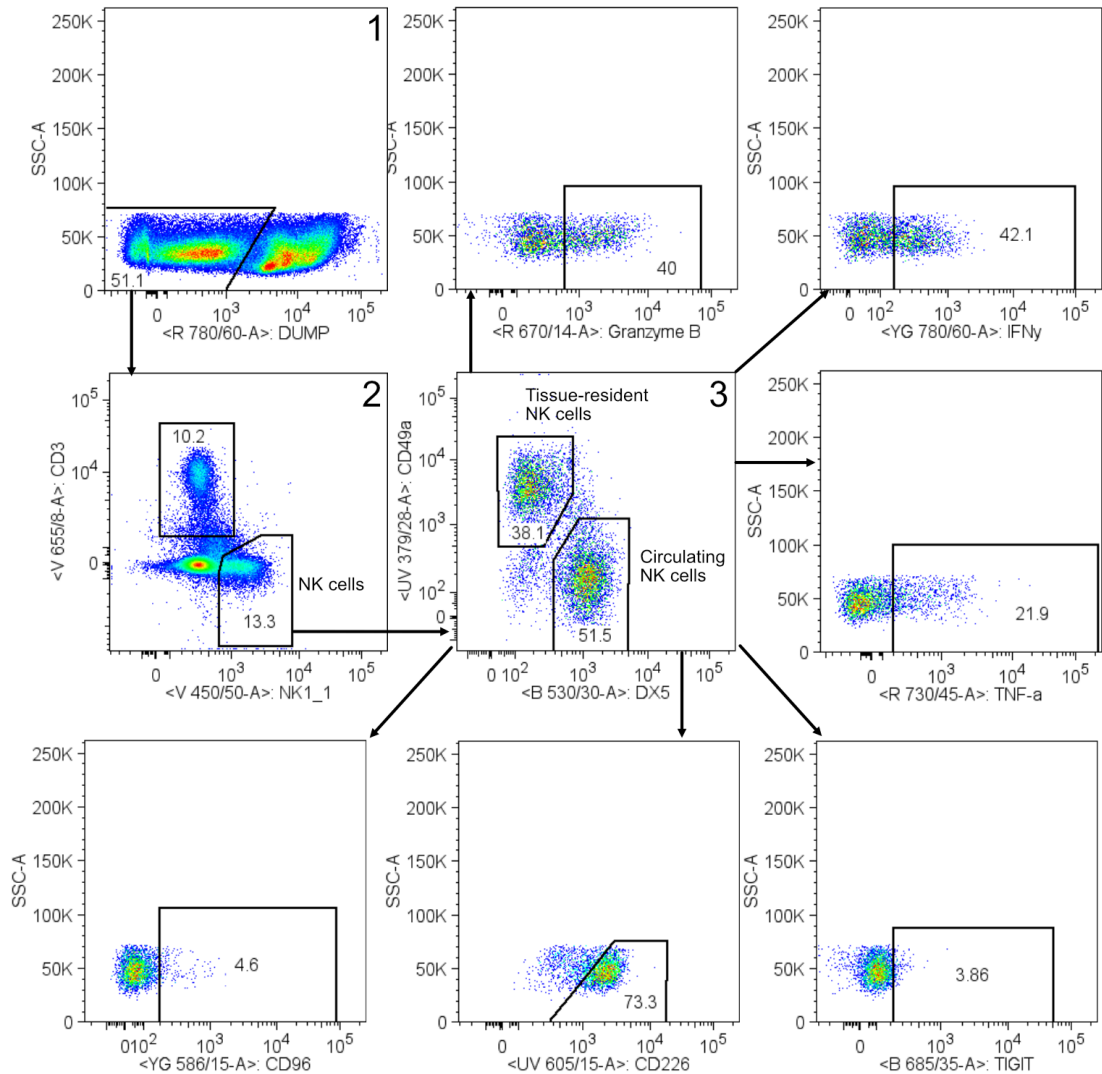
Figure 5-11 NK cells in the liver can be separated into tissue-resident (CD49a$^+$DX5$^-$) and circulating (CD49a$^-$DX5$^+$) populations.
Illustration showing the representative gating strategy where viable (1) liver NK cells (CD3$^-$NK1.1$^+$ (2) were identified and sub-categorised into tissue-resident (CD49a$^+$DX5$^-$) and circulating (CD49a$^-$ DX5$^+$) populations (3). Both tissue-resident and circulating NK cells were then assessed for activating (CD226) and inhibitory (TIGIT and CD96) receptors and cytokine production (Granzyme B, IFN-γ and TNF-α).

A

B

Circulating NK cells

C

Tissue-resident NK cells

D
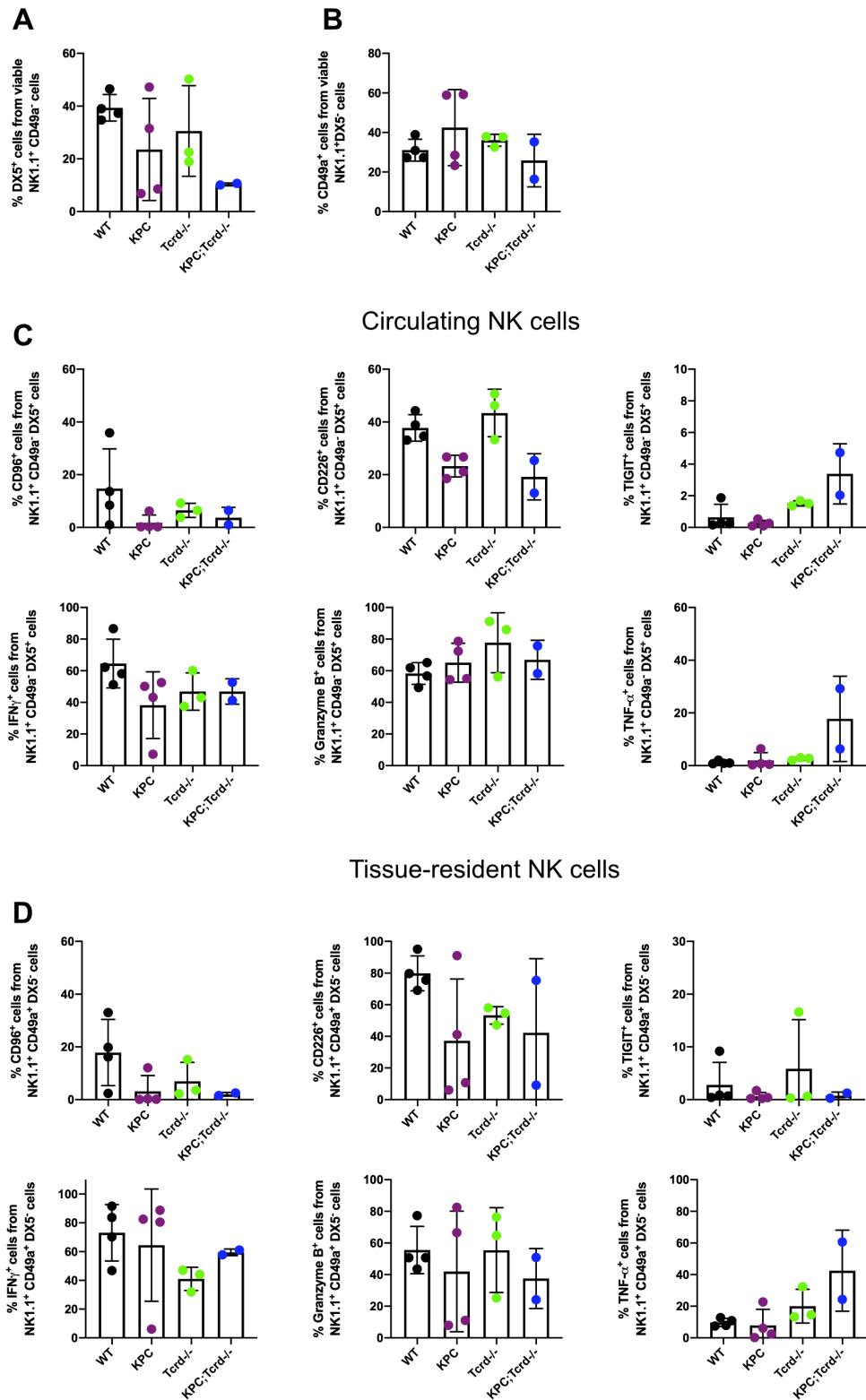
Figure 5-12 Circulating NK cells may express higher levels of inhibitory receptor TIGIT in KPC;Tcrd$^{-/-}$ liver tissue.
Liver tissue was obtained from KPC (n=4) and KPC;Tcrd$^{-/-}$ (n=2) mice that were aged to humane clinical endpoint, and liver tissue was harvested from age-matched WT (n=4) and Tcrd$^{-/-}$ (n=3) controls. Proportions of circulating (CD49a$^-$DX5$^+$) (A) and tissue resident (CD49a$^+$DX5$^-$) (B) cells from NK1.1$^+$ cells. Expression of CD96, CD226 and TIGIT receptors and production of IFN-γ, Granzyme B and TNF-α on circulating NK cells (C). Expression of CD96, CD226 and TIGIT receptors and production of IFN-γ, Granzyme B and TNF-α on tissue-resident NK cells (D).

In summary, there are no significant changes to either circulating or tissue-resident NK cells, and expression CD96 and CD226 remains unchanged by the absence of γδ T cells in KPC;Tcrd$^{-/-}$ livers. Tissue-resident NK cells display no changes to TIGIT expression in all cohorts. However, circulating NK cells in KPC;Tcrd$^{-/-}$ livers appear to express marginally higher TIGIT and potentially greater levels of TNF-α (Figure 5-12C). Higher levels of TIGIT would initially suggest that circulating NK cells are more inhibited in the absence of γδ T cells; however, the stable expression of IFN-γ, Granzyme B and the potential increase in TNF-α secretion suggests otherwise as TIGIT overexpression is normally associated with reduced IFN-γ and TNF-α production. (Meng et al 2020) Thus, whilst concrete conclusions cannot yet be drawn from this experiment, the potentially increased TIGIT expression may indicate a response to increased NK cell activation, as TIGIT also increases in response to NK cell activation as a self-limiting step to prevent excessive activation.(Schorer et al., 2020, Yin et al., 2018)

5.3.5 Histological analysis of the liver metastatic niche indicates NK cells are reduced in KPC;Tcrd$^{-/-}$ liver tissue.

To gain a greater idea of additional changes within the metastatic niche, extensive immunohistochemistry (IHC) staining was performed targeting lymphocytes, myeloid cells and other components associated with tumourigenesis. Following staining, all slides were assessed to ensure optimal staining and were then scanned for quantification on HALO® image analysis software. Firstly, I found that CD3 cells were not changed between KPC and KPC;Tcrd$^{-/-}$ livers (Figure 5-13), confirming my flow cytometry findings that proportions of CD4$^+$ and CD8$^+$ T cells were not changed in KPC;Tcrd$^{-/-}$ liver tissue (Figure 5-8A/D). I also found that F4/80$^+$ macrophages and Ly6G$^+$ neutrophils remained unchanged in KPC;Tcrd$^{-/-}$ livers (Figure 5-13). In metastatic breast cancer, pro-tumour IL-17A$^+$ γδ T cells promote the expansion of immune-suppressive neutrophils that impair anti-metastatic CD8$^+$ T cells. (Coffelt et al., 2015) These data suggests that although γδ T cells in KPC mice are pro-metastatic, they do not promote metastasis through neutrophil expansion or CD8$^+$ T cell impairment in the liver metastatic niche. Interestingly, I observed a significant reduction in NKp46 staining (NK cells) (Figure 5-13), which indicates that although there are fewer NK cells in KPC;Tcrd$^{-/-}$ liver

tissue, they produce more IFN-γ (Figure 5-10B), and so may have a greater anti-metastatic capacity. Finally, I found no differences to Ki67, Caspase 3 and FOXP3 staining, suggesting that the loss of γδ T cells in the liver metastatic niche does not significantly impact on cellular proliferation, apoptotic cell death and regulatory T cell populations, respectively (Figure 5-14).
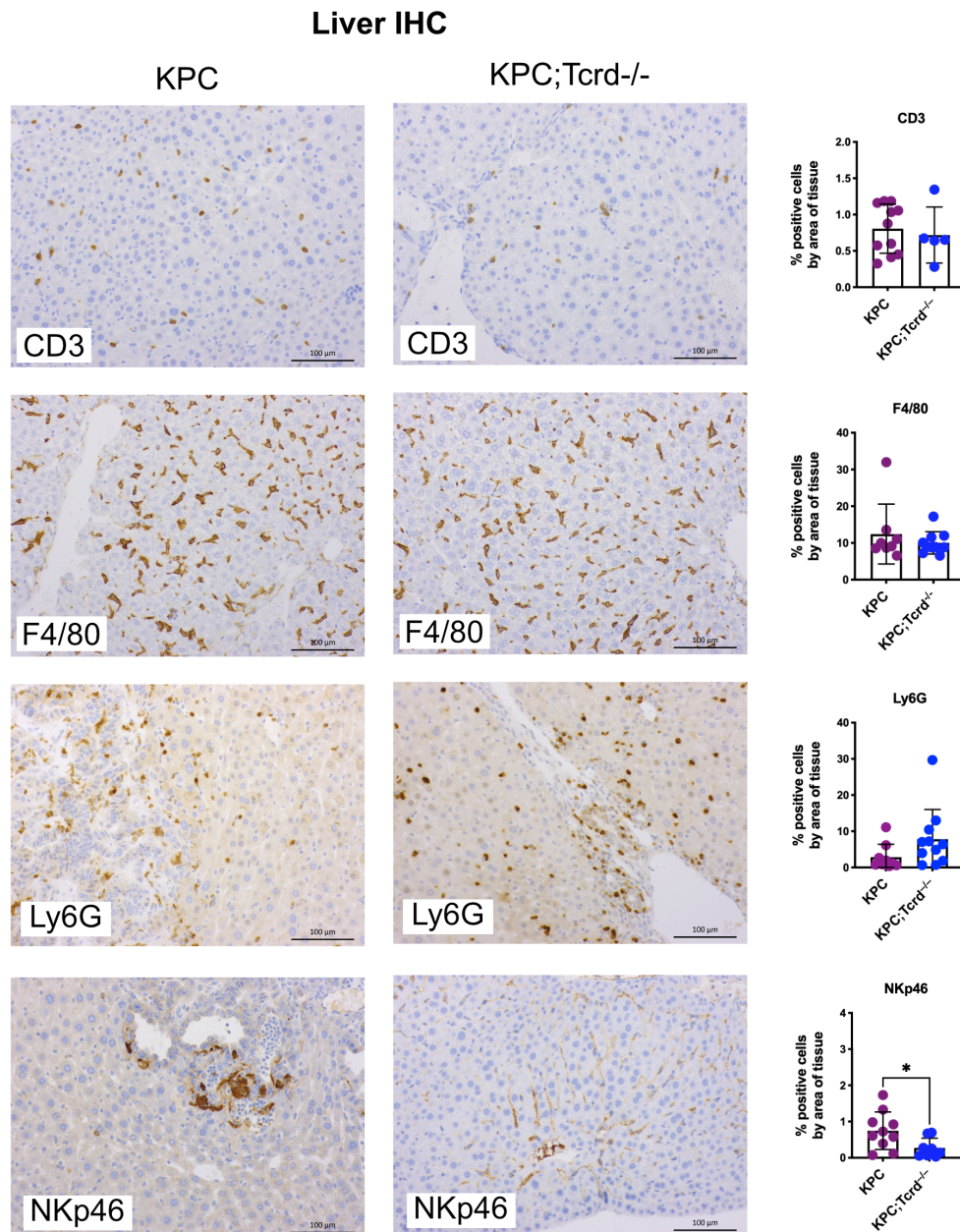
Figure 5-13 IHC reveals NK cells are reduced in KPC;Tcrd$^{-/-}$ liver tissue.
KPC (n=11) and KPC;Tcrd$^{-/-}$ (n=11) were aged to humane clinical endpoint, and IHC staining was performed on liver tissue. Representative images of staining for CD3$^+$ (T cells), F4/80$^+$ (macrophages), Ly6G$^+$ (neutrophils) and NKp46$^+$ (NK cells) are shown from KPC (left) and KPC;Tcrd$^{-/-}$ (middle), images taken at 20x magnification with scale bar representing 100μm. Quantifications of staining was performed on HALO® image analysis and are shown (right) as "*% positive cells by area of tissue*". * P < 0.05 as determined by Mann-Whitney U-Test.

Liver IHC
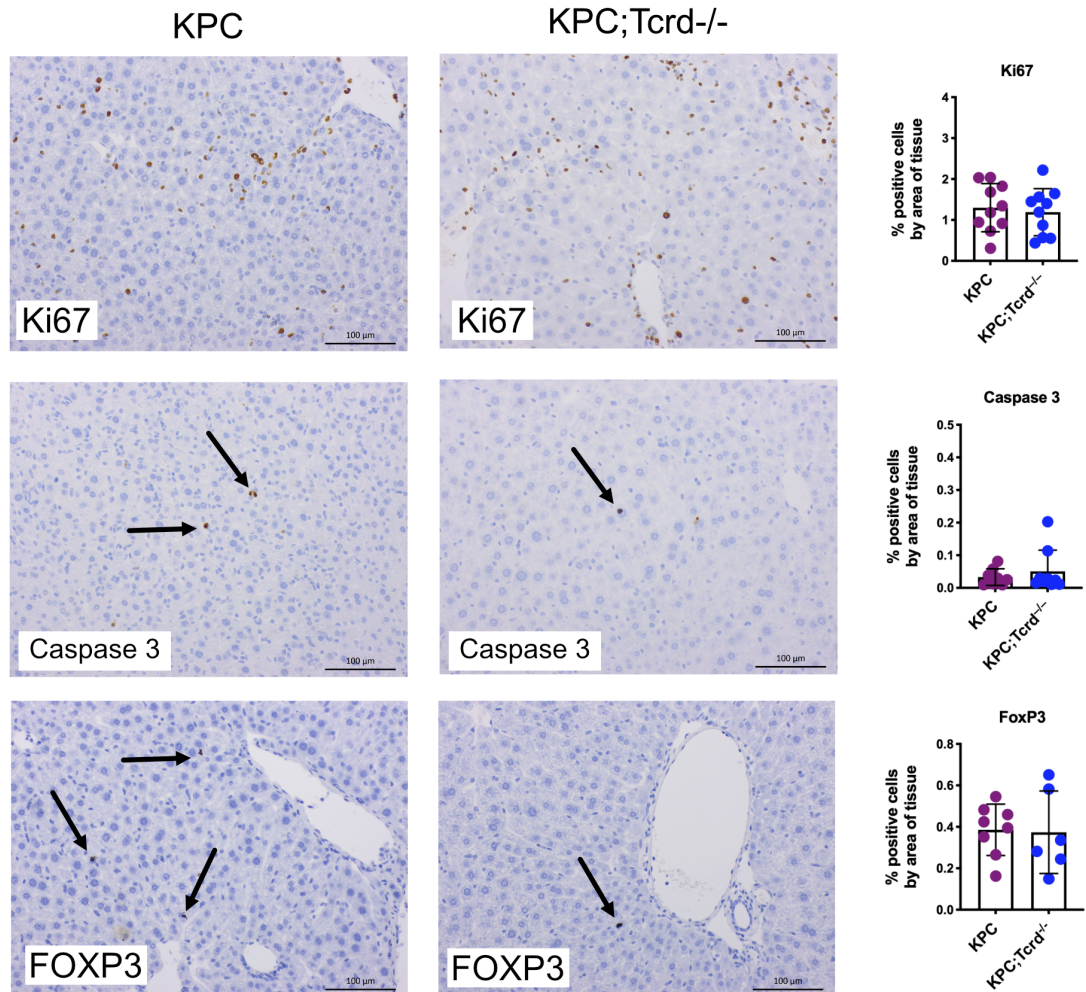
Figure 5-14 Apoptotic cell death and cellular proliferation are unchanged between KPC and KPC;Tcrd$^{-/-}$ liver tissue.
KPC (n=11) and KPC;Tcrd$^{-/-}$ (n=11) were aged to humane clinical endpoint, and IHC staining was performed on liver tissue. Representative images of staining for Ki67 (proliferation), Caspase 3 (apoptotic cell death) and FOXP3 (Tregs) are shown from KPC (left) and KPC;Tcrd$^{-/-}$ (middle), images taken at 20x magnification with scale bar representing 100μm. Quantifications of staining was performed on HALO® image analysis and are shown (right) as "*% positive cells by area of tissue*".

5.4 The role of γδ T cells in the PDAC TME.

5.4.1 The absence of γδ T cells reduces TAM populations and PDPN-expressing cells in KPC;Tcrd$^{-/-}$ PDAC tissue.

I have shown by flow cytometry that γδ T cells do not affect the activation state of αβ T cells in KPC PDAC tissue, and so I looked to further assess the impact of γδ T cells on other components of the primary tumour TME. The PDAC TME consists of a dense fibrotic stroma controlled primarily by activated fibroblasts and other stromal cells, and infiltrated immune-suppressive cells such as Tregs, TAMs and pro-metastatic neutrophils that subvert anti-tumour functions and promote tumour progression. Thus, extensive IHC staining was performed on endpoint PDAC tissue of KPC and KPC;Tcrd$^{-/-}$ mice to gain a global understanding of the impact of γδ T cells on the metastatic niche.

My focus was initially towards cell populations that are prevalent within the PDAC niche, and so performed IHC staining for T cells (CD3), Tregs (FOXP3), macrophages (F4/80) and neutrophils (Ly6G). In line with flow cytometry data, I observed no changes to CD3 staining which confirmed that γδ T cells do not control T cell infiltration into PDAC tissue (Figure 5-15). I also found there were no changes to Ly6G and FOXP3 staining in KPC;Tcrd$^{-/-}$ PDAC, showing that γδ T cells do not promote neutrophils and Tregs in the PDAC TME (Figure 5-15). Interestingly, I found a significant reduction in F4/80 staining in KPC;Tcrd$^{-/-}$ mice compared to KPC controls, indicating that γδ T cells promote PDAC TAM populations (Figure 5-15). When TAM populations are impaired in KPC mice with anti-M-CSFR (AZD7507), there is reduced Masson's Trichrome staining (collagen deposition) and reductions in myofibroblasts (α-SMA), which indicates impaired tumour stroma following TAM inhibition. (Candido et al., 2018) However, despite the reductions in TAMs, there were no corresponding changes to Ki67 (proliferation), α-SMA (myofibroblasts) or Sirius Red (collagen deposition), but there was higher Caspase 3 (apoptosis) expression in KPC;Tcrd$^{-/-}$ PDAC tissue (Figure 5-16). However, this was not combined with any additional markers, and so it cannot be attributed to either increased tumour cell death or to other populations within the TME. Thus, whilst the loss of γδ T cells significantly impacts TAM populations, this does not result in significant alterations to the stromal compartment in KPC;Tcrd$^{-/-}$ PDAC tissue.

Following on from the observation that F4/80$^+$ macrophages are reduced in KPC;Tcrd$^{-/-}$ PDAC, I then looked to establish if this was also due to impaired M-CSFR expression, which is expressed on monocytes and macrophages and has been described as an indispensable factor for TAM-mediated immune suppression within the PDAC TME.(Zhu et al., 2014) Interestingly, I found that M-CSFR expression was unchanged in KPC;Tcrd$^{-/-}$ PDAC tissue, suggesting that the reductions to TAM populations is not related to M-CSFR expression, which is expressed by both embryonic-derived and bone marrow-derived macrophages (Figure 5-17). I also looked to see if γδ T cell absence in KPC;Tcrd$^{-/-}$ PDAC influences the formation of blood vessels, so stained for CD31 which is a marker for vascular differentiation; however, CD31 was unaffected by the absence of γδ T cells in KPC;Tcrd$^{-/-}$ PDAC (Figure 5-17). Additionally, given the greater appreciation of CAF heterogeneity, I then look to determine the effect of γδ T cells on CAFs, and utilised podoplanin (PDPN) as a marker for CAFs. (Biffi et al., 2019) I found that KPC;Tcrd$^{-/-}$ PDAC have significantly lower expression of PDPN, suggesting that γδ T cells promote CAF populations in PDAC (Figure 5-17). Finally, given that TGF-β signalling has been described as a major factor in the polarisation of TAMs, I stained for pSMAD3 which is an important mediator to TGF-β signalling, but I found no changes to pSMAD3 in KPC;Tcrd$^{-/-}$ PDAC.(Ahmed et al., 2017) In summary, the absence of γδ T cells leads to a significant reduction in the F4/80$^+$ macrophages in the PDAC TME, but this is not associated with any changes to collagen deposition (Sirius Red) or to tumour cell proliferation (Ki67), which has previously been observed when PDAC TAMs are inhibited.(Candido et al., 2018) Additionally, whilst the loss of γδ T cells does not impact myofibroblasts (α-SMA), the reduction in PDPN expression suggests an impairment to other fibroblast populations in the absence of γδ T cells.

PDAC IHC
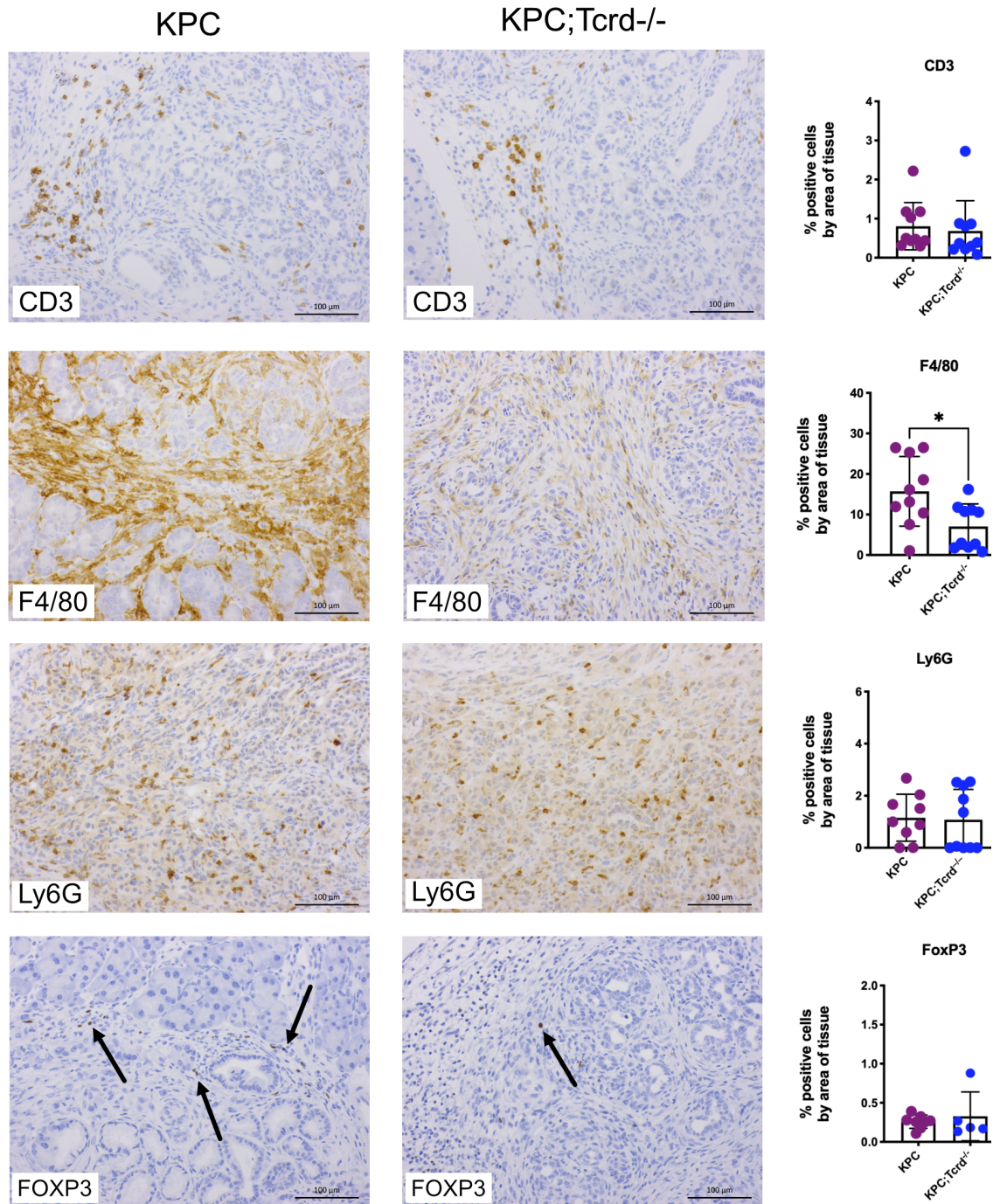
Figure 5-15 Absence of γδ T cells in KPC;Tcrd$^{-/-}$ PDAC tissue leads to a significant reduction in tumour-associated macrophage populations.
KPC (n=10) and KPC;Tcrd$^{-/-}$ (n=10) were aged to humane clinical endpoint, and IHC staining was performed on PDAC tissue. Representative images of staining for CD3 (T cells), F4/80 (macrophages) and Ly6G (neutrophils) and FOXP3 (Treg cells) (KPC n=8. KPC;Tcrd$^{-/-}$ n=6). Representative images shown from KPC (left) and KPC;Tcrd$^{-/-}$ (middle), images taken at 20x magnification and scale bar represent 100μm. Quantifications of staining was performed on HALO® image analysis, shown (right) as "*% positive cells by area of tissue*". * P < 0.05 as determined by Mann-Whitney U-Test.

PDAC IHC
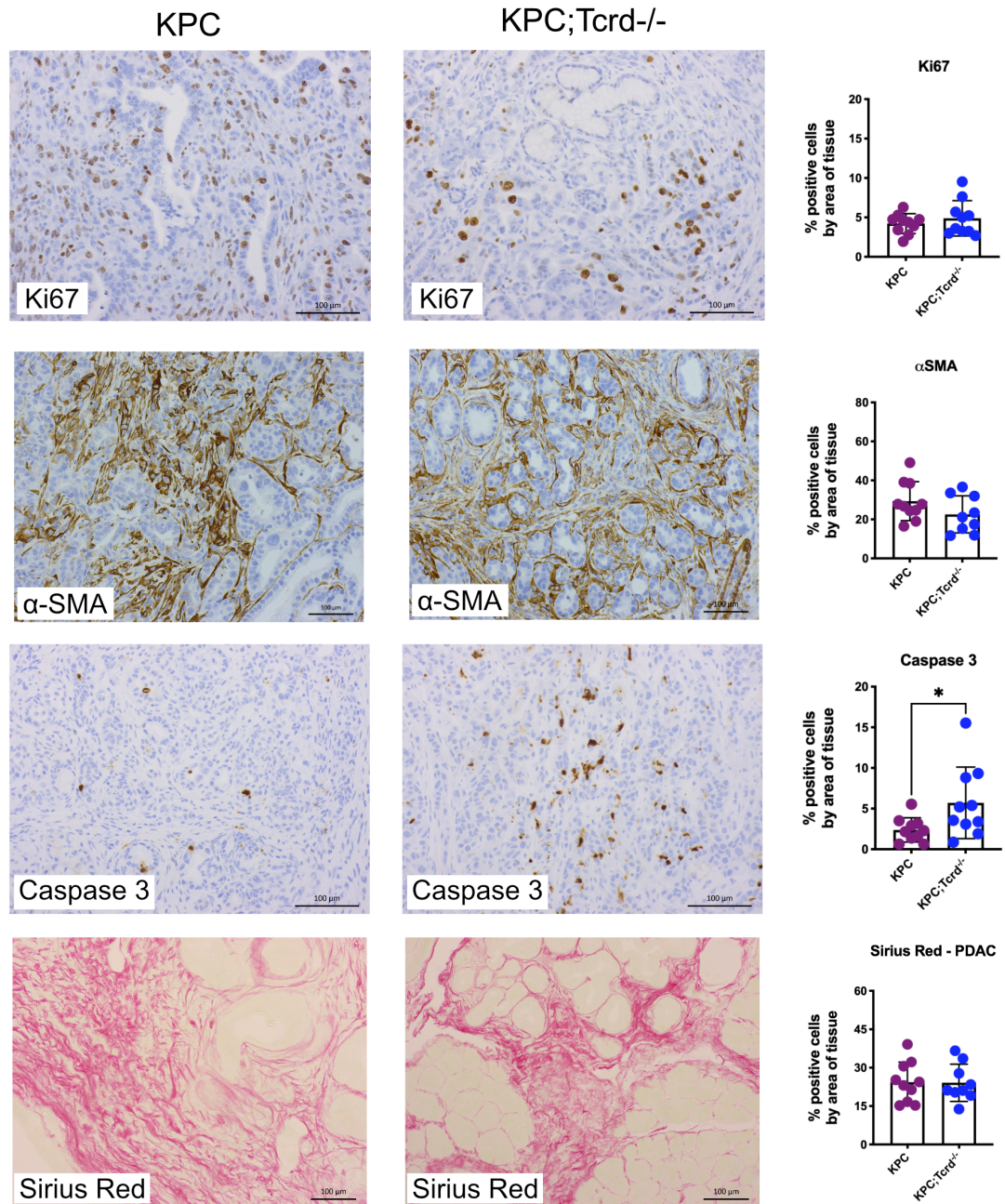
Figure 5-16 The absence of γδ T cells in KPC;Tcrd$^{-/-}$ PDAC tissue is associated with greater levels of apoptotic cell death.
KPC (n=10) and KPC;Tcrd$^{-/-}$ (n=10) were aged to humane clinical endpoint, and IHC staining was performed on PDAC tissue. Representative images of staining for Ki67 (proliferation), α-SMA (myofibroblasts), Caspase 3 (apoptotic cell death) and Sirius Red (collagen deposition). Representative images shown from KPC (left) and KPC;Tcrd$^{-/-}$ (middle), images taken at 20x magnification and scale bars represent 100μm. Quantifications of staining was performed on HALO® image analysis, shown (right) as *"% positive cells by area of tissue"*. * P < 0.05 as determined by Mann-Whitney U-Test.

PDAC IHC
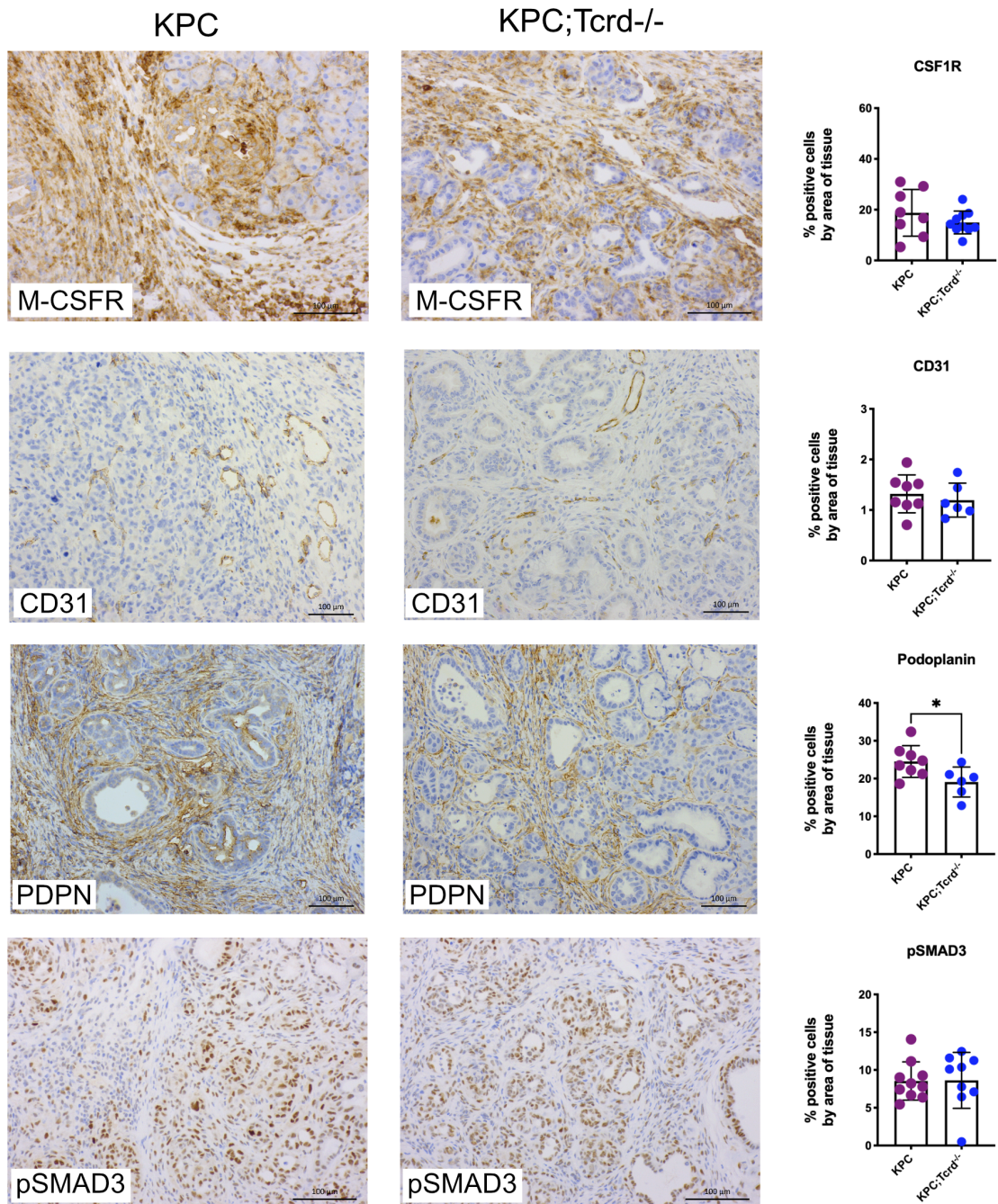
Figure 5-17 The absence of γδ T cells in KPC;Tcrd$^{-/-}$ PDAC tissue leads to significantly reduced expression of podoplanin (PDPN).
KPC and KPC;Tcrd$^{-/-}$ were aged to humane clinical endpoint, and IHC staining was performed on PDAC tissue. Representative images of staining for M-CSFR, CD31 (blood vessels), Podoplanin (PDPN), and pSMAD3 (TGF-β signalling). Representative images shown from KPC (left) and KPC;Tcrd$^{-/-}$ (middle), images taken at 20x magnification and scale bars represent 100μm. Quantifications of staining was performed on HALO® image analysis, shown (right) as "*% positive cells by area of tissue*". M-CSFR and pSMAD 3 KPC n=10 and KPC;Tcrd$^{-/-}$ n=10, CD31 and PDPN KPC n=8 and KPC;Tcrd$^{-/-}$ n=6. * P < 0.05 as determined by Mann-Whitney U-Test.

5.4.2 The absence of γδ T cells only impairs TAM populations and PDPN⁺ cells in end-stage PDAC.

I then sought to confirm if the reductions to F4/80$^+$ macrophages and PDPN$^+$ CAFs is restricted to end-stage PDAC, or if it occurs earlier in tumourigenesis. Therefore, I performed IHC staining for F4/80 and PDPN at 6-week and 10-week timepoints to understand the kinetics of these populations during PanIN progression and PDAC development. In early-stage (6wk) PanINs, both F4/80$^+$ macrophages and PDPN$^+$ CAFs are present within PanIN lesions (Figure 5-18A). However the absence of γδ T cells in 6wk KPC;Tcrd$^{-/-}$ pancreas does not significantly impact either F4/80$^+$ macrophages or PDPN$^+$ CAFs. As PanIN lesions progress to late-stage (10wk), greater levels of neoplastic transformation and stromal remodelling is also associated with increased infiltration of both F4/80$^+$ macrophages and PDPN$^+$ CAFs (Figure 5-18B). However, the absence of γδ T cells in 10wk KPC;Tcrd$^{-/-}$ pancreas does not impact on either F4/80$^+$ macrophages or PDPN$^+$ CAFs (Figure 5-18B) Therefore, as with the kinetics of γδ T cell infiltration throughout PDAC progression, the influence of γδ T cells on F4/80$^+$ macrophages and PDPN$^+$ CAFs appears to only become significant at late-stage PDAC.
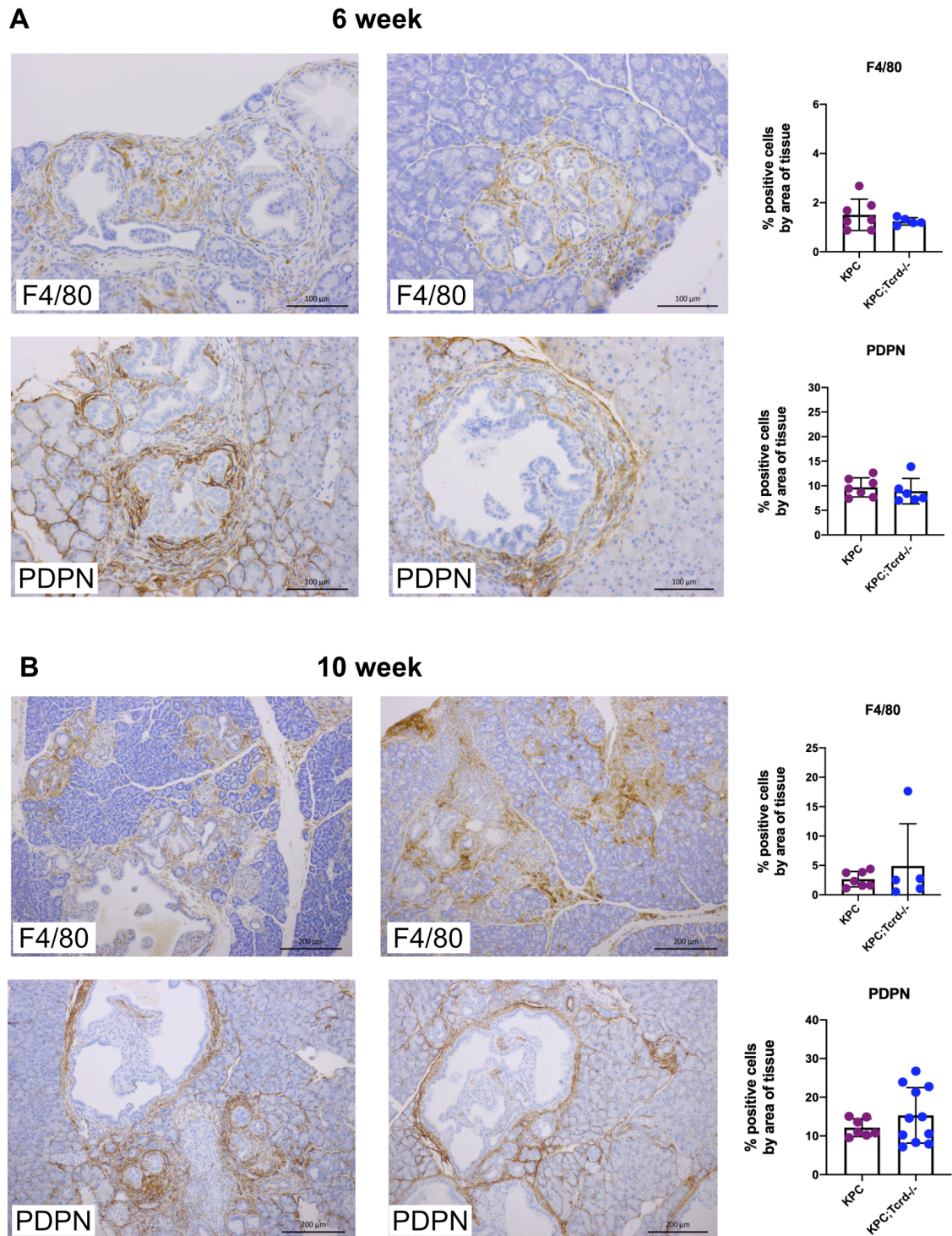
Figure 5-18 The absence of γδ T cells in KPC;Tcrd$^{-/-}$ mice only impacts TAMs and PDPN$^+$ cells in end-stage PDAC.
KPC (n=7) and KPC;Tcrd$^{-/-}$ (n=6) mice were aged to 6 weeks (A), KPC (n=7) and KPC;Tcrd$^{-/-}$ (n=5/11) were aged to 10 weeks (B). IHC staining targeting F4/80 and PDPN was performed, with representative images shown from KPC (left) and KPC;Tcrd$^{-/-}$ (middle). 6-week images taken at 20x magnification and scale bars represent 100μm. 10-week images taken at 10x magnification and scale bars represent 200μm. Quantifications of staining was performed on HALO® image analysis, shown (right) as *"% positive cells by area of tissue"*.

5.5 γδ T cell-myeloid crosstalk in the PDAC TME.

5.5.1 Distinct myeloid cell lineages are identified in PDAC tissue through the expression of F4/80 and CD11c.

Given that macrophages are a dominant cell type within the PDAC TME, and that loss of γδ T cells significantly reduces F4/80 staining in KPC;Tcrd$^{-/-}$ mice, I sought to further characterise the relationship between γδ T cells and PDAC TAMs. To achieve this, I adapted a flow cytometry panel previously described in the literature that was used to identify macrophages, monocytes, neutrophils, and dendritic cells (DCs). (Ruffell et al., 2014) The gating strategy (shown below) identified viable CD45$^+$ cells that were also negative for CD3 and CD19 to exclude T cells and B cells, respectively. F4/80 and CD11c were utilised to identify three populations of cells that were F4/80$^-$CD11c$^-$ (neutrophil/monocyte precursors), F4/80$^+$CD11c$^-$ (macrophages) and F4/80$^-$ CD11c$^+$ (DC precursors) (Figure 5-19). The neutrophil/monocyte precursor (F4/80$^-$CD11c$^-$) was then further gated on CD11b, Ly6G and Ly6C to identify neutrophils (CD11b$^+$Ly6G$^+$) and monocytes (CD11b$^+$Ly6G$^-$Ly6C$^+$). The DC precursor populations were then gated on MHC II expression, and further sub-categorised into CD11b$^+$ DCs and CD103$^+$ DCs, which induce CD4$^+$ T cells through MHC II and facilitate the cross-presentation of exogenous antigen, respectively.(Mildner and Jung, 2014, Sánchez-Paulete et al., 2017) Macrophages were then assessed for Ly6C expression, further identified through expression of CD11b, and then delineated into F4/80$^+$MHC II^{lo} and F4/80$^+$MHC II^{hi} macrophages.
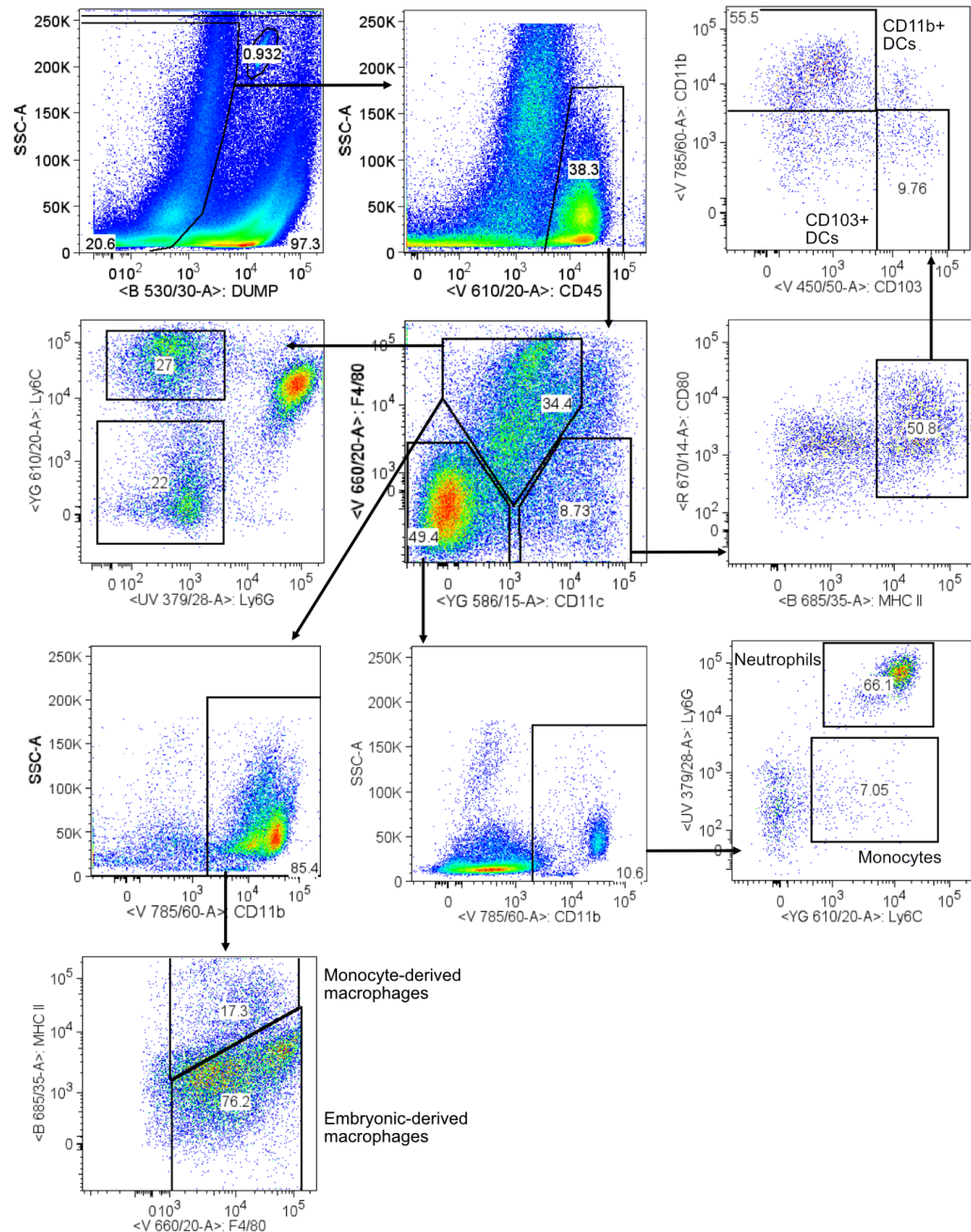
Figure 5-19 TAM populations in PDAC tissue are mainly F4/80⁺MHC II^lo embryonic-derived (tissue-resident) macrophages.
Representative flow cytometry plots from PDAC tissue showing the gating strategy implemented to identify distinct myeloid cell populations. Viable CD45⁺ cells were gated on F4/80 and CD11c to delineate between macrophage (F4/80⁺CD11c⁻), DC (F4/80⁻CD11c⁺) and neutrophil/monocyte precursor populations (F4/80⁻CD11c⁻). Macrophages were further identified through CD11b⁺ expression, and sub-categorised into embryonic-derived (F4/80⁺MHC II^lo) and monocyte derived (F4/80⁺MHC II^hi) populations. Neutrophil/monocyte precursors (F4/80⁻CD11c⁻) were then gated on CD11b⁺ to identify neutrophils (CD11b⁺F4/80⁻Ly6G⁺) and monocytes (CD11b⁺F4/80⁻Ly6C⁺Ly6G⁻). DC precursors (F4/80⁻CD11c⁺) were then further identified through MHC II expression and then sub-categorised into CD11b⁺ DCs (CD11c⁺MHC II⁺) and CD103⁺ DCs (CD11c⁺MHC II⁺).

5.5.2 γδ T cells preferentially promote embryonic-derived TAMs at the expense of monocyte-derived TAMs.

Prior to investigating distinct myeloid cell populations, I first observed that the proportion of CD45$^+$ cells in KPC;Tcrd$^{-/-}$ PDAC was not changed compared to KPC PDAC tissue (Figure 5-20A). Additionally, the proportions of neutrophils (Ly6G$^+$CD11b$^+$F4/80$^-$) remained unchanged in KPC;Tcrd$^{-/-}$ PDAC (Figure 5-20B), which corroborates the IHC findings (Figure 5-15), and I found that monocytes (Ly6C$^+$ Ly6G$^-$CD11b$^+$F4/80$^-$) were significantly increased in KPC;Tcrd$^{-/-}$ PDAC (Figure 5-20C). I also observed a significant increase in the proportion of DCs (MHC II$^+$CD11c$^+$F4/80$^-$) in KPC;Tcrd$^{-/-}$ PDAC (Figure 5-20D), however, CD103$^+$ DCs and CD11b$^+$ DCs were unchanged by the absence of γδ T cells (Figure 5-20E/F). I also found that the F4/80$^+$CD11c$^-$ macrophage population was significantly reduced in the absence of γδ T cells (Figure 5-20G), further corroborating the findings from F4/80 IHC staining (Figure 15). There was also an increase in the Ly6C$^+$ macrophage population (Figure 5-20H). The increase in both monocytes and the Ly6C$^+$ macrophage population indicates a potential disruption of monocyte differentiation into macrophages, as Ly6C$^+$MHC II monocytes normally progress to Ly6C$^-$MHC II$^+$ macrophages.(Desalegn and Pabst, 2019). Furthermore, I also confirmed that in KPC mice >90% of the macrophage population can be classed as F4/80$^+$MHC II^{lo}, whereas F4/80$^+$MHC II^{hi} TAMs account for less than 10% of TAMs (Figure 5-20I/J). In the absence of γδ T cells, MHC II^{lo} macrophages are significantly decreased in KPC;Tcrd$^{-/-}$ PDAC tissue, and MHC II^{hi} macrophages are significantly increased (Figure 5-20I/J). This data suggests that whilst γδ T cells may contribute to monocyte differentiation within the PDAC TME, γδ T cells also preferentially promote the MHC II^{lo} macrophage niche in KPC PDAC tumours.
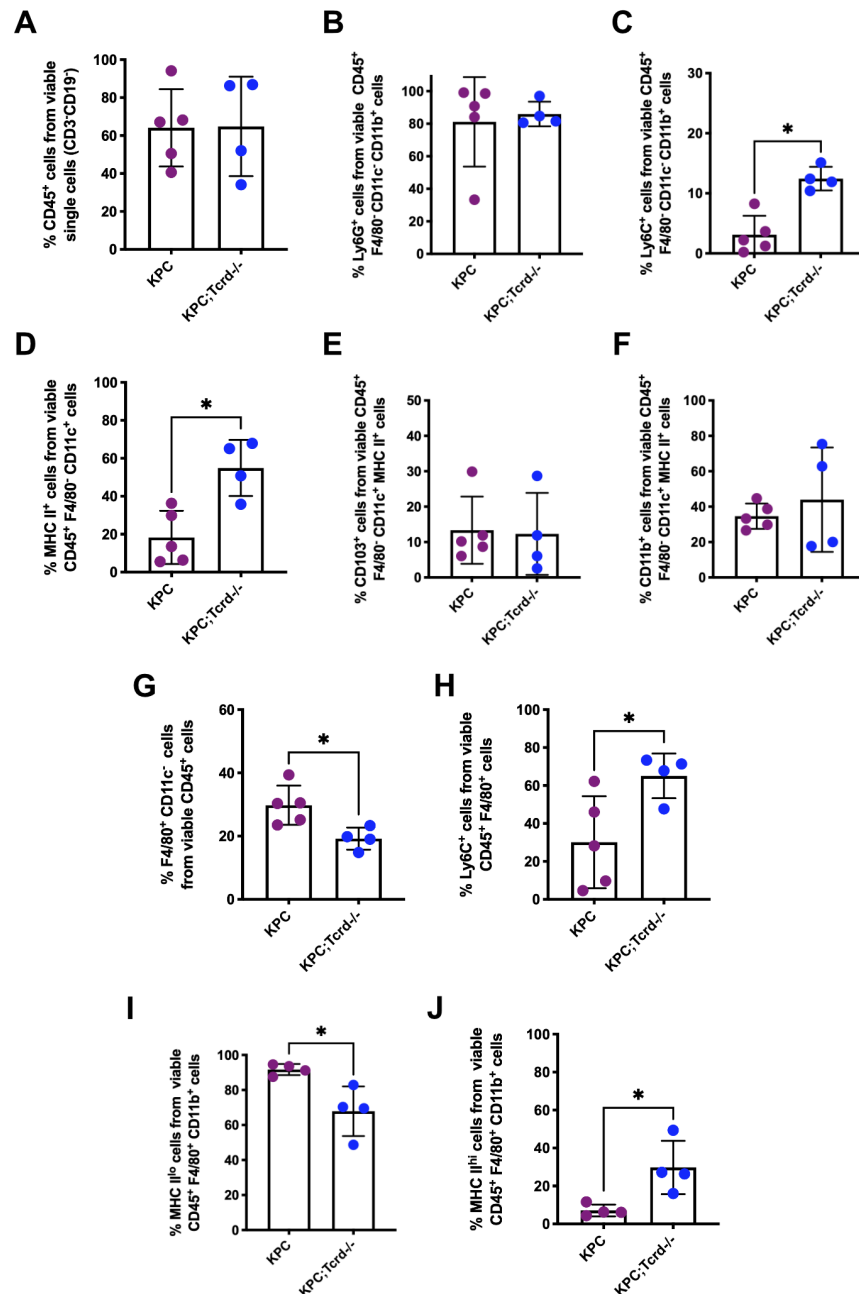
Figure 5-20 Absence of γδ T cells in KPC;Tcrd$^{-/-}$ PDAC tissue leads to decreased embryonic-derived macrophages and increased monocyte-derived macrophages.
KPC (n=5) and KPC;Tcrd$^{-/-}$ (n=4) mice were aged to humane clinical endpoint and flow cytometric analysis was performed. Proportion of viable CD45$^+$ cells following dump channel (CD3$^+$CD19$^+$Ter-119$^+$) exclusion (A). Proportions of Ly6G$^+$ neutrophils from CD11b$^+$F4/80$^-$CD11c$^-$ cells (B). Proportions of Ly6C$^+$ monocytes from Ly6G$^-$CD11b$^+$F4/80$^-$CD11c$^-$ cells (C). Proportions of MHC II$^+$ DCs from F4/80$^-$CD11c$^+$ cells (D). Proportions of CD103$^+$ DCs from F4/80$^-$CD11c$^+$ MHC II$^+$ cells (E). Proportions of CD11b$^+$ DCs from F4/80$^-$CD11c$^+$ MHC II$^+$ cells (F). Proportions of macrophages (F4/80$^+$CD11c$^-$) from viable CD45$^+$ cells (G). Proportions of Ly6C$^+$ macrophages from F4/80$^+$CD11c$^-$ cells (H). Proportions of embryonic-derived macrophages (F4/80$^+$MHC II^{lo}) from CD11b$^+$F4/80$^+$ cells (I). Proportions of monocyte-derived macrophages (F4/80$^+$MHC II^{hi}) from CD11b$^+$F4/80$^+$ cells (J). * P < 0.05 and determined by Mann-Whitey U Test.

5.5.3 Addition of CD64 helps delineate macrophages and DCs.

One limitation of the gating strategy displayed above (Figure 5-19) was in distinguishing between the F4/80$^+$ and CD11c$^+$ populations, in particular the potential contamination of CD11b$^+$ DCs in downstream macrophage populations. Therefore, I designed a new flow cytometry panel with the addition of CD64 which has been shown to help distinguish between macrophages and CD11b$^+$ DCs (Figure 5-21).(Tamoutounour et al., 2012) This new gating strategy focussed upon macrophage populations, and in particular the further classification of embryonic-derived macrophages. To further investigate the MHC II^{lo} macrophage compartment, I included additional markers such as CXCR4 and CX3CR1 chemokine receptors, as these have been shown to be upregulated in MHC II^{lo} macrophages in the literature. (Zhu et al., 2017) I retained the markers for neutrophils and monocytes to act as internal controls which would enable comparison to previous flow cytometry analysis (Figure 5-19). Finally, since I observed a change in bulk DCs (MHC II$^+$CD11c$^+$) but not in CD11b$^+$ or CD103$^+$ DCs, I decided to focus on the conventional DC populations (cDC1 and cDC2), as there is published evidence that cDC paucity in PDAC is a major contributing factor to immune cell dysfunction. (Hegde et al., 2020)
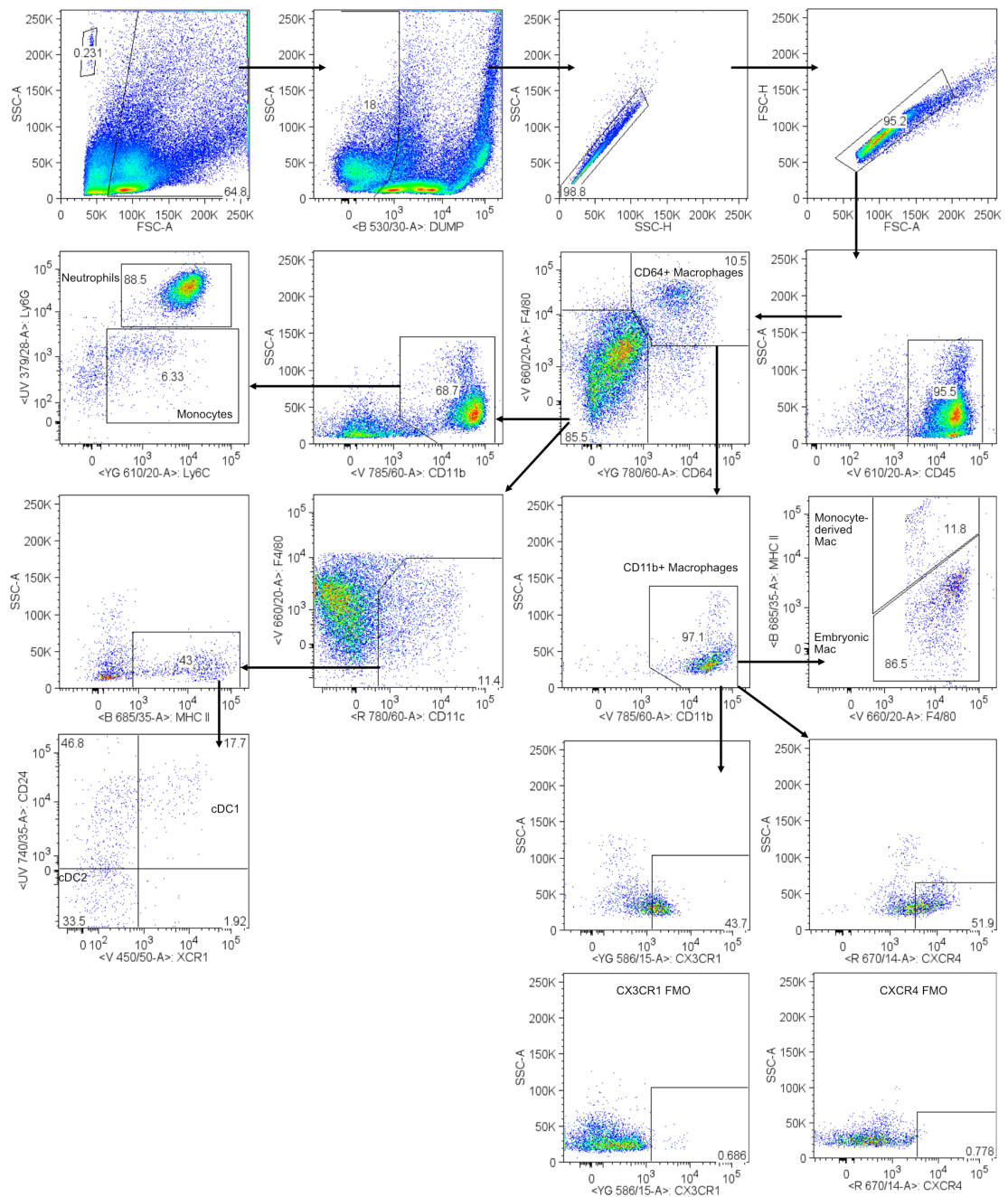
Figure 5-21 Addition of CD64 distinguishes macrophage populations from DCs in PDAC.
Representative flow cytometry plots from PDAC tissue showing the gating strategy implemented to further delineate TAM populations in PDAC. Viable CD45$^+$ cells were the gated on F4/80 and CD64 to first identify macrophages (F4/80$^+$CD64$^+$). F4/80$^-$CD64$^-$ cells were then gated on CD11b to allow for identification of neutrophils (CD11b$^+$F4/80$^-$CD64$^-$Ly6G$^+$) and monocytes (CD11b$^+$F4/80$^-$CD64$^-$Ly6C$^+$Ly6G$^-$), or were gated on F4/80 against CD11c to identify DCs (CD11c$^+$MHC II$^+$). Conventional DCs (cDCs) were then subcategories into cDC1 (XCR1$^+$CD24$^+$) and cDC2 (XCR1$^-$CD24$^-$) populations. F4/80$^+$CD64$^+$ cells where then gated on CD11b$^+$ and embryonic-derived (F4/80$^+$MHC II^{lo}) and monocyte derived (F4/80$^+$MHC II^{hi}) populations were identified. Expression of CXCR4 and CX3CR1 on macrophages (F4/80$^+$CD64$^+$CD11b$^+$) were also assessed.

5.5.4 F4/80$^+$CD64$^+$ macrophages appear reduced in KPC;Tcrd$^{-/-}$ PDAC, but chemokine receptors are not optimal markers of embryonic-derived TAMs.

Firstly, the proportions of CD45$^+$ cells and neutrophils were unchanged between KPC and KPC;Tcrd$^{-/-}$ PDAC (Figure 5-22A/B), corroborating my previous flow cytometry findings. However, monocytes (Figure 5-22C), MHC II$^+$ DCs (Figure 5-22D), cDC1s (Figure 5-22E) and in cDC2s (Figure 5-22F) were not changed in the absence of γδ T cells. There appears to be a reduction in the macrophage population (F4/80$^+$CD64$^+$) in KPC;Tcrd$^{-/-}$ PDAC (17%) compared to KPC PDAC (29%) (Figure 5-22G), however this does not reach statistical significance. Similarly, there was no statistically significant reduction in the MHC II^{lo} TAMs (Figure 5-22H) or any significant increase in the MHC II^{hi} macrophages (F4/80$^+$MHC II^{hi}) (Figure 5-22I). MHC II^{lo} macrophages consisted of nearly 80% of the F4/80$^+$CD64$^+$CD11b$^+$ macrophages (Figure 5-22H), comparable to the 90% observed in previous analysis of F4/80$^+$CD11c$^-$CD11b$^+$ cells (Figure 5-20I); similarly the MHC II^{hi} macrophages identified from F4/80$^+$CD64$^+$CD11b$^+$ macrophages made up 17% (Figure 5-22I) compared to the 7% of monocyte-derived macrophages identified from F4/80$^+$CD11c$^-$CD11b$^+$ cells (Figure 5-20J). Thus, the difference between the two analyses is roughly 10% in the KPC cohort, and less in the KPC;Tcrd$^{-/-}$ group, and indicates a similar trend in MHC II^{lo} macrophages across the two analyses. Finally, I found no differences between the expression of CXCR4 (Figure 5-22J) or CX3CR1 (Figure 5-22K) on macrophages (F4/80$^+$CD64$^+$), however, both appear to be increased in KPC;Tcrd$^{-/-}$ PDAC, which contradicts their use in the literature. (Zhu et al., 2017) Additionally, the lack of distinct CXCR4 and CX3CR1 populations requires the use of FMOs for each surface marker (Figure 5-21), further confirming their unsuitability as additional markers of MHC II^{lo} macrophages in flow cytometry.
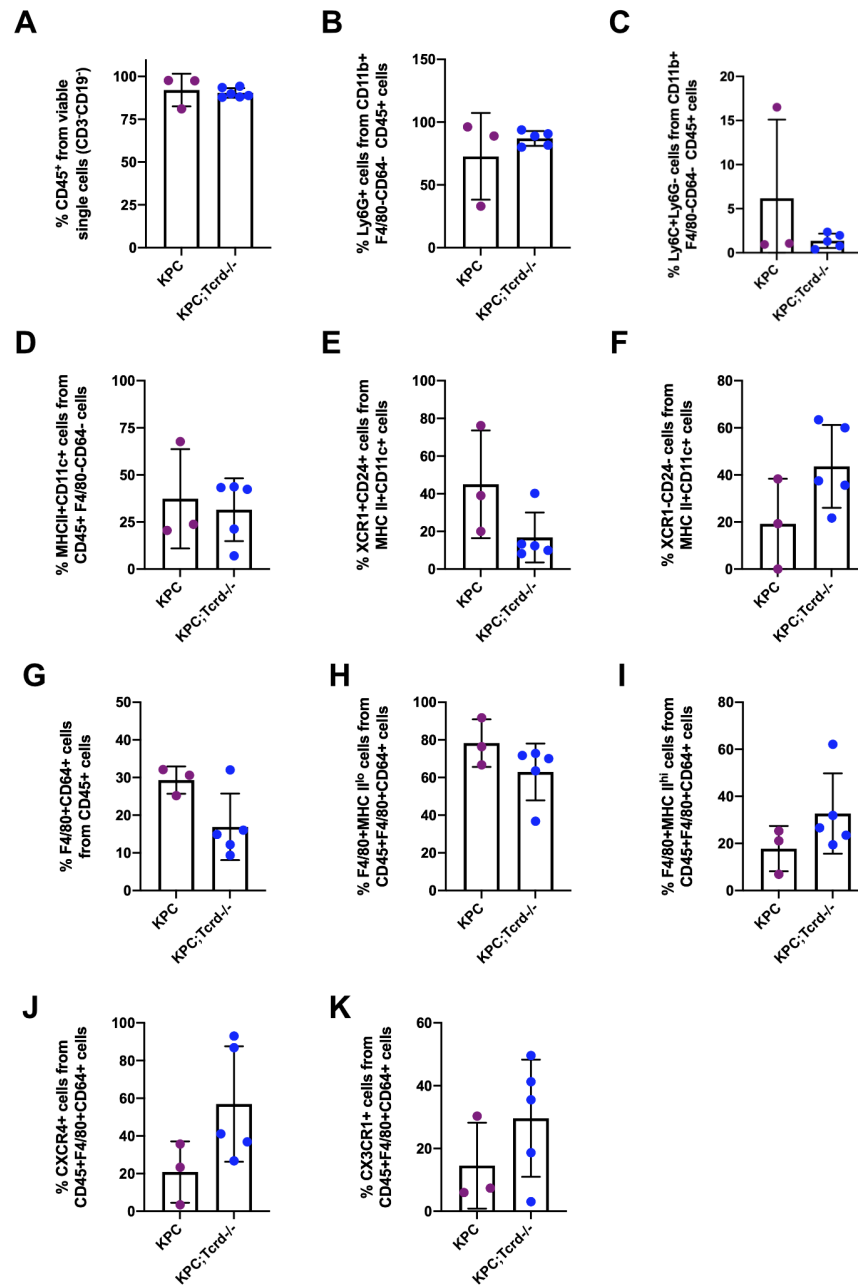
Figure 5-22 F4/80⁺CD64⁺ TAMs may be reduced in KPC;Tcrd⁻/⁻ PDAC, but chemokine receptors are not optimal markers for embryonic-derived TAMs.
KPC (n=3) and KPC;Tcrd⁻/⁻ (n=5) mice were aged to humane clinical endpoint and flow cytometric analysis was performed. Proportion of viable CD45⁺ cells following dump channel (CD3⁺CD19⁺Ter-119⁺) exclusion (A). Proportions of Ly6G⁺ neutrophils from CD11b⁺F4/80⁻CD64⁻ cells (B). Proportions of Ly6C⁺ monocytes from Ly6G⁻CD11b⁺F4/80⁻CD64⁻ cells (C). Proportions of MHC II⁺ DCs from F4/80⁻CD64⁻CD11c⁺ cells (D). Proportions of cDC1 cells (XCR1⁺CD24⁺) from F4/80⁻CD64⁻CD11c⁺MHC II⁺ cells (E). Proportions of cDC2 cells (XCR1⁻CD24⁻) from F4/80⁻CD64⁻CD11c⁺MHC II⁺ cells (F). Proportions of macrophages (F4/80⁺CD64⁺) from viable CD45⁺ cells (G). Proportions of embryonic-derived macrophages (F4/80⁺MHC II^lo) from CD11b⁺F4/80⁺ CD64⁺ cells (H). Proportions of monocyte-derived macrophages (F4/80⁺MHC II^hi) from CD11b⁺F4/80⁺CD64⁺ cells (I). Proportions of CXCR4⁺ cells from F4/80⁺CD64⁺CD11b⁺ cells (J). Proportions of CX3CR1⁺ cells from F4/80⁺CD64⁺CD11b⁺ cells (K).

5.6 γδ T cell-myeloid cell crosstalk signals.

5.6.1 Absence of γδ T cells is associated with significant reductions of IFN-γ in KPC;Tcrd$^{-/-}$ serum.

To further investigate the crosstalk between γδ T cells and TAMs in KPC mice, I performed extensive cytokine profiling using the Luminex Magnetic Bead Array, where KPC and KPC;Tcrd$^{-/-}$ serum was tested to determine the expression of systemic cytokine and chemokine signals. Serum samples were titrated and a dilution of 1:16 was determined to be the optimal dilution factor. However, following acquisition only 7/33 analytes returned results (data not shown). Given that only 7/33 analytes were recorded, I hypothesised that the majority of the remaining 26 analytes were either not expressed within the serum, or would be expressed at much lower levels. Thus, I repeated the Luminex assay a lower dilution factor (1:4) to determine if there were any changes to lowly expressed analytes in the absence of γδ T cells (Figure 5-23). With the lower dilution factor, a substantially greater number of analytes were recorded; these included CCL4, CCL5, CCL7, CCL11, CCL12, CCL21, CCL22, CXCL1, CXCL2, CXCL12, CXCL13, GM-CSF, M-CSF, IFN-γ, IL-17A, IL-1α, IL-6, IL-13 and IL-16 (Figure 5-23). However, there were no observable changes between any cohorts (WT, KPC, Tcrd$^{-/-}$, KPC;Tcrd$^{-/-}$) for CCL4, CCL5, CCL11, CCL21, CCL22, CXCL1, CXCL2, CXCL12, CXCL13, GM-CSF, M-CSF, IL-17A or IL-13A. Interestingly, I found that IFN-γ was significantly reduced in KPC;Tcrd$^{-/-}$ compared to KPC mice, but the levels of IFN-γ in KPC mice were not significantly different from WT controls (Figure 5-23). I also found that IL-6 was significantly increased in the serum of both KPC and KPC;Tcrd$^{-/-}$ mice compared to respective WT controls, but the absence of γδ T cells had no impact. The reduction in IFN-γ expression was unexpected, as I hypothesised that with reduced metastatic incidence in KPC;Tcrd$^{-/-}$ mice there may also be a corresponding increase in anti-metastatic IFN-γ expression. However, given the KPC;Tcrd$^{-/-}$ model is a global knockout of all γδ T cells (including IFN-γ^{+} γδ T cells), this may explain the reduction. In summary, my investigation into the changes in systemic chemokine\cytokine signals in KPC;Tcrd$^{-/-}$ yielded few significant results. However, these observations indicate that any cross-talk between γδ T cells and TAMs is occurring in a TME-specific manner, and that the promotion of metastasis is not mediated through the systemic signals from γδ T cells.
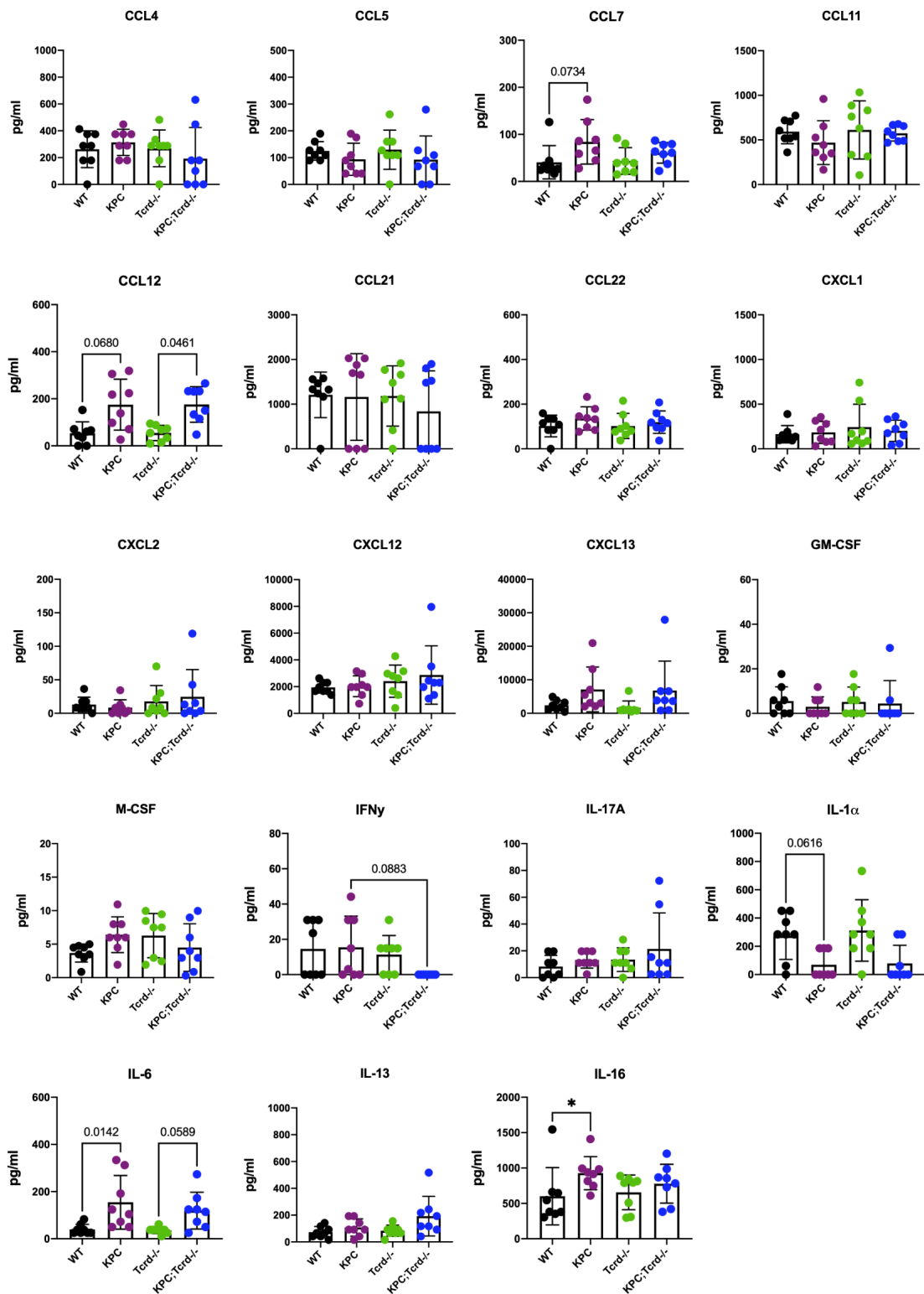
Figure 5-23 Loss of γδ T cells leads to significant reductions of IFN-γ in KPC;Tcrd$^{-/-}$ serum. KPC (n=8) and KPC;Tcrd$^{-/-}$ (n=8) mice were aged to clinical endpoint, and blood was harvested for serum preparation alongside corresponding WT (n=8) and Tcrd$^{-/-}$ (n=8) aged-matched controls. Samples were diluted 1:4 prior to plating and incubation with capture, biotinylated and then PE-Streptavidin antibodies. PE signal strength was determined on Luminex200 analyser to determine the concentration of selected analytes. * P < 0.05 as determined by Kruskal-Wallis Test.

5.6.2 Increased iCAF gene signatures suggests that γδ T cells suppress iCAF activity in the PDAC TME.

Following on from the Luminex analysis, I hypothesised that the crosstalk between γδ T cells and macrophages, and potentially PDPN⁺ CAFs, is occurring through a TME-specific signal. Therefore, I again utilised the in-house Molecular Technology Services to perform bulk RNA-Seq analysis on PDAC tumour. KPC and KPC;Tcrd⁻/⁻ mice were aged to humane clinical endpoint and tumour pieces were frozen in RNAlater, I then isolated the RNA and bulk RNA-Seq was performed by Billy Clark and bioinformatics analysis was undertaken by Robin Shaw. In this experiment I aimed to identify any differentially expressed genes that might indicate a connection between γδ T cells, macrophages and PDPN⁺ CAFs. The results from unsupervised differentially expressed gene analysis (DEGA) indicate that KPC and KPC;Tcrd⁻/⁻ PDAC tissue have distinct gene expression patterns, as KPC and KPC;Tcrd⁻/⁻ samples naturally cluster together (Figure 5-24). Surprisingly, of the significantly upregulated genes in KPC mice there were no indicators of enhanced macrophage activity compared to KPC;Tcrd⁻/⁻ PDAC, other than expression of *Cxcr3* (previously been implicated in tissue-resident PDAC TAMS) (Figure 5-24). (Zhu et al., 2017) Interestingly, in KPC;Tcrd⁻/⁻ PDAC tissue, iCAF gene products (*Il11, Ccl7, Ccl11* and *Il33)* are upregulated compared to KPC PDAC tissue (Figure 5-24). Thus, the heatmaps indicate that KPC and KPC;Tcrd⁻/⁻ PDAC tissue have distinct expression patterns, but that iCAF populations may be suppressed by γδ T cells.
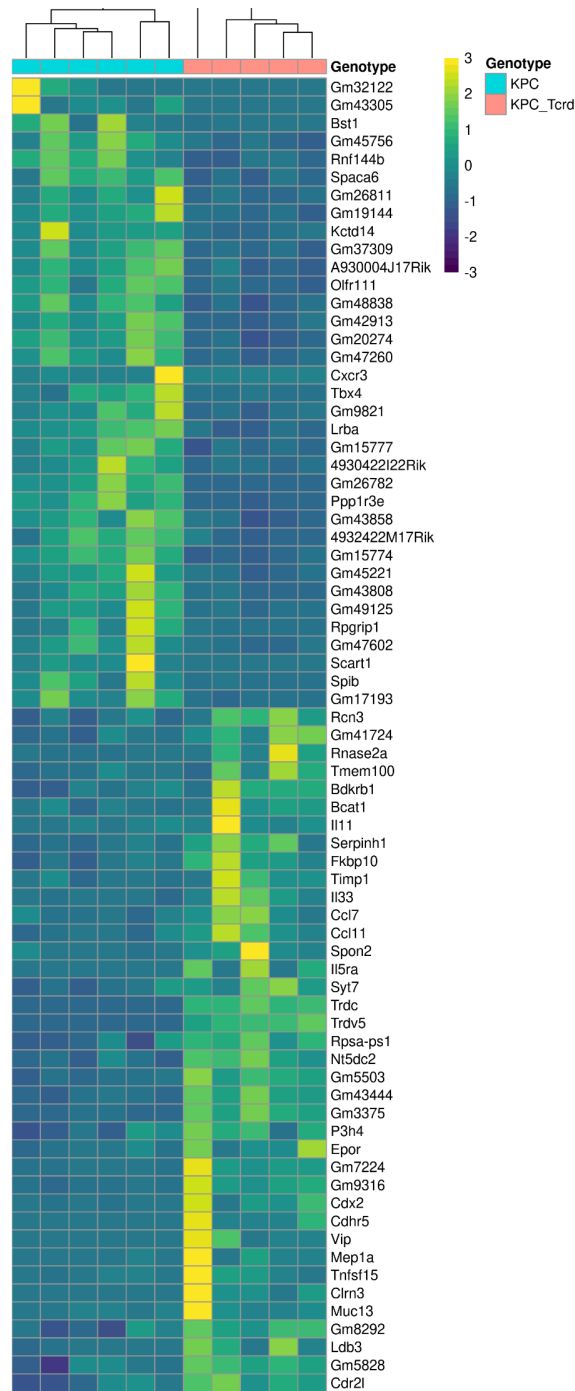
Figure 5-24 KPC;Tcrd⁻/⁻ PDAC tissue has distinct expression profiles from KPC tissue, and have increased expression of iCAF genes.
KPC (n=6) and KPC;Tcrd⁻/⁻ (n=6) mice were aged to humane clinical endpoint, RNA was isolated from PDAC tumours and bulk RNA-Seq was performed by Billy Clark (Beatson Molecular Technology Services). Bioinformatics was then performed by Robin Shaw, and heatmaps were generated to visualise clustering of KPC and KPC;Tcrd⁻/⁻ PDAC tissue, and also to visualise differential gene expression.

To better visualise which genes are significantly altered in KPC;Tcrd⁻/⁻ PDAC, volcano plots were generated from DEGA analysis results (Figure 5-25). The volcano plots confirmed that *Il11, Ccl7, Ccl11* and *Il33* are significantly increased in KPC;Tcrd⁻/⁻ PDAC tissue, indicating that γδ T cells instead suppress the iCAF

population. Interestingly, *Bst1* is significantly expressed in KPC PDAC tissue, which recapitulates the findings from previous bulk RNA-Seq showing *Bst1* expression in KPC-derived γδ T cells. *Scart1* is expressed mainly on γδ T cells, and so its increased expression in KPC PDAC indicates that γδ T cell gene signatures are an important aspect of KPC PDAC TME (Figure 5-25). It should be noted that *Tcrd* and *Trdv5* appear significantly expressed in KPC;Tcrd$^{-/-}$ mice (Figure 5-25), however, all mice were confirmed to be KPC;Tcrd$^{-/-}$, and the high expression of *Tcrd* in KPC;Tcrd$^{-/-}$ PDAC is most likely due to the alignment of incomplete transcripts, leading to increased read counts. Thus, these data from bulk RNA-seq of PDAC tumours has revealed that γδ T cells do not promote the iCAF niche as initially hypothesised following PDPN IHC reduction, but instead appear to impair this population within the PDAC TME.
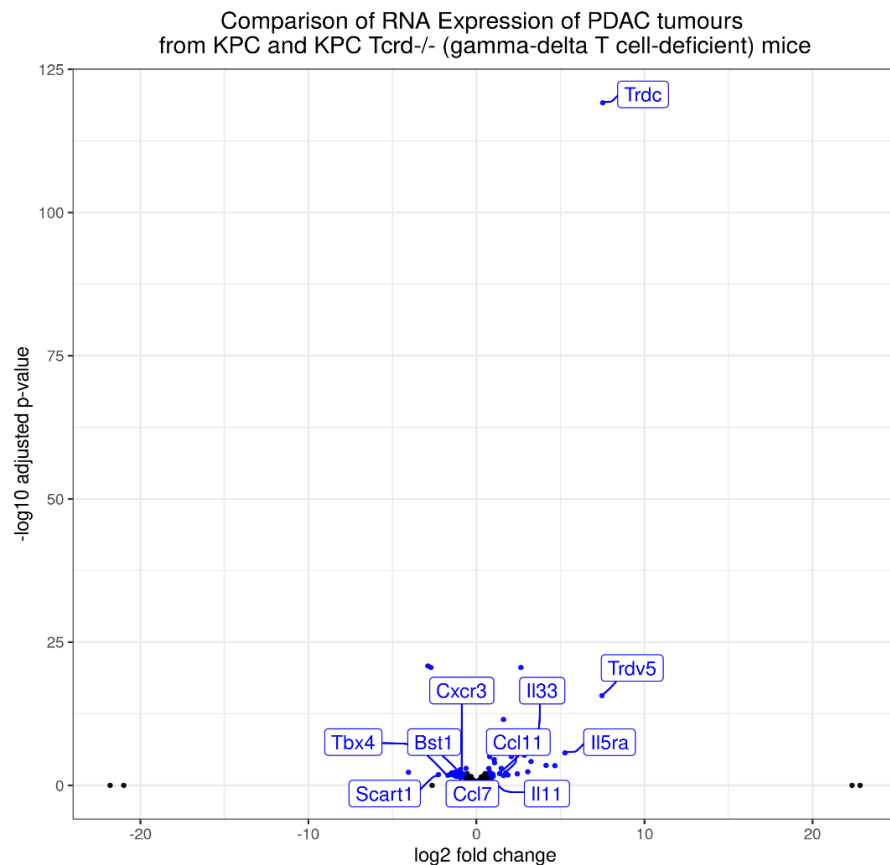
Figure 5-25 Genes associated with iCAF identity are significantly increased in KPC;Tcrd$^{-/-}$ PDAC tissue compared to KPC PDAC.
Unsupervised differentially expressed gene analysis (DEGA) was performed to identify top genes that were differentially expressed in KPC;Tcrd$^{-/-}$ PDAC tissue compared to KPC PDAC tissue. Volcano plots were used to visualise differential gene expression, with genes of interest highlighted. Bioinformatics performed by Robin Shaw.

To validate the findings from RNA-Seq, I then performed a western blot to determine the expression of IL-33 protein in KPC and KPC;Tcrd$^{-/-}$ PDAC tissue, which was shown in the RNA-Seq analysis to be upregulated in KPC;Tcrd$^{-/-}$ PDAC (Figure 5-25). Based on established literature, murine IL-33 can exist in WT and truncated forms with molecular weight of roughly 37kDA and 20kDA, respectively. (Travers et al., 2018) I performed a western blot to visualise IL-33 protein expression and observed bands with a molecular weight roughly 35kDA, shown in the representative image of an IL-33 western blot (Figure 5-26A). This indicates that WT IL-33 is the main form expressed in KPC and KPC;Tcrd$^{-/-}$ PDAC tissue (Figure 5-26A). I then sought to quantify the relative optical density to establish if IL-33 protein expression was significantly different between KPC and KPC;Tcrd$^{-/-}$ PDAC tissue, and so stained for ß-actin to serve as a protein loading control (Figure 5-26B). Using FIJI(ImageJ), I quantified the relative optical density of the bands by normalising IL-33 to ß-actin pixel density, and found no significant differences in IL-33 protein expression in KPC;Tcrd$^{-/-}$ PDAC compared to KPC PDAC (Figure 5-26C). There appears a trend towards increased IL-33 in KPC;Tcrd$^{-/-}$ PDAC, but there is significant variation of IL-33 protein expression within the KPC group, with one notable outlier. This variation is most likely attributable to the method of tissue sampling, where random tumour pieces are collected and may result in tumour pieces that have vastly different tumour architecture. Although speculative and underpowered because of the variation, this data appears to corroborate the findings from RNA-Seq and indicates that IL-33, which is a product produced by iCAFs, may be increased in KPC;Tcrd$^{-/-}$ PDAC tissue. Overall, the combined RNA-Seq and IL-33 western blot data confirms that instead of promoting iCAF populations in the PDAC TME, γδ T cells may suppress iCAF populations.
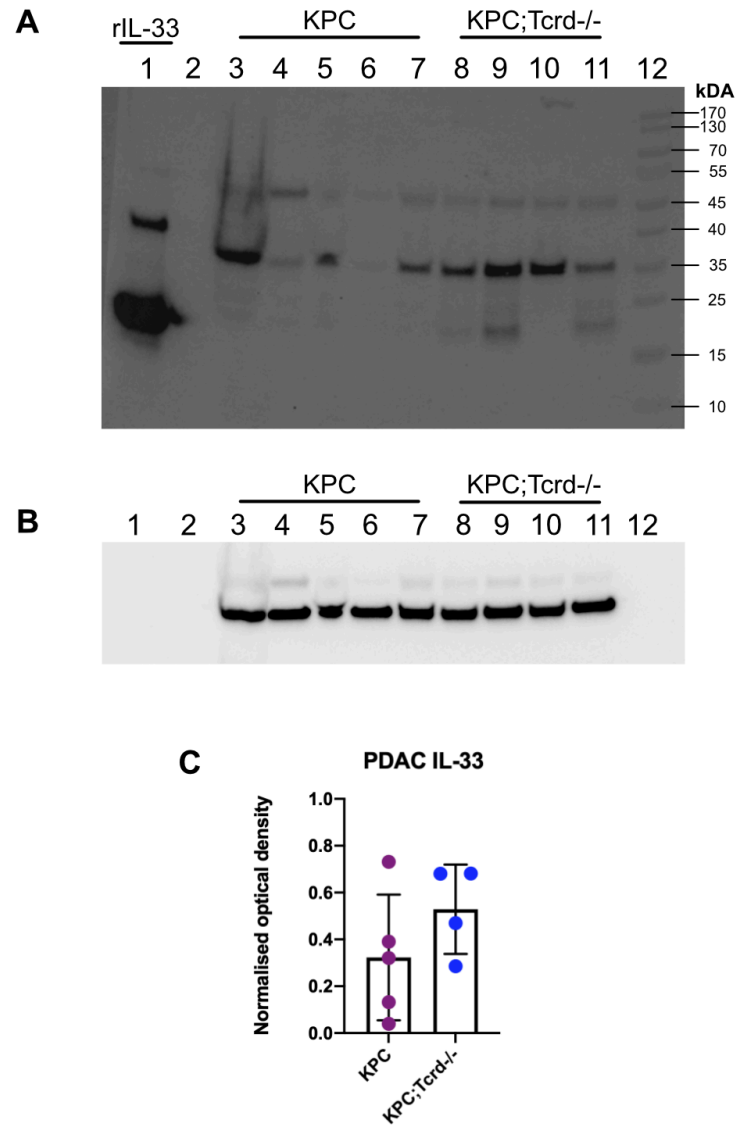
Figure 5-26 IL-33 protein is found at higher levels in KPC;Tcrd$^{-/-}$, suggesting γδ T cells suppress rather than promote iCAF populations.
KPC (n=5) (lanes 3-7) and KPC (n=4) (lanes 8-11) mice were aged to humane clinical endpoint, and PDAC tissue was snap frozen for protein lysates. Protein was extracted and western blot was performed with primary antibody targeting murine IL-33 (37kDA), recombinant murine IL-33 was included (lane 1) to act as a positive control (A). Loading control using primary antibody targeting murine β-actin (B). Quantifications of IL-33 protein expression normalised to β-actin loading control (C).

5.7 Discussion

In this chapter I aimed to uncover the impact of γδ T cells on the primary tumour TME and in the metastatic niche. I also investigated the global effects that γδ T cells have in KPC mice through cytokine profiling as well as bulk RNA sequencing.

Firstly, I assessed the function of γδ T cells within adipose tissue and investigated their role in promoting cancer-associated cachexia in KPC mice. To achieve this, I investigated if the absence of γδ T cells resulted in changes to the weight of adipose tissue depots, and if γδ T cell absence resulted in greater immune cell activation and cytokine production within adipose tissue. In short, I found that KPC and KPC;$Tcrd^{-/-}$mice both display overt adipose tissue wastage when aged to clinical endpoint, but that the absence of γδ T cells did not reverse or delay adipose tissue wastage, and so concluded that γδ T cells do not contribute to cancer-associated cachexia. However, there are additional indicators of cachexia, including skeletal muscle and cardiac muscle mass compared to body weight, so I have not investigated all cachexia readouts.(Olson et al., 2021) The KPC model has been utilised in several studies in cancer-associated cachexia, but a recent study revealed a caveat within the model, which indicates they are not optimal for studying cachexia.(Parajuli et al., 2018, Petruzzelli et al., 2014) In short, KPC mice have significantly reduced body weight regardless of pathology stage (PanIN, early PDAC or late-stage PDAC), and have lower hind limb muscle (tibialis anterior, quadriceps and gastrocnemius) weight when compared to controls. (Talbert et al., 2019) Generation of the $Kras^{G12D/+}$;$Ptf1a^{ER-Cre/+}$;$Pten^{f/f}$ (KPP) mouse enabled the temporal control of oncogenic Kras^{G12D} expression by utilising the tamoxifen-inducible Cre recombinase system; and KPP mice develop cachexia and undergo progressive muscle wastage following tamoxifen induction but had no differences in body weight prior to induction compared to controls.(Talbert et al., 2019) Although not focussed on adipose tissue wastage, this study suggests that KPC mice are not ideal models of cachexia.

Regarding the immune populations in adipose tissue, I found no significant differences to bulk γδ T cells, no changes to cytokine production, and no preferential expansion of pro- or anti-tumour γδ T cell subsets. Compared to

published literature I observed similar enrichment of γδ T cell populations in all adipose tissue depots, and so the chronic inflammatory insults associated with KPC tumourigenesis appear not to impact the adipose tissue-resident γδ T cells.(Kohlgruber et al., 2018) Given that γδ T cells have been shown to promote development of the Treg populations, I sought to confirm the impact of γδ T cells on other adipose tissue immune cells. However, I found no significant changes to the activation state, cytokine production, or proportions of CD4/CD8 T cells, and no changes to NK cell maturation or cytokine production in the absence of γδ T cells. This is in line with published data, as the increase of adipose tissue γδ T cells with age is concomitant with Treg cells, but not CD4$^+$ T cells, CD8$^+$ T cells or NK cells. (Kohlgruber et al., 2018) Therefore, my findings combined with published data indicates that γδ T cells are dispensable for the progression of cancer-associated cachexia, and that γδ T cells do not exert a significant effect on the major immune cell populations within the adipose tissue niche, which is unaffected by tumourigenesis.

Next, I assessed the impact of γδ T cells on immune cell populations in the primary tumour TME and in the metastatic niche. The rationale for this approach was due to previously published evidence that tumour-infiltrating γδ T cells in orthotopic KPC models directly restrain αß T cell activation through Galectin-9 and PD-L1 checkpoint ligation. (Daley et al., 2016) I have already confirmed that IL-17A$^+$ γδ T cells are capable of infiltrating into autochthonous KPC tumours, albeit in fairly low numbers. However, in the absence of γδ T cells I found no significant differences to bulk proportions, activation state or cytokine production of CD4/CD8 T cells in primary PDAC tissue or liver metastatic niche. As previously mentioned, orthotopic KPC models have reduced tumour cell heterogeneity and surgery induces inflammatory insults that confer greater immune diversity during tumour development. (Lee et al, 2016) The models I have used are spontaneous and display greater immune exclusion and reduced immune activation — for example, IFN-γ production by γδ T cells in orthotopic KPC models is roughly 30%, whereas IFN-γ production from spontaneous KPC tumour-derived γδ T cells were on average <5%. (Daley et al., 2016) Therefore, the PDAC TME of spontaneous KPC mice is more representative of the immune-suppressive environment in human PDAC, and so suggests that the directly immune-suppressive function of γδ T cells is less important in KPC mice than in

orthotopic models. In short, my data demonstrates that γδ T cells do not promote αß T cell impairment, and their loss has no impact on the activation state or cytokine production of PDAC-infiltrated CD4$^+$ and CD8$^+$ T cells in KPC mice.

Interestingly, I found there was impaired production of IFN-γ from mature (CD11b$^+$CD27$^-$) NK cells in KPC liver tissue, which was restored in the absence of γδ T cells. Additionally, I found that Granzyme B was also impaired in mature NK cells in KPC liver, but the absence of γδ T cells did not restore Granzyme B production, indicating a selective impairment of mature NK cell IFN-γ production by γδ T cells. This is similar to findings in PDAC patients, which show normal levels of circulating NK cells but have substantially impaired cytokine production, notably IFN-γ.(Marcon et al., 2020) Additionally, the impairment of IFN-γ in NK cells in gastric cancer has been associated with tumour size, tumour invasion and metastasis, which further indicates that impairment of IFN-γ$^+$ NK cells may be central to PDAC metastatic disease. (Lee et al., 2017) I then investigated if this phenotype was due to a either tissue-resident or circulating NK cells, and if altered inhibitory receptor expression is responsible for this observed phenotype. In short, I found no significant differences between circulating and tissue-resident NK cells in KPC mice, and there were no significant differences in activating (CD226) or inhibitory (CD96 and TIGIT) receptors in either NK cell population. I also found no changes to cytokine (IFN-γ, TNF-α or Granzyme B) production in the absence of γδ T cells. This suggests that the TIGIT/CD226 axis is not the driver of IFN-γ$^+$ NK cell impairment, which is supported by the literature where CD226 (DNAM-1) is not impaired in PDAC patients. (Marcon et al., 2020) Binding of TIGIT to activating ligand CD155 has recently been implicated in PDAC, however, it appears to have more relevance in the context of CD155$^+$ PDAC cells binding to TIGIT$^+$ CD8$^+$ T cells to restrain their activation and drive immune suppression. (Freed-Pastor et al., 2021) Interestingly, my findings indicate that NK cell-derived TNF-α should be further investigated, as the absence of γδ T cells in KPC;Tcrd$^{-/-}$ liver tissue may increase the production of TNF-α by both circulating (CD49a$^-$DX5$^+$) and tissue-resident (CD49a$^+$DX5$^-$) NK cells. TNF-alpha has been shown to synergise with IFN-γ to direct NK cell cytolytic killing, and so the TNF-α-producing capacity of mature (CD11b$^+$CD27$^-$) NK cells should also be revisited. (Wang et al., 2012)

To gain a more global understanding of the impact of γδ T cells on both the primary TME and metastatic niches, I utilised extensive IHC staining. To summarise, I found that the absence of γδ T cells leads to significantly reduced NKp46 (NK cells) in KPC;Tcrd$^{-/-}$ liver, significantly reduced F4/80$^+$ (macrophages) cells and increased Caspase 3 (apoptosis) in KPC;Tcrd$^{-/-}$ PDAC tissue. The reduction of NK cells through IHC indicates that the loss of γδ T cells results in fewer NK cells infiltrating the metastatic niche, but they display greater anti-metastatic potential through significantly increased IFN-γ expression. Evidence in the literature demonstrates that human γδ T cells can upregulate the cytotoxic function of NK cells through direct contact and the provision of costimulatory signals via CD137/CD137L.(Maniar et al., 2010) Thus, the potential for direct cell-cell contact between γδ T cells is a possible area of future investigation, as my data indicates γδ T cells negatively regulate NK cell function. Finally, the reduction observed in NKp46 IHC may also be explained through NK cell location within the metastatic niche, as I observed a significant accumulation of NK cells within the metastatic lesions of KPC mice, with NK cells found throughout liver parenchyma to a lesser extent. Given the enrichment of NK cells within metastatic lesions, the significant reduction in metastatic incidence could explain the observations from NKp46 IHC, and so this connection requires further study.

One major focus of this chapter was the investigation of γδ T cell/myeloid cell crosstalk within the primary tumour TME. I found that γδ T cells preferentially promote the expansion of F4/80$^+$MHC II^{lo} TAMs, and I found that PDAC TAM populations in KPC mice consisted of >90% F4/80$^+$MHC II^{lo} TAMs on average. F4/80$^+$MHC II^{lo} TAMs and F4/80$^+$MHC II^{hi} TAMS are more evenly balanced in orthotopic KPC models (46.4% and 53.6%, respectively), and so my findings indicate that F4/80$^+$MHC II^{lo} TAMs are significantly more dominant in autochthonous KPC models. (Zhu et al., 2017) Depletion of F4/80$^+$MHC II^{lo} (previously defined as embryonic-derived) macrophages has been shown to result in delayed tumour progression and reduced PDAC cell proliferation; embryonic-derived TAMs also produce greater amounts of collagen and display higher expression of genes associated with ECM remodelling and pro-fibrotic responses within the PDAC TME.(Zhu et al., 2017) Despite reductions of F4/80$^+$MHC II^{lo} TAMs in KPC;Tcrd$^{-/-}$ mice (92% to 68%), I observed no delay to tumour

progression, no reductions in PDAC cell proliferation, and no change to fibrosis within the PDAC TME. This indicates that whilst γδ T cells can contribute to the expansion of the F4/80$^+$MHC II^{lo} TAM populations, they do not contribute to the stromal reaction. I then looked to elucidate the kinetics of TAMs in PDAC progression, and so assessed TAMs and PDPN$^+$ CAF infiltration at 6wk and 10wk timepoints. However, I found no significant differences to these populations between KPC and KPC;Tcrd$^{-/-}$ mice. The lack of any change to PDAC progression and no significant differences to either TAMs or PDPN$^+$ CAFs in early timepoints, suggests that the impact of γδ T cells on embryonic TAMs and PDPN$^+$ CAFs is not significant until late-stage disease. Therefore, if γδ T cells are not important util late-stage disease, this may indicate a role in enhancing metastatic potential in established tumours. However, the lack of changes to tumour stroma, differentiation status and PDAC cell proliferation does not reveal an obvious mechanism that potentiates metastasis, and so the mechanism is currently undefined and requires further investigation. This could include strategies to determine if there is decreased EMT in KPC;Tcrd$^{-/-}$ PDAC tissue, if PDAC cells from KPC;Tcrd$^{-/-}$ mice have reduced invasive potential or through assessing if the number of circulating tumour cells is reduced in KPC;Tcrd$^{-/-}$ mice.

Finally, I looked to further elucidate the connection between γδ T cells, TAMs and CAFs. I first investigated the systemic cytokine/chemokine signals within KPC and and KPC;Tcrd$^{-/-}$ serum, and then looked to identify differentially expressed genes through bulk RNA-Seq to gain an understanding of the differences between the TME of KPC and KPC;Tcrd$^{-/-}$ PDAC. There were no significant changes to any chemokine/cytokine signals between KPC and KPC;Tcrd$^{-/-}$ serum, which indicates that the observed changes to macrophages and PDPN$^+$ CAFs are not driven by a systemic signal from γδ T cells. This further confirms that γδ T cells do not exert their pro-tumour function in a systemic manner in PDAC, unlike in breast cancer metastasis. Given the observed reduction in TAMs and PDPN$^+$ CAFs in KPC;Tcrd$^{-/-}$ PDAC, and the lack of systemic chemokine/cytokine signals, I hypothesised that γδ T cells may promote TAMs and CAFs through a niche-specific signal. In human PDAC, γδ T cells have been observed proximal to PSCs, and high levels of γδ T cells are associated with increased expression of ECM-related genes and the production of pro-tumour IL-6 from PSCs. (Seifert et al., 2020) Thus, I hypothesised that γδ T cells may

preferentially have an impact on iCAFs, which are the CAF subpopulation responsible for IL-6 production. (Biffi et al., 2019, Öhlund et al., 2017) Additional data from the literature further supported that the induction of IL-6 from PSCs is attributable to iCAFs. Single cell transcriptomic analysis of tumour-derived fibroblasts detailed that CAFs from mammary tumours can cluster into six different subtypes, with iCAFs identifiable through enrichment of *Il33, Il6, Ccl7, Cxcl1* and *Cxcl12* transcripts. iCAFs also had a strong association with surface markers *PDPN* and *Thy1*, indicating that iCAFs could be identified through expression of PDPN and IL-6 production. (Sebastian et al., 2020) Furthermore, IL-17A^{+} γδ T cells have been shown to mediate the production of IL-33 from PDPN^{+} stromal cells in adipose tissue. (Kohlgruber et al., 2018) Finally, IL-33 production from CAFs has been implicated in the polarisation of TAMs, which is followed by MMP9 production to aid in metastatic dissemination. (Andersson et al., 2018) Thus, I hypothesised that PDAC-infiltrating γδ T cells can preferentially promote iCAF populations to shape the TME inflammatory niche. However, from my bulk RNA-Seq data I found that gene expression of markers associated with iCAF behaviour (*Ccl11, Il33, Il11* and *Ccl7*) were instead significantly upregulated in KPC;Tcrd^{−/−} PDAC, proving my hypothesis to be incorrect. Additionally, IL-33 protein analysis by western blot further indicates that γδ T cells do not influence iCAFs, as IL-33 protein levels may increase in KPC;Tcrd^{−/−} PDAC. Finally, additional evidence from the literature indicates that PDPN cannot be utilised as a standalone marker for iCAFs, as PDPN[+] TAMs constitute roughly 30% of the TAM population in orthotopic 4T1 breast tumours.(Bieniasz-Krzywiec et al., 2019) Additionally, F4/80[+]MHC II[lo] TAMs were found to be positive for PDPN, and F4/80[+]MHC II[hi] TAMs were largely negative — suggesting that embryonic-derived TAMs may also be a significant PDPN[+] population within PDAC tumours. Finally, deletion of PDPN in TAMs in orthotopic 4T1 breast cancer models also impairs metastasis.(Bieniasz-Krzywiec et al., 2019) To conclude, this evidence suggests that γδ T cells do not influence iCAF activity; and that future focus should instead be on the influence of γδ T cells on embryonic-derived (F4/80[+]MHC II[lo]PDPN[+]) TAMs, and on uncovering their role in metastatic dissemination.

Chapter 6   Discussion

6.1 Data Summary

 have demonstrated that γδ T cells play a crucial role in metastatic dissemination in mouse PDAC, and their absence leads to a reduction in spontaneous liver metastasis incidence by more than 50%. The evidence I have shown suggests that this is not due to a delay in tumour progression, as γδ T cells display a redundant role in driving PanIN progression, and their absence in KPC;Tcrd$^{-/-}$ mice does not delay primary tumour progression or enhance survival. Within the metastatic niche, γδ T cells impair the production of IFN-γ from mature (CD11b$^+$CD27$^-$) NK cells, but whether this impairment is enough to enable metastatic colonisation has not yet been confirmed, and so requires further investigation. Previously in the literature, γδ T cells have directed pro-metastatic mechanisms through the production of systemic cytokine signals, but my data does not support this. Instead, I have shown that γδ T cells exert pro-tumour function in a TME-specific manner through the impairment of embryonic-derived (F4/80$^+$MHC II^{lo}) macrophages. Crucially, my data has been gathered from the gold standard autochthonous KPC mouse model and contradict findings from orthotopic KPC models. More specifically, I have demonstrated that IL-17A$^+$ γδ T cells infiltrate the PDAC TME, but do not impact the activation state of intra-tumoural αβ T cells. These findings detail a novel crosstalk between γδ T cells and a specific population of TAMs; however, more investigation is required to elucidate the underlying mechanism facilitating this crosstalk and the role this plays in directing metastasis.

6.2 Final Discussion

6.2.1 Phenotyping γδ T cells in KPC mice.

The first major finding of chapter 3 was that γδ T cells are capable of infiltrating into the PDAC tumour; although, this was not observed to any significant level until after 10 weeks. This was first observed through RNAscope analysis and further analysis via flow cytometry attributed this to a significant increase in the IL-17A$^+$ γδ T cell population. Crucially, this finding confirmed that whilst γδ T cells are capable of infiltrating primary PDAC tissue, they constitute a small proportion of the CD3$^+$ T cell population. In breast cancer, γδ T cells exert their

pro-metastatic function through the release of IL-17A, which mediates a systemic increase in G-CSF production to promote the expansion and polarisation of immune-suppressive neutrophils, which then suppress anti-metastatic CD8$^+$ T cells to facilitate metastatic dissemination. (Coffelt et al., 2015) My findings indicate that the influence of γδ T cells in PDAC may be niche-specific owing to their infiltration, which is the opposite to what has been observed in breast cancer, where γδ T cell infiltration into tumour tissue is negligible.

Whilst investigating Vγ chain usage in KPC mice, I observed a significant expansion of the Vγ6$^+$Vδ6.3$^+$ subset in the spleen of KPC mice, and that they produce significantly more GM-CSF than WT controls. GM-CSF is an important granulocyte-stimulating cytokine that correlates with increased infiltration of pro-tumour myeloid cells in human PDAC.(Saka et al., 2020) This presents a potentially unique phenotype, as the Vγ6$^+$ subset normally pairs with Vδ1$^+$ to produce IL-17A, and the Vγ1$^+$ subset is normally associated with Vδ6.3$^+$ and the production of IFN-γ. (Dalton et al., 2004, Silva-Santos et al., 2015) This phenotypic switch was only observed within KPC spleen and was not observed in KPC liver tissue, indicating that tissue-tropism within the KPC model may influence the expansion of specific Vγ subsets. Vγ subset domination is observed in other cancer GEMMs; in breast cancer the production of IL-17A is attributable to Vγ4$^+$ γδ T cells, and in ovarian cancer the production of IL-17A within the tumour is attributable to CD27$^-$ Vγ6$^+$ γδ T cells. (Coffelt et al., 2015, Rei et al., 2014) Current evidence indicates that IL-17A production by γδ T cells in orthotopic KPC models is attributable to intra-tumoural Vγ4 cells, but no indication of the role of Vγ6$^+$ γδ T cells. (Daley et al., 2016) Due to time constraints and restrictions resulting from the COVID-19 pandemic, I would have liked to confirm if the infiltration of γδ T cells in KPC tumours is due to either Vγ4$^+$ or Vγ6$^+$ cells, as the expansion of Vγ6$^+$Vδ6.3$^+$ cells in KPC spleen leads me to hypothesise that IL-17A$^+$ Vγ6$^+$ T cells would predominate within the PDAC TME. This could be studied in two ways; firstly, further phenotyping of γδ T cells from endpoint KPC PDAC tissue by flow cytometry would identify the dominant Vγ subset in KPC mice. Secondly, as seen in Daley et al., I could utilise a Vγ4 depleting antibody in KPC mice to confirm if Vγ4$^+$ γδ T cells were responsible for the production of IL-17A within the PDAC TME. (Daley et al., 2016) I would also have liked to confirm if GM-CSF production is also observed in PDAC-infiltrated

Vγ6⁺ γδ T cells. Recently, GM-CSF has been shown to be indispensable for the polarisation and maintenance of alveolar macrophages.(Draijer et al., 2019, McCowan et al., 2021) Additionally, tumour cell-derived GM-CSF has been shown to drive the recruitment of suppressive myeloid cells to PDAC TME, which in turn impairs anti-tumour immunity and enhances PDAC tumour growth, indicating a role for monocyte-derived macrophages in response to GM-CSF. (Bayne et al., 2012) Thus, I would have looked to establish if a specific subset of γδ T cells (either Vγ4⁺ or Vγ6⁺) can produce GM-CSF within the PDAC TME, as the potential to shape the myeloid compartment may contribute to metastatic disease. Finally, evidence within the literature has demonstrated that PDAC-infiltrated γδ T cells are capable not only of producing pro-tumour IL-17A but also the potent immune-regulatory cytokine IL-10. To achieve this I would have further interrogated γδ T cell cytokine production in the TME by flow cytometry, in particular the production of immune-modulatory cytokines, as the presence of IL-10 is a well-documented aspect of the TME that drives polarisation of pro-tumour TAMs. (Daley et al., 2016, Arango Duque and Descoteaux, 2014)

To investigate the potential cytokines produced by γδ T cells in KPC mice, I sorted γδ T cells from liver and spleen tissue of WT and KPC tumour-bearing mice and employed bulk RNA-Seq. The technical limitations of isolating γδ T cells from KPC PDAC have been discussed, but the low number of γδ T cells that could be isolated from tumour-free pancreas and KPC tumours would have resulted in inefficient read counts. However, I found that γδ T cells in both KPC liver and spleen have significant expression of *Ccl6* and *Ccl9* genes, which recruit pro-tumour myeloid cells through CCR1 to promote tumour invasion and have also been implicated in metastatic dissemination of colorectal cancer. (Kitamura et al., 2007) Given more time, I would have validated these findings by flow cytometry, and looked to identify the production of CCL6/CCL9 by γδ T cells in the PDAC TME. The function of CCL6/CCL9 in KPC mice could also be assessed through blockade of CCR1 signalling to determine their impact on myeloid cell recruitment to the TME and if this influences metastasis.

To summarise, in chapter 3 I have been able to determine that PDAC-infiltrating γδ T cells exhibit an immune-suppressive and pro-tumour phenotype through the expression of IL-17A in primary PDAC tissue. Additionally, I have shown that the

Vγ6⁺Vδ6.3⁺ population is expanded in the spleen of KPC mice. Further investigation is required to confirm Vγ chain subset expansion in PDAC tissue, determine the Vγ subset production of IL-17A and GM-CSF within the TME, and uncover if a specific Vγ chain subset contributes to tumour progression and metastasis.

6.2.2 The role of γδ T cells in PDAC progression.

In chapter 4 I was able to show that γδ T cells play a crucial role in PDAC metastasis, as KPC;Tcrd$^{-/-}$ mice have reduced metastatic incidence (16.2%) compared to KPC mice (38.46%) Additionally, I demonstrated that this reduction in metastasis was not due to delayed tumour progression, as the absence of γδ T cells did not significantly delay PanIN development or PDAC-specific survival of KPC;Tcrd$^{-/-}$mice. Established literature has previously investigated the impact of γδ T cells in spontaneous KC;Tcrδ$^{-/-}$ mice and in orthotopic KPC models implanted into Tcrδ$^{-/-}$ hosts; both of which demonstrated that the absence of γδ T cells was conferred a significant survival benefit. (Daley et al., 2016) My evidence from this study contradicts the established literature and demonstrates that although γδ T cells play a significant role in metastatic disease, they are dispensable for primary tumour progression. There are several reasons that may explain my findings; firstly, the *Tcrd^{tm1Mom}* targeted deletion results in the global loss of all γδ T cell populations. As previously described, γδ T cell subset classification reveals specific subsets that have differential γ chain usage and effector function. In short, Vγ5⁺ (DETCs) cells produce IFN-γ, Vγ6⁺ cells are major sources of IL-17A, Vγ4⁺ cells produce IL-17A and IFN-γ, and finally Vγ1⁺ cells produce IL-17A and IFN-γ. (Prinz et al., 2013, Ribot et al., 2021) Thus, although considered the gold standard PDAC GEMM, the KPC;Tcrd$^{-/-}$ model is less than optimal as it ablates both pro-tumour IL-17A⁺ and anti-tumour IFN-γ⁺ γδ T cells — and the loss of anti-tumour γδ T cells may negate any potential benefit when pro-tumour γδ T cells are absent. However, the KPC;Tcrd$^{-/-}$ model has still confirmed that γδ T cells are indispensable for metastatic dissemination, and that γδ T cells are the dominant IL-17A⁺ population in the PDAC TME. Previous studies have concluded that IL-17A production within the PDAC TME is contributed evenly from γδ T cells and CD4⁺ Th17 cells. McAllister et al. show that only 10% of CD4⁺ Th17 cells in the KC^{iMist1} model produce IL-17A, but that 50% of γδ T cells produce IL-17A, which balances out their differential

commonality within the TME.(McAllister et al., 2014) In the autochthonous KPC model, my findings are even more dramatic as I found that >20% of γδ T cells (3% of CD3$^+$ T cells) are IL-17A$^+$, contrasting to <1% of CD4$^+$ T cells (40% of CD3$^+$ T cells). However, in response to γδ T cell absence, the production of IL-17A from CD4$^+$ Th17 cells does not change and suggests that Th17 cells do not fill the niche left behind by IL-17A$^+$ γδ T cells.

The global ablation of γδ T cells is a major caveat of this model and is too blunt a tool to determine if specifically, the pro-tumour IL-17A$^+$ γδ T cells alone can drive metastasis. Therefore, given more time I would have investigated the impact of specific genetic ablation of the IL-17A$^+$ γδ T cells, namely the Vγ4$^+$ and Vγ6$^+$ subsets. To explore this, I have crossed KPC mice with Vγ4/6$^{-/-}$ mice (provided by Rebecca O'Brien) which are currently ageing to determine if the loss of specifically the Vγ4/6 (IL-17A$^+$) compartment will confer a survival benefit and reduce metastasis. Due to the COVID-19 pandemic, I was forced to maintain only breeding pairs for this colony and was unable to generate KPC tumour-bearing mice deficient for Vγ4/6 cells (KPC;Vγ4/6$^{-/-}$) for a considerable period of time. My intention was to perform survival analysis, score for metastatic incidence, and determine how loss of the Vγ4/6 cells impacts both immune cell activation and the macrophage compartment. However, delays due to the impact of the pandemic meant I was unable to perform these experiments. This is a crucial aspect of PDAC biology that must be pursued further, as various studies have linked pro-tumour IL-17A function to Vγ4$^+$ and Vγ6$^+$ γδ T cells in breast/orthotopic KPC and ovarian cancer GEMMS, respectively. Therefore, elucidating if the PDAC-infiltrating IL-17A$^+$ γδ T cells are dominated by a specific Vγ chain subset, and linking the pro-tumour subset to metastatic dissemination and myeloid cell crosstalk, is of utmost importance.

6.2.3 The impact of γδ T cells in the primary tumour TME and the metastatic niche.

In chapter 5 I sought to investigate the impact that γδ T cells have on the primary tumour TME and in the liver metastatic niche, with the aim of understanding γδ T cell-driven immune cell crosstalk and deciphering the γδ T cell driven mechanism that potentiates PDAC metastasis.

The first part of chapter 5 focused on the role of γδ T cells in cancer-associated cachexia, and if the presence of γδ T cells accelerates cachexia and alters the immune landscape within the adipose tissue niche. γδ T cells are enriched in adipose tissue and they promote the expansion of Tregs within the adipose tissue niche; therefore, I hypothesised that if γδ T cells promote cachexia in KPC mice, this may be due to alterations to activation state and cytokine production from adipose tissue immune cells.(Kohlgruber et al., 2018) My findings demonstrate that the absence of γδ T cells does not impact adipose tissue wastage in KPC;Tcrd$^{-/-}$ mice, and there are no significant alterations to immune cell populations in SubAT, EpiAT or BrAT in the absence of γδ T cells. One limitation to this approach was the restriction to adipose tissue, and it would have been interesting to explore other indicators of cachexia, such as hindlimb muscle (tibialis anterior, quadriceps and gastrocnemius) mass and cardiac muscle mass. (Talbert et al., 2019) Another route could have been to measure white adipose tissue browning; this is a process that occurs during the early stages of cachexia where brown adipose tissue deposits form in white adipose tissue and is driven through inflammatory IL-6. (Petruzzelli et al., 2014) This is identifiable through IHC staining for uncoupling protein 1 (UCP1), which drives a metabolic switch from energy storage to energy expenditure; this would explore a an early timepoint in cancer-associated cachexia and would determine if γδ T cells contribute to metabolic homeostasis in early KPC cachexia rather than end-stage tumourigenesis. Elucidating the underlying mechanisms of cachexia would benefit patients, as it is a major disease co-morbidity. Current therapies include pancreatic enzyme replacement therapy (PERT), which restores normal digestive function, enhances survival and alleviates symptoms associated with malnourishment and cachexia.(Trestini et al., 2021) However, PERT is not routinely prescribed to PDAC patients in the UK, so further elucidating the underlying mechanisms of PDAC cachexia would enable the development of new regimens that could supplement current therapies. (Landers et al., 2016)

The next major aim of this project was to ascertain whether γδ T cells can influence the activation state of immune cells in KPC mice, after I confirmed IL-17A$^+$ γδ T cells infiltrate the PDAC TME. My findings are in direct contradiction to Daley et al., as the impact of γδ T cell absence did not change the activation state or cytokine production of intra-tumoural αβ T cells. (Daley et al., 2016)

The mechanism proposed by Daley et al. detailed that tumour-infiltrating γδ T cells mediated immune suppression through Galectin-9 and PD-L1 expression, which directly impaired the activation and anti-tumour function of CD4$^+$/CD8$^+$ T cells. Given the lack of any change to αβ T cells in KPC;Tcrd$^{-/-}$ mice, I did not assess the expression of checkpoint ligands, but in retrospect it would have been informative to establish if PDAC-infiltrated IL-17A$^+$ γδ T cells expressed immune checkpoint ligands such as PD-L1, Galectin-9 or CTLA-4 in KPC mice.

Compared to orthotopic KPC models, I observed similar proportions of bulk CD4$^+$ and CD8$^+$ T cells (60% and 20% of CD3$^+$ cells, respectively) and similar levels of IFN-γ production from CD4$^+$ and CD8$^+$ T cells (roughly 10% and 20%, respectively) in my spontaneous KPC model. (Daley et al., 2016) This implies γδ T cells in spontaneous KPC mice have either distinct function or restrained activity compared to orthotopic models. This could be due to the spontaneous nature of the KPC model which strongly recapitulates the TME of human PDAC, in particular the evolution of immune escape variants and the progressive development of the dense desmoplastic stroma.(Westphalen and Olive, 2012) In comparison, orthotopic KPC mice have significantly reduced tumour heterogeneity due to *in vitro* passaging, and the combined impact of peri- and post-operative inflammatory insults may directly alter the ability of the immune system to mount an effective anti-tumour response following checkpoint blockade. (Lee et al., 2016) Alternatively, the suppression of αβ T cells may be driven through entirely different populations within the TME; for example, cancer-associated fibroblasts (CAFs) can upregulate immune checkpoint receptor on CD4$^+$ and CD8$^+$ T cells.(Ware et al., 2020) CAFs derived from human PDAC also demonstrate upregulated PD-L1, but preferentially upregulate checkpoint receptors on CD4$^+$ and CD8$^+$ T cells through soluble mediators such as prostaglandin E$_2$ (PGE$_2$) rather than through direct contact.(Gorchs et al., 2019) Given this information, the expression profiles of checkpoint receptors such as PD-1, CTLA-4 and TIM-3 on αβ T cells should be assessed, along with the corresponding ligands on CAFs. This would determine if αβ T cell activity in spontaneous KPC mice is restricted in a different manner than by γδ T cells, as seen in orthotopic models.

However, an interesting phenotype found by flow cytometry was the increased production of IFN-γ from mature (CD11b$^+$CD27$^-$) NK cells in liver tissue from KPC;Tcrd$^{-/-}$ mice. This indicates that γδ T cells can influence the production of anti-tumour cytokines from NK cells in the metastatic niche, however this was not due to a change in activating (CD226) or inhibitory (TIGIT and CD96) receptor expression, or through preferential expansion of circulating or tissue-resident NK cells by γδ T cells. Furthermore, IHC staining for NKp46 shows that NK cells are less abundant in the liver metastatic niche of KPC;Tcrd$^{-/-}$ mice. Therefore, despite being less numerous in the KPC;Tcrd$^{-/-}$ niche, NK cells appear to have greater potential for immune activation, which may promote the reduction in metastasis. Interestingly, I observed that NKp46 staining in liver tissue appeared enriched within metastatic lesions compared to liver parenchyma, and so the reductions in NKp46 staining may be explained through the corresponding reductions in metastasis incidence in KPC;Tcrd$^{-/-}$ mice. This data has not been shown as it is merely a recent observation that has not yet been quantified. Thus, NK cells may be important anti-metastatic cells in murine PDAC, owing to their increased IFN-γ production, enrichment in liver metastatic lesions, and their reduced frequency in KPC;Tcrd$^{-/-}$ that correlates with reduced metastasis. To confirm if the reduced metastasis in KPC;Tcrd$^{-/-}$ mice is driven through NK cells, KPC;Tcrd$^{-/-}$ could be treated with anti-NK1.1 antibody to selectively deplete NK cells once palpable tumours have been established. The impact of NK cell depletion could then be assessed through scoring of metastatic incidence once clinical endpoint has been reached, and then determine if metastatic incidence is restored to KPC levels.

The most important finding of chapter 5 is the connection between γδ T cells and tumour-associated macrophages (TAMs). To summarise, reductions in F4/80 IHC staining first indicated that TAMs are significantly reduced in KPC;Tcrd$^{-/-}$ PDAC TME, and was then confirmed by flow cytometry showing macrophages (F4/80$^+$CD11c$^-$) were significantly reduced. Additionally, there was also a significant increase in the number of Ly6C$^+$ macrophages (F4/80$^+$CD11c$^-$) and monocytes (Ly6C$^+$Ly6G$^-$F4/80$^-$CD11c$^-$) in KPC;Tcrd$^{-/-}$ PDAC TME. This first indicated a potential impairment of monocyte differentiation in the absence of γδ T cells. Further exploration then revealed the majority of TAMs in KPC PDAC TME are classified as F4/80$^+$MHC II^{lo} macrophages, with only a small proportion

of the TAM niche consisting of F4/80$^+$MHC II^{hi} macrophages. Crucially, the absence of γδ T cells in KPC;Tcrd$^{-/-}$ PDAC significantly increases MHC II^{hi} macrophages at the expense of the MHC II^{lo} macrophage population – indicating that γδ T cells preferentially expand the MHC II^{lo} macrophage compartment in KPC PDAC. This finding is particularly significant, as it not only reinforces the established literature that macrophages are fundamental to PDAC tumourigenesis but that γδ T cells preferentially promote a subset of TAMs. The current literature has detailed that F4/80$^+$MHC II^{lo} TAMs can develop from Flt3$^-$ precursors, potentially alluding to a connection between γδ T cells and what have been referred to as embryonic-derived TAMs. However, more investigation is needed to fully elucidate the true nature of the F4/80$^+$MHC II^{lo} subset.

To elucidate the potential connection between γδ T cells and monocyte-derived TAMs in PDAC, and how this promotes progression, I have crossed KPC;Tcrd$^{-/-}$ mice with mice deficient for chemokine receptors CCR1, CCR2, CCR3 and CCR5 (iCCRs) (KPC;iCCR$^{-/-}$). During inflammation, the induction of monocyte recruitment is controlled by the iCCRs, and deletion of the iCCRs results in significant reduction of Ly6C$^+$CD11b$^+$ circulating monocytes, and significantly impaired recruitment of monocytic cells during acute inflammation.(Dyer et al., 2019) The initial aim is to age KPC mice that are deficient for both γδ T cells and circulating monocytes (KPC;Tcrd$^{-/-}$;iCCR$^{-/-}$), and determine the impact that combined loss of these two cell populations has in KPC mice. I hypothesise that KPC;Tcrd$^{-/-}$;iCCR$^{-/-}$ mice will display similar phenotypes and survival to KPC;Tcrd$^{-/-}$ mice, as both orthotopic models and my findings show F4/80$^+$MHC II^{lo} TAMs are important to PDAC progression.(Zhu et al., 2017) An additional route to investigating the macrophage compartment could be through a fate-mapping approach, for example resident macrophages such as Kupffer cells, Langerhan's cells and alveolar macrophages are derived from CX3CR1$^+$Flt3$^-$ progenitors despite not expressing the chemokine receptor, and monocyte-derived macrophages develop from CX3CR1$^-$Flt3$^+$ progenitors. (Yona et al, 2013)

However, the loss of γδ T cells only reduces the proportion of MHC II^{lo} macrophages in the TME from 91% to 67%, so the niche is not completely ablated by the absence of γδ T cells. This suggests that MHC II^{lo} TAMs are at least partly maintained through some other signal within the TME. Additionally, despite MHC

II^{lo} TAMs having greater pro-fibrotic function and displaying increased expression of fibrosis-associated genes in the literature, I see no changes to the local TME in terms of collagen deposition or changes to α-SMA$^+$ fibroblasts. (Zhu et al., 2017) Instead, I then hypothesised that γδ T cells may also influence the inflammatory niche through iCAF stimulation, as PDPN IHC was significantly reduced in KPC;Tcrd$^{-/-}$ PDAC. My reasoning behind iCAFs was thus; γδ T cells mediate IL-6 production from PSCs and iCAFs are identifiable through IL-6 production along with IL-33, CCL7, CCL11 and CXCL1 and through surface expression of PDPN; also, IL-17A$^+$ γδ T cells have been shown to promote IL-33 production from PDPN$^+$ stromal cells in adipose tissue; and finally, IL-33 production has been implicated in TAM-driven metastasis. (Seifert et al., 2020, Sebastian et al., 2020, Kohlgruber et al., 2018, Andersson et al., 2018) However, my findings from RNAseq and western blot analysis revealed that iCAFs genes were significantly upregulated and IL-33 protein may even be increased in KPC;Tcrd$^{-/-}$ PDAC. Furthermore, MHC II^{lo} TAMs have been described as PDPN$^+$ in 4T1 breast cancer models, which may explain the reduction in PDPN staining in KPC;Tcrd$^{-/-}$ PDAC. However, I would have liked to further investigate this to ascertain if PDPN$^+$ TAMs exist in the KPC mice. This could be achieved initially through flow cytometry to identify F4/80$^+$PDPN$^+$ cells in the PDAC TME, and compare their presence between KPC and KPC;Tcrd$^{-/-}$ mice; or through immunofluorescence to visualise F4/80 and PDPN co-localisation within the PDAC TME. Further evidence has shown that fibroblasts in KPC mice are in part contributed by bone marrow-derived cells, as KPC mice that undergo bone marrow engraftment with GFP$^+$ cells display a significant proportion of GFP$^+$α-SMA$^+$ and GFP$^+$PDPN$^+$ cells in KPC pancreas.(Iwamoto et al., 2021, Watt and Morton, 2021) However, there was also evidence of GFP$^+$ F4/80$^+$PDPN$^+$ cells in KPC pancreas, suggesting that MHC II^{hi} TAMs may also exhibit an F4/80$^+$PDPN$^+$ phenotype. (Iwamoto et al., 2021, Watt and Morton, 2021) Thus, the exact connection between CAFs and TAMs requires further investigation, as does identifying the expression of CAF markers by TAM populations.

The importance of understanding the role of TAMs in PDAC tumourigenesis is reinforced when one considers the number of clinical trials that are currently underway to target TAM populations. One example is the inhibition of *Bruton's tyrosine kinase* (BTK), which has gathered notice due to its promotion of pro-

tumour macrophage function.(Weber et al., 2017) More specifically, the inhibition of BTK function by PCI32765 (Ibrutinib) in orthotopic PDAC models results in reduced TAM polarisation along with increased CD8^{+} T cell activity and suppressed PDAC tumour growth.(Gunderson et al., 2016) BTK inhibition has recently been tested in a phase III clinical trial, where BTK inhibitor in combination with nab-paclitaxel and gemcitabine standard of care regimens was compared against placebo with nab-paclitaxel and gemcitabine in metastatic PDAC (NCT02436668).(Duan and Luo, 2021) This trial was completed in December 2020, however there were no significant differences in overall survival between Ibrutinib and placebo groups, with a median survival of 9.7 and 10.8 months and progression-free survival or 5.3 and 6 months, respectively. (Tempero et al., 2021) Other clinical trials are focussed on M-CSFR inhibition, which leads to reductions in established tumour and improves survival in spontaneous KPC mice and sensitises orthotopic mice to checkpoint blockade. (Candido et al., 2018, Zhu et al., 2014) In the clinic, M-CSFR inhibition (pexidartinib) in combination with anti-PD-L1 therapy (durvalumab) has been tested in an ongoing Phase I trial for advanced/metastatic PDAC (NCT02777710). (Benner et al., 2020) Finally, numerous Phase II clinical trials are ongoing to assess the impact of combination therapies with CCR2 inhibitors in pancreatic cancer (NCT3184870, NCT03496662 and NCT03767582), further reinforcing the current focus on targeting TAM populations in PDAC patients.

6.2.4 Concluding remarks.

To summarise, the data presented in this thesis has revealed that γδ T cells play a central role in PDAC metastasis, as their absence results in the reduction of metastatic incidence by over 50%. Additionally, I have identified a connection between γδ T cells and TAMs, more specifically the embryonic-derived TAM populations. These findings present a novel crosstalk between γδ T cells and TAMs in murine PDAC and is an interaction that may potentiate the metastatic potential of PDAC. However, further investigation is required to elucidate the underlying mechanism connecting γδ T cells and TAMs, and if this indeed promotes metastasis. Understanding the connection to macrophages is crucial, as there are numerous clinical trials trying to target TAMs to provide real clinical benefit to patients, and so further investigation into the mechanism is of the utmost importance.

Chapter 7   List of References

AGUILAR-MEDINA, M., AVENDAÑO-FÉLIX, M., LIZÁRRAGA-VERDUGO, E., BERMÚDEZ, M., ROMERO-QUINTANA, J. G., RAMOS-PAYAN, R., RUÍZ-GARCÍA, E. & LÓPEZ-CAMARILLO, C. 2019. SOX9 Stem-Cell Factor: Clinical and Functional Relevance in Cancer. *J Oncol,* 2019, 6754040.

AGUIRRE, A. J., BARDEESY, N., SINHA, M., LOPEZ, L., TUVESON, D. A., HORNER, J., REDSTON, M. S. & DEPINHO, R. A. 2003. Activated Kras and Ink4a/Arf deficiency cooperate to produce metastatic pancreatic ductal adenocarcinoma. *Genes Dev,* 17, 3112-26.

AHMED, S., BRADSHAW, A. D., GERA, S., DEWAN, M. Z. & XU, R. 2017. The TGF-ß/Smad4 Signaling Pathway in Pancreatic Carcinogenesis and Its Clinical Significance. *J Clin Med,* 6.

AKDIS, C. A., JOSS, A., AKDIS, M., FAITH, A. & BLASER, K. 2000. A molecular basis for T cell suppression by IL-10: CD28-associated IL-10 receptor inhibits CD28 tyrosine phosphorylation and phosphatidylinositol 3-kinase binding. *Faseb j,* 14, 1666-8.

ANDERSSON, P., YANG, Y., HOSAKA, K., ZHANG, Y., FISCHER, C., BRAUN, H., LIU, S., YU, G., LIU, S., BEYAERT, R., CHANG, M., LI, Q. & CAO, Y. 2018. Molecular mechanisms of IL-33-mediated stromal interactions in cancer metastasis. *JCI Insight,* 3.

ARANGO DUQUE, G. & DESCOTEAUX, A. 2014. Macrophage cytokines: involvement in immunity and infectious diseases. *Front Immunol,* 5, 491.

ARISTON GABRIEL, A. N., JIAO, Q., YVETTE, U., YANG, X., AL-AMERI, S. A., DU, L., WANG, Y. S. & WANG, C. 2020. Differences between KC and KPC pancreatic ductal adenocarcinoma mice models, in terms of their modeling biology and their clinical relevance. *Pancreatology,* 20, 79-88.

AWAJI, M. & SINGH, R. K. 2019. Cancer-Associated Fibroblasts' Functional Heterogeneity in Pancreatic Ductal Adenocarcinoma. *Cancers (Basel),* 11.

BAER, R., CINTAS, C., DUFRESNE, M., CASSANT-SOURDY, S., SCHÖNHUBER, N., PLANQUE, L., LULKA, H., COUDERC, B., BOUSQUET, C., GARMY-SUSINI, B., VANHAESEBROECK, B., PYRONNET, S., SAUR, D. & GUILLERMET-GUIBERT, J. 2014. Pancreatic cell plasticity and cancer initiation induced by oncogenic Kras is completely dependent on wild-type PI 3-kinase p110α. *Genes Dev,* 28, 2621-35.

BAILEY, P., CHANG, D. K., NONES, K., JOHNS, A. L., PATCH, A. M., GINGRAS, M. C., MILLER, D. K., CHRIST, A. N., BRUXNER, T. J., QUINN, M. C., NOURSE, C., MURTAUGH, L. C., HARLIWONG, I., IDRISOGLU, S., MANNING, S., NOURBAKHSH, E., WANI, S., FINK, L., HOLMES, O., CHIN, V., ANDERSON, M. J., KAZAKOFF, S., LEONARD, C., NEWELL, F., WADDELL, N., WOOD, S., XU, Q., WILSON, P. J., CLOONAN, N., KASSAHN, K. S., TAYLOR, D., QUEK, K., ROBERTSON, A., PANTANO, L., MINCARELLI, L., SANCHEZ, L. N., EVERS, L., WU, J., PINESE, M., COWLEY, M. J., JONES, M. D., COLVIN, E. K., NAGRIAL, A. M., HUMPHREY, E. S., CHANTRILL, L. A., MAWSON, A., HUMPHRIS, J., CHOU, A., PAJIC, M., SCARLETT, C. J., PINHO, A. V., GIRY-LATERRIERE, M., ROOMAN, I., SAMRA, J. S., KENCH, J. G., LOVELL, J. A., MERRETT, N. D., TOON, C. W., EPARI, K., NGUYEN, N. Q., BARBOUR, A., ZEPS, N., MORAN-JONES, K., JAMIESON, N. B., GRAHAM, J. S., DUTHIE, F., OIEN, K., HAIR, J., GRÜTZMANN, R., MAITRA, A., IACOBUZIO-DONAHUE, C. A., WOLFGANG, C. L., MORGAN, R. A., LAWLOR, R. T., CORBO, V., BASSI, C., RUSEV, B., CAPELLI, P., SALVIA, R., TORTORA, G., MUKHOPADHYAY, D., PETERSEN, G. M., MUNZY, D. M., FISHER, W. E., KARIM, S. A.,

ESHLEMAN, J. R., HRUBAN, R. H., PILARSKY, C., MORTON, J. P., SANSOM, O. J., SCARPA, A., MUSGROVE, E. A., BAILEY, U. M., HOFMANN, O., SUTHERLAND, R. L., WHEELER, D. A., GILL, A. J., GIBBS, R. A., PEARSON, J. V., WADDELL, N., et al. 2016. Genomic analyses identify molecular subtypes of pancreatic cancer. *Nature,* 531**,** 47-52.

BARDEESY, N., CHENG, K. H., BERGER, J. H., CHU, G. C., PAHLER, J., OLSON, P., HEZEL, A. F., HORNER, J., LAUWERS, G. Y., HANAHAN, D. & DEPINHO, R. A. 2006. Smad4 is dispensable for normal pancreas development yet critical in progression and tumor biology of pancreas cancer. *Genes Dev,* 20**,** 3130-46.

BAYNE, L. J., BEATTY, G. L., JHALA, N., CLARK, C. E., RHIM, A. D., STANGER, B. Z. & VONDERHEIDE, R. H. 2012. Tumor-derived granulocyte-macrophage colony-stimulating factor regulates myeloid inflammation and T cell immunity in pancreatic cancer. *Cancer Cell,* 21**,** 822-35.

BENNER, B., GOOD, L., QUIROGA, D., SCHULTZ, T. E., KASSEM, M., CARSON, W. E., CHERIAN, M. A., SARDESAI, S. & WESOLOWSKI, R. 2020. Pexidartinib, a Novel Small Molecule CSF-1R Inhibitor in Use for Tenosynovial Giant Cell Tumor: A Systematic Review of Pre-Clinical and Clinical Development. *Drug Des Devel Ther,* 14**,** 1693-1704.

BI, Y., CAO, J., JIN, S., LV, L., QI, L., LIU, F., GENG, J. & YU, Y. 2016. Interleukin-22 promotes lung cancer cell proliferation and migration via the IL-22R1/STAT3 and IL-22R1/AKT signaling pathways. *Mol Cell Biochem,* 415**,** 1-11.

BIANKIN, A. V., WADDELL, N., KASSAHN, K. S., GINGRAS, M. C., MUTHUSWAMY, L. B., JOHNS, A. L., MILLER, D. K., WILSON, P. J., PATCH, A. M., WU, J., CHANG, D. K., COWLEY, M. J., GARDINER, B. B., SONG, S., HARLIWONG, I., IDRISOGLU, S., NOURSE, C., NOURBAKHSH, E., MANNING, S., WANI, S., GONGORA, M., PAJIC, M., SCARLETT, C. J., GILL, A. J., PINHO, A. V., ROOMAN, I., ANDERSON, M., HOLMES, O., LEONARD, C., TAYLOR, D., WOOD, S., XU, Q., NONES, K., FINK, J. L., CHRIST, A., BRUXNER, T., CLOONAN, N., KOLLE, G., NEWELL, F., PINESE, M., MEAD, R. S., HUMPHRIS, J. L., KAPLAN, W., JONES, M. D., COLVIN, E. K., NAGRIAL, A. M., HUMPHREY, E. S., CHOU, A., CHIN, V. T., CHANTRILL, L. A., MAWSON, A., SAMRA, J. S., KENCH, J. G., LOVELL, J. A., DALY, R. J., MERRETT, N. D., TOON, C., EPARI, K., NGUYEN, N. Q., BARBOUR, A., ZEPS, N., KAKKAR, N., ZHAO, F., WU, Y. Q., WANG, M., MUZNY, D. M., FISHER, W. E., BRUNICARDI, F. C., HODGES, S. E., REID, J. G., DRUMMOND, J., CHANG, K., HAN, Y., LEWIS, L. R., DINH, H., BUHAY, C. J., BECK, T., TIMMS, L., SAM, M., BEGLEY, K., BROWN, A., PAI, D., PANCHAL, A., BUCHNER, N., DE BORJA, R., DENROCHE, R. E., YUNG, C. K., SERRA, S., ONETTO, N., MUKHOPADHYAY, D., TSAO, M. S., SHAW, P. A., PETERSEN, G. M., GALLINGER, S., HRUBAN, R. H., MAITRA, A., IACOBUZIO-DONAHUE, C. A., SCHULICK, R. D., WOLFGANG, C. L., MORGAN, R. A., et al. 2012. Pancreatic cancer genomes reveal aberrations in axon guidance pathway genes. *Nature,* 491**,** 399-405.

BIE, Q., SUN, C., GONG, A., LI, C., SU, Z., ZHENG, D., JI, X., WU, Y., GUO, Q., WANG, S. & XU, H. 2016. Non-tumor tissue derived interleukin-17B activates IL-17RB/AKT/ß-catenin pathway to enhance the stemness of gastric cancer. *Sci Rep,* 6**,** 25447.

BIENIASZ-KRZYWIEC, P., MARTÍN-PÉREZ, R., EHLING, M., GARCÍA-CABALLERO, M., PINIOTI, S., PRETTO, S., KROES, R., ALDENI, C., DI MATTEO, M., PRENEN, H., TRIBULATTI, M. V., CAMPETELLA, O., SMEETS, A., NOEL, A., FLORIS,

G., VAN GINDERACHTER, J. A. & MAZZONE, M. 2019. Podoplanin-Expressing Macrophages Promote Lymphangiogenesis and Lymphoinvasion in Breast Cancer. *Cell Metab,* 30**,** 917-936.e10.

BIFFI, G., ONI, T. E., SPIELMAN, B., HAO, Y., ELYADA, E., PARK, Y., PREALL, J. & TUVESON, D. A. 2019. IL1-Induced JAK/STAT Signaling Is Antagonized by TGFß to Shape CAF Heterogeneity in Pancreatic Ductal Adenocarcinoma. *Cancer Discov,* 9**,** 282-301.

BISWAS, S. K. & MANTOVANI, A. 2010. Macrophage plasticity and interaction with lymphocyte subsets: cancer as a paradigm. *Nat Immunol,* 11**,** 889-96.

BOLM, L., CIGOLLA, S., WITTEL, U. A., HOPT, U. T., KECK, T., RADES, D., BRONSERT, P. & WELLNER, U. F. 2017. The Role of Fibroblasts in Pancreatic Cancer: Extracellular Matrix Versus Paracrine Factors. *Transl Oncol,* 10**,** 578-588.

BREMBECK, F. H., SCHREIBER, F. S., DERAMAUDT, T. B., CRAIG, L., RHOADES, B., SWAIN, G., GRIPPO, P., STOFFERS, D. A., SILBERG, D. G. & RUSTGI, A. K. 2003. The mutant K-ras oncogene causes pancreatic periductal lymphocytic infiltration and gastric mucous neck cell hyperplasia in transgenic mice. *Cancer Res,* 63**,** 2005-9.

CAMPOS, M. L., SÁNCHEZ-ARÉVALO LOBO, V. J., RODOLOSSE, A., GOTTARDI, C. J., MAFFICINI, A., BEGHELLI, S., SCARDONI, M., BASSI, C., SCARPA, A. & REAL, F. X. 2013. ICAT is a novel Ptf1a interactor that regulates pancreatic acinar differentiation and displays altered expression in tumours. *Biochem J,* 451**,** 395-405.

CANDIDO, J. B., MORTON, J. P., BAILEY, P., CAMPBELL, A. D., KARIM, S. A., JAMIESON, T., LAPIENYTE, L., GOPINATHAN, A., CLARK, W., MCGHEE, E. J., WANG, J., ESCORCIO-CORREIA, M., ZOLLINGER, R., ROSHANI, R., DREW, L., RISHI, L., ARKELL, R., EVANS, T. R. J., NIXON, C., JODRELL, D. I., WILKINSON, R. W., BIANKIN, A. V., BARRY, S. T., BALKWILL, F. R. & SANSOM, O. J. 2018. CSF1R(+) Macrophages Sustain Pancreatic Tumor Growth through T Cell Suppression and Maintenance of Key Gene Programs that Define the Squamous Subtype. *Cell Rep,* 23**,** 1448-1460.

CAO, Y., WANG, X., JIN, T., TIAN, Y., DAI, C., WIDARMA, C., SONG, R. & XU, F. 2020. Immune checkpoint molecules in natural killer cells as potential targets for cancer immunotherapy. *Signal Transduct Target Ther,* 5**,** 250.

CARSTENS, J. L., CORREA DE SAMPAIO, P., YANG, D., BARUA, S., WANG, H., RAO, A., ALLISON, J. P., LEBLEU, V. S. & KALLURI, R. 2017. Spatial computation of intratumoral T cells correlates with survival of patients with pancreatic cancer. *Nat Commun,* 8**,** 15095.

CÉSPEDES, M. V., GUILLÉN, M. J., LÓPEZ-CASAS, P. P., SARNO, F., GALLARDO, A., ÁLAMO, P., CUEVAS, C., HIDALGO, M., GALMARINI, C. M., ALLAVENA, P., AVILÉS, P. & MANGUES, R. 2016. Lurbinectedin induces depletion of tumor-associated macrophages, an essential component of its in vivo synergism with gemcitabine, in pancreatic adenocarcinoma mouse models. *Dis Model Mech,* 9**,** 1461-1471.

CHABAB, G., BARJON, C., ABDELLAOUI, N., SALVADOR-PRINCE, L., DEJOU, C., MICHAUD, H. A., BOISSIÈRE-MICHOT, F., LOPEZ-CRAPEZ, E., JACOT, W., POURQUIER, D., BONNEFOY, N. & LAFONT, V. 2020. Identification of a regulatory Vδ1 gamma delta T cell subpopulation expressing CD73 in human breast cancer. *J Leukoc Biol,* 107**,** 1057-1067.

CHAE, W. J., GIBSON, T. F., ZELTERMAN, D., HAO, L., HENEGARIU, O. & BOTHWELL, A. L. 2010. Ablation of IL-17A abrogates progression of

spontaneous intestinal tumorigenesis. *Proc Natl Acad Sci U S A,* 107, 5540-4.

CHAO, T., FURTH, E. E. & VONDERHEIDE, R. H. 2016. CXCR2-Dependent Accumulation of Tumor-Associated Neutrophils Regulates T-cell Immunity in Pancreatic Ductal Adenocarcinoma. *Cancer Immunol Res,* 4, 968-982.

CHEN, D. S. & MELLMAN, I. 2013. Oncology meets immunology: the cancer-immunity cycle. *Immunity,* 39, 1-10.

CHEN, H. C., ELING, N., MARTINEZ-JIMENEZ, C. P., O'BRIEN, L. M., CARBONARO, V., MARIONI, J. C., ODOM, D. T. & DE LA ROCHE, M. 2019a. IL-7-dependent compositional changes within the γδ T cell pool in lymph nodes during ageing lead to an unbalanced anti-tumour response. *EMBO Rep,* 20, e47379.

CHEN, J., YE, X., PITMON, E., LU, M., WAN, J., JELLISON, E. R., ADLER, A. J., VELLA, A. T. & WANG, K. 2019b. IL-17 inhibits CXCL9/10-mediated recruitment of CD8(+) cytotoxic T cells and regulatory T cells to colorectal tumors. *J Immunother Cancer,* 7, 324.

CHIOSSONE, L., CHAIX, J., FUSERI, N., ROTH, C., VIVIER, E. & WALZER, T. 2009. Maturation of mouse NK cells is a 4-stage developmental program. *Blood,* 113, 5488-96.

CODARRI, L., GYÜLVÉSZI, G., TOSEVSKI, V., HESSKE, L., FONTANA, A., MAGNENAT, L., SUTER, T. & BECHER, B. 2011. RORγt drives production of the cytokine GM-CSF in helper T cells, which is essential for the effector phase of autoimmune neuroinflammation. *Nat Immunol,* 12, 560-7.

COFFELT, S. B., KERSTEN, K., DOORNEBAL, C. W., WEIDEN, J., VRIJLAND, K., HAU, C. S., VERSTEGEN, N. J. M., CIAMPRICOTTI, M., HAWINKELS, L., JONKERS, J. & DE VISSER, K. E. 2015. IL-17-producing γδ T cells and neutrophils conspire to promote breast cancer metastasis. *Nature,* 522, 345-348.

COFFELT, S. B., WELLENSTEIN, M. D. & DE VISSER, K. E. 2016. Neutrophils in cancer: neutral no more. *Nat Rev Cancer,* 16, 431-46.

COLLISSON, E. A., SADANANDAM, A., OLSON, P., GIBB, W. J., TRUITT, M., GU, S., COOC, J., WEINKLE, J., KIM, G. E., JAKKULA, L., FEILER, H. S., KO, A. H., OLSHEN, A. B., DANENBERG, K. L., TEMPERO, M. A., SPELLMAN, P. T., HANAHAN, D. & GRAY, J. W. 2011. Subtypes of pancreatic ductal adenocarcinoma and their differing responses to therapy. *Nat Med,* 17, 500-3.

COOLS-LARTIGUE, J., SPICER, J., MCDONALD, B., GOWING, S., CHOW, S., GIANNIAS, B., BOURDEAU, F., KUBES, P. & FERRI, L. 2013. Neutrophil extracellular traps sequester circulating tumor cells and promote metastasis. *J Clin Invest,* 123, 3446-58.

COSTA-SILVA, B., AIELLO, N. M., OCEAN, A. J., SINGH, S., ZHANG, H., THAKUR, B. K., BECKER, A., HOSHINO, A., MARK, M. T., MOLINA, H., XIANG, J., ZHANG, T., THEILEN, T. M., GARCÍA-SANTOS, G., WILLIAMS, C., ARARSO, Y., HUANG, Y., RODRIGUES, G., SHEN, T. L., LABORI, K. J., LOTHE, I. M., KURE, E. H., HERNANDEZ, J., DOUSSOT, A., EBBESEN, S. H., GRANDGENETT, P. M., HOLLINGSWORTH, M. A., JAIN, M., MALLYA, K., BATRA, S. K., JARNAGIN, W. R., SCHWARTZ, R. E., MATEI, I., PEINADO, H., STANGER, B. Z., BROMBERG, J. & LYDEN, D. 2015. Pancreatic cancer exosomes initiate pre-metastatic niche formation in the liver. *Nat Cell Biol,* 17, 816-26.

CROXFORD, A. L., LANZINGER, M., HARTMANN, F. J., SCHREINER, B., MAIR, F., PELCZAR, P., CLAUSEN, B. E., JUNG, S., GRETER, M. & BECHER, B. 2015.

The Cytokine GM-CSF Drives the Inflammatory Signature of CCR2+ Monocytes and Licenses Autoimmunity. *Immunity,* 43**,** 502-14.

CUI, R., YUE, W., LATTIME, E. C., STEIN, M. N., XU, Q. & TAN, X. L. 2016. Targeting tumor-associated macrophages to combat pancreatic cancer. *Oncotarget,* 7**,** 50735-50754.

DALEY, D., ZAMBIRINIS, C. P., SEIFERT, L., AKKAD, N., MOHAN, N., WERBA, G., BARILLA, R., TORRES-HERNANDEZ, A., HUNDEYIN, M., MANI, V. R. K., AVANZI, A., TIPPENS, D., NARAYANAN, R., JANG, J. E., NEWMAN, E., PILLARISETTY, V. G., DUSTIN, M. L., BAR-SAGI, D., HAJDU, C. & MILLER, G. 2016. γδ T Cells Support Pancreatic Oncogenesis by Restraining αβ T Cell Activation. *Cell,* 166**,** 1485-1499.e15.

DALIN, S., SULLIVAN, M. R., LAU, A. N., GRAUMAN-BOSS, B., MUELLER, H. S., KREIDL, E., FENOGLIO, S., LUENGO, A., LEES, J. A., VANDER HEIDEN, M. G., LAUFFENBURGER, D. A. & HEMANN, M. T. 2019. Deoxycytidine Release from Pancreatic Stellate Cells Promotes Gemcitabine Resistance. *Cancer Res,* 79**,** 5723-5733.

DALTON, J. E., HOWELL, G., PEARSON, J., SCOTT, P. & CARDING, S. R. 2004. Fas-Fas ligand interactions are essential for the binding to and killing of activated macrophages by gamma delta T cells. *J Immunol,* 173**,** 3660-7.

DANILUK, J., LIU, Y., DENG, D., CHU, J., HUANG, H., GAISER, S., CRUZ-MONSERRATE, Z., WANG, H., JI, B. & LOGSDON, C. D. 2012. An NF-κB pathway-mediated positive feedback loop amplifies Ras activity to pathological levels in mice. *J Clin Invest,* 122**,** 1519-28.

DELGIORNO, K. E., NAEEM, R. F., FANG, L., CHUNG, C. Y., RAMOS, C., LUHTALA, N., O'CONNOR, C., HUNTER, T., MANOR, U. & WAHL, G. M. 2020. Tuft Cell Formation Reflects Epithelial Plasticity in Pancreatic Injury: Implications for Modeling Human Pancreatitis. *Front Physiol,* 11**,** 88.

DESALEGN, G. & PABST, O. 2019. Inflammation triggers immediate rather than progressive changes in monocyte differentiation in the small intestine. *Nat Commun,* 10**,** 3229.

DESEKE, M. & PRINZ, I. 2020. Ligand recognition by the γδ TCR and discrimination between homeostasis and stress conditions. *Cell Mol Immunol,* 17**,** 914-924.

DIAZ-MONTERO, C. M., SALEM, M. L., NISHIMURA, M. I., GARRETT-MAYER, E., COLE, D. J. & MONTERO, A. J. 2009. Increased circulating myeloid-derived suppressor cells correlate with clinical cancer stage, metastatic tumor burden, and doxorubicin-cyclophosphamide chemotherapy. *Cancer Immunol Immunother,* 58**,** 49-59.

DISTLER, M., AUST, D., WEITZ, J., PILARSKY, C. & GRÜTZMANN, R. 2014. Precursor lesions for sporadic pancreatic cancer: PanIN, IPMN, and MCN. *Biomed Res Int,* 2014**,** 474905.

DOUGALL, W. C., KURTULUS, S., SMYTH, M. J. & ANDERSON, A. C. 2017. TIGIT and CD96: new checkpoint receptor targets for cancer immunotherapy. *Immunol Rev,* 276**,** 112-120.

DRAIJER, C., PENKE, L. R. K. & PETERS-GOLDEN, M. 2019. Distinctive Effects of GM-CSF and M-CSF on Proliferation and Polarization of Two Major Pulmonary Macrophage Populations. *J Immunol,* 202**,** 2700-2709.

DUAN, Z. & LUO, Y. 2021. Targeting macrophages in cancer immunotherapy. *Signal Transduct Target Ther,* 6**,** 127.

DULUC, C., MOATASSIM-BILLAH, S., CHALABI-DCHAR, M., PERRAUD, A., SAMAIN, R., BREIBACH, F., GAYRAL, M., CORDELIER, P., DELISLE, M. B., BOUSQUET-DUBOUCH, M. P., TOMASINI, R., SCHMID, H., MATHONNET, M., PYRONNET,

S., MARTINEAU, Y. & BOUSQUET, C. 2015. Pharmacological targeting of the protein synthesis mTOR/4E-BP1 pathway in cancer-associated fibroblasts abrogates pancreatic tumour chemoresistance. *EMBO Mol Med,* 7, 735-53.

DUNN, G. P., OLD, L. J. & SCHREIBER, R. D. 2004. The three Es of cancer immunoediting. *Annu Rev Immunol,* 22, 329-60.

DYER, D. P., MEDINA-RUIZ, L., BARTOLINI, R., SCHUETTE, F., HUGHES, C. E., PALLAS, K., VIDLER, F., MACLEOD, M. K. L., KELLY, C. J., LEE, K. M., HANSELL, C. A. H. & GRAHAM, G. J. 2019. Chemokine Receptor Redundancy and Specificity Are Context Dependent. *Immunity,* 50, 378-389.e5.

EASH, K. J., GREENBAUM, A. M., GOPALAN, P. K. & LINK, D. C. 2010. CXCR2 and CXCR4 antagonistically regulate neutrophil trafficking from murine bone marrow. *J Clin Invest,* 120, 2423-31.

EDWARDS, S. C., HEDLEY, A., HOEVENAAR, W. H. M., GLAUNER, T., WIESHEU, R., KILBEY, A., SHAW, R., BOUFEA, K., BATADA, N., BLYTH, K., MILLER, C., KIRSCHNER, K. & COFFELT, S. B. 2021. Single-cell analysis uncovers differential regulation of lung γδ T cell subsets by the co-inhibitory molecules, PD-1 and TIM-3. *bioRxiv.*

ELYADA, E., BOLISETTY, M., LAISE, P., FLYNN, W. F., COURTOIS, E. T., BURKHART, R. A., TEINOR, J. A., BELLEAU, P., BIFFI, G., LUCITO, M. S., SIVAJOTHI, S., ARMSTRONG, T. D., ENGLE, D. D., YU, K. H., HAO, Y., WOLFGANG, C. L., PARK, Y., PREALL, J., JAFFEE, E. M., CALIFANO, A., ROBSON, P. & TUVESON, D. A. 2019. Cross-Species Single-Cell Analysis of Pancreatic Ductal Adenocarcinoma Reveals Antigen-Presenting Cancer-Associated Fibroblasts. *Cancer Discov,* 9, 1102-1123.

FAHL, S. P., KAPPES, D. J. & WIEST, D. L. 2018. TCR Signaling Circuits in αβ/γδ T Lineage Choice. *In:* SOBOLOFF, J. & KAPPES, D. J. (eds.) *Signaling Mechanisms Regulating T Cell Diversity and Function.* Boca Raton (FL): CRC Press/Taylor & Francis

FENG, L., QI, Q., WANG, P., CHEN, H., CHEN, Z., MENG, Z. & LIU, L. 2018. Serum levels of IL-6, IL-8, and IL-10 are indicators of prognosis in pancreatic cancer. *J Int Med Res,* 46, 5228-5236.

FERDEK, P. E. & JAKUBOWSKA, M. A. 2017. Biology of pancreatic stellate cells-more than just pancreatic cancer. *Pflugers Arch,* 469, 1039-1050.

FERREIRA, R. M. M., SANCHO, R., MESSAL, H. A., NYE, E., SPENCER-DENE, B., STONE, R. K., STAMP, G., ROSEWELL, I., QUAGLIA, A. & BEHRENS, A. 2017. Duct- and Acinar-Derived Pancreatic Ductal Adenocarcinomas Show Distinct Tumor Progression and Marker Expression. *Cell Rep,* 21, 966-978.

FISCHER, A. H., JACOBSON, K. A., ROSE, J. & ZELLER, R. 2008. Hematoxylin and eosin staining of tissue and cell sections. *CSH Protoc,* 2008, pdb.prot4986.

FREED-PASTOR, W. A., LAMBERT, L. J., ELY, Z. A., PATTADA, N. B., BHUTKAR, A., ENG, G., MERCER, K. L., GARCIA, A. P., LIN, L., RIDEOUT, W. M., 3RD, HWANG, W. L., SCHENKEL, J. M., JAEGER, A. M., BRONSON, R. T., WESTCOTT, P. M. K., HETHER, T. D., DIVAKAR, P., REEVES, J. W., DESHPANDE, V., DELOREY, T., PHILLIPS, D., YILMAZ, O. H., REGEV, A. & JACKS, T. 2021. The CD155/TIGIT axis promotes and maintains immune evasion in neoantigen-expressing pancreatic cancer. *Cancer Cell,* 39, 1342-1360.e14.

GARDNER, A. & RUFFELL, B. 2016. Dendritic Cells and Cancer Immunity. *Trends Immunol,* 37, 855-865.

GELMAN, I. H. 2016. How the TRAMP Model Revolutionized the Study of Prostate Cancer Progression. *Cancer Res,* 76**,** 6137-6139.

GHALEB, A. M. & YANG, V. W. 2017. Krüppel-like factor 4 (KLF4): What we currently know. *Gene,* 611**,** 27-37.

GIRARDI, M., OPPENHEIM, D. E., STEELE, C. R., LEWIS, J. M., GLUSAC, E., FILLER, R., HOBBY, P., SUTTON, B., TIGELAAR, R. E. & HAYDAY, A. C. 2001. Regulation of cutaneous malignancy by gammadelta T cells. *Science,* 294**,** 605-9.

GORCHS, L., FERNÁNDEZ MORO, C., BANKHEAD, P., KERN, K. P., SADEAK, I., MENG, Q., RANGELOVA, E. & KAIPE, H. 2019. Human Pancreatic Carcinoma-Associated Fibroblasts Promote Expression of Co-inhibitory Markers on CD4(+) and CD8(+) T-Cells. *Front Immunol,* 10**,** 847.

GREMONPREZ, F., DESCAMPS, B., IZMER, A., VANHOVE, C., VANHAECKE, F., DE WEVER, O. & CEELEN, W. 2015. Pretreatment with VEGF(R)-inhibitors reduces interstitial fluid pressure, increases intraperitoneal chemotherapy drug penetration, and impedes tumor growth in a mouse colorectal carcinomatosis model. *Oncotarget,* 6**,** 29889-900.

GRIVENNIKOV, S. I., WANG, K., MUCIDA, D., STEWART, C. A., SCHNABL, B., JAUCH, D., TANIGUCHI, K., YU, G. Y., OSTERREICHER, C. H., HUNG, K. E., DATZ, C., FENG, Y., FEARON, E. R., OUKKA, M., TESSAROLLO, L., COPPOLA, V., YAROVINSKY, F., CHEROUTRE, H., ECKMANN, L., TRINCHIERI, G. & KARIN, M. 2012. Adenoma-linked barrier defects and microbial products drive IL-23/IL-17-mediated tumour growth. *Nature,* 491**,** 254-8.

GSCHWANDTNER, M., DERLER, R. & MIDWOOD, K. S. 2019. More Than Just Attractive: How CCL2 Influences Myeloid Cell Behavior Beyond Chemotaxis. *Front Immunol,* 10**,** 2759.

GUERRA, C., SCHUHMACHER, A. J., CAÑAMERO, M., GRIPPO, P. J., VERDAGUER, L., PÉREZ-GALLEGO, L., DUBUS, P., SANDGREN, E. P. & BARBACID, M. 2007. Chronic pancreatitis is essential for induction of pancreatic ductal adenocarcinoma by K-Ras oncogenes in adult mice. *Cancer Cell,* 11**,** 291-302.

GUNDERSON, A. J., KANEDA, M. M., TSUJIKAWA, T., NGUYEN, A. V., AFFARA, N. I., RUFFELL, B., GORJESTANI, S., LIUDAHL, S. M., TRUITT, M., OLSON, P., KIM, G., HANAHAN, D., TEMPERO, M. A., SHEPPARD, B., IRVING, B., CHANG, B. Y., VARNER, J. A. & COUSSENS, L. M. 2016. Bruton Tyrosine Kinase-Dependent Immune Cell Cross-talk Drives Pancreas Cancer. *Cancer Discov,* 6**,** 270-85.

HABBE, N., SHI, G., MEGUID, R. A., FENDRICH, V., ESNI, F., CHEN, H., FELDMANN, G., STOFFERS, D. A., KONIECZNY, S. F., LEACH, S. D. & MAITRA, A. 2008. Spontaneous induction of murine pancreatic intraepithelial neoplasia (mPanIN) by acinar cell targeting of oncogenic Kras in adult mice. *Proc Natl Acad Sci U S A,* 105**,** 18913-8.

HABTEZION, A., EDDERKAOUI, M. & PANDOL, S. J. 2016. Macrophages and pancreatic ductal adenocarcinoma. *Cancer Lett,* 381**,** 211-6.

HAN, J., MENG, Q., SHEN, L. & WU, G. 2018. Interleukin-6 induces fat loss in cancer cachexia by promoting white adipose tissue lipolysis and browning. *Lipids Health Dis,* 17**,** 14.

HAYES, S. M., LAIRD, R. M. & LOVE, P. E. 2010. Beyond alphabeta/gammadelta lineage commitment: TCR signal strength regulates gammadelta T cell maturation and effector fate. *Semin Immunol,* 22**,** 247-51.

HE, W., HAO, J., DONG, S., GAO, Y., TAO, J., CHI, H., FLAVELL, R., O'BRIEN, R. L., BORN, W. K., CRAFT, J., HAN, J., WANG, P., ZHAO, L., WU, J. & YIN, Z. 2010. Naturally activated V gamma 4 gamma delta T cells play a protective role in tumor immunity through expression of eomesodermin. *J Immunol,* 185**,** 126-33.

HEGDE, S., KRISNAWAN, V. E., HERZOG, B. H., ZUO, C., BREDEN, M. A., KNOLHOFF, B. L., HOGG, G. D., TANG, J. P., BAER, J. M., MPOY, C., LEE, K. B., ALEXANDER, K. A., ROGERS, B. E., MURPHY, K. M., HAWKINS, W. G., FIELDS, R. C., DESELM, C. J., SCHWARZ, J. K. & DENARDO, D. G. 2020. Dendritic Cell Paucity Leads to Dysfunctional Immune Surveillance in Pancreatic Cancer. *Cancer Cell,* 37**,** 289-307.e9.

HENRIQUES, F., LOPES, M. A., FRANCO, F. O., KNOBL, P., SANTOS, K. B., BUENO, L. L., CORREA, V. A., BEDARD, A. H., GUILHERME, A., BIRBRAIR, A., PERES, S. B., FARMER, S. R. & BATISTA, M. L., JR. 2018. Toll-Like Receptor-4 Disruption Suppresses Adipose Tissue Remodeling and Increases Survival in Cancer Cachexia Syndrome. *Sci Rep,* 8**,** 18024.

HERREROS-VILLANUEVA, M., HIJONA, E., COSME, A. & BUJANDA, L. 2012. Mouse models of pancreatic cancer. *World J Gastroenterol,* 18**,** 1286-94.

HINGORANI, S. R., PETRICOIN, E. F., MAITRA, A., RAJAPAKSE, V., KING, C., JACOBETZ, M. A., ROSS, S., CONRADS, T. P., VEENSTRA, T. D., HITT, B. A., KAWAGUCHI, Y., JOHANN, D., LIOTTA, L. A., CRAWFORD, H. C., PUTT, M. E., JACKS, T., WRIGHT, C. V., HRUBAN, R. H., LOWY, A. M. & TUVESON, D. A. 2003. Preinvasive and invasive ductal pancreatic cancer and its early detection in the mouse. *Cancer Cell,* 4**,** 437-50.

HINGORANI, S. R., WANG, L., MULTANI, A. S., COMBS, C., DERAMAUDT, T. B., HRUBAN, R. H., RUSTGI, A. K., CHANG, S. & TUVESON, D. A. 2005. Trp53R172H and KrasG12D cooperate to promote chromosomal instability and widely metastatic pancreatic ductal adenocarcinoma in mice. *Cancer Cell,* 7**,** 469-83.

HRUBAN, R. H., MAITRA ANIRBAN AND GOGGINS, MICHAEL 2008. Update on Pancreatic Intraepithelial Neoplasia. *International Journal of Clincal and Experimental Pathology,* 1**,** 306-316.

HRUBAN, R. H., WILENTZ, R. E. & KERN, S. E. 2000. Genetic progression in the pancreatic ducts. *Am J Pathol,* 156**,** 1821-5.

HSIEH, C. L., NIEMI, E. C., WANG, S. H., LEE, C. C., BINGHAM, D., ZHANG, J., COZEN, M. L., CHARO, I., HUANG, E. J., LIU, J. & NAKAMURA, M. C. 2014. CCR2 deficiency impairs macrophage infiltration and improves cognitive function after traumatic brain injury. *J Neurotrauma,* 31**,** 1677-88.

HSU, P., SANTNER-NANAN, B., HU, M., SKARRATT, K., LEE, C. H., STORMON, M., WONG, M., FULLER, S. J. & NANAN, R. 2015. IL-10 Potentiates Differentiation of Human Induced Regulatory T Cells via STAT3 and Foxo1. *J Immunol,* 195**,** 3665-74.

HU, F., GUO, F., ZHU, Y., ZHOU, Q., LI, T., XIANG, H. & SHANG, D. 2020. IL-17 in pancreatic disease: pathogenesis and pharmacotherapy. *Am J Cancer Res,* 10**,** 3551-3564.

HU, G., WU, P., CHENG, P., ZHANG, Z., WANG, Z., YU, X., SHAO, X., WU, D., YE, J., ZHANG, T., WANG, X., QIU, F., YAN, J. & HUANG, J. 2017. Tumor-infiltrating CD39(+)γδTregs are novel immunosuppressive T cells in human colorectal cancer. *Oncoimmunology,* 6**,** e1277305.

HUNTER, M., WANG, Y., EUBANK, T., BARAN, C., NANA-SINKAM, P. & MARSH, C. 2009. Survival of monocytes and macrophages and their role in health and disease. *Front Biosci (Landmark Ed),* 14**,** 4079-102.

HUNTINGTON, N. D., CURSONS, J. & RAUTELA, J. 2020. The cancer-natural killer cell immunity cycle. *Nat Rev Cancer,* 20**,** 437-454.

IJICHI, H., CHYTIL, A., GORSKA, A. E., AAKRE, M. E., BIERIE, B., TADA, M., MOHRI, D., MIYABAYASHI, K., ASAOKA, Y., MAEDA, S., IKENOUE, T., TATEISHI, K., WRIGHT, C. V., KOIKE, K., OMATA, M. & MOSES, H. L. 2011. Inhibiting Cxcr2 disrupts tumor-stromal interactions and improves survival in a mouse model of pancreatic ductal adenocarcinoma. *J Clin Invest,* 121**,** 4106-17.

IRELAND, L., SANTOS, A., AHMED, M. S., RAINER, C., NIELSEN, S. R., QUARANTA, V., WEYER-CZERNILOFSKY, U., ENGLE, D. D., PEREZ-MANCERA, P. A., COUPLAND, S. E., TAKTAK, A., BOGENRIEDER, T., TUVESON, D. A., CAMPBELL, F., SCHMID, M. C. & MIELGO, A. 2016. Chemoresistance in Pancreatic Cancer Is Driven by Stroma-Derived Insulin-Like Growth Factors. *Cancer Res,* 76**,** 6851-6863.

IWAMOTO, C., OHUCHIDA, K., SHINKAWA, T., OKUDA, S., OTSUBO, Y., OKUMURA, T., SAGARA, A., KOIKAWA, K., ANDO, Y., SHINDO, K., IKENAGA, N., NAKATA, K., MORIYAMA, T., MIYASAKA, Y., OHTSUKA, T., ETO, M., AKASHI, K. & NAKAMURA, M. 2021. Bone marrow-derived macrophages converted into cancer-associated fibroblast-like cells promote pancreatic cancer progression. *Cancer Lett,* 512**,** 15-27.

JEWETT, A., KOS, J., KAUR, K., SAFAEI, T., SUTANTO, C., CHEN, W., WONG, P., NAMAGERDI, A. K., FANG, C., FONG, Y. & KO, M. W. 2020. Natural Killer Cells: Diverse Functions in Tumor Immunity and Defects in Pre-neoplastic and Neoplastic Stages of Tumorigenesis. *Mol Ther Oncolytics,* 16**,** 41-52.

JIN, C., LAGOUDAS, G. K., ZHAO, C., BULLMAN, S., BHUTKAR, A., HU, B., AMEH, S., SANDEL, D., LIANG, X. S., MAZZILLI, S., WHARY, M. T., MEYERSON, M., GERMAIN, R., BLAINEY, P. C., FOX, J. G. & JACKS, T. 2019. Commensal Microbiota Promote Lung Cancer Development via γδ T Cells. *Cell,* 176**,** 998-1013.e16.

JØRGENSEN, M. C., AHNFELT-RØNNE, J., HALD, J., MADSEN, O. D., SERUP, P. & HECKSHER-SØRENSEN, J. 2007. An illustrated review of early pancreas development in the mouse. *Endocr Rev,* 28**,** 685-705.

JOSS, A., AKDIS, M., FAITH, A., BLASER, K. & AKDIS, C. A. 2000. IL-10 directly acts on T cells by specifically altering the CD28 co-stimulation pathway. *Eur J Immunol,* 30**,** 1683-90.

JUNG, H., HSIUNG, B., PESTAL, K., PROCYK, E. & RAULET, D. H. 2012. RAE-1 ligands for the NKG2D receptor are regulated by E2F transcription factors, which control cell cycle entry. *J Exp Med,* 209**,** 2409-22.

JUNG, H., MITHAL, D. S., PARK, J. E. & MILLER, R. J. 2015. Localized CCR2 Activation in the Bone Marrow Niche Mobilizes Monocytes by Desensitizing CXCR4. *PLoS One,* 10**,** e0128387.

KATSUNO, Y., LAMOUILLE, S. & DERYNCK, R. 2013. TGF-ß signaling and epithelial-mesenchymal transition in cancer progression. *Curr Opin Oncol,* 25**,** 76-84.

KAUR, K., CHANG, H. H., TOPCHYAN, P., COOK, J. M., BARKHORDARIAN, A., EIBL, G. & JEWETT, A. 2018. Deficiencies in Natural Killer Cell Numbers, Expansion, and Function at the Pre-Neoplastic Stage of Pancreatic Cancer by KRAS Mutation in the Pancreas of Obese Mice. *Front Immunol,* 9**,** 1229.

KEENAN, B. P., SAENGER, Y., KAFROUNI, M. I., LEUBNER, A., LAUER, P., MAITRA, A., RUCKI, A. A., GUNDERSON, A. J., COUSSENS, L. M., BROCKSTEDT, D. G., DUBENSKY, T. W., JR., HASSAN, R., ARMSTRONG, T. D. & JAFFEE, E. M. 2014. A Listeria vaccine and depletion of T-regulatory cells activate

immunity against early stage pancreatic intraepithelial neoplasms and prolong survival of mice. *Gastroenterology,* 146**,** 1784-94.e6.

KHOSRAVI, N., CAETANO, M. S., CUMPIAN, A. M., UNVER, N., DE LA GARZA RAMOS, C., NOBLE, O., DALIRI, S., HERNANDEZ, B. J., GUTIERREZ, B. A., EVANS, S. E., HANASH, S., ALEKSEEV, A. M., YANG, Y., CHANG, S. H., NURIEVA, R., KADARA, H., CHEN, J., OSTRIN, E. J. & MOGHADDAM, S. J. 2018. IL22 Promotes Kras-Mutant Lung Cancer by Induction of a Protumor Immune Response and Protection of Stemness Properties. *Cancer Immunol Res,* 6**,** 788-797.

KIM, H. K., DE LA LUZ SIERRA, M., WILLIAMS, C. K., GULINO, A. V. & TOSATO, G. 2006. G-CSF down-regulation of CXCR4 expression identified as a mechanism for mobilization of myeloid cells. *Blood,* 108**,** 812-20.

KITAMURA, T., FUJISHITA, T., LOETSCHER, P., REVESZ, L., HASHIDA, H., KIZAKA-KONDOH, S., AOKI, M. & TAKETO, M. M. 2010. Inactivation of chemokine (C-C motif) receptor 1 (CCR1) suppresses colon cancer liver metastasis by blocking accumulation of immature myeloid cells in a mouse model. *Proc Natl Acad Sci U S A,* 107**,** 13063-8.

KITAMURA, T., KOMETANI, K., HASHIDA, H., MATSUNAGA, A., MIYOSHI, H., HOSOGI, H., AOKI, M., OSHIMA, M., HATTORI, M., TAKABAYASHI, A., MINATO, N. & TAKETO, M. M. 2007. SMAD4-deficient intestinal tumors recruit CCR1+ myeloid cells that promote invasion. *Nat Genet,* 39**,** 467-75.

KOHLGRUBER, A. C., GAL-OZ, S. T., LAMARCHE, N. M., SHIMAZAKI, M., DUQUETTE, D., KOAY, H. F., NGUYEN, H. N., MINA, A. I., PARAS, T., TAVAKKOLI, A., VON ANDRIAN, U., ULDRICH, A. P., GODFREY, D. I., BANKS, A. S., SHAY, T., BRENNER, M. B. & LYNCH, L. 2018. γδ T cells producing interleukin-17A regulate adipose regulatory T cell homeostasis and thermogenesis. *Nat Immunol,* 19**,** 464-474.

KOMORI, H. K., MEEHAN, T. F. & HAVRAN, W. L. 2006. Epithelial and mucosal gamma delta T cells. *Curr Opin Immunol,* 18**,** 534-8.

KONG, Y., CAO, W., XI, X., MA, C., CUI, L. & HE, W. 2009. The NKG2D ligand ULBP4 binds to TCRgamma9/delta2 and induces cytotoxicity to tumor cells through both TCRgammadelta and NKG2D. *Blood,* 114**,** 310-7.

KOPP, J. L., VON FIGURA, G., MAYES, E., LIU, F. F., DUBOIS, C. L., MORRIS, J. P. T., PAN, F. C., AKIYAMA, H., WRIGHT, C. V., JENSEN, K., HEBROK, M. & SANDER, M. 2012. Identification of Sox9-dependent acinar-to-ductal reprogramming as the principal mechanism for initiation of pancreatic ductal adenocarcinoma. *Cancer Cell,* 22**,** 737-50.

KRAH, N. M., DE LA, O. J., SWIFT, G. H., HOANG, C. Q., WILLET, S. G., CHEN PAN, F., CASH, G. M., BRONNER, M. P., WRIGHT, C. V., MACDONALD, R. J. & MURTAUGH, L. C. 2015. The acinar differentiation determinant PTF1A inhibits initiation of pancreatic ductal adenocarcinoma. *Elife,* 4.

KRATOCHVILL, F., NEALE, G., HAVERKAMP, J. M., VAN DE VELDE, L. A., SMITH, A. M., KAWAUCHI, D., MCEVOY, J., ROUSSEL, M. F., DYER, M. A., QUALLS, J. E. & MURRAY, P. J. 2015. TNF Counterbalances the Emergence of M2 Tumor Macrophages. *Cell Rep,* 12**,** 1902-14.

KUMAR, S. 2018. Natural killer cell cytotoxicity and its regulation by inhibitory receptors. *Immunology,* 154**,** 383-393.

KURAHARA, H., SHINCHI, H., MATAKI, Y., MAEMURA, K., NOMA, H., KUBO, F., SAKODA, M., UENO, S., NATSUGOE, S. & TAKAO, S. 2011. Significance of M2-polarized tumor-associated macrophage in pancreatic cancer. *J Surg Res,* 167**,** e211-9.

LANDERS, A., MUIRCROFT, W. & BROWN, H. 2016. Pancreatic enzyme replacement therapy (PERT) for malabsorption in patients with metastatic pancreatic cancer. *BMJ Support Palliat Care,* 6**,** 75-9.

LAURITSEN, J. P., WONG, G. W., LEE, S. Y., LEFEBVRE, J. M., CIOFANI, M., RHODES, M., KAPPES, D. J., ZÚÑIGA-PFLÜCKER, J. C. & WIEST, D. L. 2009. Marked induction of the helix-loop-helix protein Id3 promotes the gammadelta T cell fate and renders their functional maturation Notch independent. *Immunity,* 31**,** 565-75.

LAWAND, M., DÉCHANET-MERVILLE, J. & DIEU-NOSJEAN, M. C. 2017. Key Features of Gamma-Delta T-Cell Subsets in Human Diseases and Their Immunotherapeutic Implications. *Front Immunol,* 8**,** 761.

LEE, J., PARK, K. H., RYU, J. H., BAE, H. J., CHOI, A., LEE, H., LIM, J., HAN, K., PARK, C. H., JUNG, E. S. & OH, E. J. 2017. Natural killer cell activity for IFN-gamma production as a supportive diagnostic marker for gastric cancer. *Oncotarget,* 8**,** 70431-70440.

LEE, J. W., KOMAR, C. A., BENGSCH, F., GRAHAM, K. & BEATTY, G. L. 2016. Genetically Engineered Mouse Models of Pancreatic Cancer: The KPC Model (LSL-Kras(G12D/+) ;LSL-Trp53(R172H/+) ;Pdx-1-Cre), Its Variants, and Their Application in Immuno-oncology Drug Discovery. *Curr Protoc Pharmacol,* 73**,** 14.39.1-14.39.20.

LESINA, M., KURKOWSKI, M. U., LUDES, K., ROSE-JOHN, S., TREIBER, M., KLÖPPEL, G., YOSHIMURA, A., REINDL, W., SIPOS, B., AKIRA, S., SCHMID, R. M. & ALGÜL, H. 2011. Stat3/Socs3 activation by IL-6 transsignaling promotes progression of pancreatic intraepithelial neoplasia and development of pancreatic cancer. *Cancer Cell,* 19**,** 456-69.

LI, A., KING, J., MORO, A., SUGI, M. D., DAWSON, D. W., KAPLAN, J., LI, G., LU, X., STRIETER, R. M., BURDICK, M., GO, V. L., REBER, H. A., EIBL, G. & HINES, O. J. 2011a. Overexpression of CXCL5 is associated with poor survival in patients with pancreatic cancer. *Am J Pathol,* 178**,** 1340-9.

LI, Z., XU, Q., PENG, H., CHENG, R., SUN, Z. & YE, Z. 2011b. IFN-γ enhances HOS and U2OS cell lines susceptibility to γδ T cell-mediated killing through the Fas/Fas ligand pathway. *Int Immunopharmacol,* 11**,** 496-503.

LIM, S. A., KIM, J., JEON, S., SHIN, M. H., KWON, J., KIM, T. J., IM, K., HAN, Y., KWON, W., KIM, S. W., YEE, C., KIM, S. J., JANG, J. Y. & LEE, K. M. 2019. Defective Localization With Impaired Tumor Cytotoxicity Contributes to the Immune Escape of NK Cells in Pancreatic Cancer Patients. *Front Immunol,* 10**,** 496.

LIN, J. H., HUFFMAN, A. P., WATTENBERG, M. M., WALTER, D. M., CARPENTER, E. L., FELDSER, D. M., BEATTY, G. L., FURTH, E. E. & VONDERHEIDE, R. H. 2020. Type 1 conventional dendritic cells are systemically dysregulated early in pancreatic carcinogenesis. *J Exp Med,* 217.

LIN, Y., XU, J. & LAN, H. 2019. Tumor-associated macrophages in tumor metastasis: biological roles and clinical therapeutic applications. *J Hematol Oncol,* 12**,** 76.

LINDELL, D. M., MOORE, T. A., MCDONALD, R. A., TOEWS, G. B. & HUFFNAGLE, G. B. 2006. Distinct compartmentalization of CD4+ T-cell effector function versus proliferative capacity during pulmonary cryptococcosis. *Am J Pathol,* 168**,** 847-55.

LINTON, S. S., ABRAHAM, T., LIAO, J., CLAWSON, G. A., BUTLER, P. J., FOX, T., KESTER, M. & MATTERS, G. L. 2018. Tumor-promoting effects of pancreatic cancer cell exosomes on THP-1-derived macrophages. *PLoS One,* 13**,** e0206759.

LIOU, G. Y., BASTEA, L., FLEMING, A., DÖPPLER, H., EDENFIELD, B. H., DAWSON, D. W., ZHANG, L., BARDEESY, N. & STORZ, P. 2017. The Presence of Interleukin-13 at Pancreatic ADM/PanIN Lesions Alters Macrophage Populations and Mediates Pancreatic Tumorigenesis. *Cell Rep,* 19**,** 1322-1333.

LIOU, G. Y., DÖPPLER, H., NECELA, B., KRISHNA, M., CRAWFORD, H. C., RAIMONDO, M. & STORZ, P. 2013. Macrophage-secreted cytokines drive pancreatic acinar-to-ductal metaplasia through NF-κB and MMPs. *J Cell Biol,* 202**,** 563-77.

LIPSON, K. E., WONG, C., TENG, Y. & SPONG, S. 2012. CTGF is a central mediator of tissue remodeling and fibrosis and its inhibition can reverse the process of fibrosis. *Fibrogenesis Tissue Repair,* 5**,** S24.

LIU, T., ZHANG, L., JOO, D. & SUN, S. C. 2017. NF-κB signaling in inflammation. *Signal Transduct Target Ther,* 2**,** 17023-.

LIU, X., XU, J., ZHANG, B., LIU, J., LIANG, C., MENG, Q., HUA, J., YU, X. & SHI, S. 2019. The reciprocal regulation between host tissue and immune cells in pancreatic ductal adenocarcinoma: new insights and therapeutic implications. *Mol Cancer,* 18**,** 184.

LIU, Z., ELTOUM, I. E., GUO, B., BECK, B. H., CLOUD, G. A. & LOPEZ, R. D. 2008. Protective immunosurveillance and therapeutic antitumor activity of gammadelta T cells demonstrated in a mouse model of prostate cancer. *J Immunol,* 180**,** 6044-53.

LÓPEZ-SOTO, A., GONZALEZ, S., SMYTH, M. J. & GALLUZZI, L. 2017. Control of Metastasis by NK Cells. *Cancer Cell,* 32**,** 135-154.

MA, C., ZHANG, Q., YE, J., WANG, F., ZHANG, Y., WEVERS, E., SCHWARTZ, T., HUNBORG, P., VARVARES, M. A., HOFT, D. F., HSUEH, E. C. & PENG, G. 2012. Tumor-infiltrating γδ T lymphocytes predict clinical outcome in human breast cancer. *J Immunol,* 189**,** 5029-36.

MA, S., CHENG, Q., CAI, Y., GONG, H., WU, Y., YU, X., SHI, L., WU, D., DONG, C. & LIU, H. 2014. IL-17A produced by γδ T cells promotes tumor growth in hepatocellular carcinoma. *Cancer Res,* 74**,** 1969-82.

MALIK, S., WANT, M. Y. & AWASTHI, A. 2016. The Emerging Roles of Gamma-Delta T Cells in Tissue Inflammation in Experimental Autoimmune Encephalomyelitis. *Front Immunol,* 7**,** 14.

MAMEDOV, M. R., SCHOLZEN, A., NAIR, R. V., CUMNOCK, K., KENKEL, J. A., OLIVEIRA, J. H. M., TRUJILLO, D. L., SALIGRAMA, N., ZHANG, Y., RUBELT, F., SCHNEIDER, D. S., CHIEN, Y. H., SAUERWEIN, R. W. & DAVIS, M. M. 2018. A Macrophage Colony-Stimulating-Factor-Producing γδ T Cell Subset Prevents Malarial Parasitemic Recurrence. *Immunity,* 48**,** 350-363.e7.

MANIAR, A., ZHANG, X., LIN, W., GASTMAN, B. R., PAUZA, C. D., STROME, S. E. & CHAPOVAL, A. I. 2010. Human gammadelta T lymphocytes induce robust NK cell-mediated antitumor cytotoxicity through CD137 engagement. *Blood,* 116**,** 1726-33.

MARCON, F., ZUO, J., PEARCE, H., NICOL, S., MARGIELEWSKA-DAVIES, S., FARHAT, M., MAHON, B., MIDDLETON, G., BROWN, R., ROBERTS, K. J. & MOSS, P. 2020. NK cells in pancreatic cancer demonstrate impaired cytotoxicity and a regulatory IL-10 phenotype. *Oncoimmunology,* 9**,** 1845424.

MARRACHE, F., TU, S. P., BHAGAT, G., PENDYALA, S., OSTERREICHER, C. H., GORDON, S., RAMANATHAN, V., PENZ-OSTERREICHER, M., BETZ, K. S., SONG, Z. & WANG, T. C. 2008. Overexpression of interleukin-1beta in the

murine pancreas results in chronic pancreatitis. *Gastroenterology,* 135**,** 1277-87.

MARTINELLI, P., MADRILES, F., CAÑAMERO, M., PAU, E. C., POZO, N. D., GUERRA, C. & REAL, F. X. 2016. The acinar regulator Gata6 suppresses KrasG12V-driven pancreatic tumorigenesis in mice. *Gut,* 65**,** 476-86.

MATSUO, Y., OCHI, N., SAWAI, H., YASUDA, A., TAKAHASHI, H., FUNAHASHI, H., TAKEYAMA, H., TONG, Z. & GUHA, S. 2009a. CXCL8/IL-8 and CXCL12/SDF-1alpha co-operatively promote invasiveness and angiogenesis in pancreatic cancer. *Int J Cancer,* 124**,** 853-61.

MATSUO, Y., RAIMONDO, M., WOODWARD, T. A., WALLACE, M. B., GILL, K. R., TONG, Z., BURDICK, M. D., YANG, Z., STRIETER, R. M., HOFFMAN, R. M. & GUHA, S. 2009b. CXC-chemokine/CXCR2 biological axis promotes angiogenesis in vitro and in vivo in pancreatic cancer. *Int J Cancer,* 125**,** 1027-37.

MCALLISTER, F., BAILEY, J. M., ALSINA, J., NIRSCHL, C. J., SHARMA, R., FAN, H., RATTIGAN, Y., ROESER, J. C., LANKAPALLI, R. H., ZHANG, H., JAFFEE, E. M., DRAKE, C. G., HOUSSEAU, F., MAITRA, A., KOLLS, J. K., SEARS, C. L., PARDOLL, D. M. & LEACH, S. D. 2014. Oncogenic Kras activates a hematopoietic-to-epithelial IL-17 signaling axis in preinvasive pancreatic neoplasia. *Cancer Cell,* 25**,** 621-37.

MCBRIDE, J. M., JUNG, T., DE VRIES, J. E. & AVERSA, G. 2002. IL-10 alters DC function via modulation of cell surface molecules resulting in impaired T-cell responses. *Cell Immunol,* 215**,** 162-72.

MCCOWAN, J., FERCOQ, F., KIRKWOOD, P. M., T'JONCK, W., HEGARTY, L. M., MAWER, C. M., CUNNINGHAM, R., MIRCHANDANI, A. S., HOY, A., HUMPHRIES, D. C., JONES, G. R., HANSEN, C. G., HIRANI, N., JENKINS, S. J., HENRI, S., MALISSEN, B., WALMSLEY, S. R., DOCKRELL, D. H., SAUNDERS, P. T. K., CARLIN, L. M. & BAIN, C. C. 2021. The transcription factor EGR2 is indispensable for tissue-specific imprinting of alveolar macrophages in health and tissue repair. *Sci Immunol,* 6**,** eabj2132.

MENGYU TU, L. K., ELISA ESPINET, THEODOROS GEOGOMANOLIS, FLORIAN WEGWITZ, XIAOJUAN LI, LAURA URBACH, ADI DANIELI0MACKAY, STEFAN KUFFER, KAMIL BOJARCZUK, ATHANASIA MIZI, UFUK GUNESDOGAN, BJORN CHAPUY, ZUGUANG GU, ALBRECT NEESE, UDAY KISHORE, PHILIPP STROBEL, ELISABETH HESSMANN, STEPHAN A. HAHN, ANDREAS TRUMPP, ARGYRIS PAPANTONIS, VOLKER ELLENRIEDER AND SHIV K. SINGH 2021. TNF-α-producing macrophages determine subtype identity and prognosis via AP1 enhancer reprogramming in pancreatic cancer. *Nature Cancer*.

MEYER, M. A., BAER, J. M., KNOLHOFF, B. L., NYWENING, T. M., PANNI, R. Z., SU, X., WEILBAECHER, K. N., HAWKINS, W. G., MA, C., FIELDS, R. C., LINEHAN, D. C., CHALLEN, G. A., FACCIO, R., AFT, R. L. & DENARDO, D. G. 2018. Breast and pancreatic cancer interrupt IRF8-dependent dendritic cell development to overcome immune surveillance. *Nat Commun,* 9**,** 1250.

MILDNER, A. & JUNG, S. 2014. Development and function of dendritic cell subsets. *Immunity,* 40**,** 642-56.

MILLER, J. S. A. L., LEWIS L. 2018. Natural Killer Cells in Cancer Immunotherapy. *Annual Reviews,* 77-103.

MITTAL, D., GUBIN, M. M., SCHREIBER, R. D. & SMYTH, M. J. 2014. New insights into cancer immunoediting and its three component phases--elimination, equilibrium and escape. *Curr Opin Immunol,* 27**,** 16-25.

MITTAL, S. K., CHO, K. J., ISHIDO, S. & ROCHE, P. A. 2015. Interleukin 10 (IL-10)-mediated Immunosuppression: MARCH-I INDUCTION REGULATES ANTIGEN PRESENTATION BY MACROPHAGES BUT NOT DENDRITIC CELLS. *J Biol Chem*, 290**,** 27158-27167.

MOFFITT, R. A., MARAYATI, R., FLATE, E. L., VOLMAR, K. E., LOEZA, S. G., HOADLEY, K. A., RASHID, N. U., WILLIAMS, L. A., EATON, S. C., CHUNG, A. H., SMYLA, J. K., ANDERSON, J. M., KIM, H. J., BENTREM, D. J., TALAMONTI, M. S., IACOBUZIO-DONAHUE, C. A., HOLLINGSWORTH, M. A. & YEH, J. J. 2015. Virtual microdissection identifies distinct tumor- and stroma-specific subtypes of pancreatic ductal adenocarcinoma. *Nat Genet,* 47**,** 1168-78.

MORRIS, J. P. T., CANO, D. A., SEKINE, S., WANG, S. C. & HEBROK, M. 2010. Beta-catenin blocks Kras-dependent reprogramming of acini into pancreatic cancer precursor lesions in mice. *J Clin Invest,* 120**,** 508-20.

MORTON, J. P., TIMPSON, P., KARIM, S. A., RIDGWAY, R. A., ATHINEOS, D., DOYLE, B., JAMIESON, N. B., OIEN, K. A., LOWY, A. M., BRUNTON, V. G., FRAME, M. C., EVANS, T. R. & SANSOM, O. J. 2010. Mutant p53 drives metastasis and overcomes growth arrest/senescence in pancreatic cancer. *Proc Natl Acad Sci U S A,* 107, 246-51.

MUCCIOLO, G., CURCIO, C., ROUX, C., LI, W. Y., CAPELLO, M., CURTO, R., CHIARLE, R., GIORDANO, D., SATOLLI, M. A., LAWLOR, R., SCARPA, A., LUKAC, P., STAKHEEV, D., PROVERO, P., VANNUCCI, L., MAK, T. W., NOVELLI, F. & CAPPELLO, P. 2021. IL17A critically shapes the transcriptional program of fibroblasts in pancreatic cancer and switches on their protumorigenic functions. *Proc Natl Acad Sci U S A,* 118.

MURPHY, K. P. 2012. *Janeway's Immunobiology*, Garland Science.

NARASIMHAN, A., ZHONG, X., AU, E. P., CEPPA, E. P., NAKEEB, A., HOUSE, M. G., ZYROMSKI, N. J., SCHMIDT, C. M., SCHLOSS, K. N. H., SCHLOSS, D. E. I., LIU, Y., JIANG, G., HANCOCK, B. A., RADOVICH, M., KAYS, J. K., SHAHDA, S., COUCH, M. E., KONIARIS, L. G. & ZIMMERS, T. A. 2021. Profiling of Adipose and Skeletal Muscle in Human Pancreatic Cancer Cachexia Reveals Distinct Gene Profiles with Convergent Pathways. *Cancers (Basel),* 13.

NETHERBY, C. S., MESSMER, M. N., BURKARD-MANDEL, L., COLLIGAN, S., MILLER, A., CORTES GOMEZ, E., WANG, J., NEMETH, M. J. & ABRAMS, S. I. 2017. The Granulocyte Progenitor Stage Is a Key Target of IRF8-Mediated Regulation of Myeloid-Derived Suppressor Cell Production. *J Immunol,* 198**,** 4129-4139.

NIELSEN, S. R., QUARANTA, V., LINFORD, A., EMEAGI, P., RAINER, C., SANTOS, A., IRELAND, L., SAKAI, T., SAKAI, K., KIM, Y. S., ENGLE, D., CAMPBELL, F., PALMER, D., KO, J. H., TUVESON, D. A., HIRSCH, E., MIELGO, A. & SCHMID, M. C. 2016. Macrophage-secreted granulin supports pancreatic cancer metastasis by inducing liver fibrosis. *Nat Cell Biol,* 18**,** 549-60.

NOUBADE, R., MAJRI-MORRISON, S. & TARBELL, K. V. 2019. Beyond cDC1: Emerging Roles of DC Crosstalk in Cancer Immunity. *Front Immunol,* 10**,** 1014.

NOY, R. & POLLARD, J. W. 2014. Tumor-associated macrophages: from mechanisms to therapy. *Immunity,* 41**,** 49-61.

NYWENING, T. M., BELT, B. A., CULLINAN, D. R., PANNI, R. Z., HAN, B. J., SANFORD, D. E., JACOBS, R. C., YE, J., PATEL, A. A., GILLANDERS, W. E., FIELDS, R. C., DENARDO, D. G., HAWKINS, W. G., GOEDEGEBUURE, P. & LINEHAN, D. C. 2018. Targeting both tumour-associated CXCR2(+)

neutrophils and CCR2(+) macrophages disrupts myeloid recruitment and improves chemotherapeutic responses in pancreatic ductal adenocarcinoma. *Gut,* 67**,** 1112-1123.

OBERG, H. H., PEIPP, M., KELLNER, C., SEBENS, S., KRAUSE, S., PETRICK, D., ADAM-KLAGES, S., RÖCKEN, C., BECKER, T., VOGEL, I., WEISNER, D., FREITAG-WOLF, S., GRAMATZKI, M., KABELITZ, D. & WESCH, D. 2014. Novel bispecific antibodies increase γδ T-cell cytotoxicity against pancreatic cancer cells. *Cancer Res,* 74**,** 1349-60.

ÖHLUND, D., ELYADA, E. & TUVESON, D. 2014. Fibroblast heterogeneity in the cancer wound. *J Exp Med,* 211**,** 1503-23.

ÖHLUND, D., HANDLY-SANTANA, A., BIFFI, G., ELYADA, E., ALMEIDA, A. S., PONZ-SARVISE, M., CORBO, V., ONI, T. E., HEARN, S. A., LEE, E. J., CHIO, II, HWANG, C. I., TIRIAC, H., BAKER, L. A., ENGLE, D. D., FEIG, C., KULTTI, A., EGEBLAD, M., FEARON, D. T., CRAWFORD, J. M., CLEVERS, H., PARK, Y. & TUVESON, D. A. 2017. Distinct populations of inflammatory fibroblasts and myofibroblasts in pancreatic cancer. *J Exp Med,* 214**,** 579-596.

OLOVNIKOV, I. A., KRAVCHENKO, J. E. & CHUMAKOV, P. M. 2009. Homeostatic functions of the p53 tumor suppressor: regulation of energy metabolism and antioxidant defense. *Semin Cancer Biol,* 19**,** 32-41.

OLSON, B., ZHU, X., NORGARD, M. A., LEVASSEUR, P. R., BUTLER, J. T., BUENAFE, A., BURFEIND, K. G., MICHAELIS, K. A., PELZ, K. R., MENDEZ, H., EDWARDS, J., KRASNOW, S. M., GROSSBERG, A. J. & MARKS, D. L. 2021. Lipocalin 2 mediates appetite suppression during pancreatic cancer cachexia. *Nat Commun,* 12**,** 2057.

ORTH, M., METZGER, P., GERUM, S., MAYERLE, J., SCHNEIDER, G., BELKA, C., SCHNURR, M. & LAUBER, K. 2019. Pancreatic ductal adenocarcinoma: biological hallmarks, current status, and future perspectives of combined modality treatment approaches. *Radiat Oncol,* 14**,** 141.

ÖZDEMIR, B. C., PENTCHEVA-HOANG, T., CARSTENS, J. L., ZHENG, X., WU, C. C., SIMPSON, T. R., LAKLAI, H., SUGIMOTO, H., KAHLERT, C., NOVITSKIY, S. V., DE JESUS-ACOSTA, A., SHARMA, P., HEIDARI, P., MAHMOOD, U., CHIN, L., MOSES, H. L., WEAVER, V. M., MAITRA, A., ALLISON, J. P., LEBLEU, V. S. & KALLURI, R. 2014. Depletion of carcinoma-associated fibroblasts and fibrosis induces immunosuppression and accelerates pancreas cancer with reduced survival. *Cancer Cell,* 25**,** 719-34.

PANDOL, S. J. 2010. The Exocrine Pancreas. Morgan & Claypool Life Sciences.

PARAJULI, P., KUMAR, S., LOUMAYE, A., SINGH, P., ERAGAMREDDY, S., NGUYEN, T. L., OZKAN, S., RAZZAQUE, M. S., PRUNIER, C., THISSEN, J. P. & ATFI, A. 2018. Twist1 Activation in Muscle Progenitor Cells Causes Muscle Loss Akin to Cancer Cachexia. *Dev Cell,* 45**,** 712-725.e6.

PARKER, M. E. & CIOFANI, M. 2020. Regulation of γδ T Cell Effector Diversification in the Thymus. *Front Immunol,* 11**,** 42.

PATIN, E. C., SOULARD, D., FLEURY, S., HASSANE, M., DOMBROWICZ, D., FAVEEUW, C., TROTTEIN, F. & PAGET, C. 2018. Type I IFN Receptor Signaling Controls IL7-Dependent Accumulation and Activity of Protumoral IL17A-Producing γδT Cells in Breast Cancer. *Cancer Res,* 78**,** 195-204.

PAUL, S. & LAL, G. 2017. The Molecular Mechanism of Natural Killer Cells Function and Its Importance in Cancer Immunotherapy. *Front Immunol,* 8**,** 1124.

PEREIRA, B. A., VENNIN, C., PAPANICOLAOU, M., CHAMBERS, C. R., HERRMANN, D., MORTON, J. P., COX, T. R. & TIMPSON, P. 2019. CAF Subpopulations: A

New Reservoir of Stromal Targets in Pancreatic Cancer. *Trends Cancer,* 5**,** 724-741.

PERRI, F., PISCONTI, S. & DELLA VITTORIA SCARPATI, G. 2016. P53 mutations and cancer: a tight linkage. *Ann Transl Med,* 4**,** 522.

PETRIE, H. T., SCOLLAY, R. & SHORTMAN, K. 1992. Commitment to the T cell receptor-alpha beta or -gamma delta lineages can occur just prior to the onset of CD4 and CD8 expression among immature thymocytes. *Eur J Immunol,* 22**,** 2185-8.

PETRUZZELLI, M., SCHWEIGER, M., SCHREIBER, R., CAMPOS-OLIVAS, R., TSOLI, M., ALLEN, J., SWARBRICK, M., ROSE-JOHN, S., RINCON, M., ROBERTSON, G., ZECHNER, R. & WAGNER, E. F. 2014. A switch from white to brown fat increases energy expenditure in cancer-associated cachexia. *Cell Metab,* 20**,** 433-47.

POH, A. R. & ERNST, M. 2021. Tumor-Associated Macrophages in Pancreatic Ductal Adenocarcinoma: Therapeutic Opportunities and Clinical Challenges. *Cancers (Basel),* 13.

PONOMAREV, E. D., SHRIVER, L. P., MARESZ, K., PEDRAS-VASCONCELOS, J., VERTHELYI, D. & DITTEL, B. N. 2007. GM-CSF production by autoreactive T cells is required for the activation of microglial cells and the onset of experimental autoimmune encephalomyelitis. *J Immunol,* 178**,** 39-48.

PRAGER, I. & WATZL, C. 2019. Mechanisms of natural killer cell-mediated cellular cytotoxicity. *J Leukoc Biol,* 105**,** 1319-1329.

PRÉVOT, P. P., SIMION, A., GRIMONT, A., COLLETTI, M., KHALAILEH, A., VAN DEN STEEN, G., SEMPOUX, C., XU, X., ROELANTS, V., HALD, J., BERTRAND, L., HEIMBERG, H., KONIECZNY, S. F., DOR, Y., LEMAIGRE, F. P. & JACQUEMIN, P. 2012. Role of the ductal transcription factors HNF6 and Sox9 in pancreatic acinar-to-ductal metaplasia. *Gut,* 61**,** 1723-32.

PRINCIPE, D. R., DECANT, B., MASCARIÑAS, E., WAYNE, E. A., DIAZ, A. M., AKAGI, N., HWANG, R., PASCHE, B., DAWSON, D. W., FANG, D., BENTREM, D. J., MUNSHI, H. G., JUNG, B. & GRIPPO, P. J. 2016. TGFß Signaling in the Pancreatic Tumor Microenvironment Promotes Fibrosis and Immune Evasion to Facilitate Tumorigenesis. *Cancer Res,* 76**,** 2525-39.

PRINZ, I., SILVA-SANTOS, B. & PENNINGTON, D. J. 2013. Functional development of γδ T cells. *Eur J Immunol,* 43**,** 1988-94.

QUANTE, M., TU, S. P., TOMITA, H., GONDA, T., WANG, S. S., TAKASHI, S., BAIK, G. H., SHIBATA, W., DIPRETE, B., BETZ, K. S., FRIEDMAN, R., VARRO, A., TYCKO, B. & WANG, T. C. 2011. Bone marrow-derived myofibroblasts contribute to the mesenchymal stem cell niche and promote tumor growth. *Cancer Cell,* 19**,** 257-72.

RAHIB, L., SMITH, B. D., AIZENBERG, R., ROSENZWEIG, A. B., FLESHMAN, J. M. & MATRISIAN, L. M. 2014. Projecting cancer incidence and deaths to 2030: the unexpected burden of thyroid, liver, and pancreas cancers in the United States. *Cancer Res,* 74**,** 2913-21.

RAWLA, P., SUNKARA, T. & GADUPUTI, V. 2019. Epidemiology of Pancreatic Cancer: Global Trends, Etiology and Risk Factors. *World J Oncol,* 10**,** 10-27.

REI, M., GONÇALVES-SOUSA, N., LANÇA, T., THOMPSON, R. G., MENSURADO, S., BALKWILL, F. R., KULBE, H., PENNINGTON, D. J. & SILVA-SANTOS, B. 2014. Murine CD27(-) Vγ6(+) γδ T cells producing IL-17A promote ovarian cancer growth via mobilization of protumor small peritoneal macrophages. *Proc Natl Acad Sci U S A,* 111**,** E3562-70.

REID, M. D., BASTURK, O., THIRABANJASAK, D., HRUBAN, R. H., KLIMSTRA, D. S., BAGCI, P., ALTINEL, D. & ADSAY, V. 2011. Tumor-infiltrating neutrophils in pancreatic neoplasia. *Mod Pathol,* 24**,** 1612-9.

RHIM, A. D., OBERSTEIN, P. E., THOMAS, D. H., MIREK, E. T., PALERMO, C. F., SASTRA, S. A., DEKLEVA, E. N., SAUNDERS, T., BECERRA, C. P., TATTERSALL, I. W., WESTPHALEN, C. B., KITAJEWSKI, J., FERNANDEZ-BARRENA, M. G., FERNANDEZ-ZAPICO, M. E., IACOBUZIO-DONAHUE, C., OLIVE, K. P. & STANGER, B. Z. 2014. Stromal elements act to restrain, rather than support, pancreatic ductal adenocarcinoma. *Cancer Cell,* 25**,** 735-47.

RIBOT, J. C., LOPES, N. & SILVA-SANTOS, B. 2021. γδ T cells in tissue physiology and surveillance. *Nat Rev Immunol,* 21**,** 221-232.

ROARK, C. L., AYDINTUG, M. K., LEWIS, J., YIN, X., LAHN, M., HAHN, Y. S., BORN, W. K., TIGELAAR, R. E. & O'BRIEN, R. L. 2004. Subset-specific, uniform activation among V gamma 6/V delta 1+ gamma delta T cells elicited by inflammation. *J Leukoc Biol,* 75**,** 68-75.

ROBERTS, E. W., BROZ, M. L., BINNEWIES, M., HEADLEY, M. B., NELSON, A. E., WOLF, D. M., KAISHO, T., BOGUNOVIC, D., BHARDWAJ, N. & KRUMMEL, M. F. 2016. Critical Role for CD103(+)/CD141(+) Dendritic Cells Bearing CCR7 for Tumor Antigen Trafficking and Priming of T Cell Immunity in Melanoma. *Cancer Cell,* 30**,** 324-336.

RUFFELL, B., CHANG-STRACHAN, D., CHAN, V., ROSENBUSCH, A., HO, C. M., PRYER, N., DANIEL, D., HWANG, E. S., RUGO, H. S. & COUSSENS, L. M. 2014. Macrophage IL-10 blocks CD8+ T cell-dependent responses to chemotherapy by suppressing IL-12 expression in intratumoral dendritic cells. *Cancer Cell,* 26**,** 623-37.

SAINTIGNY, P., MASSARELLI, E., LIN, S., AHN, Y. H., CHEN, Y., GOSWAMI, S., EREZ, B., O'REILLY, M. S., LIU, D., LEE, J. J., ZHANG, L., PING, Y., BEHRENS, C., SOLIS SOTO, L. M., HEYMACH, J. V., KIM, E. S., HERBST, R. S., LIPPMAN, S. M., WISTUBA, II, HONG, W. K., KURIE, J. M. & KOO, J. S. 2013. CXCR2 expression in tumor cells is a poor prognostic factor and promotes invasion and metastasis in lung adenocarcinoma. *Cancer Res,* 73**,** 571-82.

SAKA, D., GÖKALP, M., PIYADE, B., CEVIK, N. C., ARIK SEVER, E., UNUTMAZ, D., CEYHAN, G. O., DEMIR, I. E. & ASIMGIL, H. 2020. Mechanisms of T-Cell Exhaustion in Pancreatic Cancer. *Cancers (Basel),* 12.

SALMON, H., IDOYAGA, J., RAHMAN, A., LEBOEUF, M., REMARK, R., JORDAN, S., CASANOVA-ACEBES, M., KHUDOYNAZAROVA, M., AGUDO, J., TUNG, N., CHAKAROV, S., RIVERA, C., HOGSTAD, B., BOSENBERG, M., HASHIMOTO, D., GNJATIC, S., BHARDWAJ, N., PALUCKA, A. K., BROWN, B. D., BRODY, J., GINHOUX, F. & MERAD, M. 2016. Expansion and Activation of CD103(+) Dendritic Cell Progenitors at the Tumor Site Enhances Tumor Responses to Therapeutic PD-L1 and BRAF Inhibition. *Immunity,* 44**,** 924-38.

SÁNCHEZ-PAULETE, A. R., TEIJEIRA, A., CUETO, F. J., GARASA, S., PÉREZ-GRACIA, J. L., SÁNCHEZ-ARRÁEZ, A., SANCHO, D. & MELERO, I. 2017. Antigen cross-presentation and T-cell cross-priming in cancer immunology and immunotherapy. *Ann Oncol,* 28**,** xii74.

SANFORD, D. E., BELT, B. A., PANNI, R. Z., MAYER, A., DESHPANDE, A. D., CARPENTER, D., MITCHEM, J. B., PLAMBECK-SUESS, S. M., WORLEY, L. A., GOETZ, B. D., WANG-GILLAM, A., EBERLEIN, T. J., DENARDO, D. G., GOEDEGEBUURE, S. P. & LINEHAN, D. C. 2013. Inflammatory monocyte

mobilization decreases patient survival in pancreatic cancer: a role for targeting the CCL2/CCR2 axis. *Clin Cancer Res,* 19**,** 3404-15.

SANO, M., IJICHI, H., TAKAHASHI, R., MIYABAYASHI, K., FUJIWARA, H., YAMADA, T., KATO, H., NAKATSUKA, T., TANAKA, Y., TATEISHI, K., MORISHITA, Y., MOSES, H. L., ISAYAMA, H. & KOIKE, K. 2019. Blocking CXCLs-CXCR2 axis in tumor-stromal interactions contributes to survival in a mouse model of pancreatic ductal adenocarcinoma through reduced cell invasion/migration and a shift of immune-inflammatory microenvironment. *Oncogenesis,* 8**,** 8.

SARAIVA, M. & O'GARRA, A. 2010. The regulation of IL-10 production by immune cells. *Nat Rev Immunol,* 10**,** 170-81.

SCHLITZER, A., SIVAKAMASUNDARI, V., CHEN, J., SUMATOH, H. R., SCHREUDER, J., LUM, J., MALLERET, B., ZHANG, S., LARBI, A., ZOLEZZI, F., RENIA, L., POIDINGER, M., NAIK, S., NEWELL, E. W., ROBSON, P. & GINHOUX, F. 2015. Identification of cDC1- and cDC2-committed DC progenitors reveals early lineage priming at the common DC progenitor stage in the bone marrow. *Nat Immunol,* 16**,** 718-28.

SCHORER, M., RAKEBRANDT, N., LAMBERT, K., HUNZIKER, A., PALLMER, K., OXENIUS, A., KIPAR, A., STERTZ, S. & JOLLER, N. 2020. TIGIT limits immune pathology during viral infections. *Nat Commun,* 11**,** 1288.

SCHÜLKE, S. 2018. Induction of Interleukin-10 Producing Dendritic Cells As a Tool to Suppress Allergen-Specific T Helper 2 Responses. *Front Immunol,* 9**,** 455.

SCHULZ, C., GOMEZ PERDIGUERO, E., CHORRO, L., SZABO-ROGERS, H., CAGNARD, N., KIERDORF, K., PRINZ, M., WU, B., JACOBSEN, S. E., POLLARD, J. W., FRAMPTON, J., LIU, K. J. & GEISSMANN, F. 2012. A lineage of myeloid cells independent of Myb and hematopoietic stem cells. *Science,* 336**,** 86-90.

SEBASTIAN, A., HUM, N. R., MARTIN, K. A., GILMORE, S. F., PERAN, I., BYERS, S. W., WHEELER, E. K., COLEMAN, M. A. & LOOTS, G. G. 2020. Single-Cell Transcriptomic Analysis of Tumor-Derived Fibroblasts and Normal Tissue-Resident Fibroblasts Reveals Fibroblast Heterogeneity in Breast Cancer. *Cancers (Basel),* 12.

SEIFERT, A. M., LIST, J., HEIDUK, M., DECKER, R., VON RENESSE, J., MEINECKE, A. C., AUST, D. E., WELSCH, T., WEITZ, J. & SEIFERT, L. 2020. Gamma-delta T cells stimulate IL-6 production by pancreatic stellate cells in pancreatic ductal adenocarcinoma. *J Cancer Res Clin Oncol,* 146**,** 3233-3240.

SHI, G., DIRENZO, D., QU, C., BARNEY, D., MILEY, D. & KONIECZNY, S. F. 2013. Maintenance of acinar cell organization is critical to preventing Kras-induced acinar-ductal metaplasia. *Oncogene,* 32**,** 1950-8.

SHI, Y., GAO, W., LYTLE, N. K., HUANG, P., YUAN, X., DANN, A. M., RIDINGER-SAISON, M., DELGIORNO, K. E., ANTAL, C. E., LIANG, G., ATKINS, A. R., ERIKSON, G., SUN, H., MEISENHELDER, J., TERENZIANI, E., WOO, G., FANG, L., SANTISAKULTARM, T. P., MANOR, U., XU, R., BECERRA, C. R., BORAZANCI, E., VON HOFF, D. D., GRANDGENETT, P. M., HOLLINGSWORTH, M. A., LEBLANC, M., UMETSU, S. E., COLLISSON, E. A., SCADENG, M., LOWY, A. M., DONAHUE, T. R., REYA, T., DOWNES, M., EVANS, R. M., WAHL, G. M., PAWSON, T., TIAN, R. & HUNTER, T. 2019. Targeting LIF-mediated paracrine interaction for pancreatic cancer therapy and monitoring. *Nature,* 569**,** 131-135.

SILVA-SANTOS, B., SERRE, K. & NORELL, H. 2015. γδ T cells in cancer. *Nat Rev Immunol,* 15**,** 683-91.

SMITH, L. K., BOUKHALED, G. M., CONDOTTA, S. A., MAZOUZ, S., GUTHMILLER, J. J., VIJAY, R., BUTLER, N. S., BRUNEAU, J., SHOUKRY, N. H., KRAWCZYK, C. M. & RICHER, M. J. 2018. Interleukin-10 Directly Inhibits CD8(+) T Cell Function by Enhancing N-Glycan Branching to Decrease Antigen Sensitivity. *Immunity,* 48, 299-312.e5.

SMITTENAAR, C. R., PETERSEN, K. A., STEWART, K. & MOITT, N. 2016. Cancer incidence and mortality projections in the UK until 2035. *Br J Cancer,* 115**,** 1147-1155.

SMYTH, M. J., CRETNEY, E., KELLY, J. M., WESTWOOD, J. A., STREET, S. E., YAGITA, H., TAKEDA, K., VAN DOMMELEN, S. L., DEGLI-ESPOSTI, M. A. & HAYAKAWA, Y. 2005. Activation of NK cell cytotoxicity. *Mol Immunol,* 42**,** 501-10.

SOJKA, D. K., PLOUGASTEL-DOUGLAS, B., YANG, L., PAK-WITTEL, M. A., ARTYOMOV, M. N., IVANOVA, Y., ZHONG, C., CHASE, J. M., ROTHMAN, P. B., YU, J., RILEY, J. K., ZHU, J., TIAN, Z. & YOKOYAMA, W. M. 2014. Tissue-resident natural killer (NK) cells are cell lineages distinct from thymic and conventional splenic NK cells. *Elife,* 3**,** e01659.

SONG, H. K. & HWANG, D. Y. 2017. Use of C57BL/6N mice on the variety of immunological researches. *Lab Anim Res,* 33**,** 119-123.

STEELE, C. W., KARIM, S. A., LEACH, J. D. G., BAILEY, P., UPSTILL-GODDARD, R., RISHI, L., FOTH, M., BRYSON, S., MCDAID, K., WILSON, Z., EBERLEIN, C., CANDIDO, J. B., CLARKE, M., NIXON, C., CONNELLY, J., JAMIESON, N., CARTER, C. R., BALKWILL, F., CHANG, D. K., EVANS, T. R. J., STRATHDEE, D., BIANKIN, A. V., NIBBS, R. J. B., BARRY, S. T., SANSOM, O. J. & MORTON, J. P. 2016. CXCR2 Inhibition Profoundly Suppresses Metastases and Augments Immunotherapy in Pancreatic Ductal Adenocarcinoma. *Cancer Cell,* 29**,** 832-845.

STORZ, P. 2017. Acinar cell plasticity and development of pancreatic ductal adenocarcinoma. *Nat Rev Gastroenterol Hepatol,* 14**,** 296-304.

STROMNES, I. M., BROCKENBROUGH, J. S., IZERADJENE, K., CARLSON, M. A., CUEVAS, C., SIMMONS, R. M., GREENBERG, P. D. & HINGORANI, S. R. 2014. Targeted depletion of an MDSC subset unmasks pancreatic ductal adenocarcinoma to adaptive immunity. *Gut,* 63**,** 1769-81.

SUZUKI, T., HAYMAN, L., KILBEY, A., EDWARDS, J. & COFFELT, S. B. 2020. Gut γδ T cells as guardians, disruptors, and instigators of cancer. *Immunol Rev,* 298**,** 198-217.

SVENSSON, J., JENMALM, M. C., MATUSSEK, A., GEFFERS, R., BERG, G. & ERNERUDH, J. 2011. Macrophages at the fetal-maternal interface express markers of alternative activation and are induced by M-CSF and IL-10. *J Immunol,* 187**,** 3671-82.

TALBERT, E. E., CUITIÑO, M. C., LADNER, K. J., RAJASEKEREA, P. V., SIEBERT, M., SHAKYA, R., LEONE, G. W., OSTROWSKI, M. C., PALEO, B., WEISLEDER, N., REISER, P. J., WEBB, A., TIMMERS, C. D., EIFERMAN, D. S., EVANS, D. C., DILLHOFF, M. E., SCHMIDT, C. R. & GUTTRIDGE, D. C. 2019. Modeling Human Cancer-induced Cachexia. *Cell Rep,* 28**,** 1612-1622.e4.

TAMOUTOUNOUR, S., HENRI, S., LELOUARD, H., DE BOVIS, B., DE HAAR, C., VAN DER WOUDE, C. J., WOLTMAN, A. M., REYAL, Y., BONNET, D., SICHIEN, D., BAIN, C. C., MOWAT, A. M., REIS E SOUSA, C., POULIN, L. F., MALISSEN, B. & GUILLIAMS, M. 2012. CD64 distinguishes macrophages from dendritic

cells in the gut and reveals the Th1-inducing role of mesenteric lymph node macrophages during colitis. *Eur J Immunol,* 42**,** 3150-66.

TAWFIK, D., GROTH, C., GUNDLACH, J. P., PEIPP, M., KABELITZ, D., BECKER, T., OBERG, H. H., TRAUZOLD, A. & WESCH, D. 2019. TRAIL-Receptor 4 Modulates γδ T Cell-Cytotoxicity Toward Cancer Cells. *Front Immunol,* 10**,** 2044.

TAYLOR, A., AKDIS, M., JOSS, A., AKKOÇ, T., WENIG, R., COLONNA, M., DAIGLE, I., FLORY, E., BLASER, K. & AKDIS, C. A. 2007. IL-10 inhibits CD28 and ICOS costimulations of T cells via src homology 2 domain-containing protein tyrosine phosphatase 1. *J Allergy Clin Immunol,* 120**,** 76-83.

TEMPERO, M., OH, D. Y., TABERNERO, J., RENI, M., VAN CUTSEM, E., HENDIFAR, A., WALDSCHMIDT, D. T., STARLING, N., BACHET, J. B., CHANG, H. M., MAUREL, J., GARCIA-CARBONERO, R., LONARDI, S., COUSSENS, L. M., FONG, L., TSAO, L. C., COLE, G., JR., JAMES, D. & MACARULLA, T. 2021. Ibrutinib in combination with nab-paclitaxel and gemcitabine for first-line treatment of patients with metastatic pancreatic adenocarcinoma: phase III RESOLVE study. *Ann Oncol,* 32**,** 600-608.

TJOMSLAND, V., SPÅNGEUS, A., VÄLILÄ, J., SANDSTRÖM, P., BORCH, K., DRUID, H., FALKMER, S., FALKMER, U., MESSMER, D. & LARSSON, M. 2011. Interleukin 1α sustains the expression of inflammatory factors in human pancreatic cancer microenvironment by targeting cancer-associated fibroblasts. *Neoplasia,* 13**,** 664-75.

TRAVERS, J., ROCHMAN, M., MIRACLE, C. E., HABEL, J. E., BRUSILOVSKY, M., CALDWELL, J. M., RYMER, J. K. & ROTHENBERG, M. E. 2018. Chromatin regulates IL-33 release and extracellular cytokine activity. *Nat Commun,* 9**,** 3244.

TRESTINI, I., CARBOGNIN, L., PERETTI, U., SPERDUTI, I., CALDART, A., TREGNAGO, D., AVANCINI, A., AURIEMMA, A., ORSI, G., PILOTTO, S., FRULLONI, L., CAPURSO, G., BRIA, E., RENI, M., TORTORA, G. & MILELLA, M. 2021. Pancreatic Enzyme Replacement Therapy in Patients Undergoing First-Line Gemcitabine Plus nab-paclitaxel for Advanced Pancreatic Adenocarcinoma. *Front Oncol,* 11**,** 688889.

TSOLI, M., SWARBRICK, M. M. & ROBERTSON, G. R. 2016. Lipolytic and thermogenic depletion of adipose tissue in cancer cachexia. *Semin Cell Dev Biol,* 54**,** 68-81.

VAN DUIJNEVELDT, G., GRIFFIN, M. D. W. & PUTOCZKI, T. L. 2020. Emerging roles for the IL-6 family of cytokines in pancreatic cancer. *Clin Sci (Lond),* 134**,** 2091-2115.

VANTOUROUT, P. & HAYDAY, A. 2013. Six-of-the-best: unique contributions of γδ T cells to immunology. *Nat Rev Immunol,* 13**,** 88-100.

WACHSMANN, M. B., POP, L. M. & VITETTA, E. S. 2012. Pancreatic ductal adenocarcinoma: a review of immunologic aspects. *J Investig Med,* 60**,** 643-63.

WAGHRAY, M., YALAMANCHILI, M., DZIUBINSKI, M., ZEINALI, M., ERKKINEN, M., YANG, H., SCHRADLE, K. A., URS, S., PASCA DI MAGLIANO, M., WELLING, T. H., PALMBOS, P. L., ABEL, E. V., SAHAI, V., NAGRATH, S., WANG, L. & SIMEONE, D. M. 2016. GM-CSF Mediates Mesenchymal-Epithelial Cross-talk in Pancreatic Cancer. *Cancer Discov,* 6**,** 886-99.

WANG, R., JAW, J. J., STUTZMAN, N. C., ZOU, Z. & SUN, P. D. 2012. Natural killer cell-produced IFN-γ and TNF-α induce target cell cytolysis through up-regulation of ICAM-1. *J Leukoc Biol,* 91**,** 299-309.

WANG, S., HUANG, S. & SUN, Y. L. 2017. Epithelial-Mesenchymal Transition in Pancreatic Cancer: A Review. *Biomed Res Int,* 2017**,** 2646148.

WANG, S. W. & SUN, Y. M. 2014. The IL-6/JAK/STAT3 pathway: potential therapeutic strategies in treating colorectal cancer (Review). *Int J Oncol,* 44**,** 1032-40.

WANG, Y., CUI, L., GONSIOREK, W., MIN, S. H., ANILKUMAR, G., ROSENBLUM, S., KOZLOWSKI, J., LUNDELL, D., FINE, J. S. & GRANT, E. P. 2009. CCR2 and CXCR4 regulate peripheral blood monocyte pharmacodynamics and link to efficacy in experimental autoimmune encephalomyelitis. *J Inflamm (Lond),* 6**,** 32.

WARE, M. B., EL-RAYES, B. F. & LESINSKI, G. B. 2020. Mirage or long-awaited oasis: reinvigorating T-cell responses in pancreatic cancer. *J Immunother Cancer,* 8.

WATERS, A. M. & DER, C. J. 2018. KRAS: The Critical Driver and Therapeutic Target for Pancreatic Cancer. *Cold Spring Harb Perspect Med,* 8.

WATT, D. M. & MORTON, J. P. 2021. Heterogeneity in Pancreatic Cancer Fibroblasts-TGFß as a Master Regulator? *Cancers (Basel),* 13.

WEBER, A. N. R., BITTNER, Z., LIU, X., DANG, T. M., RADSAK, M. P. & BRUNNER, C. 2017. Bruton's Tyrosine Kinase: An Emerging Key Player in Innate Immunity. *Front Immunol,* 8**,** 1454.

WEI, D., WANG, L., YAN, Y., JIA, Z., GAGEA, M., LI, Z., ZUO, X., KONG, X., HUANG, S. & XIE, K. 2016. KLF4 Is Essential for Induction of Cellular Identity Change and Acinar-to-Ductal Reprogramming during Early Pancreatic Carcinogenesis. *Cancer Cell,* 29**,** 324-338.

WEISSMUELLER, S., MANCHADO, E., SABOROWSKI, M., MORRIS, J. P. T., WAGENBLAST, E., DAVIS, C. A., MOON, S. H., PFISTER, N. T., TSCHAHARGANEH, D. F., KITZING, T., AUST, D., MARKERT, E. K., WU, J., GRIMMOND, S. M., PILARSKY, C., PRIVES, C., BIANKIN, A. V. & LOWE, S. W. 2014. Mutant p53 drives pancreatic cancer metastasis through cell-autonomous PDGF receptor ß signaling. *Cell,* 157**,** 382-394.

WESTPHALEN, C. B. & OLIVE, K. P. 2012. Genetically engineered mouse models of pancreatic cancer. *Cancer J,* 18**,** 502-10.

WILLEMER, S., ELSÄSSER, H. P. & ADLER, G. 1992. Hormone-induced pancreatitis. *Eur Surg Res,* 24 Suppl 1**,** 29-39.

WITKIEWICZ, A. K., MCMILLAN, E. A., BALAJI, U., BAEK, G., LIN, W. C., MANSOUR, J., MOLLAEE, M., WAGNER, K. U., KODURU, P., YOPP, A., CHOTI, M. A., YEO, C. J., MCCUE, P., WHITE, M. A. & KNUDSEN, E. S. 2015. Whole-exome sequencing of pancreatic cancer defines genetic diversity and therapeutic targets. *Nat Commun,* 6**,** 6744.

WU, D., WU, P., QIU, F., WEI, Q. & HUANG, J. 2017. Human γδT-cell subsets and their involvement in tumor immunity. *Cell Mol Immunol,* 14**,** 245-253.

WU, P., WU, D., NI, C., YE, J., CHEN, W., HU, G., WANG, Z., WANG, C., ZHANG, Z., XIA, W., CHEN, Z., WANG, K., ZHANG, T., XU, J., HAN, Y., ZHANG, T., WU, X., WANG, J., GONG, W., ZHENG, S., QIU, F., YAN, J. & HUANG, J. 2014. γδT17 cells promote the accumulation and expansion of myeloid-derived suppressor cells in human colorectal cancer. *Immunity,* 40**,** 785-800.

WU, S. Y., FU, T., JIANG, Y. Z. & SHAO, Z. M. 2020. Natural killer cells in cancer biology and therapy. *Mol Cancer,* 19**,** 120.

WYNN, T. A., CHAWLA, A. & POLLARD, J. W. 2013. Macrophage biology in development, homeostasis and disease. *Nature,* 496**,** 445-55.

XIAN, G., ZHAO, J., QIN, C., ZHANG, Z., LIN, Y. & SU, Z. 2017. Simvastatin attenuates macrophage-mediated gemcitabine resistance of pancreatic ductal adenocarcinoma by regulating the TGF-ß1/Gfi-1 axis. *Cancer Lett,* 385**,** 65-74.

XUE, J., SHARMA, V., HSIEH, M. H., CHAWLA, A., MURALI, R., PANDOL, S. J. & HABTEZION, A. 2015. Alternatively activated macrophages promote pancreatic fibrosis in chronic pancreatitis. *Nat Commun,* 6**,** 7158.

YAMAZAKI, K., MASUGI, Y., EFFENDI, K., TSUJIKAWA, H., HIRAOKA, N., KITAGO, M., SHINODA, M., ITANO, O., TANABE, M., KITAGAWA, Y. & SAKAMOTO, M. 2014. Upregulated SMAD3 promotes epithelial-mesenchymal transition and predicts poor prognosis in pancreatic ductal adenocarcinoma. *Lab Invest,* 94**,** 683-91.

YAN, K., YANG, J., QIAN, Q., XU, D., LIU, H., WEI, L., LI, M. & XU, W. 2019. Pathogenic Role of an IL-23/γδT17/Neutrophil Axis in Coxsackievirus B3-Induced Pancreatitis. *J Immunol,* 203**,** 3301-3312.

YANG, S., LIU, Q. & LIAO, Q. 2020. Tumor-Associated Macrophages in Pancreatic Ductal Adenocarcinoma: Origin, Polarization, Function, and Reprogramming. *Front Cell Dev Biol,* 8**,** 607209.

YEH, H. W., HSU, E. C., LEE, S. S., LANG, Y. D., LIN, Y. C., CHANG, C. Y., LEE, S. Y., GU, D. L., SHIH, J. H., HO, C. M., CHEN, C. F., CHEN, C. T., TU, P. H., CHENG, C. F., CHEN, R. H., YANG, R. B. & JOU, Y. S. 2018. PSPC1 mediates TGF-ß1 autocrine signalling and Smad2/3 target switching to promote EMT, stemness and metastasis. *Nat Cell Biol,* 20**,** 479-491.

YIN, X., LIU, T., WANG, Z., MA, M., LEI, J., ZHANG, Z., FU, S., FU, Y., HU, Q., DING, H., HAN, X., XU, J., SHANG, H. & JIANG, Y. 2018. Expression of the Inhibitory Receptor TIGIT Is Up-Regulated Specifically on NK Cells With CD226 Activating Receptor From HIV-Infected Individuals. *Front Immunol,* 9**,** 2341.

YIN, Z., CHEN, C., SZABO, S. J., GLIMCHER, L. H., RAY, A. & CRAFT, J. 2002. T-Bet expression and failure of GATA-3 cross-regulation lead to default production of IFN-gamma by gammadelta T cells. *J Immunol,* 168**,** 1566-71.

ZHANG, B., YE, H., REN, X., ZHENG, S., ZHOU, Q., CHEN, C., LIN, Q., LI, G., WEI, L., FU, Z., ZHANG, Y., HU, C., LI, Z. & CHEN, R. 2019. Macrophage-expressed CD51 promotes cancer stem cell properties via the TGF-ß1/smad2/3 axis in pancreatic cancer. *Cancer Lett,* 459**,** 204-215.

ZHANG, K., FAN, C., CAI, D., ZHANG, Y., ZUO, R., ZHU, L., CAO, Y., ZHANG, J., LIU, C., CHEN, Y. & LIANG, H. 2020a. Contribution of TGF-Beta-Mediated NLRP3-HMGB1 Activation to Tubulointerstitial Fibrosis in Rat With Angiotensin II-Induced Chronic Kidney Disease. *Front Cell Dev Biol,* 8**,** 1.

ZHANG, L., ZHOU, F. & TEN DIJKE, P. 2013. Signaling interplay between transforming growth factor-ß receptor and PI3K/AKT pathways in cancer. *Trends Biochem Sci,* 38**,** 612-20.

ZHANG, Y., CHANDRA, V., RIQUELME SANCHEZ, E., DUTTA, P., QUESADA, P. R., RAKOSKI, A., ZOLTAN, M., ARORA, N., BAYDOGAN, S., HORNE, W., BURKS, J., XU, H., HUSSAIN, P., WANG, H., GUPTA, S., MAITRA, A., BAILEY, J. M., MOGHADDAM, S. J., BANERJEE, S., SAHIN, I., BHATTACHARYA, P. & MCALLISTER, F. 2020b. Interleukin-17-induced neutrophil extracellular traps mediate resistance to checkpoint blockade in pancreatic cancer. *J Exp Med,* 217.

ZHANG, Y., ZOLTAN, M., RIQUELME, E., XU, H., SAHIN, I., CASTRO-PANDO, S., MONTIEL, M. F., CHANG, K., JIANG, Z., LING, J., GUPTA, S., HORNE, W.,

PRUSKI, M., WANG, H., SUN, S. C., LOZANO, G., CHIAO, P., MAITRA, A., LEACH, S. D., KOLLS, J. K., VILAR, E., WANG, T. C., BAILEY, J. M. & MCALLISTER, F. 2018. Immune Cell Production of Interleukin 17 Induces Stem Cell Features of Pancreatic Intraepithelial Neoplasia Cells. *Gastroenterology*, 155**,** 210-223.e3.

ZHU, Y., HERNDON, J. M., SOJKA, D. K., KIM, K. W., KNOLHOFF, B. L., ZUO, C., CULLINAN, D. R., LUO, J., BEARDEN, A. R., LAVINE, K. J., YOKOYAMA, W. M., HAWKINS, W. G., FIELDS, R. C., RANDOLPH, G. J. & DENARDO, D. G. 2017. Tissue-Resident Macrophages in Pancreatic Ductal Adenocarcinoma Originate from Embryonic Hematopoiesis and Promote Tumor Progression. *Immunity*, 47**,** 323-338.e6.

ZHU, Y., KNOLHOFF, B. L., MEYER, M. A., NYWENING, T. M., WEST, B. L., LUO, J., WANG-GILLAM, A., GOEDEGEBUURE, S. P., LINEHAN, D. C. & DENARDO, D. G. 2014. CSF1/CSF1R blockade reprograms tumor-infiltrating macrophages and improves response to T-cell checkpoint immunotherapy in pancreatic cancer models. *Cancer Res*, 74**,** 5057-69.